UNIVERSITY OF CALIFORNIA

Santa Barbara

Novel Magnetic Nanoparticle Adsorbents for Organic and Inorganic Contaminants

A dissertation submitted in partial satisfaction of the

requirements for the degree Doctor of Philosophy

in Environmental Science & Management

by

Yuxiong Huang

Committee in charge:

Professor Arturo A. Keller, Chair

Professor Patricia A. Holden

Professor Susannah L. Scott

December 2015

The dissertation of Yuxiong Huang is approved.

_____

Patricia A. Holden

_____

Susannah L. Scott

_____

Arturo A. Keller, Committee Chair

November 2015

Novel Magnetic Nanoparticle Adsorbents for Organic and Inorganic Contaminants

by

Yuxiong Huang

To my parents.

ACKNOWLEDGEMENTS

It was always a long struggle in the Ph.D. pursuit. Fortunately, I was fully encouraged and motivated by wonderful people along the way, which makes this journey more remarkable and rewardable.

First and foremost, I would like to express my deepest gratitude to my advisor, Professor Arturo Keller, for all his contributions of time, ideas, and funding to make my Ph.D. experience productive and stimulating. He is not only a great advisor for my research, but also a mentor and friend for life.

I am greatly thankful to my PhD committee members, Professor Patricia Holden and Professor Susannah Scott, for their helpful guidance, feedback, and encouragement.

I was very lucky to be part of Keller's group at Bren School and highly appreciate the warm friendship and strong support from my fellow labmates and colleagues. Thank you, Dongxu, Yemi, Jon, Kendra, Yiming, Hongtao, Lijuan, for the help and company in the past 4 years. And my special gratitude goes to my lab assistants, Aaron and Aarushi, who helped a great deal in the experiments.

I would like to thank the Bren community, the staff and faculty generously provide their time and resources. Special thanks to Corlei for providing motivation and resources to purse this degree. Thanks Joe, Amanda, and Rachel at MRL for technical supports on research.

I am deeply grateful to my friends, for their support, tolerance and encouragement.

Special praises to my family, for their love, encouragement and support.

I would like to deeply thank my parents for raining me up, supporting me through all the education, for encouraging me to follow my dream. This dissertation is dedicated to my dearest mum and dad.

VITA OF YUXIONG HUANG
November 2015

EDUCATION

PhD in Environmental Science and Management **2015**

Bren School of Environmental Science & Management

University of California, Santa Barbara

Dissertation: *Novel Magnetic Nanoparticle Adsorbents for Organic and Inorganic Contaminants*

Bachelor of Engineering in Chemical and Biological Engineering **2011**

Department of Chemical Engineering

Tsinghua University, Beijing, China

PUBLICATIONS

1. Adeleye, A., Conway J., Garner K., Huang, Y., Su, Y., Keller, AA. Engineered nanomaterials for water treatment and remediation: Costs, benefits, and applicability. Chemical Engineering Journal, doi:10.1016/j.cej.2015.10.105

2. Wang, H., Adeleye, A., Huang, Y., Li, F., Keller, AA. Heteroaggregation of nanoparticles with biocolloids and geocolloids. Advances in Colloid and Interface Science, doi:10.1016/j.cis.2015.07.002

3. Huang, Y., A. A. Keller. (2015) EDTA Functionalized Magnetic Nanoparticle Sorbents for Cadmium and Lead Contaminated Water Treatment. Water Research, doi:10.1016/j.watres.2015.05.011

4. Bueno, Adeleye, Bradley, Brandt, Callery, Feraud, Garner, Gentry, Huang, Y., McCullough et al. (2015). Citizen Science as a Tool for Overcoming Insufficient Monitoring and Inadequate Stakeholder Buy-in in Adaptive Management: Criteria and Evidence. Ecosystems, doi:10.1007/s10021-015-9842-4

5. Su, Y., A. Adeleye, A.A. Keller, Y. Huang, C. Dai, X. Zhou,Y. Zhang (2015). Magnetic sulfide-modified nanoscale zerovalent iron (S-nZVI) for dissolved metal ion removal. Water Research, doi:10.1016/j.watres.2015.02.004

6. Su, Y., A. Adeleye, Y. Huang, Z. Sun, C. Dai, X. Zhou, Y. Zhang, A.A. Keller (2014). Simultaneous Removal of Cadmium and Nitrate in Aqueous Media by Nanoscale Zerovalent

Iron (nZVI) and Au Doped nZVI Particles, Water Research, doi: 10.1016/j.watres.2014.06.008

7. Huang, Y., Jae-Kyu Y, Keller, AA (2014). Removal of Arsenic and phosphate from aqueous solution by (hydr-)oxide coated sand. ACS Sustainable Chemistry & Engineering, doi:10.1021/sc400484s

8. Huang, Y., Keller, AA (2013). Magnetic Nanoparticle Adsorbents for Emerging Organic Contaminants. ACS Sustainable Chemistry & Engineering, doi: 10.1021/sc400047q

9. Huang, Y., Keller, AA. The design and application of magnetic-core composite nano/micro particles for environmental remediation. Book Chapter. Rational Design of Next-Generation Nanomaterials and Nanodevices for Advanced Water Applications, International Water Association (IWA) Publishing, in press

10. Huang, Y., Keller, AA. Adsorptive Removal of Multiple Metal Ions from Contaminated Water with EDTA Functionalized Superparamagnetic Nanoparticles: Equilibrium, Kinetics and Thermodynamics. Journal of Hazardous Materials, under review

11. Luo, Huang, Y., Zhu, Tang, Ren, Ren, Wang, H., Li, F. Effects of humic and fulvic acids on the aggregation and stability of TiO2 nanoparticles. Journal of Saudi Chemical Society, under review

12. Zhao, L., Huang, Y., Hu, J., Keller, AA. 1H NMR and GC-MS based metabolomics reveal defense and detoxification mechanism of cucumber plant under nano-Cu stress. Environmental Science & Technology, under review

13. Su, Y., A. Adeleye, Y. Huang, X. Zhou, A.A. Keller, Y. Zhang. Nano-seeding Stimulated Magnetism of Sulfide-modified Nanoscale Zerovalent Iron and Its Application in Metal Removal from Aqueous Media. Environmental Science: Nano, submitted

14. Dong, Y., Li, X., Huang, Y., Wang, H., Li, F. Coagulation and dissolution of zinc oxide nanoparticles in presence of humic acid under different pHs. Environmental Engineering Science, under review

15. Zhao, L., Huang, Y., Ortiz, C., Keller, AA., Zhou, H., Mazer, S.. Exposure of Cucumber (Cucumis sativus) Plants to Soil Contaminated with Nano-Cu: A Life Cycle Study Reveals the Physiological Responses and Fruit Metabolic Profile Alteration. Environmental Science & Technology, submitted.

16. Huang, Y., Fulton, A., Keller, AA. Micelle Array Confined Superparamagnetic Nanoparticle Adsorbents Porous Structure Optimization for Higher and Faster Removal of Emerging Organic Contaminants and PAHs, in preparation.

17. Huang, Y., Fulton, A., Keller, AA. Magnetic Nanoparticle Adsorbents with Micelle Array Confined in the Framework for PAHs and Metal Contaminants Simultaneous Removal, in preparation.

RESEARCH PROJECTS

Graduate Student Researcher Aug.2011~Dec.2015

Prof. Keller's Lab, Bren School, University of California, Santa Barbara

1. *Novel Sustainable Magnetic Nanoparticle Adsorbents for Organic and Inorganic Contaminants*

- Develop novel sustainable magnetic nanoparticle sorbents (Mag-PCMAs and Mag-Ligands)
- Optimize the sorbents' removal performance by providing alternative surfactants and enlarging the pore volume and size
- Evaluate the sorption capacity of sorbents under different environmental conditions (pH, ionic strength, water hardness)
- Investigate the selective sequence of sorbents in multiple contaminants competitive sorption
- Determine the equilibrium, kinetics and thermodynamics of the adsorbents

2. *Low-Cost and Easy Available Metal(hydro-)oxide Coated Sands for Arsenic Removal*

- Prepare and optimize iron or/and manganese coated sand media sorbent
- Evaluated the sorption performance of metal(hydro-)oxide coated sand under different environmental conditions

Research Assistant Sep.2010~Jun.2011

Prof. Guangsheng Luo's Group, State Key Laboratory of Chemical Engineering, Tsinghua University

3. *Controllable Synthesis of Silica Microspheres Based on Liquid-liquid Microdispersion Technique*

- Control of morphologies of silica spheres via the liquid-liquid microdispersion technique
- Apply thermo responsive polymer in shrinking the size of silica sphere

Research Intern Jul.2010~Sep.2010

Dr. Mustafa Akbulut's Group, Department of Chemical Engineering, Texas A&M University

4. *Nanomedicine's diffusion, adsorption, and distribution in the environment*

- Determine the effect of size on sorption kinetics and thermodynamics of the nanomedicine
- Obtain a fundamental understanding of the diffusion dynamics of the nanomedicine through mathematical models

Research Assistant Oct.2008~Nov.2010

Prof. Zheng Liu's Group, Deptartment of Chemical Engineering, Tsinghua University

5. *Chromatography media for large-scale preparative separation of therapeutic plasmid: Design and characterization*

- Develop a novel reusable plasmid purification kit
- Optimize the synthesis of novel adsorption media in the terms of monolith
- Functionalize the active area of the novel adsorption
- Characterize the microstructure of the macroporous materials

TEACHING & MENTOR EXPERIENCE

Teaching Assistant, Bren School, University of California, Santa Barbara

1. ESM 222, Fate & Transport of Pollutants in the Environment — Spring 2015
2. ESM 282, Industrial Ecology/ Green Supply Chain — Winter 2015
3. ESM 223L, Laboratory in Management of Soil and Groundwater Quality — Winter 2014
4. ESM 222, Fate & Transport of Pollutants in the Environment — Spring 2013

Lab Mentor, Bren School, University of California, Santa Barbara

Provide mentorship for 3 undergraduate and 2 master's student researchers

Senior Project Mentor, College of Engineering, University of California, Santa Barbara

1. Pollutant Removal via Magnetic Nanoparticle Separation — 2014~2015
2. The Development of New Methods to Prepare Nanoparticles as Carriers for Biopesticides — 2015

CONFERENCES & PRESENTATIONS

1. Presenter, 2015 Sustainable Nanotechnology Organization meeting, Portland, OR, 2015: "Magnetic Permanently Confined Micelle Array Nanoparticles Sorbents for Simultaneous Removal of Heavy Metal Ions and PAHs"

2. Presenter, 250th National Meeting of the American Chemical Society, Boston, MA, 2015: "EDTA functionalized superparamagnetic nanoparticles for heavy metal remediation"

3. Presenter, Third Sustainable Nanotechnology Organization Conference, Boston, MA, 2014: "Removal of Lead (II), Chromium (III), Mercury (II), Copper (II) and Zinc (II) from Contaminated Water with EDTA Functionalized Superparamagnetic Nanoparticles"

4. Presenter, 248th National Meeting of the American Chemical Society, San Francisco, CA, 2014: "Novel EDTA attached magnetic nanoparticles sorbents for rapid removal of cadmium from aquatic systems"

5. Presenter, 2013 American Institute of Chemical Engineers (AIChE) Annual Meeting, San Francisco, CA, 2013: "Removal of Arsenic and phosphate from aqueous solution by (hydr-)oxide coated sand"

6. Presenter, 243rd American Chemical Society Spring National Meeting, San Diego, CA, 2012: "Using magnetic permanently confined micelle arrays (Mag-PCMA) to adsorb current and emerging organic contaminants"

FELLOWSHIPS & HONORS

1. Sustainable Nanotechnology Organization Student Award — 2015
2. Doctoral Student Travel Grants, UCSB — 2015

3. Sustainable Nanotechnology Organization Student Award 2014
4. Bren School Travel Award, UCSB 2014
5. Bren School Michael J. Connell Memorial Fellowship, UCSB 2012
6. Challenge Cup (3rd Prize), Beijing Extra-Curricular Academic Competition in the Technology Works 2011
7. Challenge Cup (2nd Prize) & Innovation Academic Award, Tsinghua University Extra-Curricular Academic Competition in the Technology Works 2010
8. Innovation of Nature Science Academic Award, Tsinghua University 2010
9. Chinese National Science and Technology Innovation Program Seed Funding (for undergraduate student) 2009
10. Public Service & Outstanding Student Volunteers Awards, Tsinghua University 2008, 2009

JOURNALS REFEREED

1. Water Research
2. Chemical Engineering Journal
3. Journal of Separation Science
4. Environmental Science and Pollution Research
5. Journal of Alloys and Compounds
6. Journal of Saudi Chemical Society
7. Soil and Sediment Contamination An International Journal
8. African Journal of Engineering Research

AFFILIATIONS

1. Student member, American Chemical Society (ACS)
2. Student member, American Institute of Chemical Engineers (AIChE)
3. Student member, Sustainable Nanotechnology Organization (SNO)

ABSTRACT

Novel Magnetic Nanoparticle Adsorbents for Organic and Inorganic Contaminants

by

Yuxiong Huang

Water is not only a resource, but a life source. However, water pollution is one of the most challenging global issues that seriously threatened to people's life and sustainable development. With the continual concern over the presence of naturally-occurring and anthropogenic organic and inorganic contaminants in the aquatic environment, there is a growing need for the implementation of innovative treatment methods for the elimination of these contaminants from natural waters and wastewater effluents. Featuring high adsorption capacity, good regenerability, and surface area accessibility, magnetic nanoparticles (MNPs) have emerged as a new generation of sorbent materials for environmental decontamination in the past few years. Due to their superparamagnetic property that can be attracted to a magnetic field, it is easy to separate these MNPs adhered with contaminants from aqueous solution or complicated matrices by simply applying an external magnetic field; no filtration, centrifugation or gravitational separation is needed, making them a much more sustainable option than more traditional approaches for removing organic and inorganic contaminants. In this doctoral research, 4 different novel magnetic-core composite nanoparticle sorbents were developed for organic and metal contaminants remediation in aquatic systems. These sorbents have a core-shell structure with a magnetite core and a silica porous layer that

permanently confines surfactant micelles (namely as Mag-PCMAs, targeting organic contaminants removal) or are functionalized with metal-binding organic ligands (namely as Mag-Ligands, targeting metal contaminants removal). The physicochemical properties of these magnetic nanoparticle sorbent was fully characterized via transmission electron microscopy, scanning electron microscopy, thermogravimetric analyses, fourier transform infrared spectroscopy, superconducting quantum interference device magnetometer, X-ray diffraction and BET porosimeter. The removal efficiencies of organic contaminants such as PAHs, emerging organic contaminants (EOCs, including pharmaceuticals, industrial additives) onto Mag-PCMAs and metal contaminants such as cadmium, lead, mercury, chromium and etc. onto Mag-Ligand were evaluated across a wide range of environmental conditions (e.g. pH, water hardness). The adsorption isotherms and kinetics of various contaminants onto the magnetic nanoparticle sorbents were determined respectively. Competitive sorption studies were conducted to determine the selectivity sequence among multiple metal ions onto Mag-Ligands. Isothermal titration microcalorimetry (ITC) was used to obtain key quantitative thermodynamic binding data of the interactions between Mag-Ligand and metal ions, providing the enthalpy, entropy and free energy of binding values as well as binding constants. Micelle swelling agent was used to optimize Mag-PCMAs' porous structure for increasing pore volume and surface area to achieve higher removal efficiency and sorption kinetics. In addition, study was investigated on simultaneous removal of metal contaminants and PAHs across a variety of environmental conditions. The regenerability and reusability of these magnetic nanoparticle sorbents were also studied; both Mag-PCMAs and Mag-Ligand can be regenerated via rinsing with methanol or dilute acid, and can be reused for several treatment cycles without significant decrease on

efficiency. This study has provided a rapid, effective and more sustainable approach for organic and metal contaminants remediation from aquatic systems.

TABLE OF CONTENTS

Chapter 1. Introduction

1.1. Organic and Inorganic Contaminants in Aquatic Systems

Water is one of the world's most abundant resources, but less than 1% of the global supply of water is available and safe for human consumption (Grey et al. 2013). According to the World Health Organization, over 760 million people were without adequate drinking water supply in 2011 (WHO 2013). Where it is available, the cost of potable water is rising due to increasing energy costs, growing populations, and climatic or other environmental issues (Grey et al. 2013, Levin et al. 2002). In addition, an increasing number of drinking water sources are showing evidence of contamination, especially by emerging pollutants like pharmaceuticals and personal care products (Houtman 2010, WHO 2012).

1.1.1. Organic Contaminants

Recently, one particular concern is 'emerging organic contaminants' (EOCs). EOCs cover not only newly developed compounds but also compounds newly discovered in the environment, and compounds that have only recently been categorized as contaminants (Lapworth et al. 2012). EOCs include a wide array of different compounds such as pharmaceuticals and personal care products (PPCPs), pesticides, veterinary products, industrial compounds/by-products, food additives, as well as engineered nano-materials (Bolong et al. 2009). It is now established that these compounds enter the environment from a number of sources and pathways: wastewater effluents from municipal treatment plants, septic tanks, hospital effluents, livestock activities including waste lagoons and manure application to soil, subsurface storage of household and industrial wastes, as well as indirectly through the process of groundwater–surface water exchange (Pal et al. 2010).

The presence of these synthetic chemicals may contaminate ecosystems and surface and drinking water supplies. This is a public health concern because little is known about potentially chronic health effects associated with long term ingestion of mixtures of biologically active compounds, such as pharmaceuticals and pesticides, through drinking water (Ikehata et al. 2008). Recent studies have shown that EOCs may have biological effects and even potential ecotoxicological impacts on invertebrates (such as daphnids), fish, algae, mussels, and also human embryonic cells (Carlsson et al. 2006, Lai et al. 2009, Lyssimachou and Arukwe 2007, Pomati et al. 2006).

1.1.2. Metal Contaminants

Another major global concern is metals contaminants, which have been excessively released into the environment due to rapid industrialization. Cadmium, zinc, copper, nickel, lead, mercury and chromium are often detected in industrial wastewaters, which originate from metal plating, mining activities, smelting, battery manufacture, tanneries, petroleum refining, paint manufacture, pesticides, pigment manufacture, printing and photographic industries, etc. (Kadirvelu et al. 2001, Williams et al. 1998). Heavy metals are persistent, and therefore, very difficult to eliminate naturally from the environment, even when present at trace amounts. Nearly all heavy metals are highly toxic, non-biodegradable, non-thermodegradable and readily accumulate to toxic levels in living tissues, causing various diseases and disorders (Tuzen et al. 2008). For example, Cd^{2+} in the environment can affect human health with the potential to cause kidney damage, renal disorder, Itai-Itai (excruciating pain in the bone), hepatic damage, cancer, and hypertension (Igwe and Abia 2007, Kurniawan et al. 2006a, b).

1.1.3. Conventional Water Treatment Technologies

Conventional water treatment technologies generally designed on the basis of bulk water chemistry, and the mechanism involves adsorption (Mittal et al. 2007, Ni et al. 2007), oxidation (Huber et al. 2005, Rosal et al. 2010), photocatalysis (Badawy et al. 2006, Wang and Lemley 2002), membrane based separation (Bhatnagar and Sillanpää 2011, Phenrat et al. 2010), biological treatment (Khan and Ongerth 2004, Onesios et al. 2008, Salgado et al. 2011), coagulation and precipitation (Baskan and Pala 2009, Song et al. 2006) etc..

There are many environmental impacts associated with the various current water treatment technologies that are largely dependent on the method used and on the situation in which is it used. While there are many effective existing technologies for treating water, many of them are expensive or inefficient, and many emerging contaminants such as PCPPs and endocrine disrupting compounds (EDCs) are not easily removed or degraded by traditional means, indicating a need for alternatives.

1.2. Application of Nanotechnology in Water Remediation

1.2.1. Nanotechnology

In recent years, nanotechnology has been developing very rapidly. Generally, nanoparticles are commonly defined as materials with at least one dimension below 100 nm (e.g. diameter, thickness, length or width) (Borm et al. 2006), although more broadly nanotechnology refers to nanomaterials incorporated into products that make use of properties that are unique to the nanoscale. Due to the size effect, the physicochemical properties of nanoparticles are different with their bulk material, with some special properties, typically including: (1) size effects (reducing the particles size can lead to the

change of solubility, color, absorption or emission wavelength, and conductivity); (2) composition effects (different compositions of nanoparticles result in a different physical and chemical behavior); and (3) surface effects (the surface behavior of nanoparticles are changed by their dispersibility, conductivity and other related properties) (Borm et al. 2006).

Engineered nanomaterials (ENMs) are now being widely manufactured and applied in multiple fields, including agriculture (Zhao et al. 2012), catalysts (Zhou et al. 2011), coatings, paints and pigments (Gopalakrishnan et al. 2011), composites (Petrov and Georgiev 2012), cosmetics (Sabitha et al. 2012), electronics & optics (Song et al. 2012), energy (Serrano et al. 2009), environmental remediation (Khin et al. 2012), filtration & purification (Dhakras 2011).

Regarding to the application of ENMs for water treatment, researchers have investigated their potential to act as effective adsorbents (Tofighy and Mohammadi 2011), filters (Brady-Estévez et al. 2008), disinfectants (Dankovich and Gray 2011, Li et al. 2008, Musico et al. 2014), and reactive agents (Chen et al. 2003, Crane and Scott 2012), as well as showing the promise for full scale water treatment and environmental remediation (Mellor et al. 2015, Qu et al. 2013, Ren et al. 2013).

1.2.2. Carbonaceous Nanomaterials for Water Treatment

Carbon nanomaterials (C-ENMs) are composed entirely (or mainly) of carbon atoms. They include carbon nanotubes (single-walled, SWCNTs or multi-walled, MWCNTs), carbon nanofibers, fullerene, graphene and derivatives, and amorphous carbonaceous composites (Chen et al. 2011c, Gupta and Saleh 2013, Iijima 1991, Zhu et al. 2010). C-ENMs characteristically have exceptionally high surface area, which make them ideal candidates for adsorption of pollutants (Bacsa et al. 2000, Gai et al. 2011, Zhang et al. 2014,

Zhu et al. 2010). In addition, the surfaces of these inherently hydrophobic materials can be functionalized to target specific pollutants via chemical or electrical interactions (Wang et al. 2013). Some C-ENMs may be aligned to form efficient filters or incorporated into conventional membranes for removal of pollutants (Han et al. 2013, Mostafavi et al. 2009).

1.2.3. Metal and metal oxides for Water Treatment

Metal and metal oxide engineered nanomaterials (Me/MeO ENMs) are a diverse class of nanomaterials that are composed of one, two, or, less commonly, three metals and their oxides (Li et al. 2008, Pradeep and Anshup 2009, Stoimenov et al. 2002, Xu et al. 2012). Although there are several types, the Me/MeO ENMs most-commonly applied for water treatment/environmental remediation are nanoscale zero-valent iron (nZVI) (Karn et al. 2009, Lacinova et al. 2012, Mueller et al. 2012), TiO_2 (Bennett and Keller 2011, Lu et al. 2013, Soni et al. 2008, Yang et al. 2002, Yang et al. 2013), Ag (Dankovich and Gray 2011, Ehdaie et al. 2014, Georgekutty et al. 2008, Ren et al. 2013, Yang et al. 2013, Zodrow et al. 2009), and ZnO (Alikhani et al. 2012, El-Kemary et al. 2010). Some of the mechanisms for water treatment or remediation include adsorption, chemical degradation, photodegradation, and chemical disinfection.

1.3. Magnetic-core Composite Nano/Micro Particles Sorbents

1.3.1. Magnetic-core Composite Nano/Micro Particles Sorbents

Known as one of the cutting edge ENMs, magnetic particles are particularly attractive due to their superparamagnetic nature as well as their unique physicochemical properties such as high dispersibility, relative large surface area and the high ratio of surface to volume resulting in a higher adsorption capacity. Generally the core consists of magnetic elements

such as iron, nickel, cobalt or their oxides and alloys, such that magnetic particles show ferromagnetic or superparamagnetic properties, which make them behave like small permanent magnets once magnetized as well as form lattice or aggregate due to magnetic interaction. Specifically, ferromagnetic particles have a permanent magnetism and removal of the magnetic field results in a lattice form, while superparamagnetic particles are attracted to a magnetic field but retain no residual magnetism after the field is removed. Superparamagnetic nano-adsorbents are particularly attractive as they can be easily retained and separated from treated water by applying external magnetic fields (as shown in Figure 1), which overcomes many of the issues present in filtration, centrifugation or gravitational separation, generally requiring less energy to achieve a given level of separation.

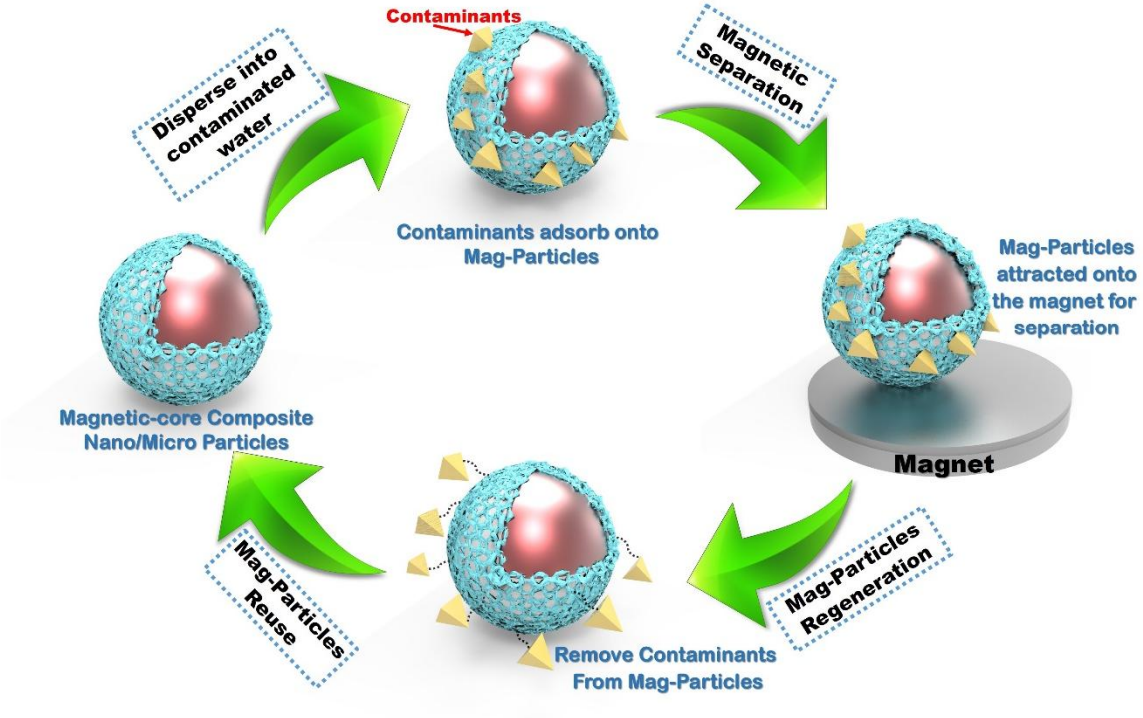

Figure 1. Procedure of applying magnetic-core composite nano/micro particles in water treatment

Iron oxides, such as magnetite (Fe_3O_4) and maghemite (γ-Fe_2O_3), are the most popular option owning to their small size and high surface area. However, pure iron oxide particles are prone to the formation of large aggregates due to the magnetic interaction, which results in changes of their magnetic properties, such as the loss of magnetism (Chen et al. 2011b). In addition, their bare surface lacks selectivity, which eliminates their range of application and remediation capacity (Giakisikli and Anthemidis 2013). Thus, researchers usually modify the surface of the iron oxide particles (as magnetic core) with specific functional groups and coatings forming a core-shell structure to overcome the above limitations (Giakisikli and Anthemidis 2013). The coating onto MPs' surface, also known as a shell, can be obtained by the attachment or binding of inorganic components (e.g., silica or alumina, etc.) (Jiang et al. 2012, Karatapanis et al. 2011) or organic molecules (e.g., polymer or surfactant, etc.) (Faraji et al. 2010b, Huang et al. 2010). With appropriate surface coating in this core-shell structure, it can help to improve their chemical stability (Ditsch et al. 2005), prevent their oxidation (Li et al. 2010b) as well as lower their implication to the environment (Chen et al. 2011a), and provide specific functionalities like selectivity for ion uptake (Koehler et al. 2009) or enhancing the water solubility of HOCs (Wang et al. 2009).

The synthesis of a magnetic-core composite nano/micro particles typically involves three steps (shown as Figure 2.):

1. Synthesis of magnetic particles, usually iron oxide (magnetite or maghemite) nanoparticles. Some studies (Huang and Keller 2013) may use the commercial iron oxide nanoparticles to skip this step.

2. Coating onto the magnetic core.

3. Surface modification of the coating layer.

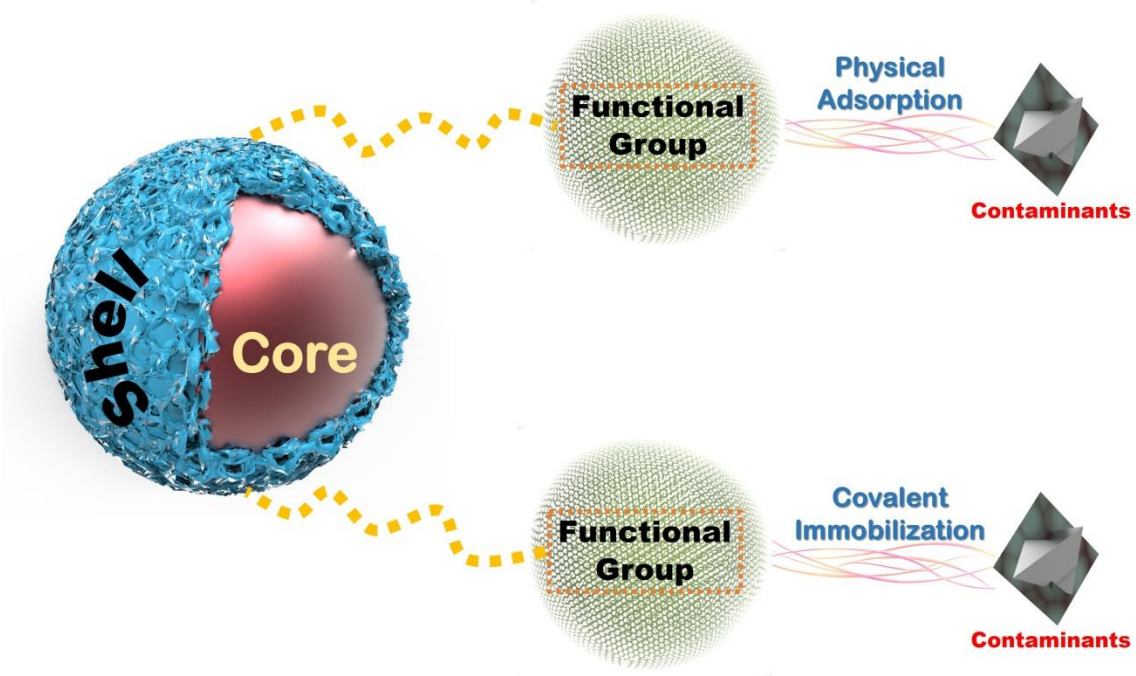

Figure 2. Functionalization of a core–shell type structure of magnetic-core composite nano/micro particles

1.3.2. Synthesis of Magnetic Nanoparticles

There are many chemical methods that can be chosen to prepare magnetic nanoparticles, including classical chemical coprecipitation (Cornell and Schwertmann 2006, Schwarzer and Peukert 2004, Sugimoto 2003), sol-gel syntheses (Dai et al. 2005, Duraes et al. 2005, Fouad et al. 2006), hydrothermal and high temperature reactions (Hyeon et al. 2001, Sun et al. 2004), surfactant mediate/template syntheses (in constrained environments) (Deng et al. 2003, Inouye et al. 1982), sonochemical reactions (Koltypin et al. 1996, Shafi et al. 1997), hydrolysis and thermolysis of precursors (Kimata et al. 2003), flow injection syntheses(Salazar-Alvarez et al. 2006), microemulsions (Geng et al. 2006, Solans et al. 2005), biomimetic mineralization (Allen et al. 2003, Rice et al. 2004), aerosol/vapor methods (Alexandrescu et al. 2005, Morales et al. 2003), and electrospray syntheses (Pascal

et al. 1999, Reetz et al. 1996). Among these methods, the chemical coprecipitation synthesis is one of the simplest and most efficient way for the preparation of magnetite particles (Laurent et al. 2010). In this method, iron oxides (Fe_3O_4 or γFe_2O_3) are prepared by an aging stoichiometric mixture of ferrous and ferric salts in aqueous medium (generally involves the dissolution of a mixture of a solution of $FeCl_3 \cdot 6H_2O$ and $FeCl_2 \cdot 4H_2O$ in deionized water under nitrogen atmosphere with vigorous stirring at 70–85 °C and the immediate addition of aqueous ammonia) (Jolivet et al. 2004).

1.3.3. Coating onto Magnetic Core

Nowadays, there are various materials to coat the magnetic core, including silica (Huang and Keller 2013, Wang et al. 2009), alumina (Tavallali 2011), carbon (including carbon-based materials, e.g. activated carbon (Faraji et al. 2010a), carbon nanotube (CNT) (Rastkari and Ahmadkhaniha 2013) and graphene/graphene oxide (Liu et al. 2011)), polymer (Li et al. 2010a), surfactant(Zhao et al. 2008) and biomass (e.g. pollen grains) (Thio et al. 2011). The mechanism of coating varies from covalent binding to electrostatic force, and the coating process also varies from sol-gel reaction to dissolution. For example, to conduct a silica coating onto magnetic core, the Stôber method (Stöber et al. 1968) through a sol–gel reaction (generally using an alkoxy silane (e.g. tetraethoxysilane) in acidic or basic media) is preferred. And during the coating process, the silane polymer can bind the magnetic iron oxide particles via a covalent bond (Yamaura et al. 2004), and enable the particles to have a strong affinity toward silica coating.

1.3.4. Surface Modifications

To enhance remediation efficiency (Huang and Keller 2013, Wang et al. 2009), the modifications with functional groups onto magnetic-core composite nano/micro particles'

surface are usually needed. Typically, the surface modifications may involve the attachment of surfactants (Huang and Keller 2013, Wang et al. 2009), cyclic oligosaccharides (e.g. β-Cyclodextrin (Ji et al. 2009)), functional groups (e.g. amine(Chen et al. 2013), thiol (Suleiman et al. 2009), carboxylic (Carpio et al. 2012) and C_{18} (Sha et al. 2008)), chelators (e.g. EDTA (Koehler et al. 2009)) and etc..

1.3.5. Silica-coated Magnetic-core Composite Nano/Micro Particle Sorbents

Silica is the most popular option for coating in terms of the mechanical and chemical stability under various environment (e.g. acidic conditions), high mass exchange as well as the high thermal resistance (Chen et al. 2011b). Another advantage of a silica coating is that different functional groups can be attached onto the surface of silica-coated MPs by silanation using silane coupling agents (e.g. amine (Chen et al. 2013), thiol (Suleiman et al. 2009), carboxylic (Carpio et al. 2012) and C_{18} (Sha et al. 2008)) to enhance the selectivity and sorption capacity. A basic schematic diagram for the synthesis of silica-coated magnetic-core composite nano/micro particles modified with different functional groups is shown in Figure 3.

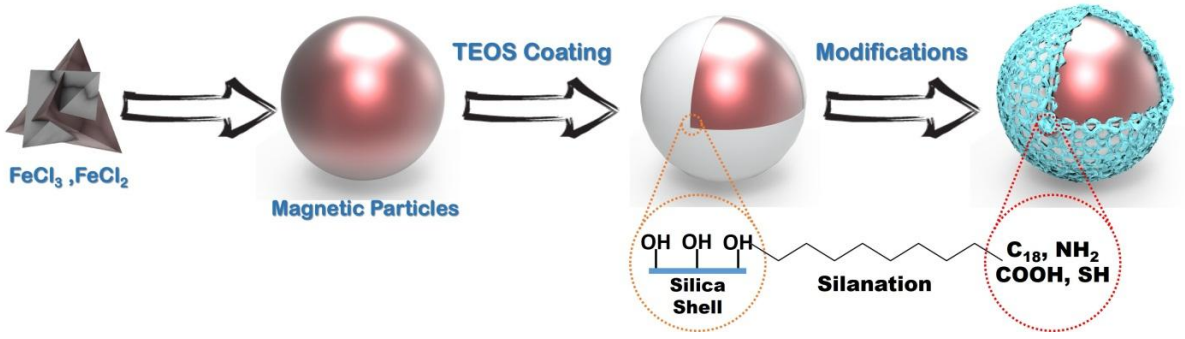

Figure 3. Schematic diagram of the synthesis of silica-coated magnetic-core composite nano/micro particles (MNPs) modified with different functional groups.

Recently magnetic permanently confined micelle arrays (Mag-PCMAs) were developed to treat hydrophobic organic contaminants (Wang et al. 2009). Mag-PCMAs are a novel composite material consisting of a mesoporous silica matrix, a co-deposited cationic surfactant micelle array, and a nano-scale magnetic silica iron oxide core. They have been applied to the removal of very hydrophobic compounds (Wang et al. 2009), pesticides (Clark and Keller 2012b), natural organic matter (Wang et al. 2011), oxyanions (Clark and Keller 2012a) and emerging organic contaminants (Huang and Keller 2013). Mag-PCMAs can be recovered and reused many times, reporting nearly all (>95%) of the sorbed hydrophobic organic compounds (HOCs) could be recovered, with easy regeneration of Mag-PCMAs in five cycles of regeneration and reuse (Wang et al. 2009). The relatively low cost (~$4/kg)(Huang and Keller 2013) make it a sustainable approach for water treatment. In addition, researchers also studied the different types of confined surfactants' (cationic and nonionic surfactant) performance on HOCs' remediation (Clark and Keller 2012b). The cationic surfactant (3-(trimethoxysily)propyl-octadecyldimethyl-ammonium chloride (TPODAC))-based Mag-PCMAs had better average recovery of the HOCs studied compared to the nonionic surfactant (Triton X-100)-based Mag-PCMAs, and was, in general, comparable to activated carbon.

1.3.6. Other Materials Coated Magnetic-core Composite Nano/Micro Particle Sorbents

Carbon-based nanomaterials (e.g. activated carbon (Oliveira et al. 2002), CNTs (Gupta et al. 2011), graphene/graphene oxide (Ai et al. 2011)) can exhibit high chemical and thermal stability and biocompatibility, and the possibility of surface modification and additional porosity make them a promising coating material for magnetic particles (Xie et al. 2014).

Besides silica and carbon-based materials, there are other inorganic substance (e.g. hydrous aluminum oxide (Zhao et al. 2010), manganese oxide (Kim et al. 2013), zirconium dioxide (Sarkar et al. 2010), titanium dioxide (Chang and Man 2011)) that have been used to coat magnetic-core composite nano/micro particles, to stabilize the magnetic particles under different environmental conditions (e.g. acidic solutions) and/or to provide high affinity binding sides to specific contaminants (Pommerenk and Schafran 2005).

Polymers can also be chemically or physically anchored on magnetic particles by covalent bonding or by electrostatic interaction (Xie et al. 2014). Other organic materials such as dimercaptosuccinic acid (DMSA) (Yantasee et al. 2007), EDTA (Warner et al. 2010), chitosan (Zhou et al. 2009), and humic acid (Liu et al. 2008), etc., can form coating shell or surface functional groups for magnetic-core composite nano/micro particles to be tailored to adsorb different pollutants.

1.4. Organization of the Dissertation

This dissertation focuses on developing novel magnetic nanoparticle sorbents to remediate contaminants in aquatic systems. The objective is to develop a fast, convenient, efficient, and sustainable approach to treating both organic and inorganic pollutants in aquatic systems, while also developing recommendations for using the sorbents to eliminate contaminants under various environmental conditions.

In Chapter 2, a regenerable magnetic ligand particle (Mag-Ligand) which includes a metal-binding organic ligand (EDTA) attached to an iron oxide nanoparticle was developed for rapid removal of Cd^{2+} and Pb^{2+} as well as other metals from contaminated water. The adsorption capacity of Cd^{2+} and Pb^{2+}onto Mag-Ligand was evaluated, the adsorption isotherms and kinetics was determined as well. In addition, the remediation performance of

Mag-Ligand for Cd^{2+} removal under various environmental conditions (e.g. range of pH and water hardness) as well as the regenerability and reusability were studied. This Chapter has been published in Water Research (Huang and Keller 2015).

Natural aquatic systems contain a wide variety of dissolved heavy metal ions at trace level (e.g. Cr, Pb, Cd, Hg, Zn and Cu). It's important to evaluate the remediation performance of Mag-Ligand for multiple metal ions in competitive sorption. In addition, though the primary application of Mag-Ligand is wastewater treatment, it could be extended to adsorb or collect ions of valuable elements, for instance, rare earth elements from process water, contaminated groundwater or mining leachate. Furthermore, to scale the use of Mag-Ligand for real world applications, a quantitative knowledge of the kinetics and thermodynamics of Mag-Ligand/metal ion interactions is needed to ascertain the minimum amount of Mag-Ligand particles needed to remove metal cations to a specified level in complex matrices with multiple metals. Thus, in Chapter 3, the adsorption capacity, isotherms and kinetics of nine different metal ions, including three rare earth elements, onto Mag-Ligand, at different initial metal ion concentrations in individual sorption was evaluated. Furthermore, the isothermal titration calorimeter technology was applied for the thermodynamic quantification of the interactions between nanoparticle sorbents and metal ions.

On the other side, the recognition that pharmaceuticals, personal care product chemicals, and endocrine disruptors, collectively known as EOCs can cause deleterious effects on humans and organisms has led to search for new approaches for removing them from contaminated waters (Petrovic et al. 2003). So far, only a few studies have investigated EOC removal. Based on Mag-PCMAs' great performance on the removal of hydrophobic compounds (Wang et al. 2009), pesticides (Clark and Keller 2012b), natural organic matter

(Wang et al. 2011) and oxyanions (Clark and Keller 2012a), extending Mag-PCMAs to treat EOCs in the aquatic systems would be a potential novel solution. In Chapter 4, study was investigated to determine the effectiveness of Mag-PCMAs to remove EOCs from water. For comparison, two legacy contaminants (e.g., ethylbenzene, 2-chlorophenol) were also evaluated. This Chapter has been published in ACS Sustainable Chemistry & Engineering (Huang and Keller 2013).

Current structure of Mag-PCMAs contains a magnetite core and a silica porous layer that permanently confines surfactant micelles within the mesopores. The surfactant, TPODAC, has a reactive endgroup $–Si(OCH_3)_3$ on its hydrophilic head, which permanently anchor on the silica framework through –Si–O–Si– covalent bonding. This feature can help to completely eliminate surfactant loss during its applications and thus allows for sorbent regeneration. However, the pore space within the mesoporous silica framework is almost completely filled by surfactant, leaving less space for contaminant adsorption, which limits the adsorption capacity. Thus, Chapter 5 investigated study on increasing the surface area and pore volume of Mag-PCMA by introducing swelling agent during the synthesis. The adsorption capacity of EOCs and PAHs onto modified Mag-PCMAs was evaluated, the adsorption isotherms and kinetics was determined as well.

Numerous wastewater is contaminated with both heavy metal ions and organic compounds, posing a major threat to public health and the environment. Thus, finding effective ways to treat these pollutants, especially for their simultaneous removal is considered as one of the most challenging areas of water treatment. Chapter 6 focuses on developing Mag-PCMAs with a silica porous layer that permanently confines nonionic surfactant micelles within the mesopores. The removal efficiency of Mag-PCMAs on Cd^{2+} and acenaphthene was evaluated under a range of initial ions concentrations and sorbent

dosage, as well as the competitive adsorption with both simultaneous presence across various environmental conditions.

Chapter 7 concludes this doctoral research, and proposes future works.

1.5. References

Ai, L.H., Zhang, C.Y. and Chen, Z.L. (2011) Removal of methylene blue from aqueous solution by a solvothermal-synthesized graphene/magnetite composite. Journal of Hazardous Materials 192(3), 1515-1524.

Alexandrescu, R., Morjan, I., Voicu, I., Dumitrache, F., Albu, L., Soare, I. and Prodan, G. (2005) Combining resonant/non-resonant processes: Nanometer-scale iron-based material preparation via CO< sub> 2</sub> laser pyrolysis. Applied surface science 248(1), 138-146.

Alikhani, M.-Y., Lee, S.-M., Yang, J.-K., Shirzad-Siboni, M., Peeri-Dogaheh, H., Khorasani, M.-S., Nooshak, M.-A. and Samarghandi, M.-R. (2012) Photocatalytic removal of Escherichia coli from aquatic solutions using synthesized ZnO nanoparticles: a kinetic study. Water Science & Technology 67(3), 557-563.

Allen, M., Willits, D., Young, M. and Douglas, T. (2003) Constrained synthesis of cobalt oxide nanomaterials in the 12-subunit protein cage from Listeria innocua. Inorganic chemistry 42(20), 6300-6305.

Bacsa, R.R., Laurent, C., Peigney, A., Bacsa, W.S., Vaugien, T. and Rousset, A. (2000) High specific surface area carbon nanotubes from catalytic chemical vapor deposition process. Chemical Physics Letters 323(5–6), 566-571.

Badawy, M.I., Ghaly, M.Y. and Gad-Allah, T.A. (2006) Advanced oxidation processes for the removal of organophosphorus pesticides from wastewater. Desalination 194(1–3), 166-175.

Baskan, M.B. and Pala, A. (2009) Determination of arsenic removal efficiency by ferric ions using response surface methodology. Journal of Hazardous Materials 166(2–3), 796-801.

Bennett, S.W. and Keller, A.A. (2011) Comparative photoactivity of CeO2, gamma-Fe2O3, TiO2 and ZnO in various aqueous systems. Applied Catalysis B-Environmental 102(3-4), 600-607.

Bhatnagar, A. and Sillanpää, M. (2011) A review of emerging adsorbents for nitrate removal from water. Chemical Engineering Journal 168(2), 493-504.

Bolong, N., Ismail, A.F., Salim, M.R. and Matsuura, T. (2009) A review of the effects of emerging contaminants in wastewater and options for their removal. Desalination 239(1-3), 229-246.

Borm, P.J., Robbins, D., Haubold, S., Kuhlbusch, T., Fissan, H., Donaldson, K., Schins, R., Stone, V., Kreyling, W. and Lademann, J. (2006) The potential risks of nanomaterials: a review carried out for ECETOC. Particle and fibre toxicology 3(1), 11.

Brady-Estévez, A.S., Kang, S. and Elimelech, M. (2008) A Single-Walled-Carbon-Nanotube Filter for Removal of Viral and Bacterial Pathogens. Small 4(4), 481-484.

Carlsson, C., Johansson, A.K., Alvan, G., Bergman, K. and Kuhler, T. (2006) Are pharmaceuticals potent environmental pollutants? Part I: Environmental risk assessments of selected active pharmaceutical ingredients. Science of the Total Environment 364(1-3), 67-87.

Carpio, A., Mercader-Trejo, F., Arce, L. and Valcarcel, M. (2012) Use of carboxylic group functionalized magnetic nanoparticles for the preconcentration of metals in juice samples prior to the determination by capillary electrophoresis. Electrophoresis 33(15), 2446-2453.

Chang, C.F. and Man, C.Y. (2011) Titania-Coated Magnetic Composites as Photocatalysts for Phthalate Photodegradation. Industrial & Engineering Chemistry Research 50(20), 11620-11627.

Chen, B., Hu, B., He, M., Huang, Q., Zhang, Y. and Zhang, X. (2013) Speciation of selenium in cells by HPLC-ICP-MS after (on-chip) magnetic solid phase extraction. Journal of Analytical Atomic Spectrometry 28(3), 334-343.

Chen, J., Liu, M., Zhang, L., Zhang, J. and Jin, L. (2003) Application of nano TiO2 towards polluted water treatment combined with electro-photochemical method. Water Res 37(16), 3815-3820.

Chen, J.W., Xiu, Z.M., Lowry, G.V. and Alvarez, P.J.J. (2011a) Effect of natural organic matter on toxicity and reactivity of nano-scale zero-valent iron. Water Research 45(5), 1995-2001.

Chen, L.G., Wang, T. and Tong, J. (2011b) Application of derivatized magnetic materials to the separation and the preconcentration of pollutants in water samples. Trac-Trends in Analytical Chemistry 30(7), 1095-1108.

Chen, Q., Wang, J. and Li, F. (2011c) Formation of Carbon Nanofibers from Supported Pt Catalysts through Catalytic Chemical Vapor Deposition from Acetylene. Industrial & Engineering Chemistry Research 50(15), 9034-9042.

Clark, K.K. and Keller, A.A. (2012a) Adsorption of perchlorate and other oxyanions onto magnetic permanently confined micelle arrays (Mag-PCMAs). Water research 46(3), 635-644.

Clark, K.K. and Keller, A.A. (2012b) Investigation of two magnetic permanently confined micelle array sorbents using nonionic and cationic surfactants for the removal of PAHs and pesticides from aqueous media. Water, Air, & Soil Pollution 223(7), 3647-3655.

Cornell, R.M. and Schwertmann, U. (2006) The iron oxides: structure, properties, reactions, occurrences and uses, John Wiley & Sons.

Crane, R.A. and Scott, T.B. (2012) Nanoscale zero-valent iron: Future prospects for an emerging water treatment technology. Journal of Hazardous Materials 211–212(0), 112-125.

Dai, Z., Meiser, F. and Möhwald, H. (2005) Nanoengineering of iron oxide and iron oxide/silica hollow spheres by sequential layering combined with a sol–gel process. Journal of colloid and interface science 288(1), 298-300.

Dankovich, T.A. and Gray, D.G. (2011) Bactericidal Paper Impregnated with Silver Nanoparticles for Point-of-Use Water Treatment. Environmental Science & Technology 45(5), 1992-1998.

Deng, Y., Wang, L., Yang, W., Fu, S. and Elaıssari, A. (2003) Preparation of magnetic polymeric particles via inverse microemulsion polymerization process. Journal of magnetism and magnetic materials 257(1), 69-78.

Dhakras, P.A. (2011) Nanotechnology applications in water purification and waste water treatment: A review, pp. 285-291.

Ditsch, A., Laibinis, P.E., Wang, D.I.C. and Hatton, T.A. (2005) Controlled clustering and enhanced stability of polymer-coated magnetic nanoparticles. Langmuir 21(13), 6006-6018.

Duraes, L., Costa, B., Vasques, J., Campos, J. and Portugal, A. (2005) Phase investigation of as-prepared iron oxide/hydroxide produced by sol–gel synthesis. Materials Letters 59(7), 859-863.

Ehdaie, B., Krause, C. and Smith, J.A. (2014) Porous Ceramic Tablet Embedded with Silver Nanopatches for Low-Cost Point-of-Use Water Purification. Environmental Science & Technology 48(23), 13901-13908.

El-Kemary, M., El-Shamy, H. and El-Mehasseb, I. (2010) Photocatalytic degradation of ciprofloxacin drug in water using ZnO nanoparticles. Journal of Luminescence 130(12), 2327-2331.

Faraji, M., Yamini, Y. and Rezaee, M. (2010a) Extraction of trace amounts of mercury with sodium dodecyle sulphate-coated magnetite nanoparticles and its determination by flow injection inductively coupled plasma-optical emission spectrometry. Talanta 81(3), 831-836.

Faraji, M., Yamini, Y., Saleh, A., Rezaee, M., Ghambarian, M. and Hassani, R. (2010b) A nanoparticle-based solid-phase extraction procedure followed by flow injection inductively coupled plasma-optical emission spectrometry to determine some heavy metal ions in water samples. Analytica Chimica Acta 659(1-2), 172-177.

Fouad, O., Ismail, A., Zaki, Z. and Mohamed, R. (2006) Zinc oxide thin films prepared by thermal evaporation deposition and its photocatalytic activity. Applied Catalysis B: Environmental 62(1), 144-149.

Gai, K., Shi, B., Yan, X. and Wang, D. (2011) Effect of Dispersion on Adsorption of Atrazine by Aqueous Suspensions of Fullerenes. Environmental Science & Technology 45(14), 5959-5965.

Geng, F., Zhao, Z., Cong, H., Geng, J. and Cheng, H.-M. (2006) An environment-friendly microemulsion approach to α-FeOOH nanorods at room temperature. Materials research bulletin 41(12), 2238-2243.

Georgekutty, R., Seery, M.K. and Pillai, S.C. (2008) A highly efficient Ag-ZnO photocatalyst: Synthesis, properties, and mechanism. Journal of Physical Chemistry C 112(35), 13563-13570.

Giakisikli, G. and Anthemidis, A.N. (2013) Magnetic materials as sorbents for metal/metalloid preconcentration and/or separation. A review. Analytica Chimica Acta 789, 1-16.

Gopalakrishnan, K., Birgisson, B., Taylor, P. and Attoh-Okine, N.O. (2011) Nanotechnology in Civil Infrastructure: A Paradigm Shift, Springer.

Grey, D., Garrick, D., Blackmore, D., Kelman, J., Muller, M. and Sadoff, C. (2013) Water security in one blue planet: twenty-first century policy challenges for science. Philosophical Transactions of the Royal Society A: Mathematical, Physical and Engineering Sciences 371(2002), 20120406.

Gupta, V. and Saleh, T. (2013) Sorption of pollutants by porous carbon, carbon nanotubes and fullerene- An overview. Environmental Science and Pollution Research 20(5), 2828-2843.

Gupta, V.K., Agarwal, S. and Saleh, T.A. (2011) Chromium removal by combining the magnetic properties of iron oxide with adsorption properties of carbon nanotubes. Water Research 45(6), 2207-2212.

Han, Y., Xu, Z. and Gao, C. (2013) Ultrathin Graphene Nanofiltration Membrane for Water Purification. Advanced Functional Materials 23(29), 3693-3700.

Houtman, C.J. (2010) Emerging contaminants in surface waters and their relevance for the production of drinking water in Europe. Journal of Integrative Environmental Sciences 7(4), 271-295.

Huang, Y. and Keller, A.A. (2015) EDTA functionalized magnetic nanoparticle sorbents for cadmium and lead contaminated water treatment. Water Research 80, 159-168.

Huang, Y.F., Li, Y., Jiang, Y. and Yan, X.P. (2010) Magnetic immobilization of amine-functionalized magnetite microspheres in a knotted reactor for on-line solid-phase extraction coupled with ICP-MS for speciation analysis of trace chromium. Journal of Analytical Atomic Spectrometry 25(9), 1467-1474.

Huang, Y.X. and Keller, A.A. (2013) Magnetic Nanoparticle Adsorbents for Emerging Organic Contaminants. Acs Sustainable Chemistry & Engineering 1(7), 731-736.

Huber, M.M., GÖbel, A., Joss, A., Hermann, N., LÖffler, D., McArdell, C.S., Ried, A., Siegrist, H., Ternes, T.A. and von Gunten, U. (2005) Oxidation of Pharmaceuticals during

Ozonation of Municipal Wastewater Effluents: A Pilot Study. Environmental Science & Technology 39(11), 4290-4299.

Hyeon, T., Lee, S.S., Park, J., Chung, Y. and Na, H.B. (2001) Synthesis of highly crystalline and monodisperse maghemite nanocrystallites without a size-selection process. Journal of the American Chemical Society 123(51), 12798-12801.

Igwe, J.C. and Abia, A.A. (2007) Equilibrium sorption isotherm studies of Cd(II), Pb(II) and Zn(II) ions detoxification from waste water using unmodified and EDTA-modified maize husk. Electronic Journal of Biotechnology 10(4), 536-548.

Iijima, S. (1991) Helical microtubules of graphitic carbon. Nature 354(6348), 56-58.

Ikehata, K., Gamal El-Din, M. and Snyder, S.A. (2008) Ozonation and advanced oxidation treatment of emerging organic pollutants in water and wastewater. Ozone-Science & Engineering 30(1), 21-26.

Inouye, K., Endo, R., Otsuka, Y., Miyashiro, K., Kaneko, K. and Ishikawa, T. (1982) Oxygenation of ferrous ions in reversed micelle and reversed microemulsion. The Journal of Physical Chemistry 86(8), 1465-1469.

Ji, Y.S., Liu, X.Y., Guan, M., Zha, C.D., Huang, H.Y., Zhang, H.X. and Wang, C.M. (2009) Preparation of functionalized magnetic nanoparticulate sorbents for rapid extraction of biphenolic pollutants from environmental samples. Journal of Separation Science 32(12), 2139-2145.

Jiang, H.M., Yan, Z.P., Zhao, Y., Hu, X. and Lian, H.Z. (2012) Zincon-immobilized silica-coated magnetic Fe3O4 nanoparticles for solid-phase extraction and determination of trace lead in natural and drinking waters by graphite furnace atomic absorption spectrometry. Talanta 94, 251-256.

Jolivet, J.-P., Chanéac, C. and Tronc, E. (2004) Iron oxide chemistry. From molecular clusters to extended solid networks. Chemical Communications (5), 481-483.

Kadirvelu, K., Thamaraiselvi, K. and Namasivayam, C. (2001) Removal of heavy metals from industrial wastewaters by adsorption onto activated carbon prepared from an agricultural solid waste. Bioresource Technology 76(1), 63-65.

Karatapanis, A.E., Fiamegos, Y. and Stalikas, C.D. (2011) Silica-modified magnetic nanoparticles functionalized with cetylpyridinium bromide for the preconcentration of metals after complexation with 8-hydroxyquinoline. Talanta 84(3), 834-839.

Karn, B., Kuiken, T. and Otto, M. (2009) Nanotechnology and in Situ Remediation: A Review of the Benefits and Potential Risks. Environmental Health Perspectives 117(12), 1823-1831.

Khan, S.J. and Ongerth, J.E. (2004) Modelling of pharmaceutical residues in Australian sewage by quantities of use and fugacity calculations. Chemosphere 54(3), 355-367.

Khin, M.M., Nair, A.S., Babu, V.J., Murugan, R. and Ramakrishna, S. (2012) A review on nanomaterials for environmental remediation. Energy & Environmental Science 5(8), 8075-8109.

Kim, E.J., Lee, C.S., Chang, Y.Y. and Chang, Y.S. (2013) Hierarchically Structured Manganese Oxide-Coated Magnetic Nanocomposites for the Efficient Removal of Heavy Metal Ions from Aqueous Systems. Acs Applied Materials & Interfaces 5(19), 9628-9634.

Kimata, M., Nakagawa, D. and Hasegawa, M. (2003) Preparation of monodisperse magnetic particles by hydrolysis of iron alkoxide. Powder technology 132(2), 112-118.

Koehler, F.M., Rossier, M., Waelle, M., Athanassiou, E.K., Limbach, L.K., Grass, R.N., Gunther, D. and Stark, W.J. (2009) Magnetic EDTA: coupling heavy metal chelators to metal nanomagnets for rapid removal of cadmium, lead and copper from contaminated water. Chemical Communications (32), 4862-4864.

Koltypin, Y., Katabi, G., Cao, X., Prozorov, R. and Gedanken, A. (1996) Sonochemical preparation of amorphous nickel. Journal of non-crystalline solids 201(1), 159-162.

Kurniawan, T.A., Chan, G.Y.S., Lo, W.H. and Babel, S. (2006a) Comparisons of low-cost adsorbents for treating wastewaters laden with heavy metals. Science of the Total Environment 366(2-3), 409-426.

Kurniawan, T.A., Chan, G.Y.S., Lo, W.H. and Babel, S. (2006b) Physico-chemical treatment techniques for wastewater laden with heavy metals. Chemical Engineering Journal 118(1-2), 83-98.

Lacinova, L., Kvapil, P. and Cernik, M. (2012) A field comparison of two reductive dechlorination (zero-valent iron and lactate) methods. Environ Technol 33(7-9), 741-749.

Lai, H.T., Hou, J.H., Su, C.I. and Chen, C.L. (2009) Effects of chloramphenicol, florfenicol, and thiamphenicol on growth of algae Chlorella pyrenoidosa, Isochrysis galbana, and Tetraselmis chui. Ecotoxicology and Environmental Safety 72(2), 329-334.

Lapworth, D.J., Baran, N., Stuart, M.E. and Ward, R.S. (2012) Emerging organic contaminants in groundwater: A review of sources, fate and occurrence. Environmental Pollution 163, 287-303.

Laurent, S., Forge, D., Port, M., Roch, A., Robic, C., Elst, L.V. and Muller, R.N. (2010) Magnetic Iron Oxide Nanoparticles: Synthesis, Stabilization, Vectorization, Physicochemical Characterizations, and Biological Applications (vol 108, pg 2064, 2008). Chemical Reviews 110(4), 2574-2574.

Levin, R., Epstein, P., Ford, T., Harrington, W., Olson, E. and Reichard, E. (2002) US drinking water challenges in the twenty-first century. Environmental Health Perspectives 110, 43-52.

Li, Q., Mahendra, S., Lyon, D.Y., Brunet, L., Liga, M.V., Li, D. and Alvarez, P.J.J. (2008) Antimicrobial nanomaterials for water disinfection and microbial control: Potential applications and implications. Water Res 42(18), 4591-4602.

Li, Q.L., Lam, M.H.W., Wu, R.S.S. and Jiang, B.W. (2010a) Rapid magnetic-mediated solid-phase extraction and pre-concentration of selected endocrine disrupting chemicals in natural waters by poly(divinylbenzene-co-methacrylic acid) coated Fe3O4 core-shell magnetite microspheres for their liquid chromatography-tandem mass spectrometry determination. Journal of Chromatography A 1217(8), 1219-1226.

Li, Z.Q., Greden, K., Alvarez, P.J.J., Gregory, K.B. and Lowry, G.V. (2010b) Adsorbed Polymer and NOM Limits Adhesion and Toxicity of Nano Scale Zerovalent Iron to E. coli. Environmental Science & Technology 44(9), 3462-3467.

Liu, J.F., Zhao, Z.S. and Jiang, G.B. (2008) Coating Fe3O4 magnetic nanoparticles with humic acid for high efficient removal of heavy metals in water. Environmental Science & Technology 42(18), 6949-6954.

Liu, M.C., Chen, C.L., Hu, J., Wu, X.L. and Wang, X.K. (2011) Synthesis of Magnetite/Graphene Oxide Composite and Application for Cobalt(II) Removal. Journal of Physical Chemistry C 115(51), 25234-25240.

Lu, S.Y., Wang, Q.L., Wu, D., Li, X.D. and Yan, J.H. (2013) Photocatalytic decomposition of hexachlorobenzene on nano-titanium dioxide filmsExperimental study and mechanistic considerations. Environmental Progress & Sustainable Energy 32(3), 458-464.

Lyssimachou, A. and Arukwe, A. (2007) Alteration of brain and interrenal StAR protein, P450scc, and Cyp11 beta mRNA levels in Atlantic salmon after nominal waterborne exposure to the synthetic pharmaceutical estrogen ethynylestradiol. Journal of Toxicology and Environmental Health-Part a-Current Issues 70(7), 606-613.

Mellor, J.E., Kallman, E., Oyanedel-Craver, V. and Smith, J.A. (2015) Comparison of Three Household Water Treatment Technologies in San Mateo Ixtatan, Guatemala. Journal of Environmental Engineering 141(5).

Mittal, A., Malviya, A., Kaur, D., Mittal, J. and Kurup, L. (2007) Studies on the adsorption kinetics and isotherms for the removal and recovery of Methyl Orange from wastewaters using waste materials. Journal of Hazardous Materials 148(1–2), 229-240.

Morales, M., Bomati-Miguel, O., Pérez de Alejo, R., Ruiz-Cabello, J., Veintemillas-Verdaguer, S. and O'Grady, K. (2003) Contrast agents for MRI based on iron oxide nanoparticles prepared by laser pyrolysis. Journal of magnetism and magnetic materials 266(1), 102-109.

Mostafavi, S.T., Mehrnia, M.R. and Rashidi, A.M. (2009) Preparation of nanofilter from carbon nanotubes for application in virus removal from water. Desalination 238(1–3), 271-280.

Mueller, N., Braun, J., Bruns, J., Cernik, M., Rissing, P., Rickerby, D. and Nowack, B. (2012) Application of nanoscale zero valent iron (NZVI) for groundwater remediation in Europe. Environmental Science and Pollution Research 19(2), 550-558.

Musico, Y.L.F., Santos, C.M., Dalida, M.L.P. and Rodrigues, D.F. (2014) Surface Modification of Membrane Filters Using Graphene and Graphene Oxide-Based Nanomaterials for Bacterial Inactivation and Removal. ACS Sustainable Chemistry & Engineering 2(7), 1559-1565.

Ni, Z.-M., Xia, S.-J., Wang, L.-G., Xing, F.-F. and Pan, G.-X. (2007) Treatment of methyl orange by calcined layered double hydroxides in aqueous solution: Adsorption property and kinetic studies. Journal of Colloid and Interface Science 316(2), 284-291.

Oliveira, L.C.A., Rios, R.V.R.A., Fabris, J.D., Garg, V., Sapag, K. and Lago, R.M. (2002) Activated carbon/iron oxide magnetic composites for the adsorption of contaminants in water. Carbon 40(12), 2177-2183.

Onesios, K., Yu, J. and Bouwer, E. (2008) Biodegradation and removal of pharmaceuticals and personal care products in treatment systems: a review - Springer. Biodegradation.

Pal, A., Gin, K.Y.H., Lin, A.Y.C. and Reinhard, M. (2010) Impacts of emerging organic contaminants on freshwater resources: Review of recent occurrences, sources, fate and effects. Science of the Total Environment 408(24), 6062-6069.

Pascal, C., Pascal, J., Favier, F., Elidrissi Moubtassim, M. and Payen, C. (1999) Electrochemical synthesis for the control of γ-Fe2O3 nanoparticle size. Morphology, microstructure, and magnetic behavior. Chemistry of materials 11(1), 141-147.

Petrov, P.D. and Georgiev, G.L. (2012) Fabrication of super-macroporous nanocomposites by deposition of carbon nanotubes onto polymer cryogels. European Polymer Journal 48(8), 1366-1373.

Petrovic, M., Gonzalez, S. and Barcelo, D. (2003) Analysis and removal of emerging contaminants in wastewater and drinking water. Trac-Trends in Analytical Chemistry 22(10), 685-696.

Phenrat, T., Song, J.E., Cisneros, C.M., Schoenfelder, D.P., Tilton, R.D. and Lowry, G.V. (2010) Estimating Attachment of Nano- and Submicrometer-particles Coated with Organic Macromolecules in Porous Media: Development of an Empirical Model. Environmental Science & Technology 44(12), 4531-4538.

Pomati, F., Castiglioni, S., Zuccato, E., Fanelli, R., Vigetti, D., Rossetti, C. and Calamari, D. (2006) Effects of a complex mixture of therapeutic drugs at environmental levels on human embryonic cells. Environmental Science & Technology 40(7), 2442-2447.

Pommerenk, P. and Schafran, G.C. (2005) Adsorption of inorganic and organic ligands onto hydrous aluminum oxide: Evaluation of surface charge and the impacts on particle and

NOM removal during water treatment. Environmental Science & Technology 39(17), 6429-6434.

Pradeep, T. and Anshup (2009) Noble metal nanoparticles for water purification: A critical review. Thin Solid Films 517(24), 6441-6478.

Qu, X., Alvarez, P.J. and Li, Q. (2013) Applications of nanotechnology in water and wastewater treatment. water research 47(12), 3931-3946.

Rastkari, N. and Ahmadkhaniha, R. (2013) Magnetic solid-phase extraction based on magnetic multi-walled carbon nanotubes for the determination of phthalate monoesters in urine samples. Journal of Chromatography A 1286, 22-28.

Reetz, M., Helbig, W., Quasick, S. and Furster, A. (1996) ActiVe Metals, Preparation, Characterization, Applications, Furster, A., Ed.

Ren, D., Colosi, L.M. and Smith, J.A. (2013) Evaluating the Sustainability of Ceramic Filters for Point-of-Use Drinking Water Treatment. Environmental Science & Technology 47(19), 11206-11213.

Rice, G., Tang, L., Stedman, K., Roberto, F., Spuhler, J., Gillitzer, E., Johnson, J.E., Douglas, T. and Young, M. (2004) The structure of a thermophilic archaeal virus shows a double-stranded DNA viral capsid type that spans all domains of life. Proceedings of the National Academy of Sciences of the United States of America 101(20), 7716-7720.

Rosal, R., Rodríguez, A., Perdigón-Melón, J.A., Petre, A., García-Calvo, E., Gómez, M.J., Agüera, A. and Fernández-Alba, A.R. (2010) Occurrence of emerging pollutants in urban wastewater and their removal through biological treatment followed by ozonation. Water Res 44(2), 578-588.

Sabitha, M., Jose, S., Raj, S. and Sumod, U. (2012) Nanotechnology in cosmetics: Opportunities and challenges. Journal of Pharmacy And Bioallied Sciences 4(3), 186-193.

Salazar-Alvarez, G., Muhammed, M. and Zagorodni, A.A. (2006) Novel flow injection synthesis of iron oxide nanoparticles with narrow size distribution. Chemical engineering science 61(14), 4625-4633.

Salgado, R., Marques, R., Noronha, J., Carvalho, G., Oehmen, A. and Reis, M. (2011) Assessing the removal of pharmaceuticals and personal care products in a full-scale activated sludge plant - Springer.

Sarkar, A., Biswas, S.K. and Pramanik, P. (2010) Design of a new nanostructure comprising mesoporous ZrO 2 shell and magnetite core (Fe 3 O 4@ mZrO 2) and study of its phosphate ion separation efficiency. Journal of Materials Chemistry 20(21), 4417-4424.

Schwarzer, H.-C. and Peukert, W. (2004) Tailoring particle size through nanoparticle precipitation. Chemical Engineering Communications 191(4), 580-606.

Serrano, E., Rus, G. and García-Martínez, J. (2009) Nanotechnology for sustainable energy. Renewable and Sustainable Energy Reviews 13(9), 2373-2384.

Sha, Y., Deng, C. and Liu, B. (2008) Development of C< sub> 18</sub>-functionalized magnetic silica nanoparticles as sample preparation technique for the determination of ergosterol in cigarettes by microwave-assisted derivatization and gas chromatography/mass spectrometry. Journal of Chromatography A 1198, 27-33.

Shafi, K.V., Koltypin, Y., Gedanken, A., Prozorov, R., Balogh, J., Lendvai, J. and Felner, I. (1997) Sonochemical preparation of nanosized amorphous NiFe2O4 particles. The Journal of Physical Chemistry B 101(33), 6409-6414.

Solans, C., Izquierdo, P., Nolla, J., Azemar, N. and Garcia-Celma, M. (2005) Nano-emulsions. Current Opinion in Colloid & Interface Science 10(3), 102-110.

Song, L., Toth, G., Vajtai, R., Endo, M. and Ajayan, P.M. (2012) Fabrication and characterization of single-walled carbon nanotube fiber for electronics applications. Carbon 50(15), 5521-5524.

Song, S., Lopez-Valdivieso, A., Hernandez-Campos, D.J., Peng, C., Monroy-Fernandez, M.G. and Razo-Soto, I. (2006) Arsenic removal from high-arsenic water by enhanced coagulation with ferric ions and coarse calcite. Water Res 40(2), 364-372.

Soni, S.S., Henderson, M.J., Bardeau, J.F. and Gibaud, A. (2008) Visible-light photocatalysis in titania-based mesoporous thin films. Advanced Materials 20(8), 1493-+.

Stöber, W., Fink, A. and Bohn, E. (1968) Controlled growth of monodisperse silica spheres in the micron size range. Journal of colloid and interface science 26(1), 62-69.

Stoimenov, P.K., Klinger, R.L., Marchin, G.L. and Klabunde, K.J. (2002) Metal Oxide Nanoparticles as Bactericidal Agents. Langmuir 18(17), 6679-6686.

Sugimoto, T. (2003) Formation of Monodispersed Nano‐and Micro‐Particles Controlled in Size, Shape, and Internal Structure. Chemical engineering & technology 26(3), 313-321.

Suleiman, J.S., Hu, B., Peng, H.Y. and Huang, C.Z. (2009) Separation/preconcentration of trace amounts of Cr, Cu and Pb in environmental samples by magnetic solid-phase extraction with Bismuthiol-II-immobilized magnetic nanoparticles and their determination by ICP-OES. Talanta 77(5), 1579-1583.

Sun, S., Zeng, H., Robinson, D.B., Raoux, S., Rice, P.M., Wang, S.X. and Li, G. (2004) Monodisperse MFe2O4 (M= Fe, Co, Mn) nanoparticles. Journal of the American Chemical Society 126(1), 273-279.

Tavallali, H. (2011) Alumina-coated magnetite nanoparticles for solid phase extraction of Cd in water samples. Chem Tech 3, 1647-1651.

Thio, B.J.R., Clark, K.K. and Keller, A.A. (2011) Magnetic pollen grains as sorbents for facile removal of organic pollutants in aqueous media. Journal of Hazardous Materials 194, 53-61.

Tofighy, M.A. and Mohammadi, T. (2011) Adsorption of divalent heavy metal ions from water using carbon nanotube sheets. Journal of Hazardous Materials 185(1), 140-147.

Tuzen, M., Saygi, K.O., Usta, C. and Soylak, M. (2008) Pseudomonas aeruginosa immobilized multiwalled carbon nanotubes as biosorbent for heavy metal ions. Bioresource Technology 99(6), 1563-1570.

Wang, H., Keller, A.A. and Clark, K.K. (2011) Natural organic matter removal by adsorption onto magnetic permanently confined micelle arrays. Journal of hazardous materials 194, 156-161.

Wang, P., Shi, Q.H., Shi, Y.F., Clark, K.K., Stucky, G.D. and Keller, A.A. (2009) Magnetic Permanently Confined Micelle Arrays for Treating Hydrophobic Organic Compound Contamination. Journal of the American Chemical Society 131(1), 182-188.

Wang, Q. and Lemley, A.T. (2002) Oxidation of diazinon by anodic Fenton treatment. Water Res 36(13), 3237-3244.

Wang, S., Sun, H., Ang, H.M. and Tadé, M.O. (2013) Adsorptive remediation of environmental pollutants using novel graphene-based nanomaterials. Chemical Engineering Journal 226, 336-347.

Warner, C.L., Addleman, R.S., Cinson, A.D., Droubay, T.C., Engelhard, M.H., Nash, M.A., Yantasee, W. and Warner, M.G. (2010) High-Performance, Superparamagnetic, Nanoparticle-Based Heavy Metal Sorbents for Removal of Contaminants from Natural Waters. Chemsuschem 3(6), 749-757.

WHO (2012) Pharmaceuticals in drinking-water, World Health Organization.

WHO (2013) Progress on Sanitation and Drinking-Water - 2013 Update, p. 40.

Williams, C.J., Aderhold, D. and Edyvean, R.G.J. (1998) Comparison between biosorbents for the removal of metal ions from aqueous solutions. Water research 32(1), 216-224.

Xie, L.J., Jiang, R.F., Zhu, F., Liu, H. and Ouyang, G.F. (2014) Application of functionalized magnetic nanoparticles in sample preparation. Analytical and Bioanalytical Chemistry 406(2), 377-399.

Xu, P., Zeng, G.M., Huang, D.L., Feng, C.L., Hu, S., Zhao, M.H., Lai, C., Wei, Z., Huang, C., Xie, G.X. and Liu, Z.F. (2012) Use of iron oxide nanomaterials in wastewater treatment: A review. Science of The Total Environment 424, 1-10.

Yamaura, M., Camilo, R.L., Sampaio, L.C., Macedo, M.A., Nakamura, M. and Toma, H.E. (2004) Preparation and characterization of (3-aminopropyl) triethoxysilane-coated magnetite nanoparticles. Journal of Magnetism and Magnetic Materials 279(2-3), 210-217.

Yang, J., Li, D., Wang, X., Yang, X.J. and Lu, L.D. (2002) Rapid synthesis of nanocrystalline TiO2/SnO2 binary oxides and their photoinduced decomposition of methyl orange. Journal of Solid State Chemistry 165(1), 193-198.

Yang, X.H., Fu, H.T., Wong, K., Jiang, X.C. and Yu, A.B. (2013) Hybrid Ag@ TiO2 core-shell nanostructures with highly enhanced photocatalytic performance. Nanotechnology 24(41).

Yantasee, W., Warner, C.L., Sangvanich, T., Addleman, R.S., Carter, T.G., Wiacek, R.J., Fryxell, G.E., Timchalk, C. and Warner, M.G. (2007) Removal of heavy metals from aqueous systems with thiol functionalized superparamagnetic nanoparticles. Environmental Science & Technology 41(14), 5114-5119.

Zhang, S., Zeng, M., Li, J., Li, J., Xu, J. and Wang, X.-K. (2014) Porous magnetic carbon sheets from biomass as super adsorbent for fast removal of organic pollutants from aqueous solution. Journal of Materials Chemistry A.

Zhao, L., Peralta-Videa, J.R., Varela-Ramirez, A., Castillo-Michel, H., Li, C., Zhang, J., Aguilera, R.J., Keller, A.A. and Gardea-Torresdey, J.L. (2012) Effect of surface coating and organic matter on the uptake of CeO2 NPs by corn plants grown in soil: Insight into the uptake mechanism. J. Hazard. Mater. DOI: .

Zhao, X.L., Shi, Y.L., Ca, Y.Q. and Mou, S.F. (2008) Cetyltrimethylammonium bromide-coated magnetic nanoparticles for the preconcentration of phenolic compounds from environmental water samples. Environmental Science & Technology 42(4), 1201-1206.

Zhao, X.L., Wang, J.M., Wu, F.C., Wang, T., Cai, Y.Q., Shi, Y.L. and Jiang, G.B. (2010) Removal of fluoride from aqueous media by Fe3O4@Al(OH)(3) magnetic nanoparticles. Journal of Hazardous Materials 173(1-3), 102-109.

Zhou, Y.-T., Nie, H.-L., Branford-White, C., He, Z.-Y. and Zhu, L.-M. (2009) Removal of Cu< sup> 2+</sup> from aqueous solution by chitosan-coated magnetic nanoparticles modified with< i> α</i>-ketoglutaric acid. Journal of colloid and interface science 330(1), 29-37.

Zhou, Z.-Y., Tian, N., Li, J.-T., Broadwell, I. and Sun, S.-G. (2011) Nanomaterials of high surface energy with exceptional properties in catalysis and energy storage. Chemical Society Reviews 40(7), 4167-4185.

Zhu, Y., Murali, S., Cai, W., Li, X., Suk, J.W., Potts, J.R. and Ruoff, R.S. (2010) Graphene and Graphene Oxide: Synthesis, Properties, and Applications. Advanced Materials 22(35), 3906-3924.

Zodrow, K., Brunet, L., Mahendra, S., Li, D., Zhang, A., Li, Q. and Alvarez, P.J.J. (2009) Polysulfone ultrafiltration membranes impregnated with silver nanoparticles show improved biofouling resistance and virus removal. Water Res 43(3), 715-723.

Chapter 2. EDTA Functionalized Magnetic Nanoparticle Sorbents for Cadmium and Lead Contaminated Water Treatment[1]

2.1. Introduction

Heavy metal ions such as cadmium (Cd) and lead (Pb) are considered as serious threat to the environment and human health due to their high toxicity and non-degradable characteristics (Kah et al. 2012). Cd can be released into the environment both from natural sources (e.g. volcanic eruptions and forest fires) (Bandara et al. 2008) and anthropogenic activities (e.g. non-ferrous metals production (Vromman et al. 2008), electroplating (Islamoglu et al. 2006), manufacturing of Ni-Cd batteries and pigments (Fthenakis 2004), application of phosphate fertilizers (Mortvedt and Osborn 1982), and burning of fossil fuels (Vouk and Piver 1983)). Pb also is emitted from natural sources and anthropogenic activities (e.g. lead-based batteries, residual lead paint, lead-based fuel additives) (Reimann and de Caritat 2005). They are bioaccumulated (Tête et al. 2014), so even at trace levels they can concentrate in living organisms acting as carcinogens. For example cadmium may cause damage to lungs (Boudreau et al. 1988), kidneys (Jamall et al. 1989), livers (Koyuturk et al. 2007), and reproductive organs (Alvarez et al. 2004, Bonda et al. 2004). Recently, studies have been reported that grains such as rice and soybean have been contaminated by cadmium (Su et al. 2014), and this has become an emerging food chain supply threat, especially in Asian countries (Shute and Macfie 2006). On the other hand, lead contamination could occur when water flows through lead-containing pipes (Xie and Giammar 2011), which also would

[1] This chapter was published in Water Research: Huang, Y., A. A. Keller. (2015) EDTA Functionalized Magnetic Nanoparticle Sorbents for Cadmium and Lead Contaminated Water Treatment. Water Research, doi: 10.1016/j.watres.2015.05.011.

enter the food chain through drinking water. Therefore, to develop effective and rapid cadmium and lead remediation technique is of great importance.

Chelating agents, for instance ethylenediaminetetraacetic acid (EDTA), are widely used as extractive reagents for heavy metals decontamination (Martinez et al. 2006, Ngah and Hanafiah 2008). Due to its strong metal chelating ability and low cost, EDTA has been used to functionalize a variety of materials from inorganic oxides to biomass, including silica gel (Repo et al. 2009), chitosan (Repo et al. 2010), polyamine composites (Hughes and Rosenherg 2007), polystyrene (Wang et al. 2010), mercerized cellulose and sugarcane bagasse (Júnior et al. 2009), wood sawdust and sugarcane bagasse (Pereira et al. 2010), rice husk (Xiong et al. 2010), and baker's yeast biomass (Yu et al. 2008). However, a comparison of results shows that the adsorption efficiency was significantly influenced by the type of supporting material (Repo et al. 2011), and post-treatment separation needs to be taken into consideration.

In the past few years, nano-scaled magnetic particles have been proposed as sorbents for environmental decontamination (Huang and Keller 2013, Su et al. 2015), and due to their superparamagnetic nature as well as their unique physical and chemical properties such as high dispersibility, relatively large surface area, and high ratio of surface-to-volume, they exhibit a high adsorption capacity (Bagheri et al. 2012). With an appropriate coating, which can be either inorganic (e.g., silica or alumina) (Jiang et al. 2012, Karatapanis et al. 2011) or organic (e.g., modified with polymer or surfactant, etc.) (Faraji et al. 2010, Huang et al. 2010), these magnetic core hybrid particles can be applied to remove heavy metal ions (Ge et al. 2012), hydrophobic compounds (Wang et al. 2008), pesticides (Clark and Keller 2012b), natural organic matter (Wang et al. 2011), oxyanions (Clark and Keller 2012a) and emerging organic contaminants (Huang and Keller 2013).

Recent studies investigated EDTA-modified magnetic nanoparticles for metals remediation. Zhang et al. (2011) reported a route for EDTA immobilization on the surface of amine-terminated Fe_3O_4 nanoparticles ($Fe_3O_4 - NH_2$/PEI-EDTA) for treatment of Cu^{2+}, Cd^{2+}, and Pb^{2+} from aqueous solutions. The results suggested that solution pH plays an important role on removal efficiency, with 98.8% Pb^{2+} removal at pH 5, but decreasing removal at higher pH. Dupont et al. (2014) decorated magnetic (Fe_3O_4) nanoparticles with N-[(3-trimethoxysilyl)propyl]ethylenediamine triacetic acid (TMS-EDTA) for rare earth elements adsorption, and found increasing removal of Gd^{3+} as solution pH increased. However, none of the previous researchers considered the potential competitive adsorption between heavy metal ions and Ca^{2+} or Mg^{2+}, which usually are present at much higher concentration than these trace heavy metal ions.

To decrease the impact of solution pH and water hardness (i.e. Ca^{2+} or Mg^{2+}), we developed a nanomaterial (Mag-Ligand) with a magnetic core covered by an organic ligand (EDTA) that can serve as an effective sorbent for metal ions from realistic aquatic systems. The initial application under consideration is the treatment of industrial wastewater, but Mag-Ligand could be to remove metal ions from contaminated groundwater or mining leachate. We evaluated the adsorption capacity of Cd^{2+} and Pb^{2+} onto Mag-Ligand at different initial Cd^{2+} and Pb^{2+} concentrations as well as determined the adsorption isotherms and kinetics. In addition, the remediation performance of Mag-Ligand for Cd^{2+} removal under various environmental conditions (e.g. range of pH and water hardness) as well as the regenerability and reusability were studied. The results demonstrated that Mag-Ligand is a rapid, effective, regenerable and more sustainable sorbent for Cd^{2+} and Pb^{2+} and thus a promising material for metal ion decontamination.

2.2. Experimental

2.2.1. Chemicals

Maghemite (iron (III) oxide) nanoparticles (30 nm in diameter) and pyridine were purchased from Alfa Aesar (USA).Cadmium and lead standard for AAS (1000 mg/L Cd^{2+}/Pb^{2+} in nitric acid) and (3-aminopropyl)triethoxysilane (99%) were purchased from Sigma-Aldrich (USA). Cadmium chloride anhydrous, lead chloride, ethylenediaminetetraacetic acid (EDTA), nitric acid, hydrochloric acid, citric acid, tris (hydroxymethyl)aminomethane, acetic acid, sodium bicarbonate and sodium carbonate were purchased from Fisher Scientific (USA). Diethylether and sodium dihydrogen phosphate were purchased from Acros Organics (Geel, Belgium). Sodium hydroxide and toluene were purchased from EMD Millipore (USA). All chemicals were used as received, without further purification. All solutions were prepared with deionized water (18 MΩ-cm) from a Barnstead NANOpure Diamond Water Purification System (USA).

2.2.2. Synthesis of Mag-Ligand

Maghemite nanoparticles (1.0 g) were dispersed into 40 mL of toluene in a flask. After mixing well, 0.4 mL of 3-aminopropyltriethoxysilane (APTES) were added to attach an amino group to the maghemite particles. Then the flask was connected to a reflux system (WU-28615-06, Cole-Parmer, USA), which was then rotated at 30 rpm (revolutions/minute) in a water bath at 90 ºC, and refluxed for 2 h. After the solution cooled to room temperature (22 ºC), 2 mM EDTA and 60 mL pyridine were added. The mixture was again rotated at 30 rpm in a water bath at 90 ºC in the reflux system for 2 h. After the solution cooled down to room temperature, 100 mL of sodium bicarbonate (0.5 M) was added to adjust pH. A magnet

(Eclipse Magnetics N821 permanent, 50 mm ×50 mm ×12.5 mm; 243.8 g; pull force: 40.1 N) was applied to the bottom of the flask to recover the nanoparticles while the supernatant was decanted. Deionized (DI) water was used to rinse the particles twice and then decanted while retaining the particles with the magnet. The same rinsing procedure was performed twice with ethanol and then diethylether. The particles were dried at room temperature for 24 h, and stored in a capped bottle prior to use.

2.2.3 Characterization of Mag-Ligand

Transmission electron microscopy (TEM) images were obtained using a JEOL 1230 Transmission Electron Microscope operated at 80 kV. Scanning electron microscopy (SEM) studies were performed on an FEI XL40 Sirion FEG Digital Scanning Microscope with an Oxford EDS analysis system. The thermogravimetric analyses (TGA) were used to investigate the amount of EDTA coated on the magnetic core, using a Mettler Toledo TGA/sDTA851e apparatus with an air flow of 100 mL/min and a heating rate of 5 °C/min. Magnetization measurements were performed on a Quantum Design MPMS 5XL SQUID Magnetometer. The functional groups of the Mag-Ligand composite were detected using a Fourier transform infrared (FTIR) spectrometer on a Nicolet iS 10 FT-IR Spectrometer.

2.2.4. Batch Sorption of Cd^{2+} and Pb^{2+}

For most experiments 5.0 mg of Mag-Ligand particles were mixed with 25 mL of Cd^{2+} or Pb^{2+} solution (10 mg/L) in 50 mL conical tubes, and the pH was adjusted to the desired condition (range from 4 to 10) by using a pH buffer. An acetic acid buffer was used for the pH interval between 3.5 to 5.5, citric acid was used for pH 6.0; pH 7.0 was obtained by using sodium dihydrogen phosphate buffer, pH between 7.5 to 9.5 was obtained by using tris (hydroxymethyl)aminomethane buffer, and sodium carbonate buffer was used to obtain pH

10.0. All buffer solutions were prepared at 100 mM concentration but the concentration of pH buffer was always kept below 10 mM to minimize other interactions. Then, these tubes were placed in an end-over-end shaker on a Dayton-6Z412A Parallel Shaft (USA) roller mixer with a speed of 70 rpm at room temperature for 24 h to ensure sufficient equilibration time. Adsorption kinetics studies were carried out at the same conditions as previously stated but for a set amount of time, varying from 15 min to 24 h, with pH = 7. After this mixing, the Mag-Ligand particles were separated from the mixture with the Eclipse magnet. All experiments were conducted at ambient temperature (22-25 °C).

The concentration of adsorbent was varied from 0.04 to 0.28 g/L to study the adsorption isotherms of Cd^{2+} or Pb^{2+} onto Mag-Ligand at pH 7. Additionally, solutions with varying initial concentrations of Cd^{2+} or Pb^{2+}, which ranged from 1 mg/L to 100 mg/L were treated with the same procedure as above at pH 7 and 5.0 mg Mag-Ligand.

In order to study the effect of ionic strength (e.g. water hardness), on the removal efficiency of Mag-Ligand, Ca^{2+} (ranging from 1 mg/L to 100 mg/L) and Mg^{2+} (ranging from 0.6 mg/L to 60 mg/L) were added to some of the experiments, at pH 7.

2.2.5. Regeneration and Reuse of Mag-Ligand

To investigate the regeneration and reuse of Mag-Ligand, 10 mg/L Cd^{2+} were used with the same adsorption process, followed by separation of the Mag-Ligand from solution with the handheld magnet. The Mag-Ligand collected was then washed with 1% HCl (10 minutes, room temperature), and the Cd^{2+} concentration in the supernatant solution (the solution pH is around 1.70) was determined by ICP. The regenerated Mag-Ligand particles were then reused for subsequent Cd^{2+} sorption experiments. The sorption, extraction, and reuse

processes were repeated for five times. Changes in sorption capacity and Mag-Ligand particle recovery were determined at every cycle.

2.2.6. Analysis

A Thermo iCAP 6300 inductively coupled plasma with atomic emission spectroscopy (ICP-AES) was used to analyze the concentration of Cd^{2+} and Pb^{2+} (Adeleye et al. 2013, Adeleye and Keller 2014, Huang et al. 2014). All tests were performed in triplicate and analysis of variance (ANOVA) was used to test the significance of results. A $p<0.05$ was considered to be statistically significant.

Metal ions removal efficiency and sorption capacity was calculated as:

$$Removal\ efficiency = \frac{C_0 - C_t}{C_0} \times 100\% \quad (1)$$

$$Sorption\ capacity = q_e = \frac{(C_0 - C_t) \cdot V}{m} \quad (2)$$

where C_0 and C_t are the initial and final concentrations of metal ions (mg/L), m is the mass of Mag-Ligand (g), and V is the volume of solution (L).

Mag-Ligand recovery efficiency was calculated as:

$$Recovery\ efficiency = \frac{C_w}{C_0} \times 100\% \quad (3)$$

where C_0 (mg/L) is the initial concentrations of Cd^{2+} ions in solution, and C_w (mg/L) is the concentrations of Cd^{2+} ions in the extracted solution (after regeneration).

The Cd^{2+} and Pb^{2+} equilibrium adsorption was evaluated according to Langmuir and Freundlich isotherms using Eq. 4 and Eq. 5, respectively (Morel and Hering 1993):

$$\frac{C_e}{q_e} = \frac{1}{K_L \cdot q_m} + \frac{C_e}{q_m} \quad (4)$$

$$\log q_e = \log K_F + \frac{1}{n}\log C_e \quad (5)$$

where C_e is solute concentration (mg/L) at equilibrium and q_e is amount adsorbed (mg/g), q_m is the maximum sorption capacity (mg/g). K_L and K_F is the Langmuir and Freundlich sorption equilibrium constant (L/mg), respectively.

Kinetics were analyzed using the pseudo-first-order and pseudo-second-order models using Eq. 6 and Eq. 7 (Coleman et al. 1956):

$$\ln(q_e - q_t) = \ln(q_e) - k_1 t \quad (6)$$

$$\frac{t}{q_t} = \frac{1}{k_2 q_e^{\,2}} + \frac{1}{q_e} t \quad (7)$$

where k_1 (h^{-1}) and k_2 ($\frac{g}{mg \cdot h}$) are the equilibrium rate constants of kinetics.

2.3. Results and discussion

2.3.1. Mag-Ligand Synthesis and Characterization

The synthesis of Mag-Ligand consists of two steps, which are schematically presented in Figure 1. First, the maghemite nanoparticles were coated with APTES to deposit aminopropylalkoxysilane on the surface of the magnetite core. In the hydrolysis reaction, the alkoxide groups ($-OC_2H_5$) of APTES were replaced by hydroxyl groups (OH) to form reactive silanol groups, which condensed with other silanol groups to produce siloxane bonds (Si–O–Si) to generate silane polymer (Yamaura et al. 2004). Then these polymers coated the maghemite nanoparticles to form a covalent bond with OH groups (Yamaura et al. 2004). After APTES coating, the maghemite nanoparticles were functionalized with an amino group.

Then, EDTA was attached to the APTES coated maghemite nanoparticles. The covalent attachment of EDTA to particles was achieved by the formation of amide bonds between the carboxylic acid groups of the complexing agent and amino groups provided by the APTES coating (Bernkop-Schnürch and Krajicek 1998). The SEM micrograph (Figure 2A and B) shows the porous surface structure of Mag-Ligand. The core/shell structure of Mag-Ligand is shown in the TEM micrograph (Figure 2C and D), and the shell layer (attached EDTA) is approximately 100 nm as determined by TEM (Figure 2D). Figure 2 demonstrates that the hydrated particles are 1 to 10 μm in size with very high porosity in the nanoscale. Figure S3 (Supplementary Material) indicates that Mag-Ligand is negatively charged (zeta potential from -27 to -47 mV) for pH ranging from 4 to 10.

The FTIR spectra of unmodified maghemite nanoparticles and Mag-Ligand are shown in Figure 3A. The Mag-Ligand presented peaks for N-H (v_{N-H}, 3267 cm^{-1}), C=O ($v_{C=O}$, 1633 cm^{-1}), N-H (v_{N-H}, 1580 cm^{-1}), C-N (v_{C-H}, 1400 cm^{-1}) and C-NH_2 (v_{C-H}, 1119 cm^{-1}); all these functional groups are expected from EDTA. These peaks were not present in the spectra of unmodified maghemite nanoparticles, indicating that the synthesis procedure had successfully attached EDTA on the surface of maghemite nanoparticles.

The TGA curves of as-synthesized Mag-Ligand (Figure 3B) show four weight loss steps at about 220, 292, 338, 424, and 742 °C, as demonstrated in the derivative curve, which can be ascribed to the decomposition of quaternary ammonium group (Wang et al. 2008), the decomposition of EDTA and transition from Na_2EDTA to Na_2CO_3, the decomposition of Na_2EDTA, and the complete oxidation of carbon, respectively (Wendlandt 1960). The weight percentage of EDTA attached onto iron oxide particles of Mag-Ligand can be determined by the difference of initial and final mass of the sample in the TGA curve

(Figure 3B) and was approximately 12.5% of the total mass of Mag-Ligand. The high fraction of EDTA and porous surface structure provides many active binding sites for metal ion removal.

Magnetic characterization with a superconducting quantum interference device (SQUID) magnetometer at 300 K indicated that maghemite and Mag-Ligand have magnetization saturation values of 59.0 and 52.8 emu/g, respectively (Figure 4A), indicating a high magnetization. The maghemite content in the macroporous composites is calculated to be as high as 35 weight %. Additionally, no remanence was detected in either maghemite or Mag-Ligand particles, indicating a superparamagnetism feature due to the nanosized maghemite. Due to the strong magnetization, Mag-Ligand suspended in water (0.2 g/L) can be quickly separated from the dispersion with a magnet (1000 Oe), as shown in Figure 4 B and C. These results indicate that the Mag-Ligand possesses excellent magnetic responsivity.

2.3.2. Sorption isotherms of Cd^{2+} and Pb^{2+}

Adsorption isotherms of Cd^{2+} and Pb^{2+} onto Mag-Ligand were obtained at pH 7 as shown in Figure 5. Both Cd^{2+} and Pb^{2+} removal efficiency gradually increased up to the optimum dosage (0.2 and 0.125g/L for Cd^{2+} and Pb^{2+}, respectively), beyond which the removal efficiency (above 97%) did not change with increasing adsorbent dosage (Figure 5A), since there are a fixed number of adsorption sites (Sekar et al. 2004).

The effect of initial [Cd^{2+}] (ranging from 1 mg/L to 50 mg/L) and [Pb^{2+}] (ranging from 1 mg/L to 30 mg/L) on adsorption is shown in Figure 5B. For both ions, removal increased first and then decreased with increasing initial ion concentration, once the maximum adsorption capacity was reached. The initial ion concentration provides the necessary driving force to overcome the resistance to mass transfer of ions between the aqueous and solid

phases, and enhances the interaction between Cd^{2+}/ Pb^{2+} and Mag-Ligand (Kumar et al. 2010). Figure 5B indicates that Mag-Ligand has stronger affinity for Pb^{2+} than Cd^{2+}.

The Pb^{2+} and Cd^{2+} isotherm sorption data was fitted using the Langmuir (Figure 5C) and Freundlich (Figure 5D) adsorption isotherm models. The Langmuir model provided a slightly better fit for Cd^{2+}, while the Freundlich model fitted Pb^{2+} adsorption better (Table 1). Results of adsorption experiments in this study showed that the maximum adsorption capacity of 79.4 mg/g for Cd^{2+} and 100.2 mg/g for Pb^{2+} onto Mag-Ligand. This agrees with the sequence of the EDTA complex formation constants (log K, 25 °C): 18.04 and 16.46 for Pb^{2+} and Cd^{2+}, respectively(Harris 2010). Table S1 (Supplementary Material) presents a direct comparison between the collected results from this study versus other previously published data of magnetic ligand particles, indicating Mag-Ligand has a higher sorption capacity for Pb^{2+} and Cd^{2+} than previous materials, as well as a wide range of optimum pH.

2.3.3. Sorption kinetics of Cd^{2+} and Pb^{2+}

Time dependent removal of metal ions (initial concentration = 10 mg/L) by Mag-Ligand (0.2 g/L) showed rapid adsorption of Cd^{2+} in the first hour (~95% removal efficiency), and thereafter, the adsorption rate decreased gradually. Cd^{2+} equilibrium adsorption was reached (above 97% removal efficiency) in about 2 h (Figure 6A). Equilibrium for Pb^{2+} was achieved much faster (~15 min) with above 97% removal efficiency, as shown in Figure 6A. Mag-Ligand has very fast metal ion sorption kinetics due to the large amount of EDTA accessible to the metal ions in solution, and the difference in kinetics between the metal ions also corresponds with the EDTA affinity sequence (Harris 2010).

The pseudo-first-order (Figure 6B) and pseudo-second-order (Figure 6C) kinetic models were used to investigate the adsorption rate of Cd^{2+} and Pb^{2+} onto Mag-Ligand. The removal

of both Cd^{2+} and Pb^{2+} by Mag-Ligand followed pseudo-second order rate (R^2>0.99) better than pseudo-first-order (R^2<0.88) (Table 2). The k_2 values (in $\frac{g}{mg \cdot h}$) for Cd^{2+} and Pb^{2+} were determined as 0.235 and 7.960, respectively, indicating Mag-Ligand has a much faster removal rate for Pb^{2+} which is due to the stronger binding constant with EDTA (Harris 2010).

2.3.4. Effect of pH on Cd^{2+} removal

The influence of pH on the removal efficiency is important in industrial wastewater, particularly for cadmium. No significant difference in Cd^{2+} removal efficiency was found between pH 3 and 7, and the removal efficiency stabilized at around 97% (Figure 7). Above pH 7, Cd^{2+} removal efficiency decreased gradually as pH increased, to about 86% at pH 10.

Simulation of the aqueous speciation of cadmium using Visual MINTEQ (Gustafsson 2006) software indicates that for pH from 3 to 10, cadmium in DI water at these concentrations is mostly present as Cd^{2+}. Cd^{2+} has a strong complex formation constant with EDTA (at 25ºC, $Cd^{2+} + EDTA^{4-} \leftrightharpoons Cd(EDTA)^{2-}$, log K=14.7; $Cd(EDTA)^{2-} + H^{+} \leftrightharpoons Cd(HEDTA)^{-}$, log K=2.5) (Martell and Smith 1989), which agrees well with our result: Mag-Ligand showed high removal efficiency across different pH, especially from pH 3 to 7. However, starting from pH 8 there is increasing formation of $Cd(OH)_2$ (Zirino and Yamamoto 1972), which decreases $Cd(EDTA)^{2-}$ and $Cd(HEDTA)^{-}$ formation.

2.3.5. Effect of water hardness on Cd^{2+} removal

Water hardness varies in different water matrices, such as tap water, groundwater, river water, lake water and sea water, which is usually expressed as the total amount of Ca^{2+} and

Mg^{2+} present in the water. Compared to the trace heavy metal ions, the concentrations of Ca^{2+} and Mg^{2+} ions present in natural water systems is typically much higher, and they can also interact with EDTA to form complexes (Yappert and DuPre 1997). Figure 8 shows the removal performance of Cd^{2+} using Mag-Ligand in the presence of different concentrations of Ca^{2+} or Mg^{2+}. No significant difference in Cd^{2+} removal efficiency was found as Mg^{2+} concentration increased up to 60 mg/L in the solution (Figure 8A). Only at high concentration of Ca^{2+} (above 50 mg/L) was there a decrease in Cd^{2+} removal efficiency (Figure 8B). These results indicate that Ca^{2+} or Mg^{2+} did not compete strongly with Cd^{2+} in the complexation reaction with EDTA; this agrees with the sequence of the EDTA complex formation constants (log K, 25 °C): 8.79, 10.69 and 16.46 for Mg^{2+}, Ca^{2+} and Cd^{2+}, respectively (Harris 2010).

2.3.6. Regeneration and reuse of Mag-Ligand

To demonstrate the regenerability and reuseability of the Mag-Ligand, the recovery of Cd^{2+} sorbed onto the Mag-Ligand was investigated using a 1% HCl wash. Cd^{2+} removal and Mag-Ligand recovery during five continuous cycles of regeneration and reuse are shown in Figure 9. It was found that a large fraction of the sorbed Cd^{2+} (>80%, over 8 mg/L) could be recovered, indicating easy regeneration of Mag-Ligand (Figure 9). Some loss (within 10% change) of Cd^{2+} sorption capacity was observed for the regenerated Mag-Ligand after 5 cycles (Figure 9), indicating good reusability of Mag-Ligand. The decreased chelating capacity was likely due to irreversibly bound metals or loss of chelator (Koehler et al. 2009).

2.4. Conclusions

Mag-Ligand represents a significant improvement in metal ion decontamination in a wide range of aqueous matrices, since (1) Mag-Ligand only requires a simple synthesis

procedure and exhibits high metal ion removal capacity; (2) the superparamagnetic Fe_2O_3 core allows rapid separation of Mag-Ligand after sorption; (3) Mag-Ligand can be easily recovered, regenerated and reused, significantly increasing treatment efficiency and reducing operation cost; (4) Mag-Ligand exhibits high removal efficiency under different environmental conditions (e.g. pH range from 4 to 10; up to 60 mg/L Ca^{2+} or Mg^{2+} present in the solution); (5) the residual Cd^{2+} and Pb^{2+} in solution represents a very small fraction of the initial contaminated mass and volume; and (6) sorption kinetics indicate fast removal of metal ions. The most likely mechanisms of Cd^{2+}adsorption onto Mag-Ligand are (1) complexation reactions with EDTA and (2) adsorption of Cd^{2+} or Pb^{2+} on the surface porous structures. Future work will address the current synthesis process, seeking a more sustainable approach with an aqueous-based synthesis.

Therefore, Mag-Ligand are reusable sorbents for the fast, convenient, and highly efficient removal of Cd^{2+} and Pb^{2+} from contaminated aquatic systems. It is expected that the Mag-Ligand will have potentially wide application in the removal of other heavy metal pollutants from aquatic systems.

Table 1. Isotherm parameters for Cd^{2+} and Pb^{2+} sorption on Mag-Ligand

	Langmuir			Freundlich		
	q_m (mg/g)	K_L (L/mg)	R^2	K_F (L/mg)	1/n	R^2
Cd^{2+}	79.365	7.200	0.951	72.755	0.550	0.946
Pb^{2+}	100.200	13.152	0.924	239.939	2.226	0.998

Table 2. Kinetic parameters for Cd^{2+} and Pb^{2+} sorption on Mag-Ligand

	Pseudo-first order			Pseudo-second order		
	q_e (mg/g)	k_1 (h^{-1})	R^2	q_e (mg/g)	k_2 (g/h·mg)	R^2
Cd^{2+}	12.117	0.699	0.879	52.549	0.235	1.000
Pb^{2+}	3.403	0.061	0.441	50.865	7.960	1.000

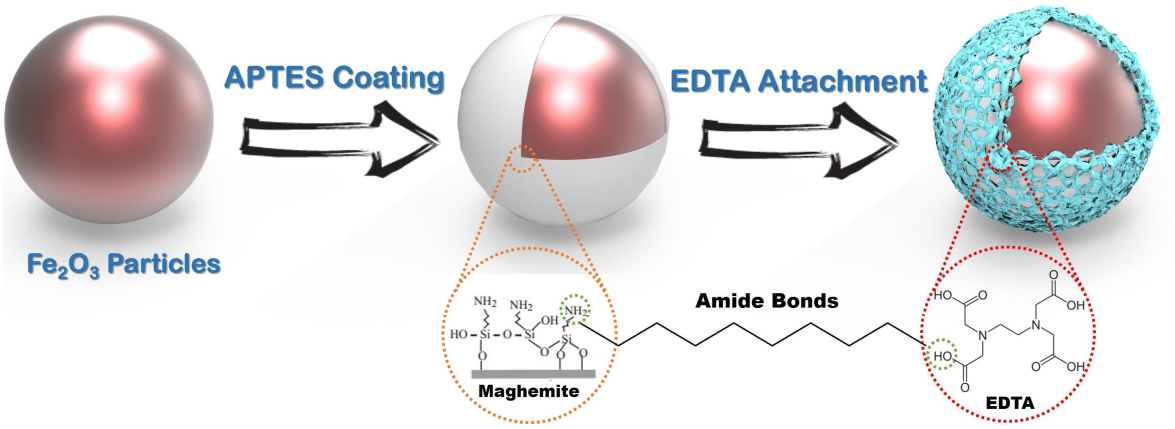

Figure 1. Schematic representation of Mag-Ligand synthesis (note: the core and shell are not drawn to scale).

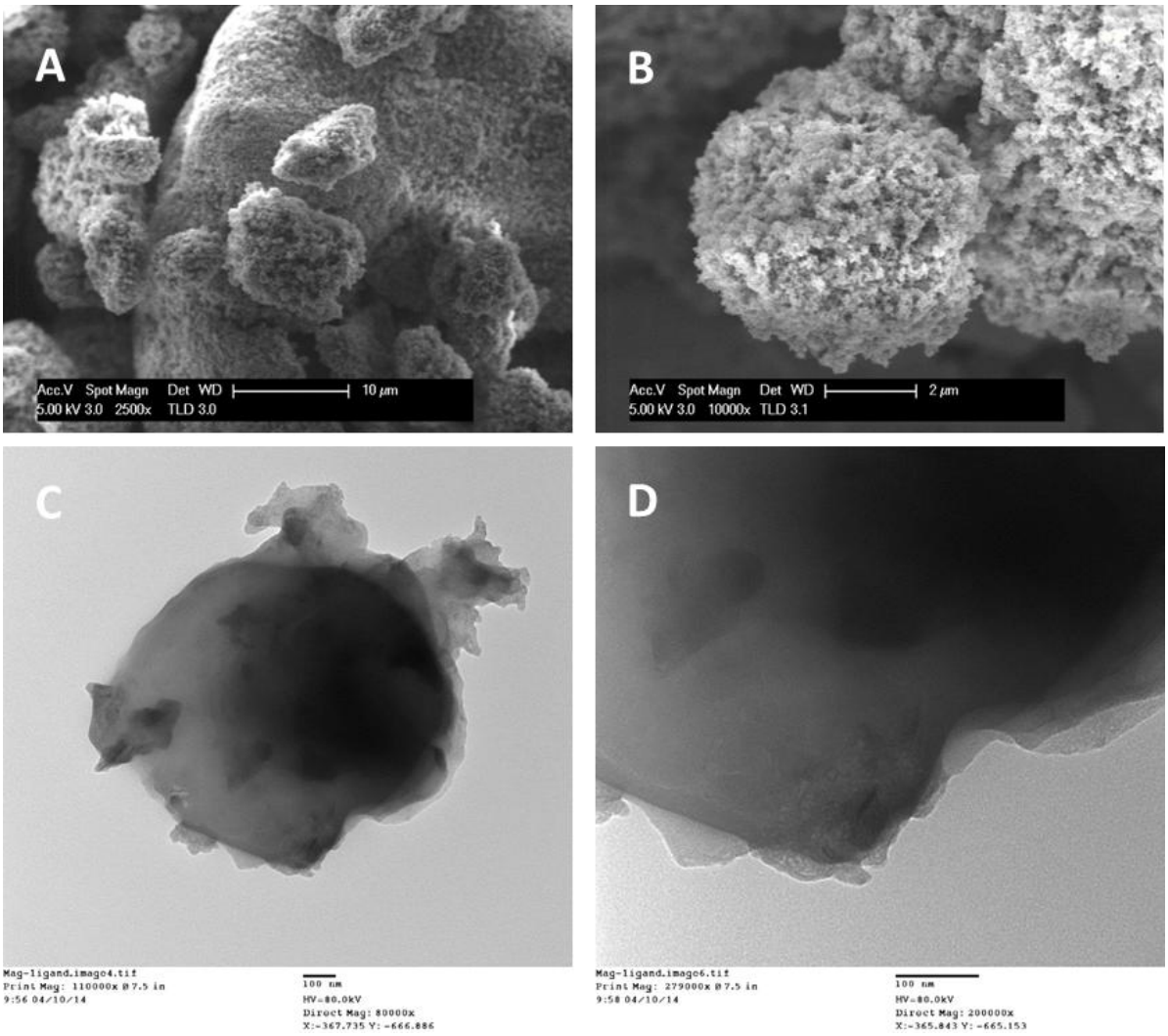

Figure 2. (A) SEM micrographs of Mag-Ligand at 2500×, scale bar=10 μm and (B) at 10,000×, scale bar=2 μm; (C) TEM micrographs of Mag-Ligand at 80,000×, scale bar =100nm and (D) at 200,000, scale bar=100nm.

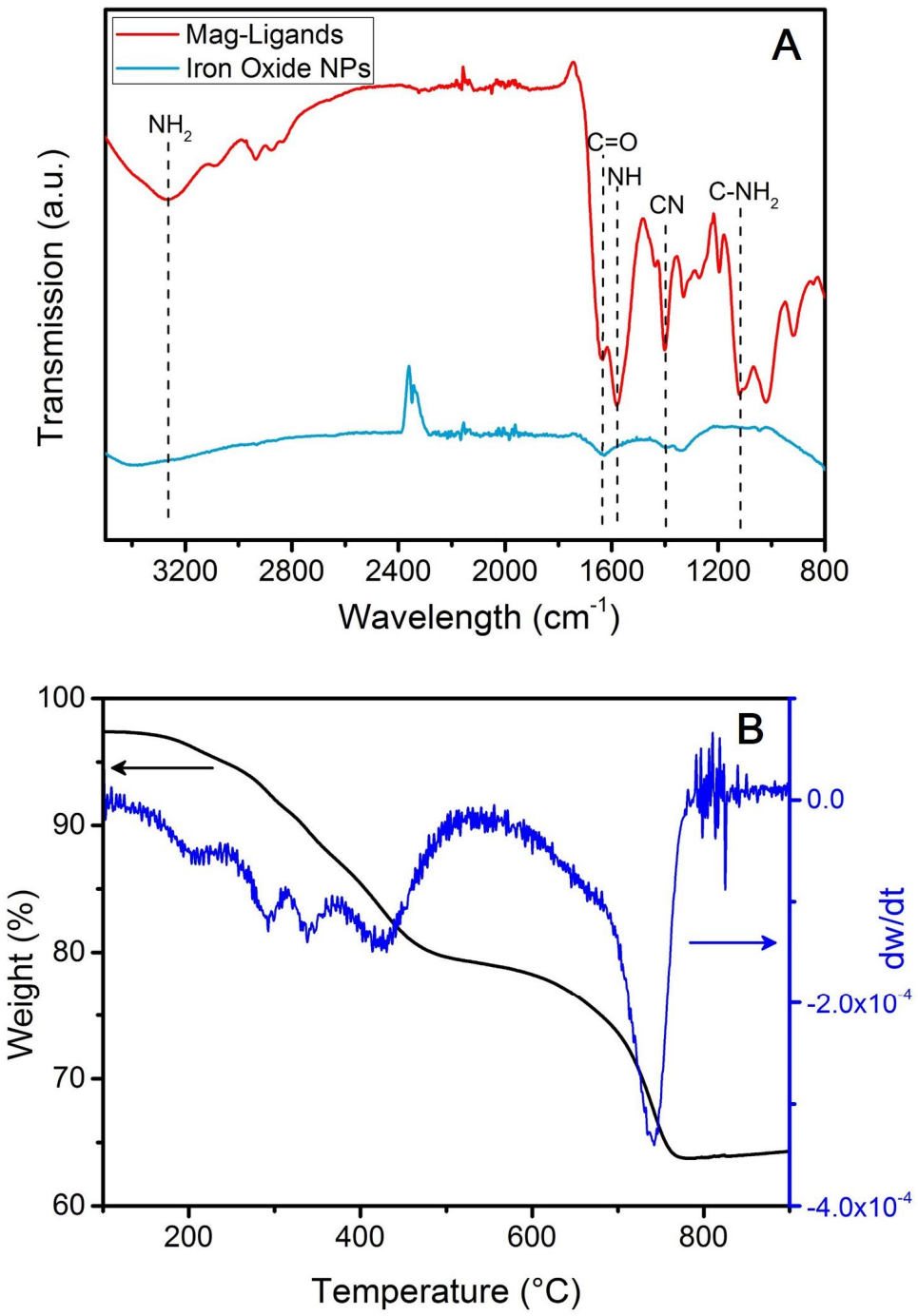

Figure 3. (A) FTIR spectra of unmodified magnetite nanoparticles and Mag-Ligand; (B) Thermogravimetric analysis (TGA) of Mag-Ligand.

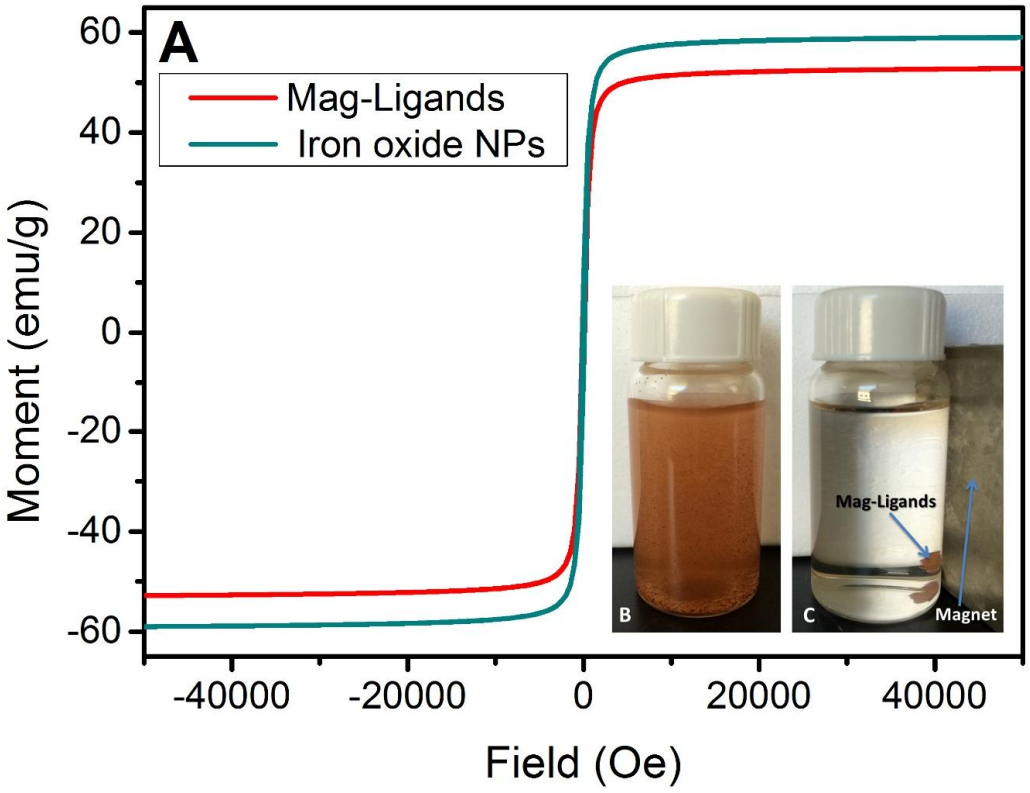

Figure 4. (A) The magnetic hysteresis loops of iron oxide nanoparticles and Mag-Ligand; (B) Mag-Ligand particles are introduced into a vial containing contaminated water; (C) A permanent magnet is placed at the side of the vial to attract the magnetic particles, demonstrating the rapid removal of Mag-Ligand from the suspension within seconds of applying a magnetic field.

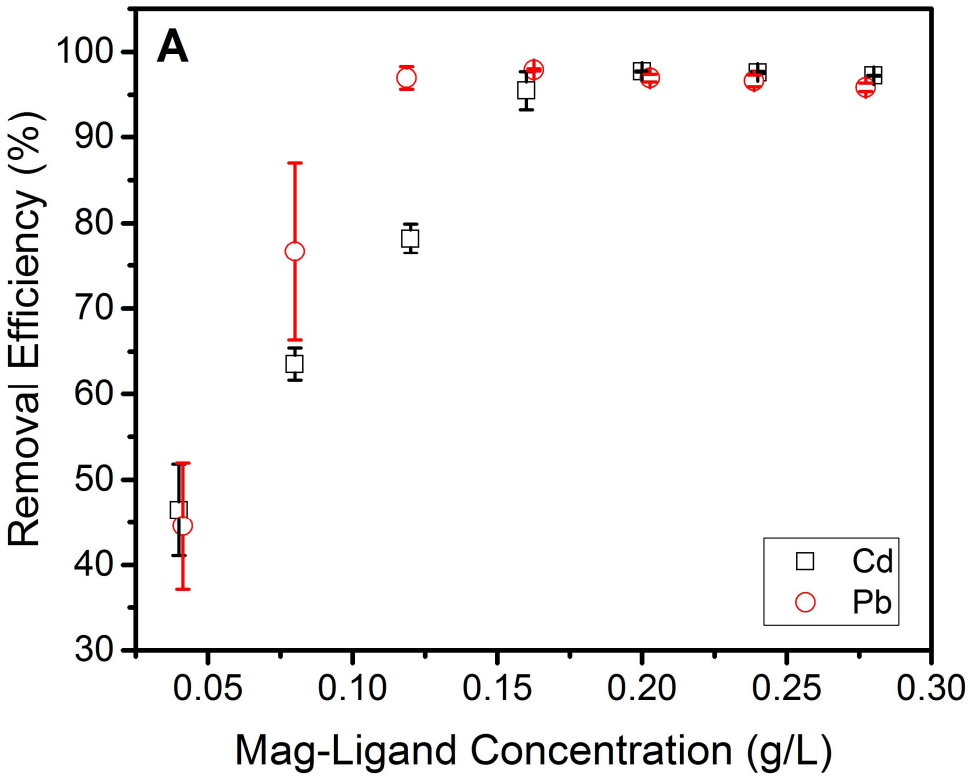
A
Removal Efficiency (%)
100
90
80
70
60
50
40
30
0.05
0.10
0.15
0.20
0.25
0.30
Mag-Ligand Concentration (g/L)
Cd
Pb

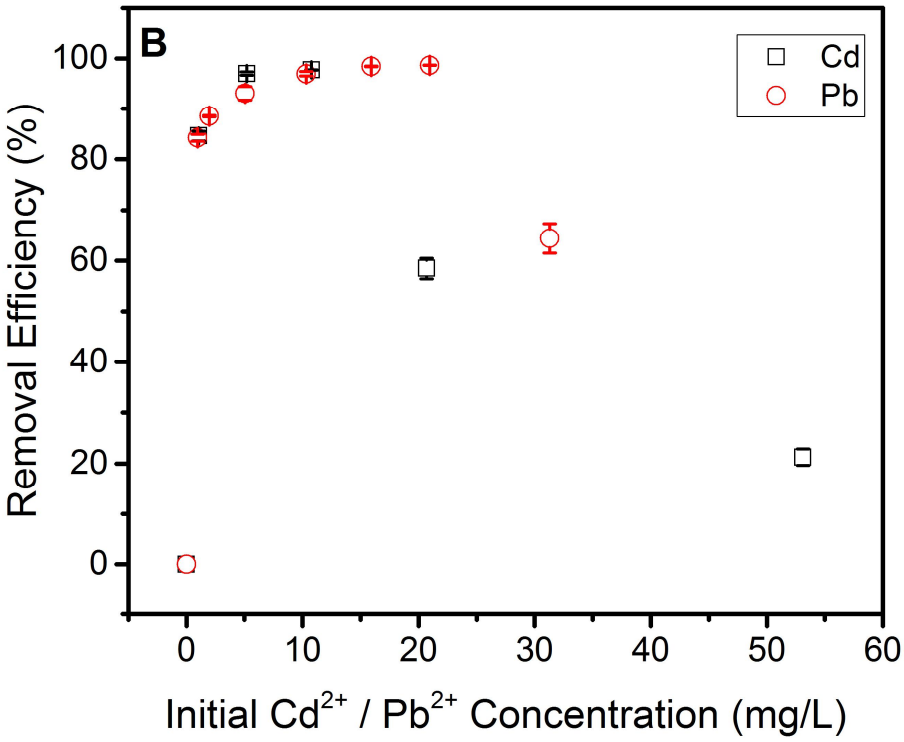
B
Removal Efficiency (%)
100
80
60
40
20
0
0
10
20
30
40
50
60
Initial Cd2+ / Pb2+ Concentration (mg/L)
Cd
Pb

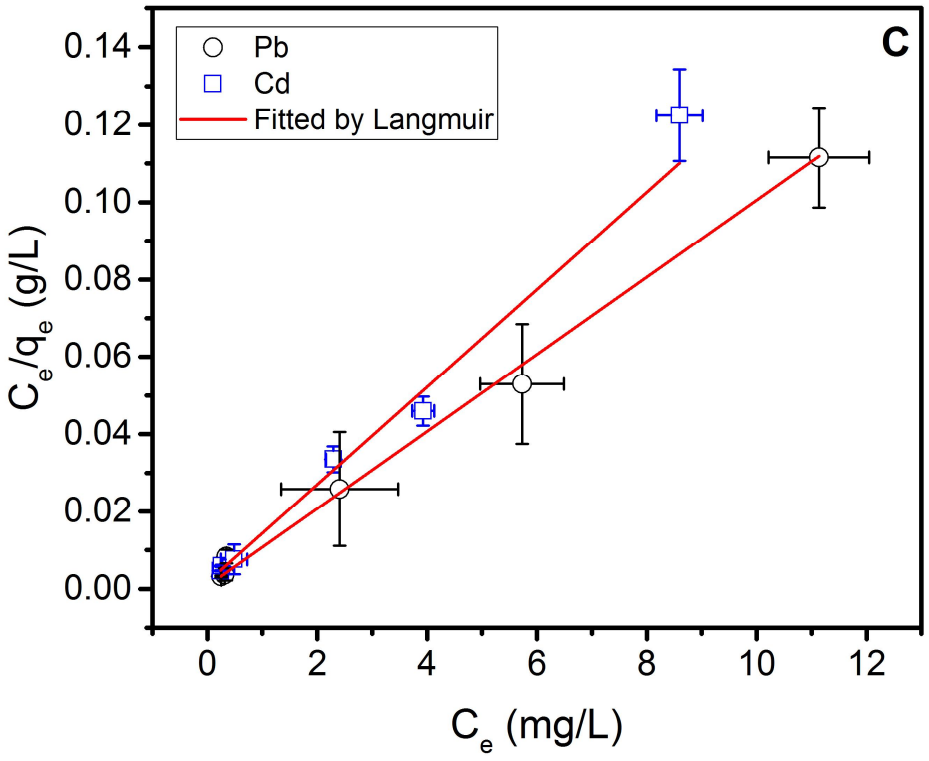
C
Pb
Cd
Fitted by Langmuir
0.14
0.12
0.10
0.08
0.06
0.04
0.02
0.00
C_e/q_e (g/L)
0
2
4
6
8
10
12
C_e (mg/L)

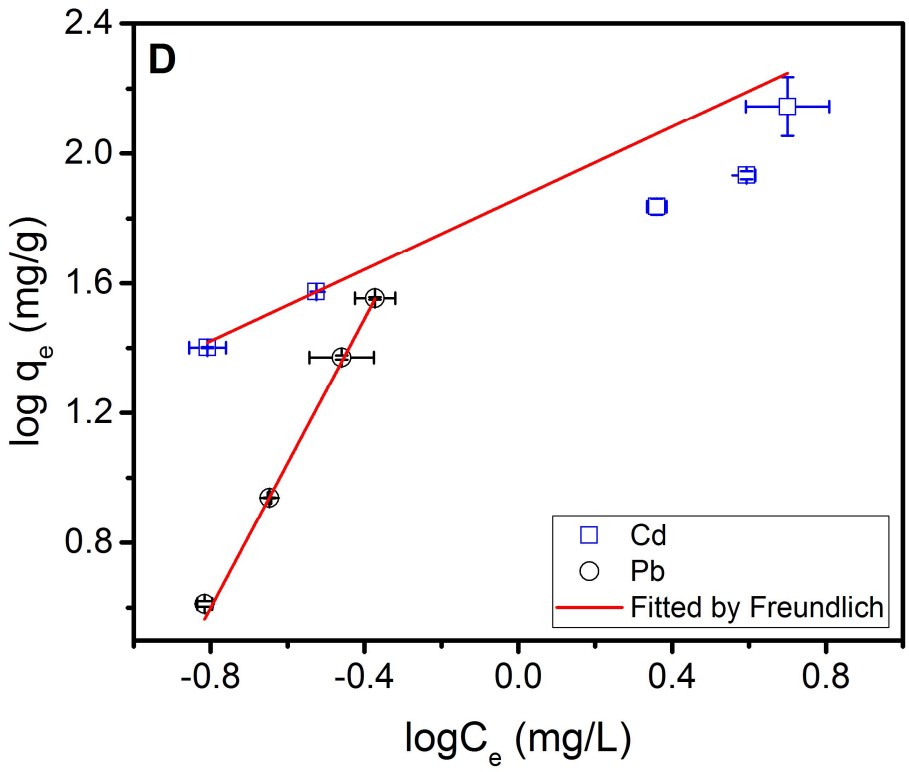
D
2.4
2.0
1.6
1.2
0.8
log q_e (mg/g)
Cd
Pb
Fitted by Freundlich
-0.8
-0.4
0.0
0.4
0.8
logC_e (mg/L)

Figure 5. Adsorption of Cd^{2+} and Pb^{2+} onto Mag-Ligand (characterized by Cd^{2+} (□) and Pb^{2+} (○)) (A) at pH 7 as a function of adsorbent dose with a fixed initial ions concentration of 10 mg/L; (B) at pH 7 as a function of initial ions concentration with a fixed adsorbent concentration of 2 g/L; (C) Langmuir and (D) Freundlich adsorption isotherms fit at pH 7, symbols represent experimental data, and red line represents model prediction.

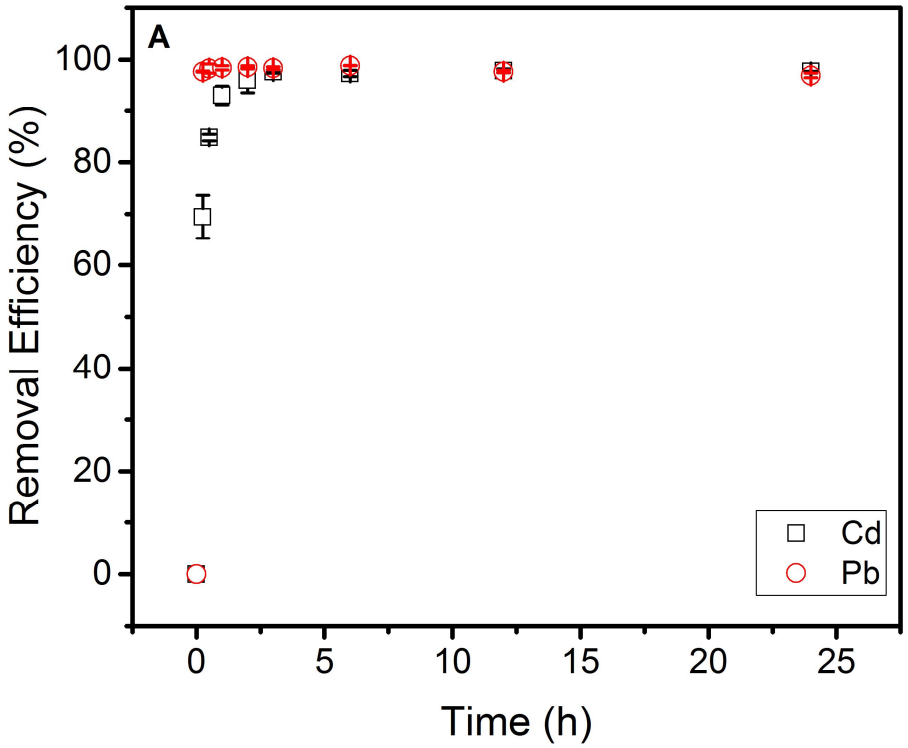
A
Removal Efficiency (%)
100
80
60
40
20
0
0
5
10
15
20
25
Time (h)
Cd
Pb

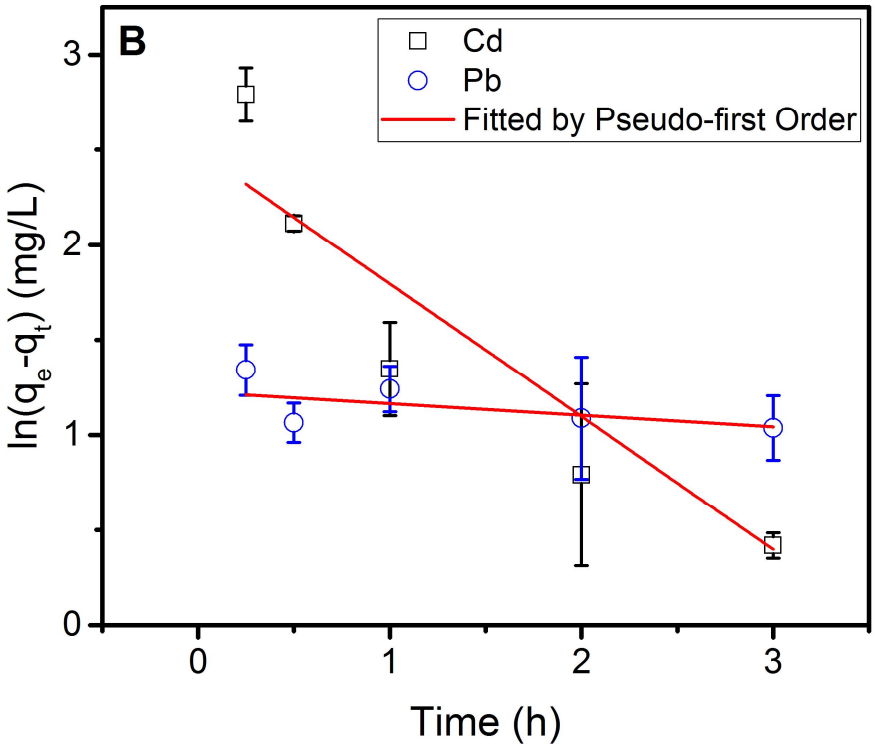
B
Cd
Pb
Fitted by Pseudo-first Order
ln(qe-qt) (mg/L)
3
2
1
0
0
1
2
3
Time (h)

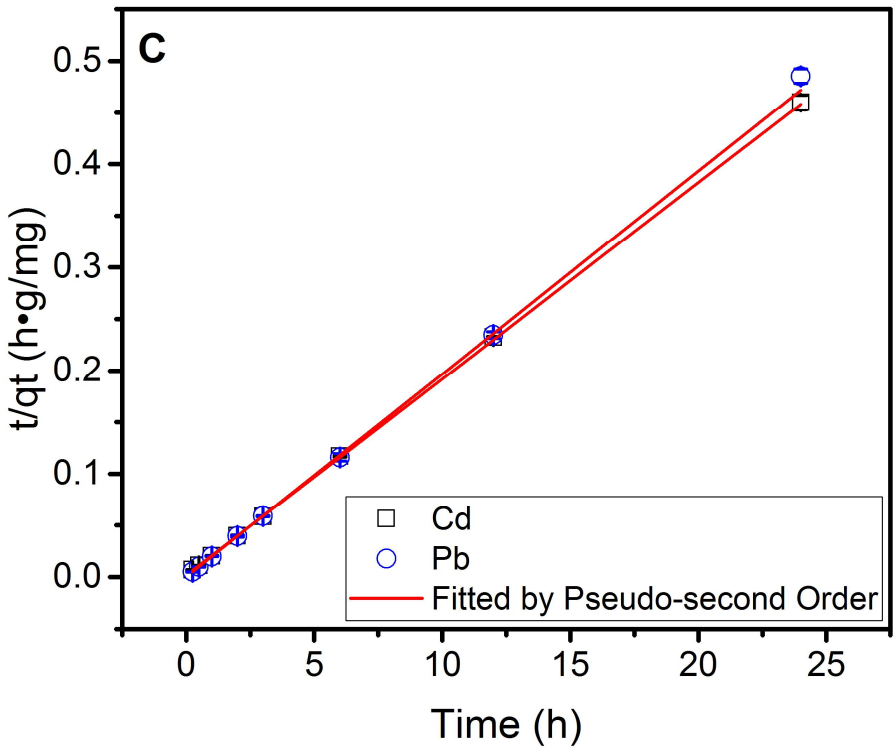

Figure 6. Cd^{2+} and Pb^{2+} (A) sorption uptake versus time; and sorption kinetics fitted by (B) Pseudo-first order and (C) Pseudo-second order onto Mag-Ligand in solution at pH 7.

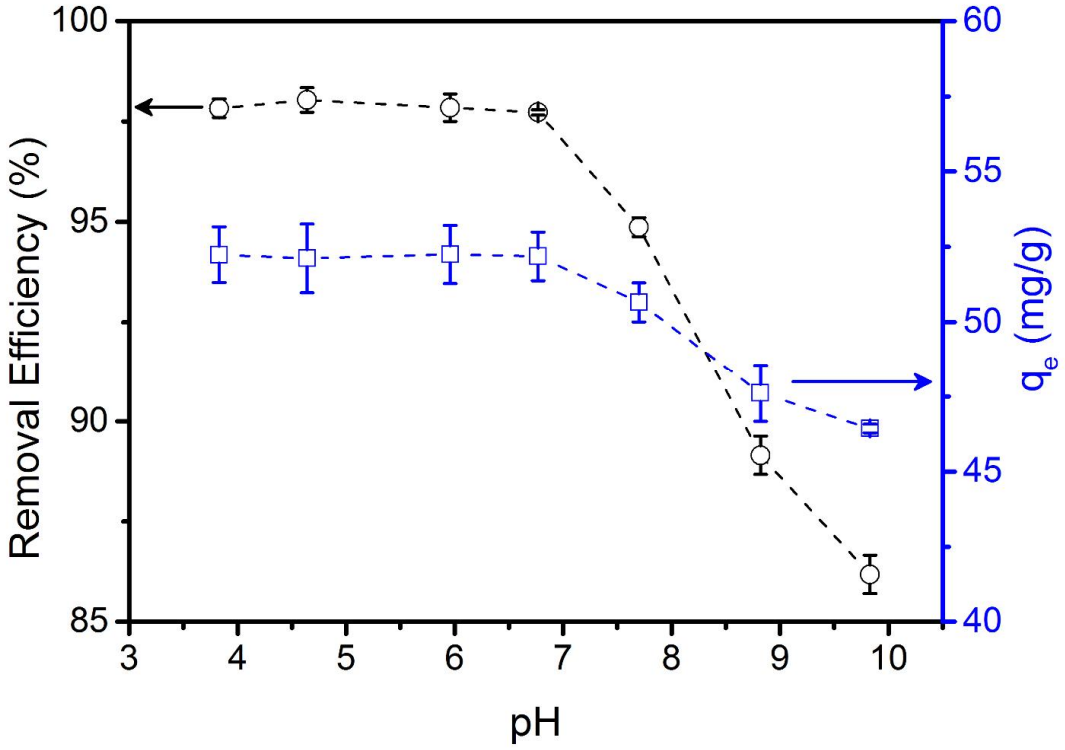

Figure 7. Adsorption of Cd^{2+} onto Mag-Ligand in solution as a function of pH, characterized by the removal efficiency (○) and adsorption capacity (□).

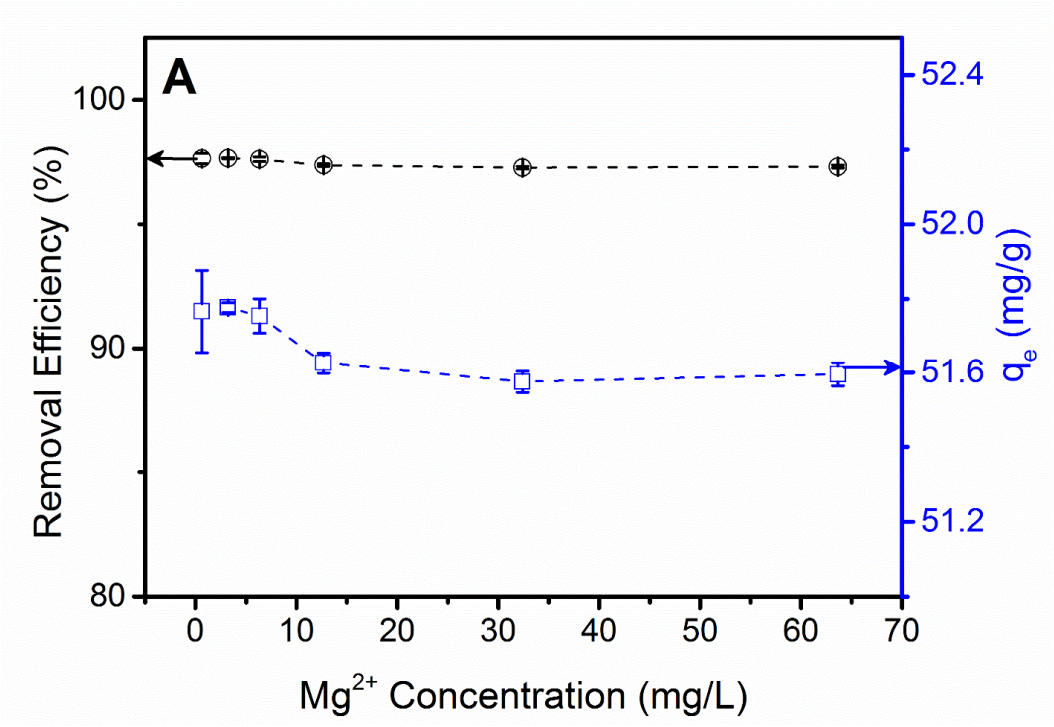
A
Removal Efficiency (%)
100
90
80
52.4
52.0
51.6
51.2
q_e (mg/g)
0
10
20
30
40
50
60
70
Mg^{2+} Concentration (mg/L)

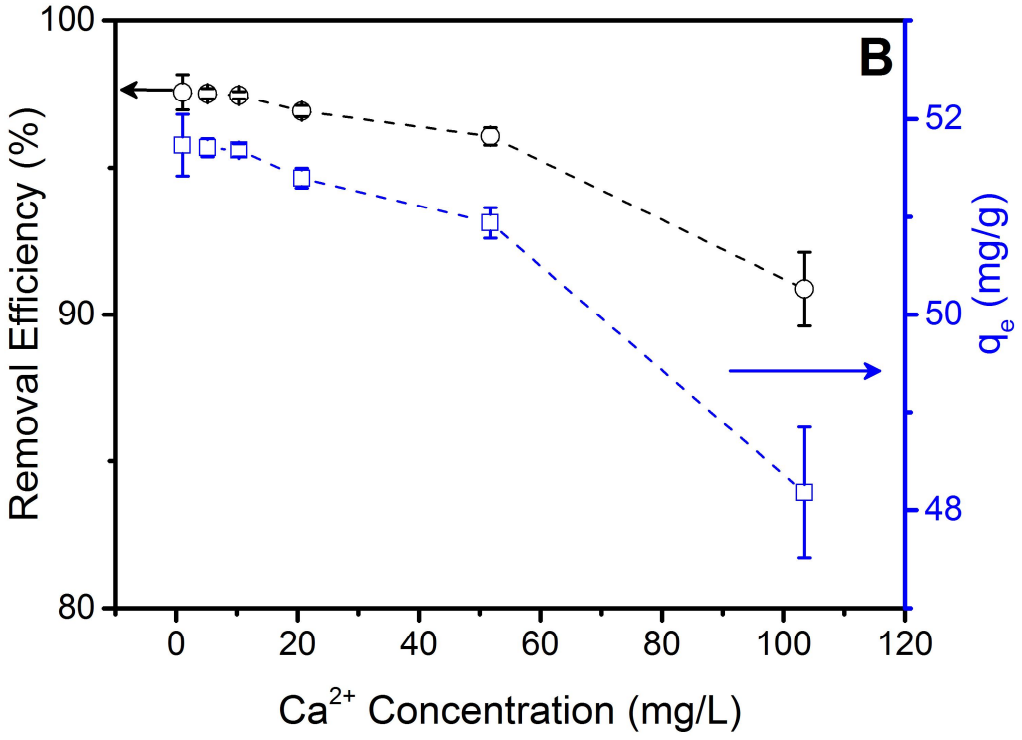
B
Removal Efficiency (%)
100
90
80
52
50
48
q_e (mg/g)
0
20
40
60
80
100
120
Ca^{2+} Concentration (mg/L)

Figure 8. Adsorption of Cd^{2+} (10 mg/L initial concentration) onto Mag-Ligand (removal efficiency (○) and adsorption capacity (□)) in the presence of (A) Mg^{2+} (from 0.6 mg/L to 60 mg/L) and (B) Ca^{2+} (from 1 mg/L to 100 mg/L) at pH 7.

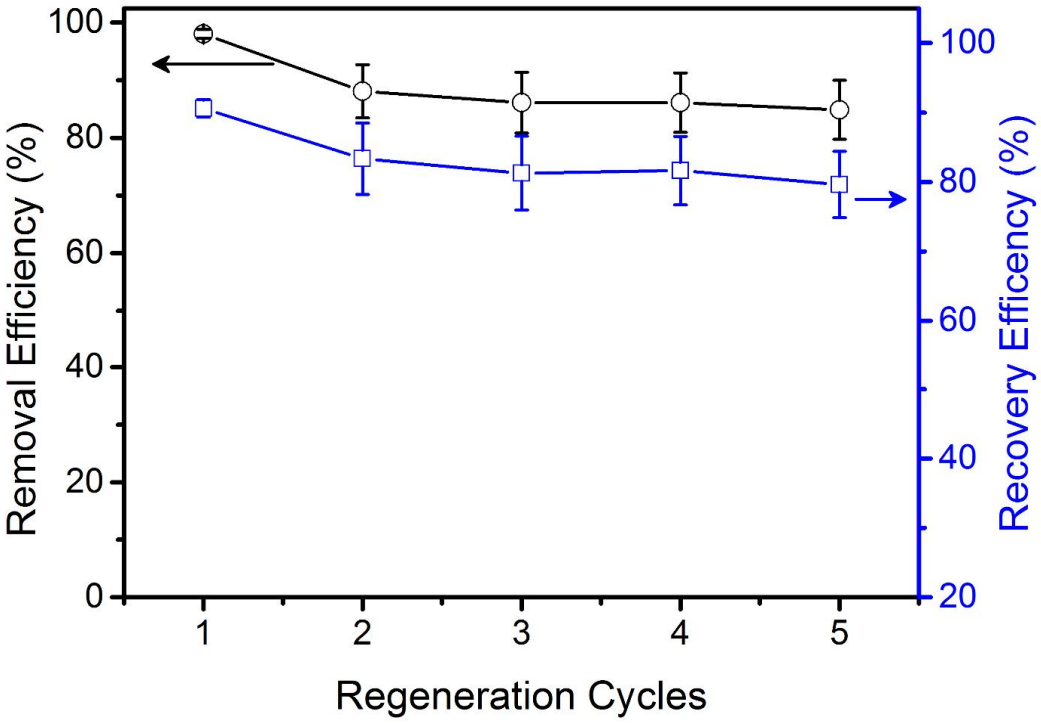

Figure 9. Cd^{2+} (10 mg/L initial concentration) removal efficiency (○) from solution and Cd^{2+} recovery (□) from Mag-Ligand during five regeneration cycles

2.5. Appendix. Supporting Information

2.5.1. Characterization of Mag-Ligand post acid wash regeneration treatment

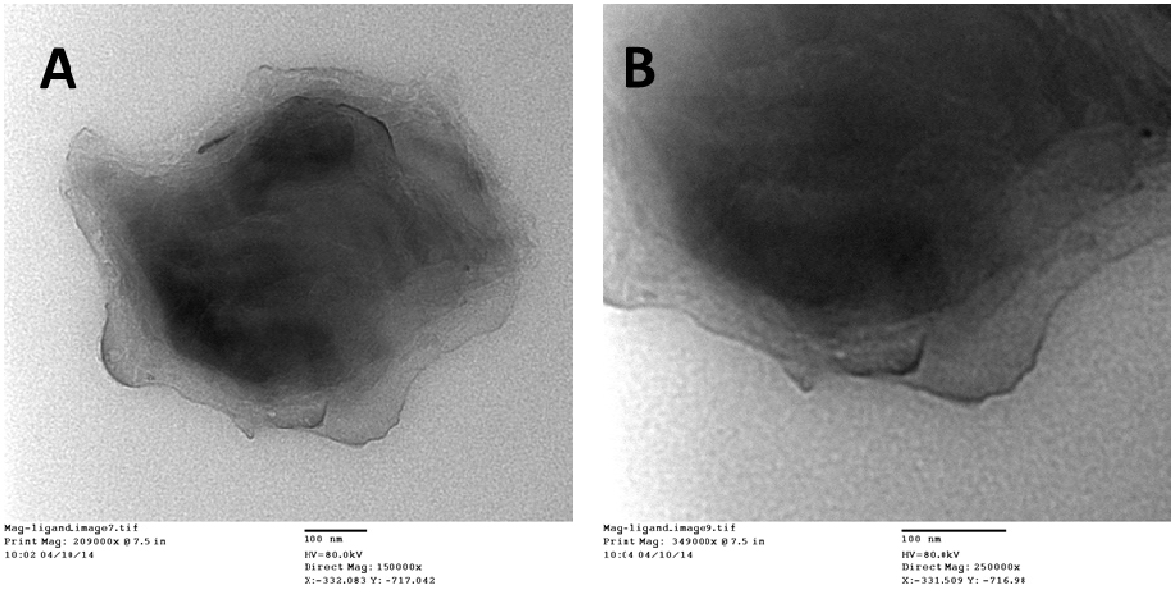

Figure S1. **(**A) TEM micrographs of Mag-Ligand at 150,000×, scale bar =100nm and (B) at 250,000, scale bar=100nm.

The TEM image (Figure S1.) shows the core/shell structure of Mag-Ligand particles after acid wash treatment. Comparing Figure 2 C. & D. with Figure S1., no significant difference can be noted before and after dilute acid wash, which indicates that 1% HCl wash did not cause the dissolution of maghemite particles. Furthermore, since acid wash treatment is a short period (Mag-Ligand was mixed with 1% HCl for 10 minutes at room temperature), not significant dissolution of maghemite was detected when using the ICP to determine the Cd (II) and Fe concentration in the supernatant solution.

2.5.2. Effect of pH (With/without pH Buffers)

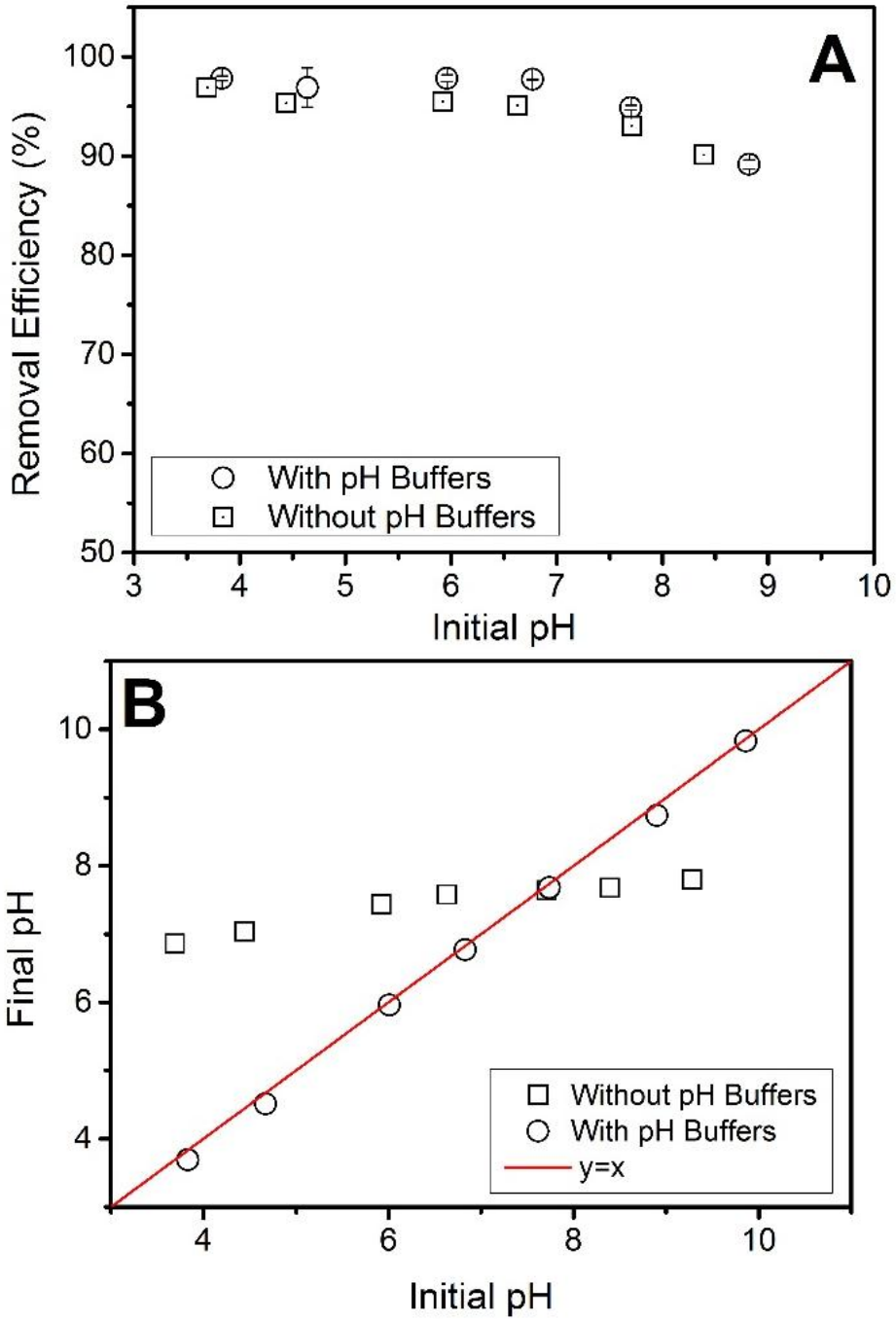

Figure S2. (A) Adsorption of Cd^{2+} onto Mag-Ligand in solution as a function of pH with and without pH buffers presented; (B) Cd^{2+} contaminated water pH change prior and post Mag-Ligand sorption treatment.

Considering pH effect on Mag-Ligand sorption performance, sorption experiments either with or without pH buffers was performed; no significant difference was found in the removal efficiency, as shown in Figure S2 A. However, without buffers present, the pH of Cd(II) contaminated water would vary significantly after treatment, while with buffers presented, we can report the pH of actual treatment, as shown in Figure S2 B.

The concentrations of these buffers was based on the minimum needed to adjust the solution to the desired pH. Furthermore, these buffers increased the ionic strength, which is very common in actual water treatment, so it is more realistic.

Considering the possible competitive sorption between Cd(II) and the ions from pH buffers, we chose sodium salt pH buffers, which has very low complex formation constant (log K=1.66, 25 °C) with EDTA. Furthermore, as noted in the manuscript as "3.4. Effect of water hardness", we discussed competitive sorption between Cd(II) and Ca(II) or Mg(II), and no significance impacts on the sorption capacity were found even regarding to higher concentration (up to 100 mg/L) and higher complex formation constant (Ca(II): log K=10.69; Mg(II): log K=8.79, 25 °C).

The results indicate that the use of pH buffers would not have a significant impact on the Mag-Ligand sorption capacity of Cd^{2+}, and they can help to control the solution pH for testing.

2.5.3. Surface charge

The surface charge (zeta (ζ) potential) of the Mag-Ligand was measured with a Zetasizer Nano-ZS90 (Malvern, UK) using folded capillary cells. Each data point obtained with the Zetasizer was an average of three repetitions of 10 or more runs each. Figure S3 indicated the zeta (ζ) potential of Mag-Ligands as a function of pH.

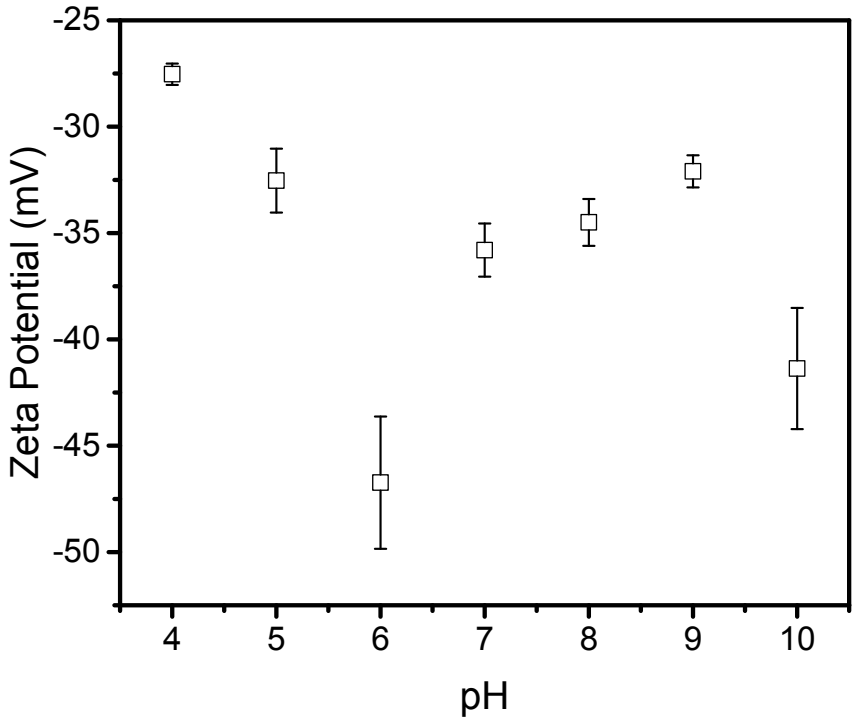

Figure S3. Mag-Ligand zeta potential as a function of pH.

Table S1. Comparison of adsorption capacities of various magnetic adsorbents for heavy metal ions (Dupont et al. 2014, Liu et al. 2013, Mahmoud et al. 2013, Zhang et al. 2011).

Magnetic Adsorbent	Metal	Optimum pH	Isotherm	q_{max}/mg/g	Ref.
Nano-Fe_3O_4-EDTA	Cu(II)	6.0	Langmuir	46.27	(Liu et al. 2013)
Nano-Fe_3O_4-SiO_2-TETA	Cu(II)	7.0	N/A	~30.50	(Mahmoud et al. 2013)
	Pb(II)	7.0	N/A	~62.1	
Fe_3O_4-NH_2/PEI-EDTA	Pb(II)	5.05	N/A	~19.76	(Zhang et al. 2011)
	Cu(II)	5.05	N/A	~19	
	Cd(II)	5.05	N/A	~18	
Fe_3O_4-TMS-EDTA	Gd(III)	6.3	N/A	113 ± 6	(Dupont et al. 2014)
Nano-Fe_2O_3-APTES-EDTA	Pb(II)		Langmuir	100.2	This work
	Cd(II)	3-7	Langmuir	79.4	

2.6. References

Adeleye, A., Keller, A., Miller, R. and Lenihan, H. (2013) Persistence of commercial nanoscaled zero-valent iron (nZVI) and by-products. Journal of Nanoparticle Research 15(1), 1-18.

Adeleye, A.S. and Keller, A.A. (2014) Long-term colloidal stability and metal leaching of single wall carbon nanotubes: effect of temperature and extracellular polymeric substances. Water Res 49(0), 236-250.

Alvarez, S.M., Gomez, N.N., Scardapane, L., Zirulnik, F., Martinez, D. and Gimenez, M.S. (2004) Morphological changes and oxidative stress in rat prostate exposed to a non-carcinogenic dose of cadmium. Toxicology Letters 153(3), 365-376.

Bagheri, H., Afkhami, A., Saber-Tehrani, M. and Khoshsafar, H. (2012) Preparation and characterization of magnetic nanocomposite of Schiff base/silica/magnetite as a preconcentration phase for the trace determination of heavy metal ions in water, food and biological samples using atomic absorption spectrometry. Talanta 97, 87-95.

Bandara, J.M.R.S., Senevirathna, D.M.A.N., Dasanayake, D.M.R.S.B., Herath, V., Bandara, J.M.R.P., Abeysekara, T. and Rajapaksha, K.H. (2008) Chronic renal failure among farm families in cascade irrigation systems in Sri Lanka associated with elevated dietary cadmium levels in rice and freshwater fish (Tilapia). Environmental Geochemistry and Health 30(5), 465-478.

Bernkop-Schnürch, A. and Krajicek, M.E. (1998) Mucoadhesive polymers as platforms for peroral peptide delivery and absorption: synthesis and evaluation of different chitosan–EDTA conjugates. Journal of controlled release 50(1), 215-223.

Bonda, E., Wlostowski, T. and Krasowska, A. (2004) Testicular toxicity induced by dietary cadmium is associated with decreased testicular zinc and increased hepatic and renal metallothionein and zinc in the bank vole (Clethrionomys glareolus). Biometals 17(6), 615-624.

Boudreau, J., Vincent, R., Nadeau, D., Trottier, B., Fournier, M., Krzystyniak, K. and Chevalier, G. (1988) Toxicity of Inhaled Cadmium Chloride - Early Responses of the Antioxidant and Surfactant Systems in Rat Lungs. Journal of Toxicology and Environmental Health 23(2), 241-256.

Clark, K.K. and Keller, A.A. (2012a) Adsorption of perchlorate and other oxyanions onto magnetic permanently confined micelle arrays (Mag-PCMAs). Water research 46(3), 635-644.

Clark, K.K. and Keller, A.A. (2012b) Investigation of two magnetic permanently confined micelle array sorbents using nonionic and cationic surfactants for the removal of PAHs and pesticides from aqueous media. Water, Air, & Soil Pollution 223(7), 3647-3655.

Coleman, N.T., Mcclung, A.C. and Moore, D.P. (1956) Formation Constants for Cu(Ii)-Peat Complexes. Science 123(3191), 330-331.

Dupont, D., Brullot, W., Bloemen, M., Verbiest, T. and Binnemans, K. (2014) Selective Uptake of Rare Earths from Aqueous Solutions by EDTA-Functionalized Magnetic and Nonmagnetic Nanoparticles. ACS Applied Materials & Interfaces 6(7), 4980-4988.

Faraji, M., Yamini, Y., Saleh, A., Rezaee, M., Ghambarian, M. and Hassani, R. (2010) A nanoparticle-based solid-phase extraction procedure followed by flow injection inductively coupled plasma-optical emission spectrometry to determine some heavy metal ions in water samples. Analytica Chimica Acta 659(1-2), 172-177.

Fthenakis, V.M. (2004) Life cycle impact analysis of cadmium in CdTe PV production. Renewable and Sustainable Energy Reviews 8(4), 303-334.

Ge, F., Li, M.M., Ye, H. and Zhao, B.X. (2012) Effective removal of heavy metal ions Cd2+, Zn2+, Pb2+, Cu2+ from aqueous solution by polymer-modified magnetic nanoparticles. Journal of Hazardous Materials 211, 366-372.

Gustafsson, J.P. (2006) Visual minteq. Capturado em de 26.

Harris, D.C. (2010) Quantitative chemical analysis, Macmillan.

Huang, Y.F., Li, Y., Jiang, Y. and Yan, X.P. (2010) Magnetic immobilization of amine-functionalized magnetite microspheres in a knotted reactor for on-line solid-phase extraction coupled with ICP-MS for speciation analysis of trace chromium. Journal of Analytical Atomic Spectrometry 25(9), 1467-1474.

Huang, Y.X. and Keller, A.A. (2013) Magnetic Nanoparticle Adsorbents for Emerging Organic Contaminants. Acs Sustainable Chemistry & Engineering 1(7), 731-736.

Huang, Y.X., Yang, J.K. and Keller, A.A. (2014) Removal of Arsenic and Phosphate from Aqueous Solution by Metal (Hydr-)oxide Coated Sand. Acs Sustainable Chemistry & Engineering 2(5), 1128-1138.

Hughes, M.A. and Rosenherg, E. (2007) Characterization and applications of poly-acetate modified silica polyamine composites. Separation science and technology 42(2), 261-283.

Islamoglu, S., Yilmaz, L. and Ozbelge, H.O. (2006) Development of a precipitation based separation scheme for selective removal and recovery of heavy metals from cadmium rich electroplating industry effluents. Separation Science and Technology 41(15), 3367-3385.

Jamall, I.S., Naik, M., Sprowls, J.J. and Trombetta, L.D. (1989) A Comparison of the Effects of Dietary-Cadmium on Heart and Kidney Antioxidant Enzymes - Evidence for the Greater Vulnerability of the Heart to Cadmium Toxicity. Journal of Applied Toxicology 9(5), 339-345.

Jiang, H.M., Yan, Z.P., Zhao, Y., Hu, X. and Lian, H.Z. (2012) Zincon-immobilized silica-coated magnetic Fe3O4 nanoparticles for solid-phase extraction and determination of trace lead in natural and drinking waters by graphite furnace atomic absorption spectrometry. Talanta 94, 251-256.

Júnior, O.K., Gurgel, L.V.A., de Freitas, R.P. and Gil, L.F. (2009) Adsorption of Cu (II), Cd (II), and Pb (II) from aqueous single metal solutions by mercerized cellulose and mercerized sugarcane bagasse chemically modified with EDTA dianhydride (EDTAD). Carbohydrate Polymers 77(3), 643-650.

Kah, M., Levy, L. and Brown, C. (2012) Potential for Effects of Land Contamination on Human Health. 1. The Case of Cadmium. Journal of Toxicology and Environmental Health-Part B-Critical Reviews 15(5), 348-363.

Karatapanis, A.E., Fiamegos, Y. and Stalikas, C.D. (2011) Silica-modified magnetic nanoparticles functionalized with cetylpyridinium bromide for the preconcentration of metals after complexation with 8-hydroxyquinoline. Talanta 84(3), 834-839.

Koehler, F.M., Rossier, M., Waelle, M., Athanassiou, E.K., Limbach, L.K., Grass, R.N., Gunther, D. and Stark, W.J. (2009) Magnetic EDTA: coupling heavy metal chelators to metal nanomagnets for rapid removal of cadmium, lead and copper from contaminated water. Chemical Communications (32), 4862-4864.

Koyuturk, M., Yanardag, R., Bolkent, S. and Tunali, S. (2007) The potential role of combined anti-oxidants against cadmium toxicity on liver of rats. Toxicology and Industrial Health 23(7), 393-401.

Kumar, P.S., Ramalingam, S., Senthamarai, C., Niranjanaa, M., Vijayalakshmi, P. and Sivanesan, S. (2010) Adsorption of dye from aqueous solution by cashew nut shell: Studies on equilibrium isotherm, kinetics and thermodynamics of interactions. Desalination 261(1-2), 52-60.

Liu, Y., Chen, M. and Yongmei, H. (2013) Study on the adsorption of Cu(II) by EDTA functionalized Fe3O4 magnetic nano-particles. Chemical Engineering Journal 218(0), 46-54.

Mahmoud, M.E., Abdelwahab, M.S. and Fathallah, E.M. (2013) Design of novel nano-sorbents based on nano-magnetic iron oxide–bound-nano-silicon oxide–immobilized-triethylenetetramine for implementation in water treatment of heavy metals. Chemical Engineering Journal 223(0), 318-327.

Martell, A.E. and Smith, R.M. (1989) Critical stability constants, Springer.

Martinez, M., Miralles, N., Hidalgo, S., Fiol, N., Villaescusa, I. and Poch, J. (2006) Removal of lead(II) and cadmium(II) from aqueous solutions using grape stalk waste. Journal of Hazardous Materials 133(1-3), 203-211.

Morel, F.M.M. and Hering, J.G. (1993) Principles and Applications of Aquatic Chemistry, Wiley.

Mortvedt, J.J. and Osborn, G. (1982) Studies on the Chemical Form of Cadmium Contaminants in Phosphate Fertilizers. Soil Science 134(3), 185-192.

Ngah, W.S.W. and Hanafiah, M.A.K.M. (2008) Removal of heavy metal ions from wastewater by chemically modified plant wastes as adsorbents: A review. Bioresource Technology 99(10), 3935-3948.

Pereira, F.V., Gurgel, L.V.A. and Gil, L.F. (2010) Removal of Zn2+ from aqueous single metal solutions and electroplating wastewater with wood sawdust and sugarcane bagasse modified with EDTA dianhydride (EDTAD). Journal of hazardous materials 176(1-3), 856-863.

Reimann, C. and de Caritat, P. (2005) Distinguishing between natural and anthropogenic sources for elements in the environment: regional geochemical surveys versus enrichment factors. Science of the Total Environment 337(1-3), 91-107.

Repo, E., Kurniawan, T.A., Warchol, J.K. and Sillanpaa, M.E.T. (2009) Removal of Co(II) and Ni(II) ions from contaminated water using silica gel functionalized with EDTA and/or DTPA as chelating agents. Journal of hazardous materials 171(1-3), 1071-1080.

Repo, E., Warchol, J.K., Bhatnagar, A. and Sillanpaa, M. (2011) Heavy metals adsorption by novel EDTA-modified chitosan-silica hybrid materials. Journal of Colloid and Interface Science 358(1), 261-267.

Repo, E., Warchol, J.K., Kurniawan, T.A. and Sillanpaa, M.E.T. (2010) Adsorption of Co(II) and Ni(II) by EDTA- and/or DTPA-modified chitosan: Kinetic and equilibrium modeling. Chemical Engineering Journal 161(1-2), 73-82.

Sekar, M., Sakthi, V. and Rengaraj, S. (2004) Kinetics and equilibrium adsorption study of lead(II) onto activated carbon prepared from coconut shell. Journal of Colloid and Interface Science 279(2), 307-313.

Shute, T. and Macfie, S.M. (2006) Cadmium and zinc accumulation in soybean: A threat to food safety? Science of the Total Environment 371(1-3), 63-73.

Su, Y., Adeleye, A.S., Keller, A.A., Huang, Y., Dai, C., Zhou, X. and Zhang, Y. (2015) Magnetic sulfide-modified nanoscale zerovalent iron (S-nZVI) for dissolved metal ion removal. Water Research.

Su, Y.M., Adeleye, A.S., Huang, Y.X., Sun, X.Y., Dai, C.M., Zhou, X.F., Zhang, Y.L. and Keller, A.A. (2014) Simultaneous removal of cadmium and nitrate in aqueous media by nanoscale zerovalent iron (nZVI) and Au doped nZVI particles. Water Research 63, 102-111.

Tête, N., Durfort, M., Rieffel, D., Scheifler, R. and Sánchez-Chardi, A. (2014) Histopathology related to cadmium and lead bioaccumulation in chronically exposed wood mice, Apodemus sylvaticus, around a former smelter. Science of the Total Environment 481, 167-177.

Vouk, V.B. and Piver, W.T. (1983) Metallic Elements in Fossil-Fuel Combustion Products - Amounts and Form of Emissions and Evaluation of Carcinogenicity and Mutagenicity. Environmental Health Perspectives 47(Jan), 201-225.

Vromman, V., Saegerman, C., Pussemier, L., Huyghebaert, A., Temmerman, L.D., Pizzolon, J.-C. and Waegeneers, N. (2008) Cadmium in the food chain near non-ferrous metal production sites. Food additives and contaminants 25(3), 293-301.

Wang, H., Keller, A.A. and Clark, K.K. (2011) Natural organic matter removal by adsorption onto magnetic permanently confined micelle arrays. Journal of Hazardous Materials 194, 156-161.

Wang, L.Y., Yang, L.Q., Li, Y.F., Zhang, Y., Ma, X.J. and Ye, Z.F. (2010) Study on adsorption mechanism of Pb(II) and Cu(II) in aqueous solution using PS-EDTA resin. Chemical Engineering Journal 163(3), 364-372.

Wang, P., Shi, Q., Shi, Y., Clark, K.K., Stucky, G.D. and Keller, A.A. (2008) Magnetic permanently confined micelle arrays for treating hydrophobic organic compound contamination. Journal of the American Chemical Society 131(1), 182-188.

Wendlandt, W.W. (1960) Thermogravimetric and Differential Thermal Analysis of (Ethylenedinitrilo)Tetraacetic Acid and Its Derivatives. Analytical Chemistry 32(7), 848-850.

Xie, Y. and Giammar, D.E. (2011) Effects of flow and water chemistry on lead release rates from pipe scales. Water Research 45(19), 6525-6534.

Xiong, Z.G., Zhang, L.L., Ma, J.Z. and Zhao, X.S. (2010) Photocatalytic degradation of dyes over graphene-gold nanocomposites under visible light irradiation. Chemical Communications 46(33), 6099-6101.

Yamaura, M., Camilo, R.L., Sampaio, L.C., Macedo, M.A., Nakamura, M. and Toma, H.E. (2004) Preparation and characterization of (3-aminopropyl) triethoxysilane-coated magnetite nanoparticles. Journal of Magnetism and Magnetic Materials 279(2-3), 210-217.

Yappert, M.C. and DuPre, D.B. (1997) Complexometric titrations: Competition of complexing agents in the determination of water hardness with EDTA. Journal of Chemical Education 74(12), 1422-1423.

Yu, J.X., Tong, M., Sun, X.M. and Li, B.H. (2008) Enhanced and selective adsorption of Pb2+ and Cu2+ by EDTAD-modified biomass of baker's yeast. Bioresource Technology 99(7), 2588-2593.

Zhang, F., Zhu, Z., Dong, Z., Cui, Z., Wang, H., Hu, W., Zhao, P., Wang, P., Wei, S., Li, R. and Ma, J. (2011) Magnetically recoverable facile nanomaterials: Synthesis, characterization and application in remediation of heavy metals. Microchemical Journal 98(2), 328-333.

Zirino, A. and Yamamoto, S. (1972) A pH-dependent model for the chemical speciation of copper, zinc, cadmium and lead in seawater. Limnol. Oceanogr 17(5), 661-671.

Chapter 3. Adsorptive Removal of Multiple Metal Ions from Contaminated Water with EDTA Functionalized Superparamagnetic Nanoparticles: Equilibrium, Kinetics and Thermodynamics

3.1. Introduction

Chromium (Cr), mercury (Hg), cadmium (Cd), lead (Pb), zinc (Zn) and copper (Cu) are considered hazardous metals as well as significant threat to the environment and public health due to their high toxicity and accumulative characteristics (Ge et al. 2012). They can be released into the environment through a number of activities, such as mining, metal processing and finishing, welding and alloy manufacturing (Fu and Wang 2011) , the use of metals in vehicles, coal combustion, as well as volcanic eruptions and forest fires (Huang and Keller 2015). These metals can enter the food supply chain via pesticides or fertilizers where they are found as impurities, causing progressive toxic effects with gradual accumulation in living organisms over their life span (Huang et al. 2014, Su et al. 2015, Su et al. 2014). Therefore, to develop effective and rapid metal remediation techniques is of great importance.

Recently, magnetic core hybrid nanoparticles have been proposed as sorbents for environmental decontamination (Huang and Keller 2013, 2015, Su et al. 2015, Su et al. 2014). Besides the relatively large surface area, and high ratio of surface-to-volume, these novel sorbents could take advantage of their superparamagnetic nature in post-treatment separation, which simply involves applying an external magnetic field to extract the adsorbents. In this way, these sorbents can overcome many of the issues present in filtration, centrifugation or gravitational separation, generally requiring less energy to achieve a given

level of separation, providing a more sustainable approach. In previous studies, these magnetic nanoparticle sorbents had successfully been applied to remove heavy metal ions (Huang and Keller 2015), hydrophobic compounds (Wang et al. 2008), pesticides (Clark and Keller 2012b), natural organic matter (Wang et al. 2011), oxyanions (Clark and Keller 2012a) and emerging organic contaminants (Huang and Keller 2013).

In a recent study (Huang and Keller 2015), we reported a magnetic nanoparticle sorbent, namely Mag-Ligand, which is structured as a magnetic nano-scale core coated with a silica porous layer that covalently bonds with an organic ligand, ethylenediaminetetraacetic acid (EDTA). The attached EDTA can bind the dissolved metal ion contaminant, while the magnetic core allows for rapid separation of the Mag-Ligand from solution by applying a magnetic field. Mag-Ligands have proven to be effective sorbents for removal of individual metal ions such as Cd^{2+} and Pb^{2+} under various environmental conditions (e.g. range of pH and water hardness) as well as showing good regenerability and reusability.

However, in realistic aquatic systems, like industrial wastewater, there are usually several metal ions. It's important to evaluate the remediation performance of Mag-Ligand for multiple metal ions in competitive sorption. In addition, though the primary application of Mag-Ligand is wastewater treatment, it could be extended to adsorb or collect ions of valuable elements, for instance, rare earth elements from process water, contaminated groundwater or mining leachate. Furthermore, to scale the use of Mag-Ligand for real world applications, a quantitative knowledge of the kinetics and thermodynamics of Mag-Ligand/metal ion interactions is needed to ascertain the minimum amount of Mag-Ligand particles needed to remove metal cations to a specified level in complex matrices with multiple metals.

In this study, we evaluated the adsorption capacity, isotherms and kinetics of nine different metal ions, including three rare earth elements, onto Mag-Ligand, at different initial metal ion concentrations in individual sorption. In addition, we determined the remediation performance of Mag-Ligand for Pb^{2+} removal under various environmental conditions (e.g. range of pH and water hardness). Three groups of competitive sorption studies were conducted to determine the selectivity sequence among multiple metal ions. Isothermal titration microcalorimetry (ITC) was used to obtain key quantitative thermodynamic binding data of the interactions between Mag-Ligand and metal ions, providing the enthalpy, entropy and free energy of binding values as well as binding constants. The results demonstrated that Mag-Ligand is a rapid, effective, regenerable and more sustainable sorbent for removal of multiple metal ions. Furthermore, Mag-Ligand can also have wide application in the recovery of highly valuable elements such as rare earth elements with stable removal performance across a range of pH and water hardness.

3.2. Experimental

3.2.1. Chemicals

Maghemite (iron (III) oxide) nanoparticles (30 nm in diameter), indium (III) chloride and pyridine were purchased from Alfa Aesar (USA). (3-aminopropyl)triethoxysilane (99%) were purchased from Sigma-Aldrich (USA). Cadmium chloride anhydrous, lead chloride, ethylenediaminetetraacetic acid (EDTA), sodium bicarbonate were purchased from Fisher Scientific (USA). Mercury (II) nitrate monohydrate, zinc (II) chloride, copper (II) chloride, gallium (III) chloride, cerium (III) chloride, chromium (III) chloride and diethylether were purchased from Acros Organics (Geel, Belgium). Toluene was purchased from EMD Millipore (USA). All chemicals were used as received, without further purification. All

solutions were prepared with deionized water (18 MΩ-cm) from a Barnstead NANOpure Diamond Water Purification System (USA).

3.2.2. Batch sorption of metal ions

For most experiments 5.0 mg of Mag-Ligand particles were mixed with 25 mL of metal ion (Cd^{2+}/Pb^{2+}/Cu^{2+}/Zn^{2+}/Hg^{2+}/Cr^{3+}/Ga^{3+}/In^{3+}/Ce^{3+}) solution (10 mg/L) in 50 mL conical tubes, and pH was adjusted by using 0.1 M NaOH and HCl. Then, these tubes were mixed in an end-over-end shaker on a Dayton-6Z412A Parallel Shaft (USA) roller mixer with a speed of 70 rpm at room temperature for 24 h to ensure sufficient equilibration time. Adsorption kinetics studies were carried out at the same conditions as previously stated but for a set amount of time, varying from 1 min to 24 h, with pH = 7. After mixing the Mag-Ligand particles with dissolved contaminants for a specified time, the particles were separated from the mixture with the Eclipse magnet. All experiments were conducted at ambient temperature (22-25 °C).

Competitive sorption was conducted in three groups: (1) Cd^{2+} and Pb^{2+}, for which Mag-Ligand has the highest sorption capacity; (2) rare earth elements: Ga^{3+}, In^{3+} and Ce^{3+}; (3) six non-rare earth elements: Cd^{2+}, Pb^{2+}, Cu^{2+}, Zn^{2+}, Hg^{2+} and Cr^{3+}. In each group, 10 mg of Mag-Ligand particles were mixed with 25 mL of equal concentrations (varied from 1 to 20 mg/L) of each metal ion.

The concentration of adsorbent was varied from 0.04 to 0.28 g/L to study the adsorption isotherms of metal ions onto Mag-Ligand at pH 7. Additionally, solutions with varying initial concentrations of metal ions, which ranged from 1 mg/L to 30 mg/L were treated with the same procedure as above at pH 7 and 5.0 mg Mag-Ligand.

A Thermo iCAP 6300 inductively coupled plasma with atomic emission spectroscopy (ICP-AES) was used to analyze the concentration of metal ions.

3.2.3. Binding constant between metal ions and Mag-Ligand

A TA Instruments Nano Isothermal Titration Calorimeter（ITC) instrument was used to measure the heat exchange between Mag-Ligand particles and metal ions at 298 K to determine the binding constants. Generally, a well-dispersed suspension of Mag-Ligand particles (degassed DI water) was placed in the 1 mL ITC sample cell, and a metal ion(s) solution (1000 mg/L) was loaded into the 100 μL injection syringe. Metal ions were titrated into the sample cell as a sequence of 20 injections of 4.91 μL aliquots. The rotational speed of the stirrer was 250 min^{-1} and the equilibrium time between two injections was set at 800 s for the signal to return to the baseline.

Estimated binding parameters were obtained from the ITC data using the NanoAnalyze Data Analysis software (Version 3.30). Data fits were obtained using the independent set of multiple binding sites model (Freire et al. 1990), for which the analytical solution for the total heat measured, Q (kJ) is determined by the formula:

$$Q = \frac{\left(1+[M]nK+K_d[L_T]\right)-\left[\left(1+[M]nK_d+K_d[L_T]\right)^2-4[M]nK_d{}^2[L_T]\right]^{1/2}}{\frac{2K_d}{V\Delta H}} \quad (1)$$

Where V is the volume of the calorimeter cell, ΔH is enthalpy (kJ/mol), $[L_T]$ is metal ions concentration, [M] is Mag-Ligand particles concentration, n is the molar ratio of interacting species, and K_d (M^{-1}) is the equilibrium binding constant. Free energy, ΔG (kJ/mol), was determined from the binding constant ($\Delta G = -RT\ln K$, where R is the gas

constant and T is the absolute temperature in Kelvin) and entropy, ΔS (kJ/mol), from the second law of thermodynamics ($\Delta G = \Delta H - T\Delta S$).

3.3. Results and discussion

3.3.1. Sorption isotherms of individual metal ions

Figure 1 presents the experimental results of the non-competitive sorption for each metal ion (Cr^{3+}, Cu^{2+}, Ce^{3+}, Zn^{2+}, In^{3+}, Ga^{3+}, Hg^{2+}, Cd^{2+} and Pb^{2+}) for the range of concentrations studied, as well as the fit of the Langmuir isotherm model (fitted parameter values are summarized in Table 1.).

Pb^{2+} exhibited the highest adsorption capacity onto Mag-Ligand (112.4 mg/g) while Cr^{3+} exhibited the lowest sorption capacity (18.17 mg/g). These differences reflect the different interaction strengths between the individual metal ions and Mag-Ligand particles. Interestingly these results do not follow the sequence in conventional formation constants for metal-EDTA complexes(Harris 2010) (log K, 25 °C) strictly, which are 23.40 for Cr^{3+} and 18.04 for Pb^{2+}. According to our previous study(Huang and Keller 2015), EDTA was covalently attached to the APTES coated maghemite nanoparticles by the formation of amide bonds between the carboxylic acid groups of the complexing agent and amino groups provided by the APTES coating. This covalent attachment would make EDTA loose at least one of its carboxylic acid groups, which would have influence on its complexing capability (BernkopSchnurch et al. 1997). Therefore, the binding capacity of EDTA attached to Mag-Ligand particles is different from the unbound EDTA. The binding constants and thermodynamic data between Mag-Ligand particles and each individual metal ion specifically will be investigated in the following sections.

3.3.2. Sorption kinetics of individual metal ions

Time dependent removal of metal ions (initial concentration= 10 mg/L) by Mag-Ligand (0.2 g/L) showed rapid adsorption of Pb^{2+} in the first 15 minutes with above 97% removal efficiency, and thereafter, the rate decreased gradually and reached equilibrium, as shown in Figure 2A. Since most of the metal ion sorption onto Mag-Ligand occurred in the first 15 minutes, the individual metal ions sorption kinetics were conducted with mixing times of 1, 5, 10, 15 and 30 minutes. The kinetic model was then used to investigate the adsorption rate (Figure 2B). The removal of metal ions by Mag-Ligand particles followed pseudo-second-order (R^2>0.99), as summarized in Table 2. The effective ionic radius of each metal ion serves to determine the adsorption rate (Unlu and Ersoz 2006), as generally reflected by the relation between ionic radius and k_2 (Figure 2C). Smaller metal ions such as Cr^{3+} and Cu^{2+} have much faster equilibrium rates than larger ions (e.g. Cd^{2+} and Pb^{2+}). This result can be expected because the adsorption is controlled either by diffusion into Mag-Ligand's porous structure or by a second-order chemical reaction (Kantipuly et al. 1990) with the chelating functional groups present on Mag-Ligand's surface (Huang and Keller 2015), both of which are influenced by metal ion size.

3.3.3. Competitive sorption of multiple metal ions

Since waste water usually contains a wide variety of dissolved metal ions we conducted competitive sorption with three groups of metal ions, with equal initial metal ion concentrations ranging from 1 to 20 mg/L. In Group 1 (Cd^{2+} and Pb^{2+}) removal efficiency of both metal ions increased first and then decreased with increasing initial ion concentration, once the maximum adsorption capacity was reached (Figure 3A). In Group 2 (Ga^{3+}, In^{3+} and Ce^{3+}) and Group 3 (Cd^{2+}, Pb^{2+}, Cu^{2+},Zn^{2+}, Hg^{2+} and Cr^{3+}), the removal efficiency of all the

metal ions decreased with increasing initial ion concentration, as shown in Figure 3B and 3C, respectively.

Figure 3A indicates that Mag-Ligand has stronger affinity for Pb^{2+} than Cd^{2+} in competitive sorption, with the maximum adsorption capacity of 49.6 mg/g for Pb^{2+} and 19.3 mg/g for Cd^{2+} (Table S3), which agreed with the trend in individual sorption (Table 1). A similar trend was observed in Group 2 (Figure 3 B), where the affinity was $Ga^{3+} > In^{3+} > Ce^{3+}$, which also followed the sequence of individual sorption (Table 1).

However, in Group 3 Cu^{2+} had much higher sorption capacity (21.4 mg/g) than other metal ions, especially at the higher initial concentration range (Figure 3C), while, Cu^{2+} exhibited relatively lower sorption capacity in individual sorption compared to other metal ions (Table 1). This could reflect the faster kinetics of Cu^{2+} (Table 2), with a larger rate constant (7.6 g/h·mg).

The competitive isotherm sorption data was analyzed using the Langmuir isotherm model (Figure S3A, S3B and S3C), and the fitted parameters are listed in Table S1. The maximum adsorption capacities of all metal ions onto Mag-Ligand in competitive sorption (Table S1) are noticeably lower than that in individual sorption (Table 1). This is expected since there are a fixed number of adsorption sites on the Mag-Ligand particles which are shared by the various metal ions (Huang and Keller 2015).

As shown in Figure 4, the trend in maximum adsorption capacity of metal ions onto Mag-Ligand in competitive sorption (based on the Langmuir model) generally agreed with the sequence of k_2 (equilibrium kinetic rate constant). Thus, in competitive sorption, as the number of binding sites on Mag-Ligand particles is limited, metal ions with higher adsorption rate occupy the sites first, leading to higher removal rate, regardless of the affinity. This also explains the fact that Cu^{2+} showed slightly lower removal efficiency than other

metal ions at low initial concentration (Figure 3C), as there were sufficient absorption sites and Cu^{2+} has lower affinity to Mag-Ligand.

3.3.4. Binding constants between Mag-Ligand and metal ions

To quantify the strength of binding of various metal ions to the Mag-Ligand particles, nine different metal cations were titrated into a suspension with Mag-Ligand particles in individual experiments using ITC. The integrated binding isotherms for metal ions are presented in Figure 5 (A), and the independent set of multiple binding sites model (Equation 1) was applied to calculate the thermodynamic parameters (Table 3). Cr^{3+} has the weakest interaction toward Mag-Ligand with a binding constant of 3.492×10^2 M^{-1}, while Pb^{2+} showed the highest affinity with a binding constant of 4.412×10^3 M^{-1}, which is more than a 10-fold difference. Table 3 indicates the sequence of the metal ion affinity to Mag-Ligand, which follows the pattern $Cr^{3+} < Cu^{2+} < Zn^{2+} < Ga^{3+} < Cd^{2+} < In^{3+} < Ce^{3+} < Hg^{2+} < Pb^{2+}$. This trend is similar to the sequence of maximum sorption capacity predicted by the Langmuir isotherm sorption model (Figure 5B).

The difference in magnitude of binding for Mag-Ligand with different metal ions is likely the result of a combination of several factors, including the geometry of the metal complexes, ionic radii of the metal cations and metal valence. A similar trend in sorption capacity and kinetic rate and binding constants indicated that the most likely mechanisms of interactions between metal ions and Mag-Ligand are complexation reactions and adsorption onto porous structures.

All metal Mag-Ligand interactions showed negative enthalpy (ΔH) of reaction values at 25 °C (Table 3), implying that these interactions are all enthalpically favored. We obtained negative changes in the entropy (ΔS) of binding and negative changes in the free energy (ΔG)

of reaction values in our experiments, indicating all of the studied metal Mag-Ligand interactions are enthalpically driven reactions as well as energetically favored at 25 °C.

3.4. Conclusions

We demonstrated that the Mag-Ligand is an effective and efficient sorbents because of fast removal rate, high sorption capacity and convenient application to removal of multiple metal ions from contaminated aqueous systems. Mag-Ligand can also have wide application in the recovery of highly valuable elements such as rare earths. Mag-Ligand exhibits stable removal performance across a range of pH and water hardness. In individual sorption experiments, Pb^{2+} showed highest sorption capacity (112.4 mg/g) following by Cd^{2+}, Hg^{2+}, Ga^{3+}, In^{3+}, Zn^{2+}, Ce^{3+}, Cu^{2+}, while Cr^{3+} has the lowest sorption capacity (18.17 mg/g). A similar trend was observed in competitive sorption experiments, except that Cu^{2+} is preferentially adsorbed due to its higher sorption kinetic rate constant. The kinetic and thermodynamic parameters for chelation reactions between metal cation and Mag-Ligand particles were determined, giving the sequence of binding constants as: $Cr^{3+} < Cu^{2+} < Zn^{2+} < Ga^{3+} < Cd^{2+} < In^{3+} < Ce^{3+} < Hg^{2+} < Pb^{2+}$. The difference in magnitude of binding of Mag-Ligand with different metal ions is likely the result of a combination of several factors, including the geometry of the metal complexes, ionic radii of the metal cations and metal valence. The similar trend in sorption capacity and kinetic rate constant and binding constants indicated that the most likely mechanisms of interactions between metal ions and Mag-Ligand are complexation reactions and adsorption onto porous structures.

Table 1. Langmuir isotherm model fitted parameters for sorption of each individual metal ion onto Mag-Ligand

Element	q_m (mg/g)	K_L (L/mg)	R^2
Cr^{3+}	18.17	3.154	1.000
Cu^{2+}	23.09	-2.221	0.937
Ce^{3+}	27.56	14.69	0.988
Zn^{2+}	33.28	4.645	0.973
In^{3+}	34.21	4.684	0.967
Ga^{3+}	36.91	3.229	0.990
Hg^{2+}	74.97	12.83	0.961
Cd^{2+}	79.37	7.200	0.980
Pb^{2+}	112.4	12.30	0.769

Table 2. Pseudo-second-order model fitted parameters for the adsorption kinetics of each individual metal ion onto Mag-Ligand

Element	q_e (mg/g)	k_2 (g/h·mg)	R^2
Cu^{2+}	25.71	7.566	0.997
Hg^{2+}	42.02	2.832	1.000
Cd^{2+}	34.84	2.746	0.991
Pb^{2+}	55.87	1.602	0.999
Zn^{2+}	23.26	1.027	0.999
Cr^{3+}	5.084	17.59	0.995
Ga^{3+}	13.64	5.373	0.990
In^{3+}	16.50	4.590	0.998
Ce^{3+}	22.37	2.220	0.996

Table 3. Fitting parameters ΔH, Kd and n from ITC analysis of the integrated heats with independent model and calculated ΔG and ΔS from K_d and ΔH values.

Element	ΔH (kJ/mol)	K_d (M^{-1})	n	ΔG (kJ/mol)	ΔS (kJ/K·mol)
Cr^{3+}	-2.167×10^{3}	3.492×10^{2}	0.100	-15.44	-7.220
Cu^{2+}	-2.068×10^{3}	6.554×10^{2}	0.100	-16.87	-6.883
Zn^{2+}	-2.084×10^{3}	5.816×10^{2}	0.100	-16.48	-6.938
Ga^{3+}	-4.414×10^{2}	8.065×10^{2}	0.685	-16.75	-1.425
Cd^{2+}	-3.230×10^{3}	7.915×10^{2}	0.100	-17.86	-10.78
In^{3+}	-3.431×10^{2}	1.299×10^{3}	0.666	-17.98	-1.091
Ce^{3+}	-2.450×10^{2}	1.448×10^{3}	0.569	-18.13	-0.761
Hg^{2+}	-1.937×10^{3}	3.275×10^{3}	0.100	-21.46	-6.428
Pb^{2+}	-5.578×10^{2}	4.412×10^{3}	0.100	-21.10	-1.801

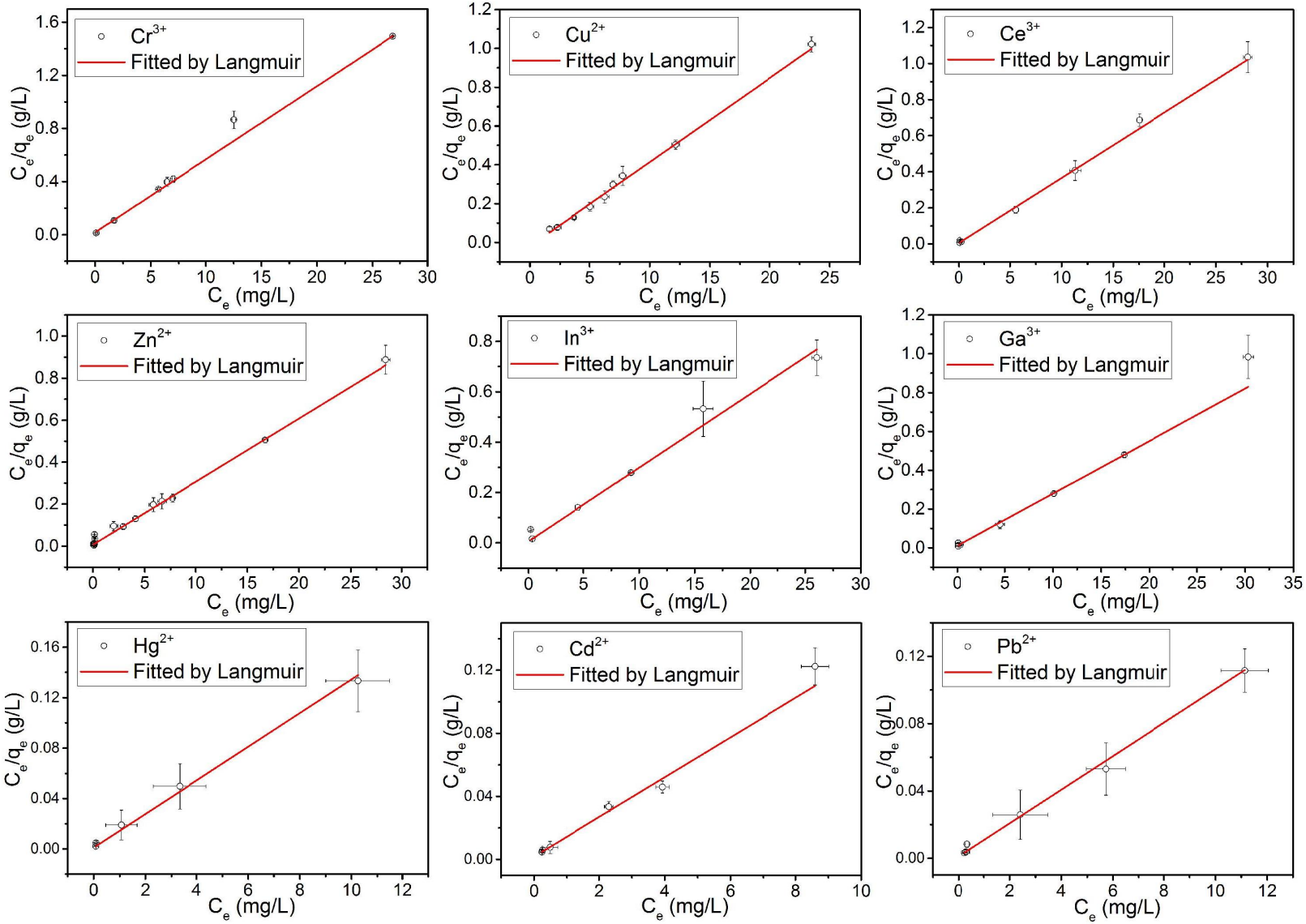
Cr3+
Fitted by Langmuir
Cu2+
Fitted by Langmuir
Ce3+
Fitted by Langmuir
Zn2+
Fitted by Langmuir
In3+
Fitted by Langmuir
Ga3+
Fitted by Langmuir
Hg2+
Fitted by Langmuir
Cd2+
Fitted by Langmuir
Pb2+
Fitted by Langmuir
Ce/qe (g/L)
Ce (mg/L)

Figure 1. Adsorption of individual metal ions (Cr^{3+}, Cu^{2+}, Ce^{3+}, Zn^{2+}, In^{3+}, Ga^{3+}, Hg^{2+}, Cd^{2+} and Pb^{2+}) onto Mag-Ligand with Langmuir adsorption isotherms fit at pH 7, symbols represent experimental data, error bars represent standard deviation from the mean (n =3), and red line represents model prediction.

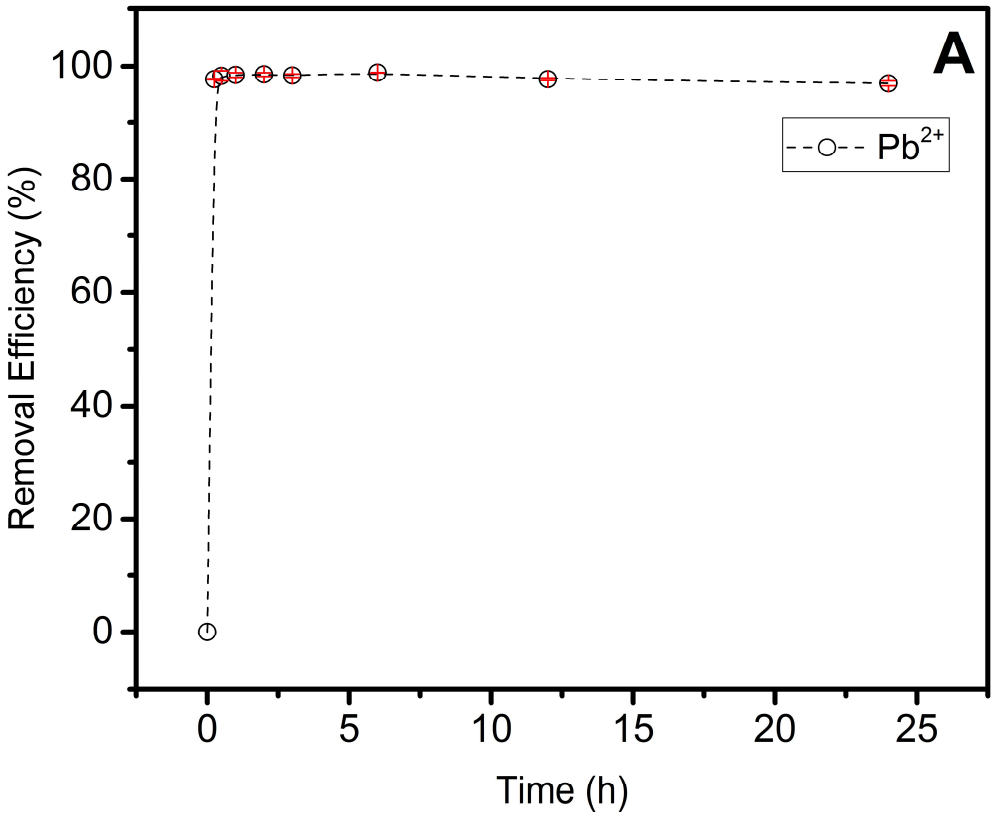

B

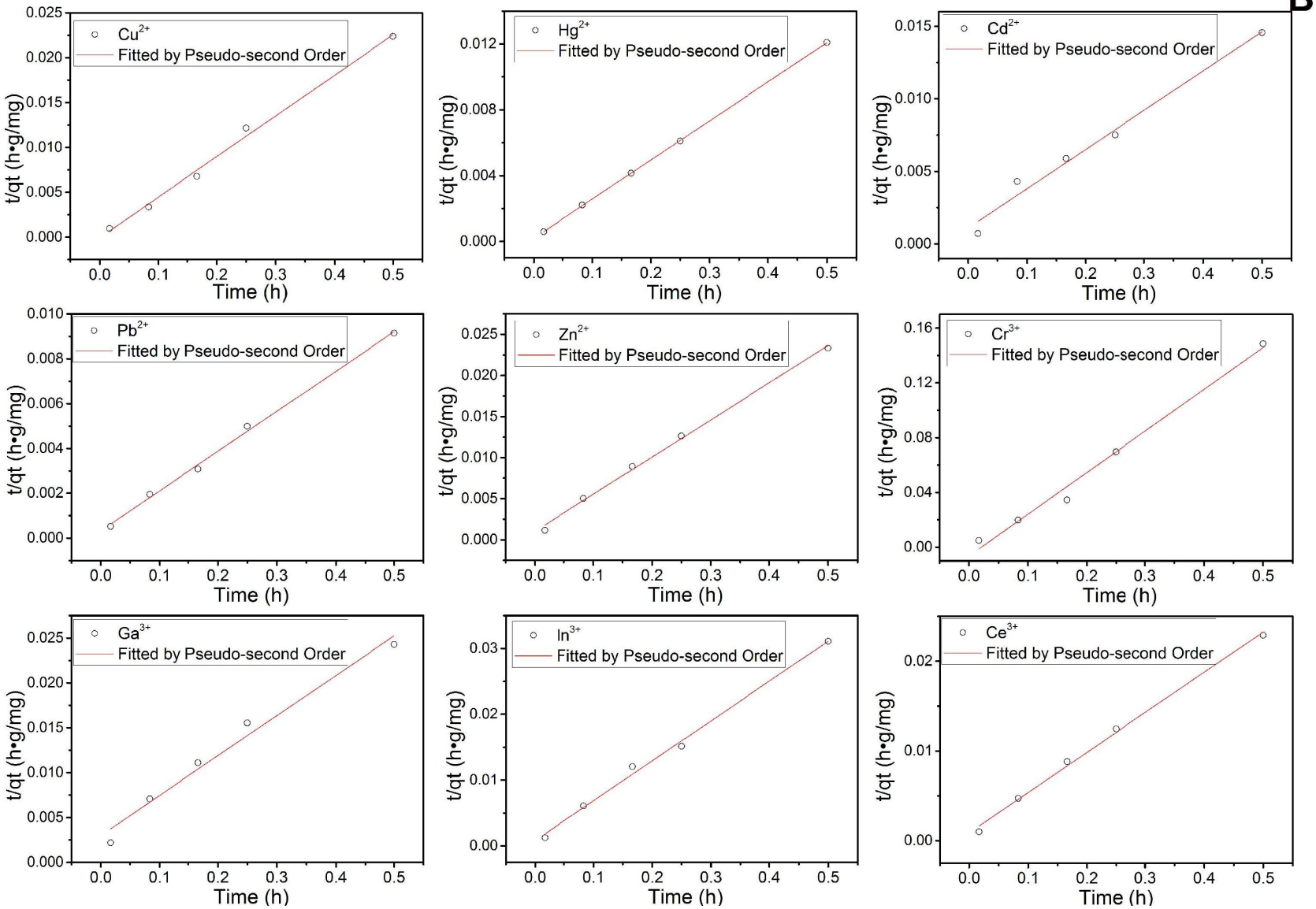
Cu2+
Fitted by Pseudo-second Order
Hg2+
Fitted by Pseudo-second Order
Cd2+
Fitted by Pseudo-second Order
Pb2+
Fitted by Pseudo-second Order
Zn2+
Fitted by Pseudo-second Order
Cr3+
Fitted by Pseudo-second Order
Ga3+
Fitted by Pseudo-second Order
In3+
Fitted by Pseudo-second Order
Ce3+
Fitted by Pseudo-second Order
t/qt (h•g/mg)
Time (h)

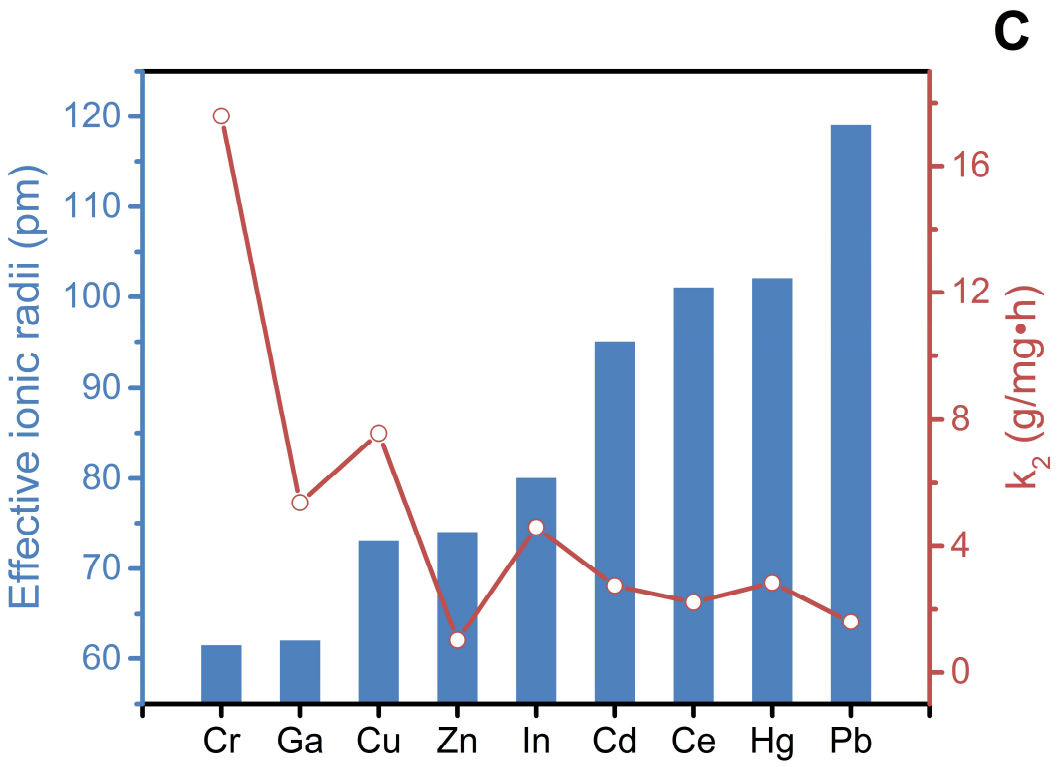

Figure 2. (A) Pb^{2+} sorption uptake versus time at pH 7; (B) individual metal ions (Cu^{2+}, Hg^{2+}, Cd^{2+}, Pb^{2+}, Zn^{2+}, Cr^{3+}, Ga^{3+}, In^{3+} and Ce^{3+}) sorption kinetics fitted by Pseudo-second order onto Mag-Ligand in solution at pH 7; (C) equilibrium rate constants of kinetics k_2 (red dots) versus effective ionic radii (blue bars)(Shannon 1976) (in pm, 1 pm=10^{-12}m), data for ionic radii from Shannon, 1976 (Shannon 1976),

A

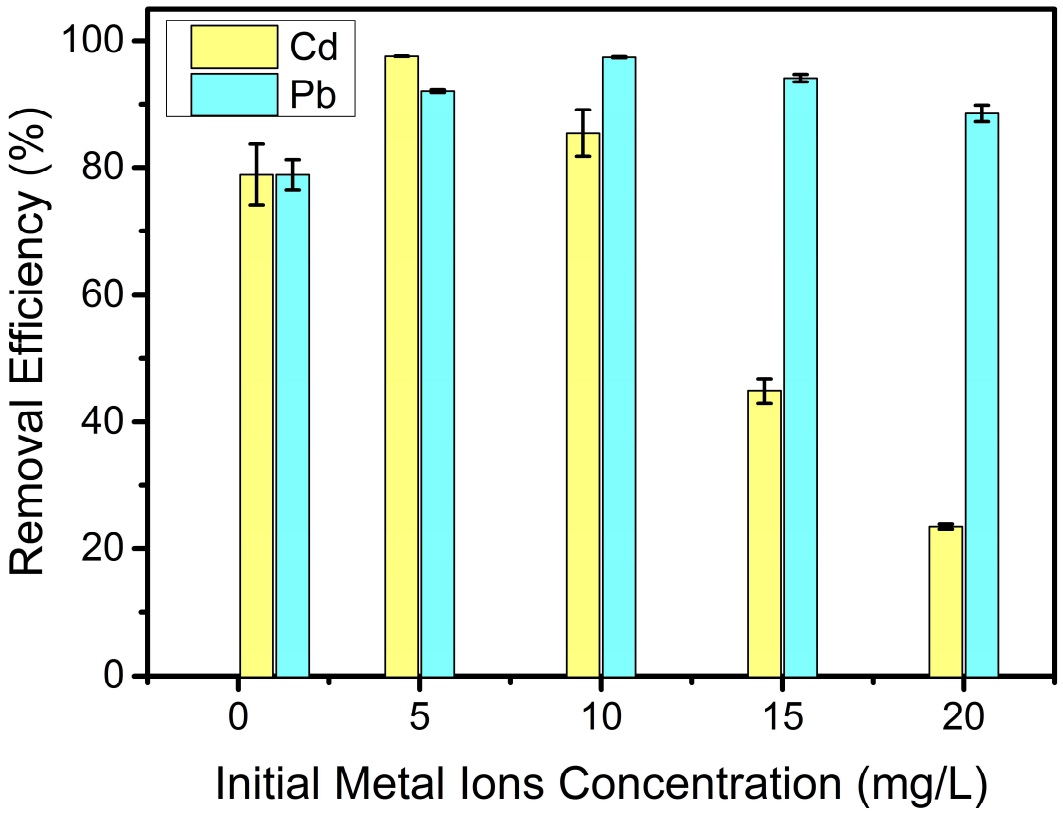
Cd
Pb
Removal Efficiency (%)
100
80
60
40
20
0
0
5
10
15
20
Initial Metal Ions Concentration (mg/L)

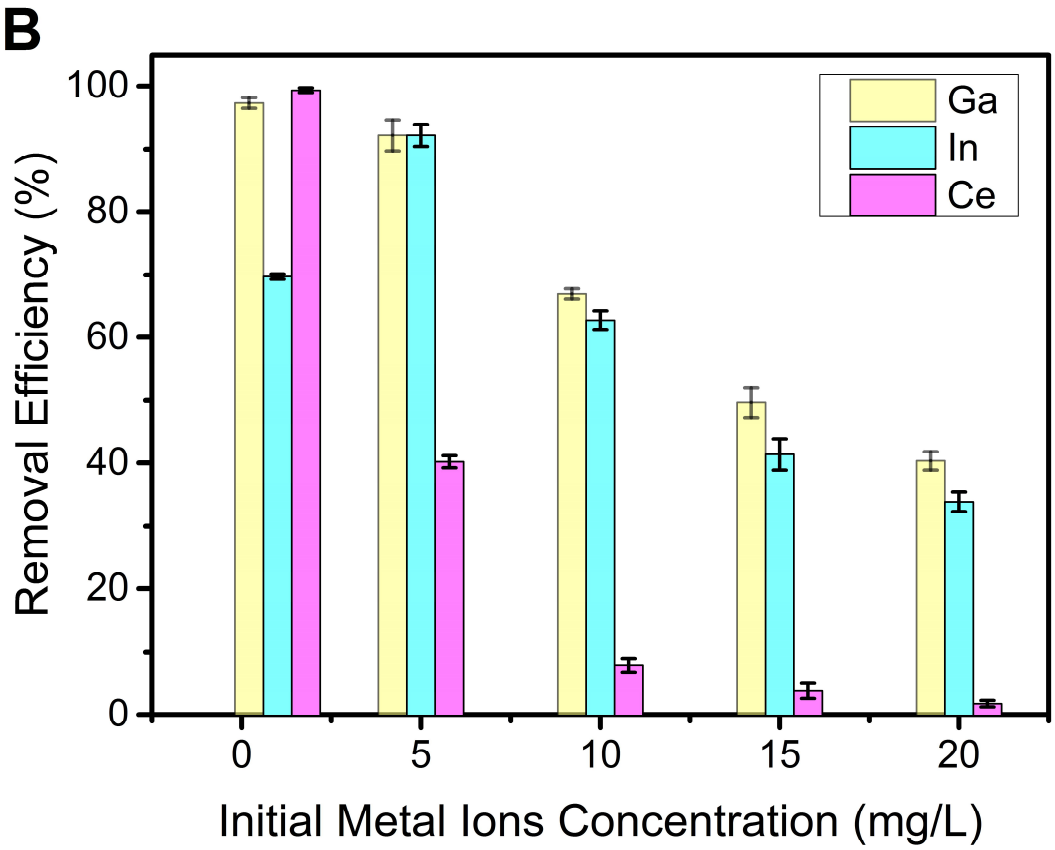
B
Removal Efficiency (%)
100
80
60
40
20
0
0
5
10
15
20
Initial Metal Ions Concentration (mg/L)
Ga
In
Ce

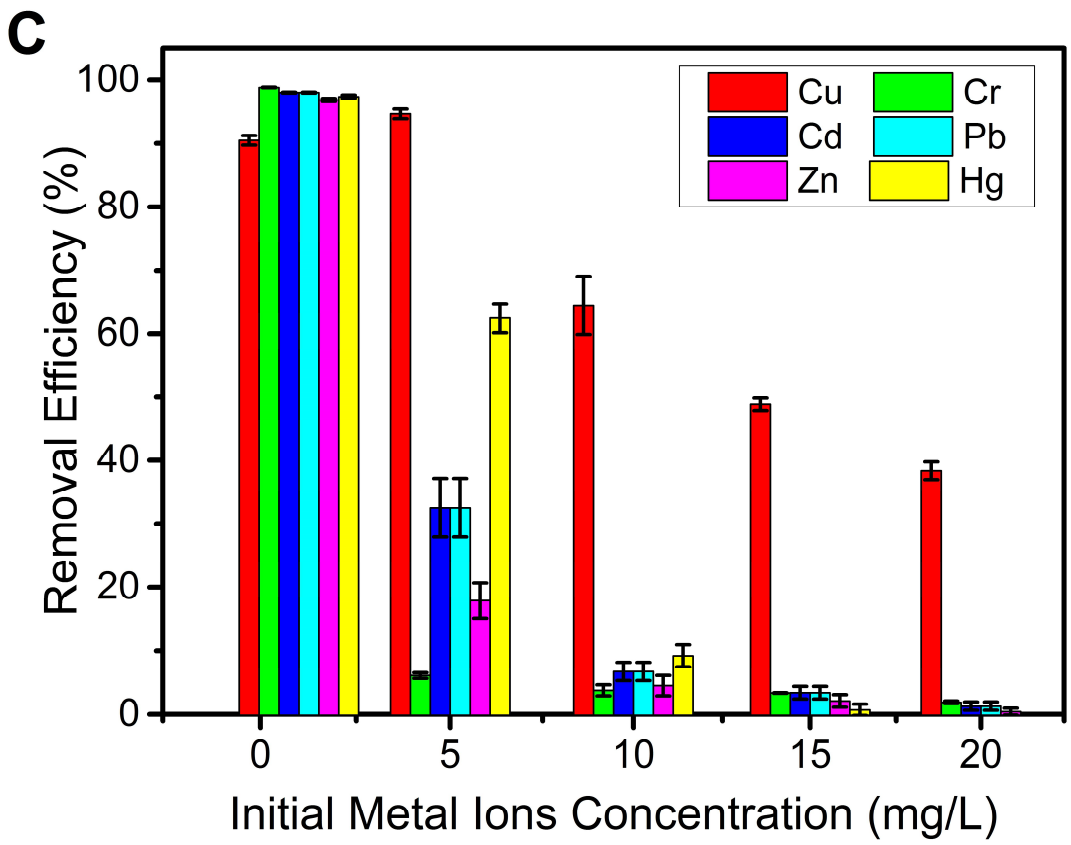

Figure 3. Competitive sorption of multiple metal ions (A) Group 1: Cd^{2+} and Pb^{2+}; (B) Group 2: Ce^{3+} In^{3+} and Ga^{3+}; and (C) Group 3: Cr^{3+}, Zn^{2+}, Cd^{2+}, Hg^{2+}, Pb^{2+} and Cu^{2+} onto Mag-Ligand at pH7 as a function of initial ions concentration with a fixed adsorbent concentration of 4 g/L;

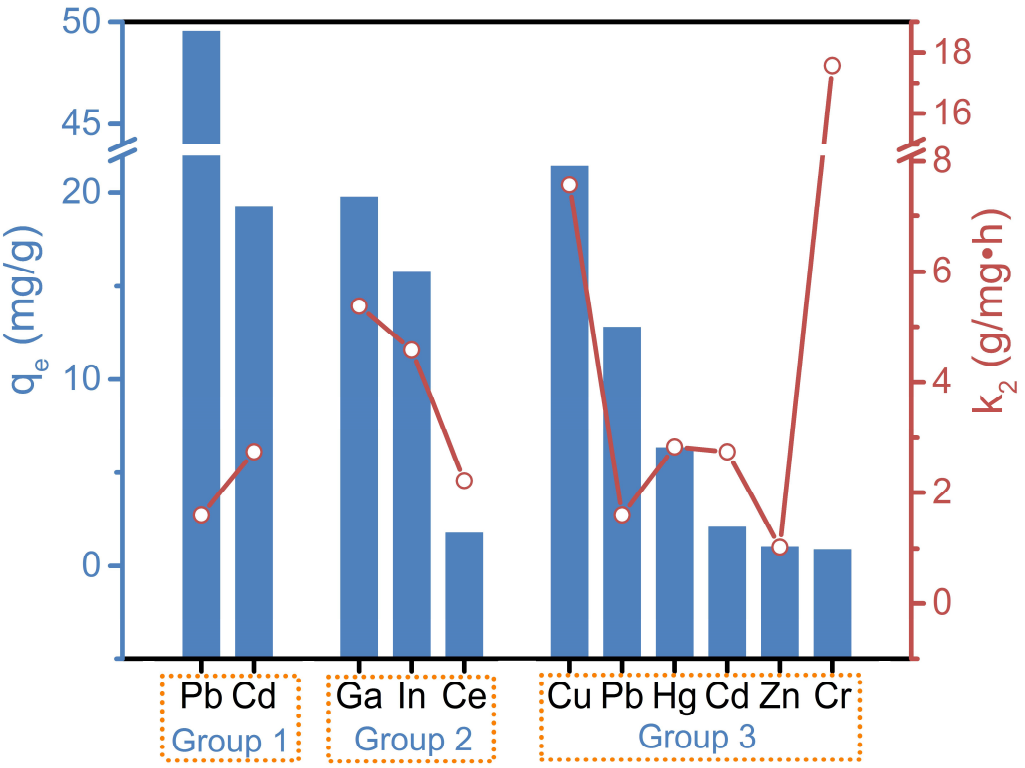

Figure 4. Langmuir model predicted maximum adsorption capacity (q_e) of metal ions onto Mag-Ligand in group competitive sorption (blue bars) versus the equilibrium kinetic rate constant, k_2 (red dots).

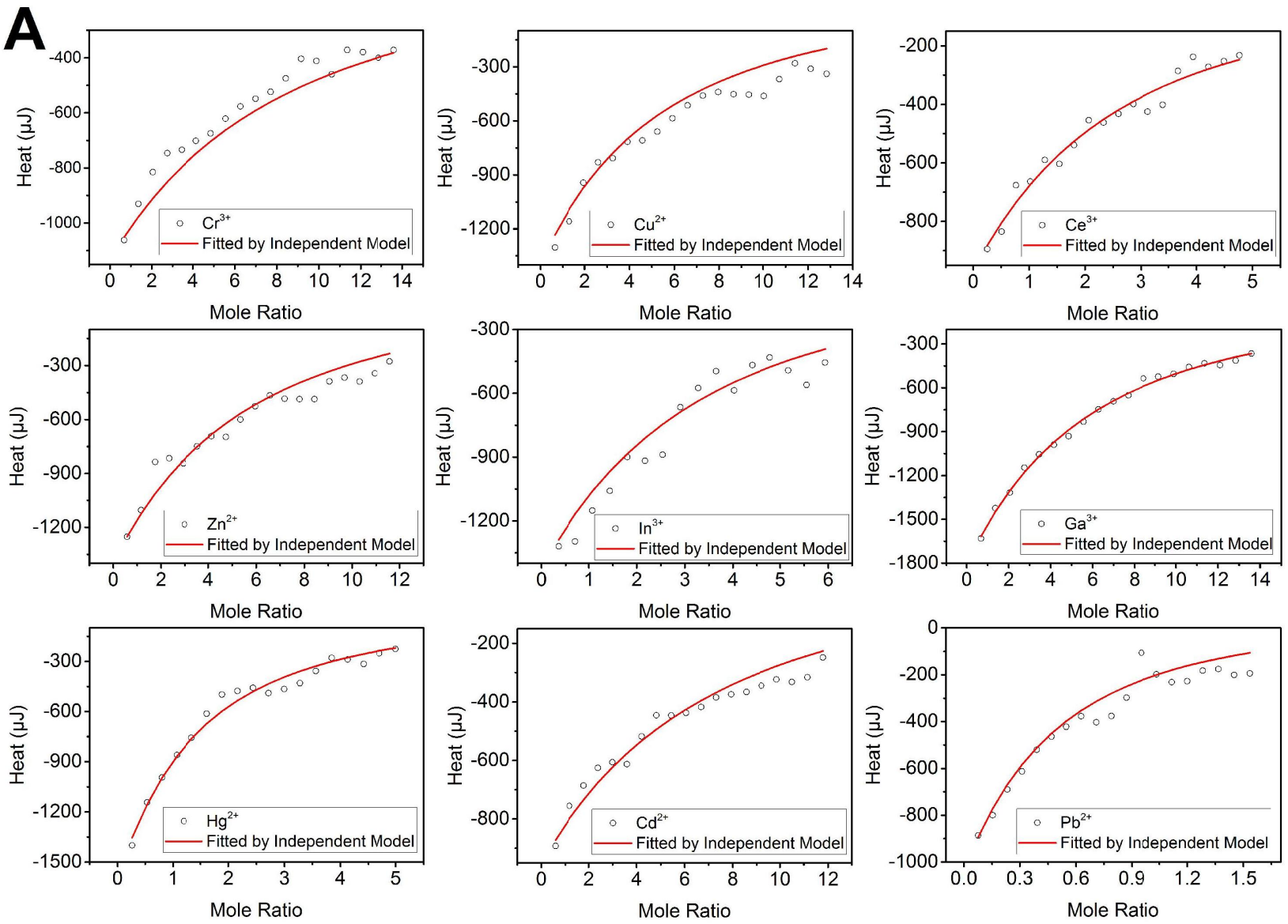
A
Heat (μJ)
Mole Ratio
Cr3+
Fitted by Independent Model
Cu2+
Fitted by Independent Model
Ce3+
Fitted by Independent Model
Zn2+
Fitted by Independent Model
In3+
Fitted by Independent Model
Ga3+
Fitted by Independent Model
Hg2+
Fitted by Independent Model
Cd2+
Fitted by Independent Model
Pb2+
Fitted by Independent Model

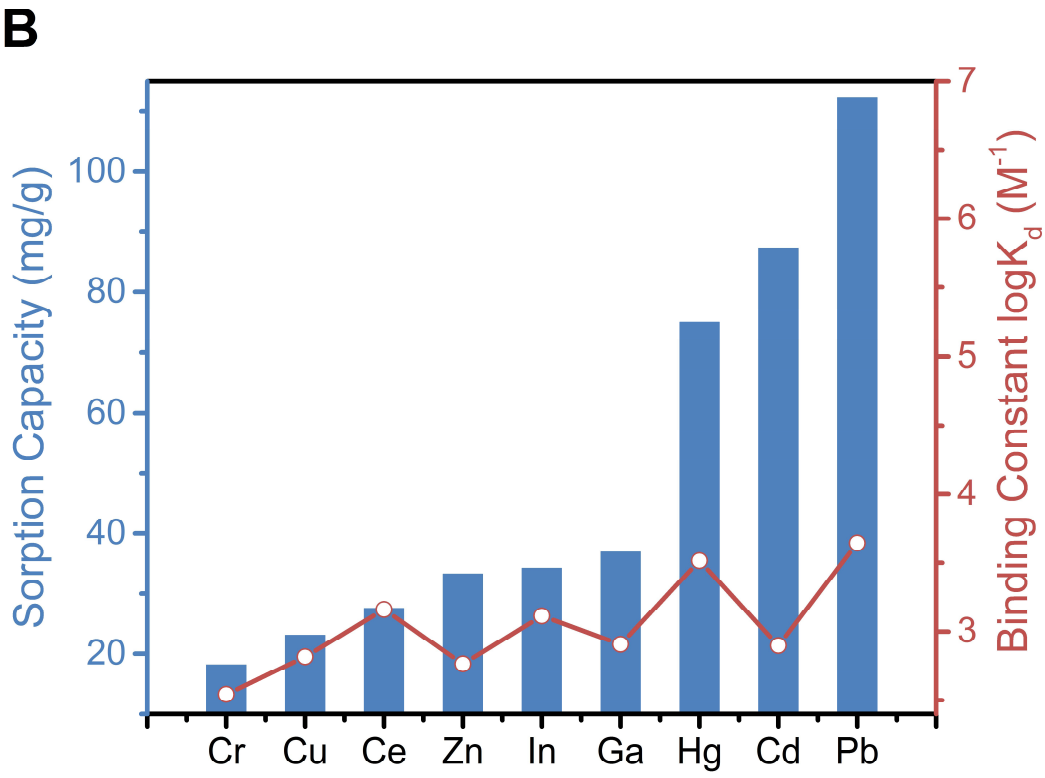

Figure 5. (A) The integrated binding isotherms as a function of molar ratio of metal ions (Cr^{3+}, Cu^{2+}, Ce^{3+}, Zn^{2+}, In^{3+}, Ga^{3+}, Hg^{2+}, Cd^{2+} and Pb^{2+}) to Mag-Ligand particles were fitted with independent model, symbols represent experimental data, and red line represents model prediction; (B) Langmuir model predicted maximum adsorption capacity of metal ions onto Mag-Ligand in individual sorption (blue bars) versus the binding constant log K_d (red dots).

3.5. Appendix. Supporting Information

3.5.1. Synthesis of Mag-Ligand

The synthesis protocol followed our previously reported method (Huang and Keller 2015). Briefly, Maghemite nanoparticles (1.0 g) were dispersed into 40 mL of toluene in a flask. After adding 0.4 mL of 3-aminopropyltriethoxysilane (APTES), the flask was connected to a reflux system (WU-28615-06, Cole-Parmer, USA), which was then rotated at 30 rpm (revolutions/minute) in a water bath at 90 ºC, and refluxed for 2 h. After the solution cooled to room temperature (22 ºC), 2 mM EDTA and 60 mL pyridine were added. The mixture was again rotated at 30 rpm in a water bath at 90 ºC in the reflux system for 2 h. After the solution cooled down to room temperature, 100 mL of sodium bicarbonate (0.5 M/L) was added to adjust pH. A magnet (Eclipse Magnetics N821 permanent, 50 mm ×50 mm ×12.5 mm; 243.8 g; pull force: 40.1 N) was applied to the bottom of the flask to recover the nanoparticles while the supernatant was decanted. Deionized (DI) water was used to rinse the particles twice and then decanted while retaining the particles with the magnet. The same rinsing procedure was performed twice with ethanol and then diethylether. The particles were dried at room temperature for 24 h, and stored in a capped bottle prior to use. The characterization of Mag-Ligand particles were reported in our previous study (Huang and Keller 2015).

3.5.2. Analysis

A Thermo iCAP 6300 inductively coupled plasma with atomic emission spectroscopy (ICP-AES) was used to analyze the concentration of metal ions. All tests were performed in

triplicate and analysis of variance (ANOVA) was used to test the significance of results. A $p<0.05$ was considered to be statistically significant.

Metal ions removal efficiency and sorption capacity were calculated as:

$$Removal\ efficiency = \frac{C_0 - C_t}{C_0} \times 100\% \quad \text{(S1)}$$

$$Sorption\ capacity = q_e = \frac{(C_0 - C_t) \cdot V}{m} \quad \text{(S2)}$$

where C_0 and C_t are the initial and final concentrations of metal ions (mg/L), m is the mass of Mag-Ligand (g), and V is the volume of solution (L).

Mag-Ligand recovery efficiency was calculated as:

$$Recovery\ efficiency = \frac{C_w}{C_0} \times 100\% \quad \text{(S3)}$$

where C_0 (mg/L) is the initial concentrations of Cd^{2+} ions in solution, and C_w (mg/L) is the concentrations of Cd^{2+} ions in the extracted solution (after regeneration).

The Cd^{2+} and Pb^{2+} equilibrium adsorption was evaluated according to Langmuir isotherms using Eq. 4, respectively (Morel and Hering 1993):

$$\frac{C_e}{q_e} = \frac{1}{K_L \cdot q_m} + \frac{C_e}{q_m} \quad \text{(S4)}$$

where C_e is solute concentration (mg/L) at equilibrium and q_e is amount adsorbed (mg/g), q_m is the maximum sorption capacity (mg/g). K_L is the Langmuir sorption equilibrium constant (L/mg).

Kinetics were analyzed using the pseudo-second-order models using Eq. 5 (Coleman et al. 1956):

$$\frac{t}{q_t} = \frac{1}{k_2 q_e^{\ 2}} + \frac{1}{q_e} t \quad \text{(S5)}$$

where k_2 ($\frac{g}{mg \cdot h}$) is the equilibrium rate constant of kinetics.

3.5.3. Effect of pH on Pb^{2+} removal

Adsorption of Pb2+ onto Mag-Ligand was also performed at various solution pH. The pH was varied from 4 to 7, and pH was adjusted by using 0.1 M NaOH and HCl. In order to study the effect of ionic strength, especially water hardness, on the removal efficiency of Mag-Ligand on metal ions, two different common ions, Ca2+ and Mg2+ were used at concentrations ranging from 1 mg/L to 100 mg/L. The experiments were done as described earlier at pH 7.

Pb^{2+} was selected as an example to study the influence of pH on the removal efficiency, given its high abundance in waste water. The removal efficiency was found to decrease gradually as pH increased between pH 3 and 7, while the sorption capacity stabilized at around 50 mg/g at the range of pH 3 to 6 (Figure S1). This is not due to a decrease in affinity, but rather a change in Pb^{2+} speciation. Based on the simulation of lead species using Visual MINTEQ (Gustafsson 2006) software, the main Pb species present in the pH range 3 to 6 is Pb^{2+}, while the formation of solid $Pb(OH)_2$ starts at pH 6.3 and $PbOH^{3-}$ dominates above pH 7.0 (Issabayeva et al. 2006). Pb^{2+} has a strong complex formation constant with EDTA (at 25ºC log K=18.04)(Harris 2010), which agrees well with our result: Mag-Ligand showed high sorption capacity across different pH, especially from pH 3 to 6.

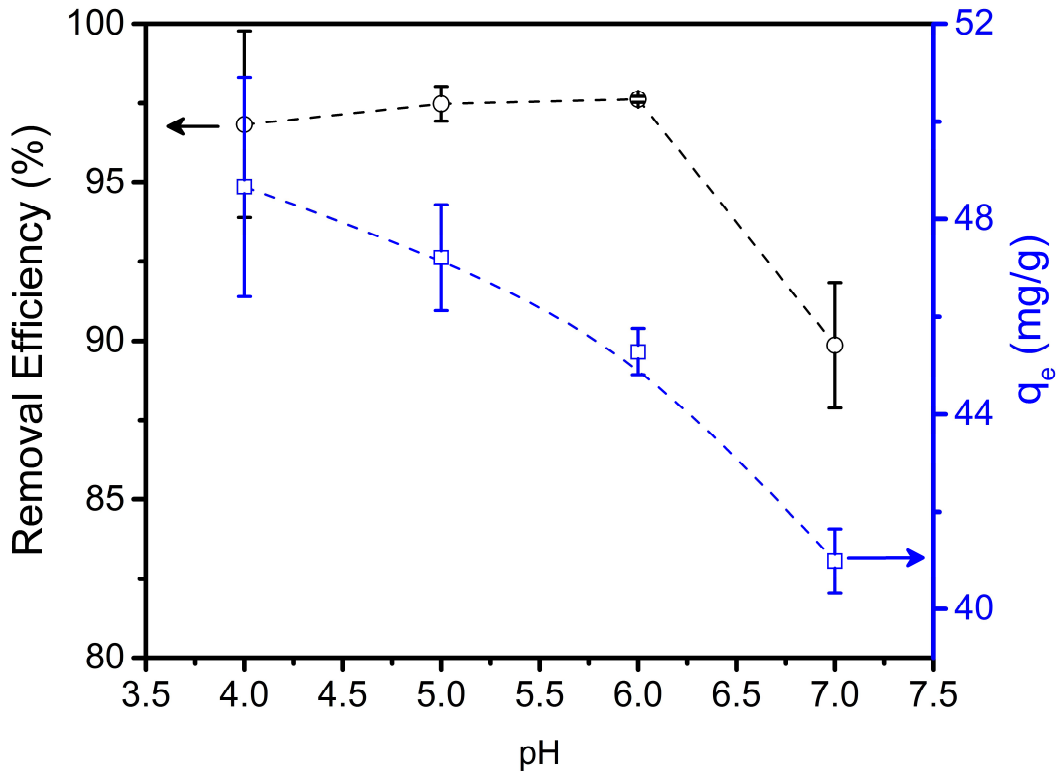

Figure S1 Adsorption of Pb^{2+} onto Mag-Ligand in solution as a function of pH, characterized by the removal efficiency (○) and adsorption capacity (□).

3.5.4. Effect of water hardness on Pb^{2+} removal

Water hardness, usually expressed as the total amount of Ca^{2+} and Mg^{2+} present in the water, varies in different water matrices, and both Ca^{2+} and Mg^{2+} can also interact with EDTA to form complexes (Yappert and DuPre 1997). Figure S2 shows the remediation performance of Pb^{2+} as a representative metal ion by Mag-Ligand in the presence of different concentrations of Ca^{2+} or Mg^{2+}. No significant difference in Pb^{2+} removal efficiency was found as Mg^{2+} or Ca^{2+}concentration increased up to 100 mg/L in solution (Figure S2). These results indicate that Ca^{2+} or Mg^{2+} did not compete strongly with Pb^{2+} in the complexation

reaction with EDTA due to relative low complex formation constants between Ca^{2+} or Mg^{2+} and EDTA (log K is 8.79 for Ca^{2+} and 10.69 for Mg^{2+} at 25 °C) (Harris 2010).

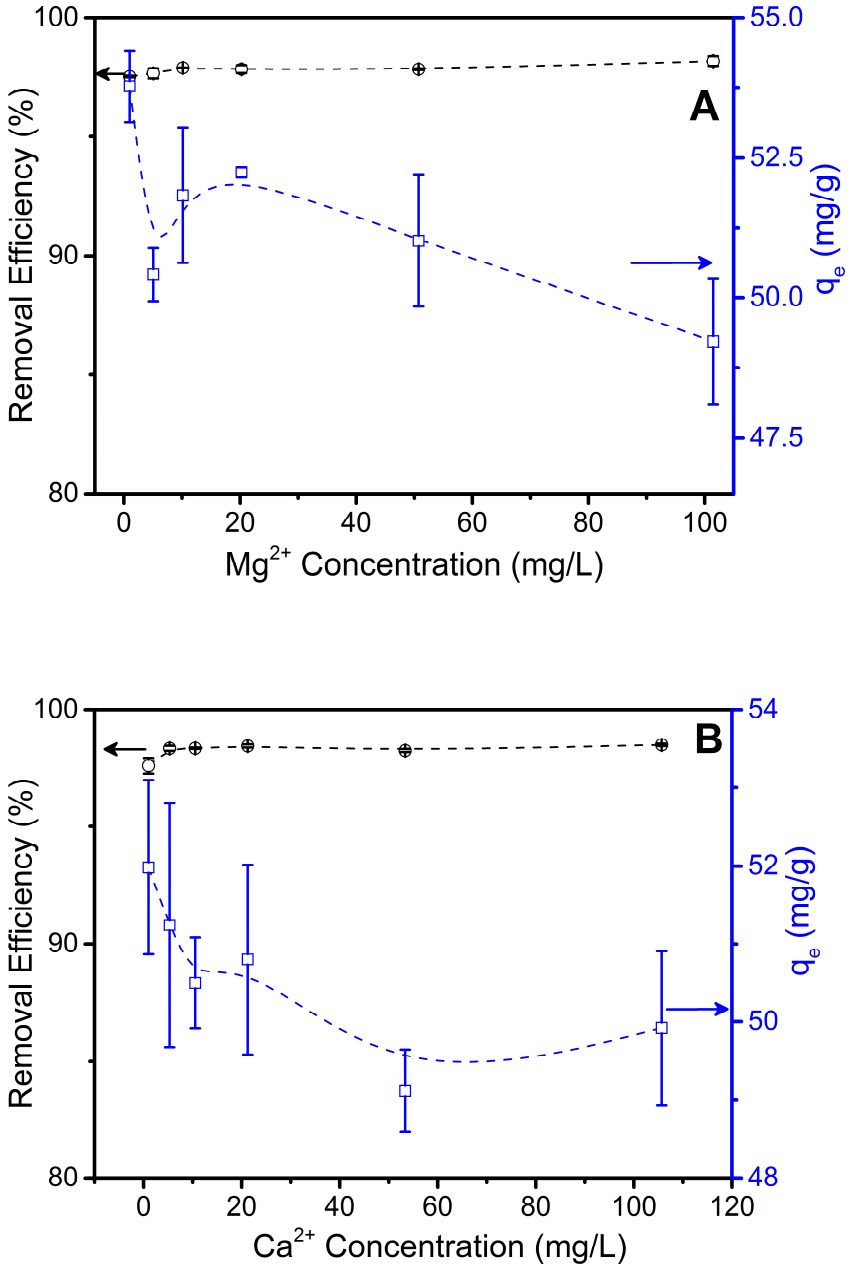

Figure S2 Adsorption of Pb^{2+} (10 mg/L initial concentration) onto Mag-Ligand (removal efficiency (○) and adsorption capacity (□)) in the presence of (A) Mg^{2+} (from 1 mg/L to 100 mg/L) and (B) Ca^{2+} (from 1 mg/L to 100 mg/L) at pH 7.

3.5.5. Competitive sorption of multiple metal ions

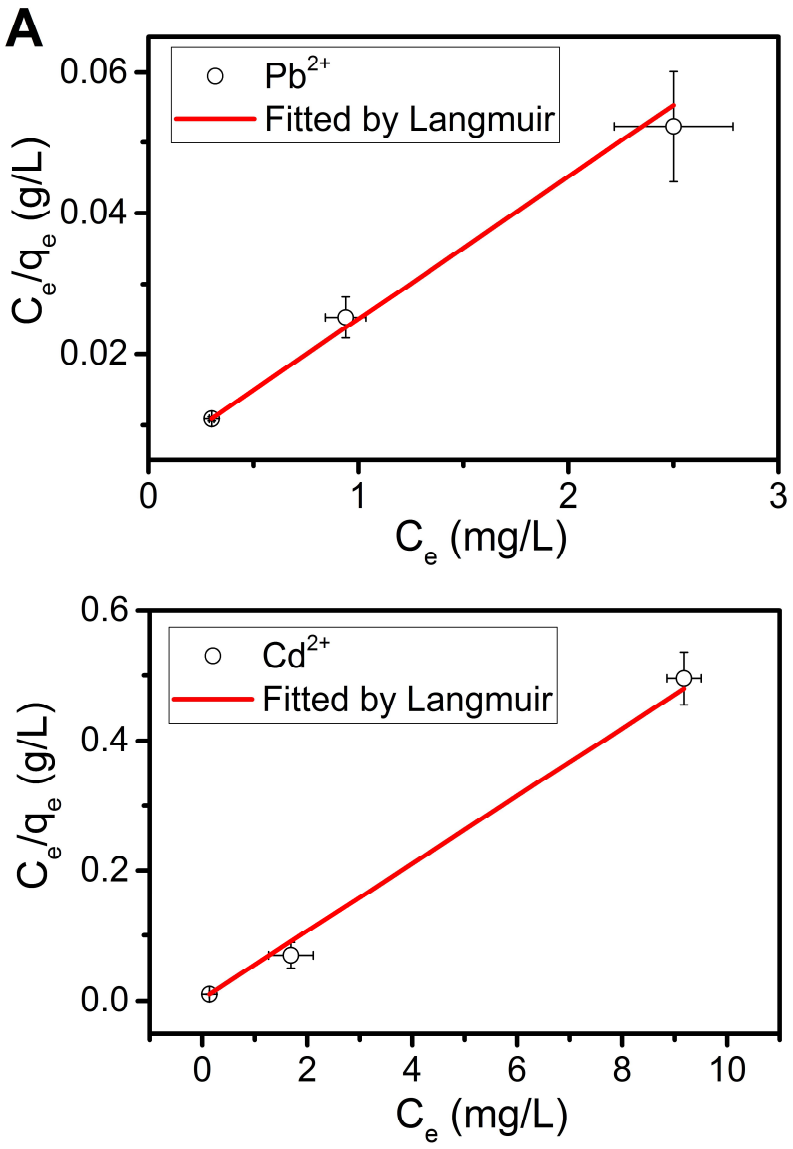

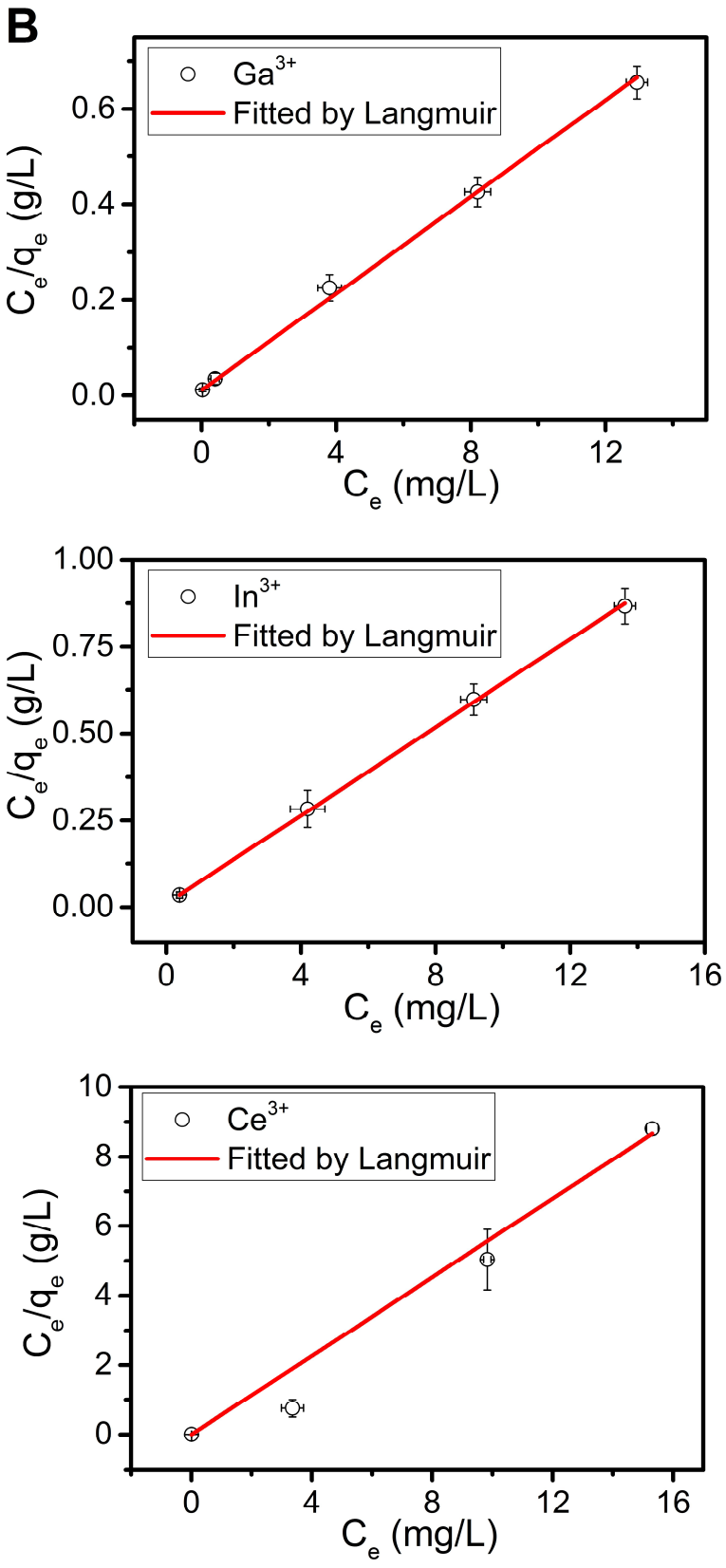
B
Ga3+
Fitted by Langmuir
Ce/qe (g/L)
Ce (mg/L)
0.0
0.2
0.4
0.6
0
4
8
12
In3+
Fitted by Langmuir
Ce/qe (g/L)
Ce (mg/L)
0.00
0.25
0.50
0.75
1.00
0
4
8
12
16
Ce3+
Fitted by Langmuir
Ce/qe (g/L)
Ce (mg/L)
0
2
4
6
8
10
0
4
8
12
16

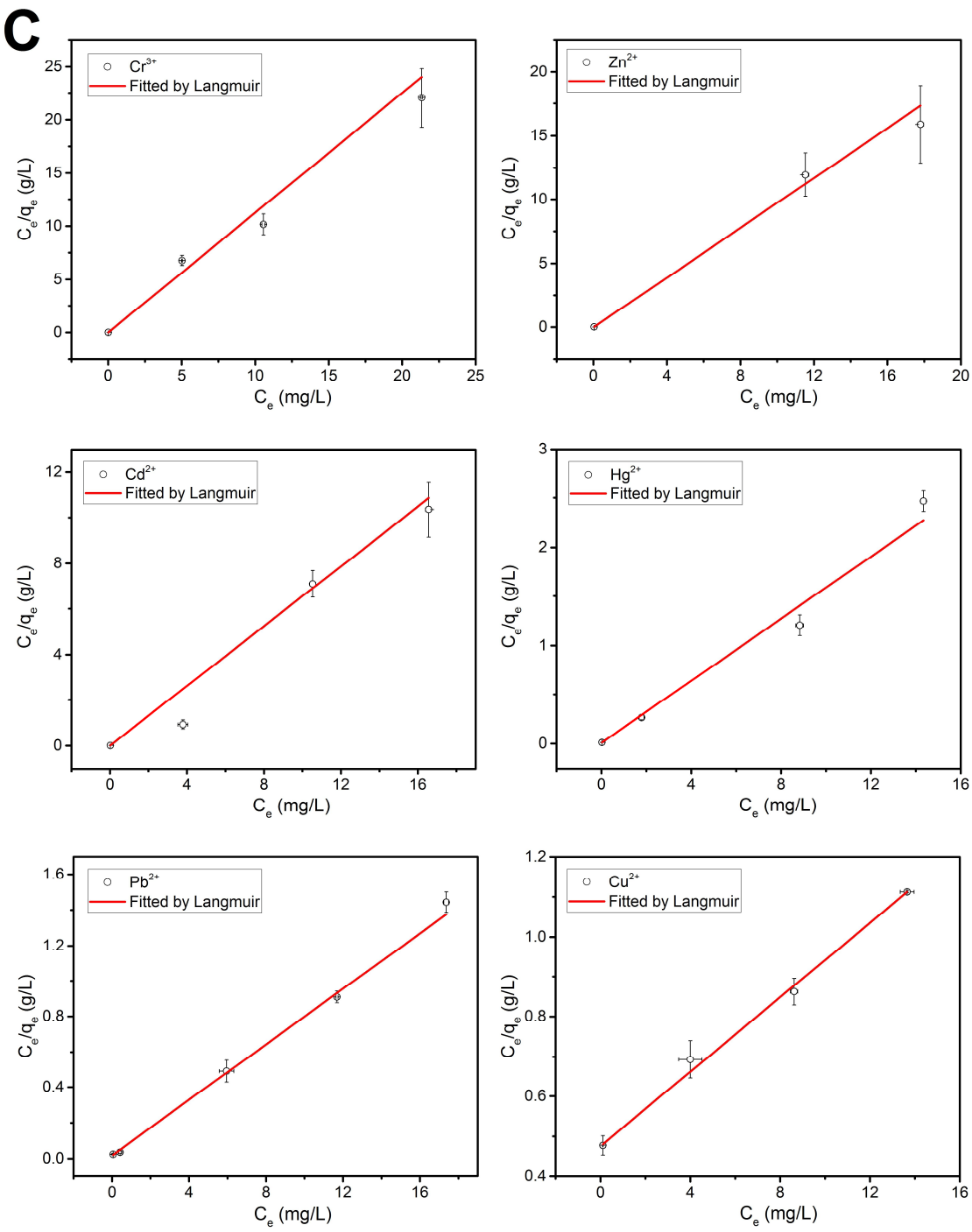

Figure S3 Competitive sorption of multiple metal ions fitted by Langmuir adsorption isotherms model: (A) Group 1: Cd^{2+} and Pb^{2+}; (B) Group 2: Ce^{3+} In^{3+} and Ga^{3+}; and (C)

Group 3: Cr^{3+}, Zn^{2+}, Cd^{2+}, Hg^{2+}, Pb^{2+} and Cu^{2+} at pH 7, symbols represent experimental data, and red line represents model prediction.

Table S1. Langmuir isotherm model fitted parameters for each metal ion in group competitive sorption onto Mag-Ligand

	Element	q_m (mg/g)	K_L (L/mg)	R^2
Group 1	Cd^{2+}	19.25	16.59	0.996
	Pb^{2+}	49.55	4.187	0.996
Group 2	Ce^{3+}	1.767	-393.0	0.996
	In^{3+}	15.75	6.335	1.000
	Ga^{3+}	19.76	4.592	0.999
Group3	Cr^{3+}	0.888	-113.61	0.988
	Zn^{2+}	1.025	-39.00	0.997
	Cd^{2+}	2.073	-72.54	0.999
	Hg^{2+}	6.326	20.40	0.995
	Pb^{2+}	12.78	4.846	0.997
	Cu^{2+}	21.44	0.098	1.000

3.6. References

BernkopSchnurch, A., Paikl, C. and Valenta, C. (1997) Novel bioadhesive chitosan-EDTA conjugate protects leucine enkephalin from degradation by aminopeptidase N. Pharmaceutical Research 14(7), 917-922.

Clark, K.K. and Keller, A.A. (2012a) Adsorption of perchlorate and other oxyanions onto magnetic permanently confined micelle arrays (Mag-PCMAs). Water research 46(3), 635-644.

Clark, K.K. and Keller, A.A. (2012b) Investigation of two magnetic permanently confined micelle array sorbents using nonionic and cationic surfactants for the removal of PAHs and pesticides from aqueous media. Water, Air, & Soil Pollution 223(7), 3647-3655.

Coleman, N.T., Mcclung, A.C. and Moore, D.P. (1956) Formation Constants for Cu(Ii)-Peat Complexes. Science 123(3191), 330-331.

Freire, E., Mayorga, O.L. and Straume, M. (1990) Isothermal titration calorimetry. Analytical chemistry 62(18), 950A-959A.

Fu, F.L. and Wang, Q. (2011) Removal of heavy metal ions from wastewaters: A review. Journal of Environmental Management 92(3), 407-418.

Ge, F., Li, M.M., Ye, H. and Zhao, B.X. (2012) Effective removal of heavy metal ions Cd2+, Zn2+, Pb2+, Cu2+ from aqueous solution by polymer-modified magnetic nanoparticles. Journal of Hazardous Materials 211, 366-372.

Gustafsson, J.P. (2006) Visual minteq. Capturado em de 26.

Harris, D.C. (2010) Quantitative chemical analysis, Macmillan.

Huang, Y., Yang, J.-K. and Keller, A.A. (2014) Removal of arsenic and phosphate from aqueous solution by metal (hydr-) oxide coated sand. Acs Sustainable Chemistry & Engineering 2(5), 1128-1138.

Huang, Y.X. and Keller, A.A. (2013) Magnetic Nanoparticle Adsorbents for Emerging Organic Contaminants. Acs Sustainable Chemistry & Engineering 1(7), 731-736.

Huang, Y.X. and Keller, A.A. (2015) EDTA functionalized magnetic nanoparticle sorbents for cadmium and lead contaminated water treatment. Water Research 80, 159-168.

Issabayeva, G., Aroua, M.K. and Sulaiman, N.M.N. (2006) Removal of lead from aqueous solutions on palm shell activated carbon. Bioresource Technology 97(18), 2350-2355.

Kantipuly, C., Katragadda, S., Chow, A. and Gesser, H.D. (1990) Chelating Polymers and Related Supports for Separation and Preconcentration of Trace-Metals. Talanta 37(5), 491-517.

Morel, F.M.M. and Hering, J.G. (1993) Principles and Applications of Aquatic Chemistry, Wiley.

Shannon, R.D. (1976) Revised Effective Ionic-Radii and Systematic Studies of Interatomic Distances in Halides and Chalcogenides. Acta Crystallographica Section A 32(Sep1), 751-767.

Su, Y., Adeleye, A.S., Keller, A.A., Huang, Y., Dai, C., Zhou, X. and Zhang, Y. (2015) Magnetic sulfide-modified nanoscale zerovalent iron (S-nZVI) for dissolved metal ion removal. Water Research.

Su, Y.M., Adeleye, A.S., Huang, Y.X., Sun, X.Y., Dai, C.M., Zhou, X.F., Zhang, Y.L. and Keller, A.A. (2014) Simultaneous removal of cadmium and nitrate in aqueous media by nanoscale zerovalent iron (nZVI) and Au doped nZVI particles. Water Research 63, 102-111.

Unlu, N. and Ersoz, M. (2006) Adsorption characteristics of heavy metal ions onto a low cost biopolymeric sorbent from aqueous solutions. Journal of Hazardous Materials 136(2), 272-280.

Wang, H., Keller, A.A. and Clark, K.K. (2011) Natural organic matter removal by adsorption onto magnetic permanently confined micelle arrays. Journal of Hazardous Materials 194, 156-161.

Wang, P., Shi, Q., Shi, Y., Clark, K.K., Stucky, G.D. and Keller, A.A. (2008) Magnetic permanently confined micelle arrays for treating hydrophobic organic compound contamination. Journal of the American Chemical Society 131(1), 182-188.

Yappert, M.C. and DuPre, D.B. (1997) Complexometric titrations: Competition of complexing agents in the determination of water hardness with EDTA. Journal of Chemical Education 74(12), 1422-1423.

Chapter 4. Magnetic Nanoparticle Adsorbents for Emerging Organic Contaminants[2]

4.1. Introduction

Recent attention has been directed at chemicals that are historically unregulated or not commonly regulated as contaminants but has the potential to enter the environment and cause known or suspected adverse ecological and human health effects, such as pharmaceuticals, personal care products, surfactants, various industrial additives and endocrine disruptors, including hormones (Bolong et al. 2009, Kuster et al. 2008, Murray et al. 2010). These chemicals are collectively defined as Emerging Organic Contaminants (EOCs) (http://toxics.usgs.gov/regional/emc). The presence of these synthetic chemicals in the wastewater or surface water may contaminate ecosystems, and surface and drinking water supplies. Recent studies have shown that EOCs may have biological effects, and even potential ecotoxicological impacts on invertebrates (such as daphnids), fish, algae, mussels, and also human embryonic cells (Carlsson et al. 2006, Hoeger et al. 2005, Kim et al. 2007, Kolok et al. 2007, Lai et al. 2009, Lyssimachou and Arukwe 2007, Pomati et al. 2006). To date, most of the studies have been focused on the occurrence and/or fate of EOCs in surface waters (Hao et al. 2006, Lin et al. 2006, Pedrouzo et al. 2007, Xu et al. 2007, Zhang et al. 2007) and/or wastewater (Chang et al. 2008, Kuster et al. 2008, Nakada et al. 2008, Santos et al. 2009, Stulten et al. 2008). However, there are few studies on approaches to remove EOCs

[2] This chapter was published in ACS Sustainable Chemistry & Engineering: Huang, Y, Keller, AA (2013). Magnetic Nanoparticle Adsorbents for Emerging Organic Contaminants. ACS Sustainable Chemistry & Engineering, doi: 10.1021/sc400047q.

from aqueous media. Therefore, the development of technologies to remove legacy and emerging organic contaminants from water is of great importance.

In recent years, magnetic particles have received a lot of attention as powerful adsorbents because of their inherent superparamagnetic properties make them desirable for magnetic field assisted separations (Ambashta and Sillanpaa 2010, Latham and Williams 2008, Toprak et al. 2007, Yavuz et al. 2006). For instance, magnetic iron oxides (Fe_2O_3 and Fe_3O_4) have been reported as potential adsorbents for the removal of pollutants from aqueous media (Ai et al. 2008, Shannon et al. 2008, Tuutijarvi et al. 2009, Yantasee et al. 2007).

The surface characteristics of the sorbents are very important to the effectiveness of the adsorption process. Since sorption of organic chemicals can be enhanced by coating of surfactants onto the sorbent, in a previous study we synthesized Magnetic Permanently Confined Micelle Arrays (Mag-PCMAs), with a magnetite core and a silica porous layer that permanently confines surfactant micelles within the mesopores (Wang et al. 2009). The magnetic core allows for rapid separation of the Mag-PCMAs from solution by applying a magnetic field. Mag-PCMAs have been applied to the removal of very hydrophobic compounds (Wang et al. 2009), natural organic matter (Wang et al. 2011) and oxyanions (Clark and Keller 2012).

The objective of this study was to determine the effectiveness of Mag-PCMAs to remove EOCs from water. For comparison, two legacy contaminants (e.g. ethylbenzene, 2-chlorophenol) were also evaluated. The microenvironment of the interactions between the mesoporous layers of the Mag-PCMAs and the multiple binding sites on EOCs make it a significant study for sorbents in complex chemical environments, such as water treatment. Mag-PCMAs have low energy requirements in their synthesis, use and regeneration,

compared to other adsorbents such as granular activated carbon (GAC), resulting in a much more sustainable material.

4.2. Experimental

4.2.1. Chemicals

Tetramethyl ammonium hydroxide (TMAOH) (25 wt. % in water), 3-(trimethoxysily)propyl-octadecyldimethyl-ammonium chloride (TPODAC) (72 wt.% in methanol), ammonia (28%), methanol, and tetraethyl orthosilicate (TEOS), atenolol, gemfibrozil, sulfamethoxazole, d-gluconic acid sodium salt, succinic acid disodium salt were purchased from Sigma-Aldrich (St. Louis, MO, USA). Methyl orange, l-3-(3,4-dihydroxyphenyl)alanine (L-Dopa) were purchased from Acros Organics (Geel, Beligum). Ethylbenzene and 2-chlorophenol were purchased from Fisher Scientific (Pittsburgh, PA, USA). Maghemite iron (III) oxide nanoparticles (30 nm in diameter) were purchased from Alfa Aesar (Ward Hill, MA, USA). All chemicals were used as received, without further purification. Relevant physicochemical properties for the contaminants are presented in Table 1.

4.2.2. Synthesis of Mag-PCMAs

The synthesis procedure for Mag-PCMAs was improved compared to the previous study to improve yield and reduce the use of ethanol (Wang et al. 2009). The core-shell structured Mag-PCMAs were synthesized through a solvothermal reaction, which is cooperative assembly of silica oligomers and TPODAC on the Fe2O3 nanoparticles. This three-step preparation of Mag-PCMAs is illustrated in Figure 1. Maghemite iron(III) oxide nanoparticles were dispersed in 40 mL of TMAOH solution (25% by weight) under constant

mixing overnight to activate the surface. Then 0.5 mL of TPODAC, a cationic surfactant, was added to the maghemite suspension under constant stirring. Next, 5 mL of 28% ammonium hydroxide were added for base catalyzed sol-gel hydrolysis of TEOS (1.1 mL) to cross-link the surfactant onto the magnetic iron core. The three steps are done at room temperature (22 ^{o}C).

4.2.3 Scanning electronic microscopy

Scanning electronic microscopy (SEM) imaging was performed under vacuum on an FEI XL40 FEG Digital Scanning Microscope using an accelerating voltage of 5.00kV.

4.2.4. Batch sorption of emerging organic contaminants

The adsorption kinetics was determined by batch experiments. 2.0 mg of Mag-PCMAs were mixed with 20 mL of a given organic contaminant in 20 mL vials. The initial concentration of contaminant was 100 mg/L in all cases. All experiments were conducted at pH = 7.0. These vials were shaken in an end-over-end shaker on Dayton-6Z412A Parallel Shaft roller mixer with a speed of 70 rpm at room temperature. The concentration of the sample was measured at the end of 5 min, 15 min, 30 min, 60 min, 90 min, 120 min and 180 min. Then the Mag-PCMAs particles with adsorbed contaminants were separated from the mixture with a Eclipse Magnetics N821permanent hand-held magnet (Dimension: 50mm× 50mm×12.5mm; Weight: 0.2438kg; Pull force: 40.1N)

To develop adsorption isotherms, solutions with varying initial concentrations were treated with the same procedure as above at room temperature. The equilibration time was 24 hours uniformly, which was determined to be sufficient to reach the adsorption equilibrium. Preliminary experiments indicated that more than 99% of adsorption occurred

within the first 120 min. The contaminant concentrations ranged from 10 mg/L to 3000 mg/L, and the Mag-PCMAs concentration were 100 mg/L.

The solid-phase concentrations were determined by mass balance, according to Equation (1):

$$q_e = \frac{V \times (C_0 - C_e)}{M} \quad (1)$$

where C_0 and C_e = the initial and equilibrium concentration of EOC in the liquid phase (mg/L), respectively, q_e = the equilibrium concentration of contaminants adsorbed on the unit mass of Mag-PCMAs (mg/g), V = the volume of solution, and M = the mass of dry Mag-PCMAs (g)..

4.2.5. Analysis by UV-Spectrophotometry and HPLC

Two instruments were used: a high performance liquid chromatography HPLC system (SPD-M10AVP, Shimadzu, MD), or a UV-Vis spectrometer (BIOSPEC-1601, Shimadzu, MD). Each instrument was used to determine the final concentration of organic contaminants after adsorption occurred. HPLC was used for the analysis of L-Dopa. The HPLC system was equipped with two LC-10AT VP pumps, a Sil-10AF autosampler, a DGU-14A degasser, and a SPD-M10AVP diode-array detector. A TSKgel ODS-120A column (length, 250 mm; inner diameter, 4.6 mm;) was used. The HPLC analyses were carried out with a mobile phase comprised of 30% methanol/70% water. The analyses were performed at a constant flow rate of 1.0 ml/min. The ultraviolet detector monitored the absorbance at 261 nm for L-Dopa. The UV-Vis spectrometer was used to monitor the concentration of organics in water at the absorption maximum for each compound: methyl orange at 400 nm, ethylbenzene at 261 nm, 2-chlorophenol at 272.93 nm, atenolol at 274 nm,

succinic acid at 218 nm, d-glueonic at 208 nm, sulfamethoxazole at 268 nm, gemfibrozil at 275 nm. Calibration curves were performed daily with a regression (R^2 value) of 0.99 or greater.

4.3. Results and discussion

4.3.1. Mag-PCMA Characterization

SEM images show the hydrated particles are 600 nm to 1 um in size (Figure 2). Figure 3 presents the separation of Mag-PCMAs from the suspension using a simple magnet. The dispersed Mag-PCMAs can be separated within a few seconds from the suspension, with a very high recovery of the Mag-PCMAs. The energy requirements for the separation of the magnetic particles is minimal, particularly if a permanent magnet is used.

4.3.2. Non-competitive sorption studies

Figure 4 presents the experimental results for the non-competitive sorption for each compound for the range of concentration studies, as well as the fit of a Freundlich isotherm, linearized by taking the logarithm of both sides of the equation (Lee 2003):

$$\log q = \log K_f + n \log C_e \qquad (2)$$

where q is the amount of contaminant adsorbed at equilibrium (mg/g), C_e is the equilibrium concentration of contaminant in solution (mg/L), K_f is the Freundlich adsorption constant ($mg^{1-n}\ g^{-1}\ L^n$), and n is a measure of adsorption intensity (dimensionless). The Freundlich parameters K_f and n were determined from the intercept and slope of Equation 2. Table 2 summarizes the fitted values from all compounds. The Freundlich isotherm was used since it provided a better fit than linear or Langmuir models. Additionally, 2-

chlorophenol, , ethylbenzene, succinic acid and L-dopa were fitted using a non-linear exponential model (Langmuir 1997) to provide a better fit:

$$log\ q = nlogC_e + n_2(logC_e)^2 + logK_f \quad (3)$$

Based on the equilibrium sorption concentrations, q, at a given C_e Mag-PCMAs exhibited the highest sorption capacity for L-dopa, and the lowest for D-gluconic acid. While for more conventional non-ionic and contaminants such as petroleum hydrocarbons and chlorinated solvents there is a strong correlation between removal efficiency and the octanol-water partitioning coefficient (K_{ow}) (Wang et al. 2009) and for anionic compounds removal efficiency can be predicted by their Gibbs free energy of adsorption (Clark and Keller 2012), the EOC present multiple characteristics that control their affinity for the cationic TPODAC surfactant. In general the amount sorbed decreases with increasing K_{ow} (Figure 5), with L-dopa and D-gluconic acid representing major outliers. The large number of –OH groups on both of these compounds results in very different behavior than the other compounds studied. The trend is much less conclusive than for a sequence of hydrophobic organic contaminants where in fact adsorption increases with hydrophobicity. For ionizable compounds, their adsorption onto Mag-PCMAs generally increases with pKa (Figure 6), although the behavior is not easily predictable based on this physicochemical characteristic alone. Further work will be done with a broader range of compounds to elucidate more clearly the relationships.

For nonionic compounds, removal was strongly correlated with the K_{ow} of the compounds, a common indicator of hydrophobicity (Figure 6). In general, removal rate was found to decrease with hydrophobicity, except for ethylbenzene. Repeated adsorption experiments for ethylbenzene resulted in similar results, indicating that some additional adsorption mechanism must be involved for this compound.

4.3.3. Adsorption Kinetics for Methyl Orange

Methyl orange was used to evaluate the adsorption kinetics onto Mag-PCMA, given the high sorption capacity for this compound. Sorption occured rapidly, even for an initial concentration of 100 mg/L. Within the first 60 min almost all of the methyl orange was adsorbed, with minimal additional sorption after 2 hours (Figure 8A). Figure 8B shows the evident color change in the mixture solution with the passage of time indicating the concentration of methyl orange decreased quickly. Note that the image was made after concentrating the Mag-PCMAs at the bottom of the vial using a permanent magnet.

4.4. Conclusions

Mag-PCMAs with a core-shell structure are fast, convenient, and efficient sorbents for removing rather soluble organic contaminants from water. This study has extended the application of Mag-PCMAs from removing very hydrophobic compounds, natural organic matter and oxyanions to consider emerging organic compounds, including pharmaceuticals and personal care compounds. The most likely mechanisms of adsorption of organic contaminants onto Mag-PCMAs are hydrophobic interactions, hydrogen bonding and electrostatic interactions. Since all of these mechanisms are at play for these mixed functionality compounds, it is not easy to predict the adsorption capacity simply on the basis of one physicochemical property (e.g. K_{ow} or pKa). Further work will be done with a broader range of compounds to elucidate more clearly the relationships.

The synthesis procedure for Mag-PCMAs is simple and requires low energy and relatively low cost (~$4/kg), and the Mag-PCMAs with adsorbed organic contaminants can be easily removed from water via magnetic separation. This can be compared to carbon nanotubes (CNTs) which have been considered as adsorbents, with a cost of $500-1,000/kg.

This is in part because manufacturing CNTs requires high pressure and temperature, i.e. considerable energy. Granular activated carbon (GAC) is < $1/kg, but synthesis of GAC requires heating the carbon source several hundreds of degrees to activate the carbonaceous surface. Increasing the input energy can shorten the time needed for equilibrium. The regeneration of Mag-PCMAs, presented in previous studies (Wang et al. 2009), can be done at room temperature using ethanol or methanol to desorb the low K_{ow} compounds, or changing pH for the ionic compounds. The Mag-PCMAs perform well in a wide range of different organic contaminants with different solubility and pK_a. It is expected that the Mag-PCMAs will have potentially wide application in the removal of emerging organic contaminants from water.

Table 1. Properties of the compounds for sorption studies

Compound	Molecular Mass (g/mol)	Log_{10} Octanol-Water Partition Coefficient (log_{10} K_{ow})	pK_a
2-Chlorophenol	128.560	2.17	8.29
Atenolol	266.336	0.16	9.6
D-Gluconic	218.139	-6.00	3.7
Ethylbenzene	106.170	3.11	--
Gemfibrozil	250.333	4.77	4.75
L-Dopa	197.190	0.28	8.7
Methyl Orange	327.330	0.68	3.47
Succinic Acid	118.090	-0.59	4.2
Sulfamethoxazole	253.279	0.89	5.7

Table 2. Fitted parameter values for each compound in non-competitive sorption

Compounds		n	95% LCL for n	95% UCL for n	$logK_f$	95% LCL for $logK_f$	95% UCL for $logK_f$	K_f	r^2
Freundlich Model									
D-Gluconic		0.867	0.867	0.867	-0.467	-0.467	-0.467	0.34	0.999
Atenolol		0.967	0.967	0.967	0.080	0.080	0.080	1.20	0.999
Gemfibrozil		0.257	0.257	0.257	1.34	1.34	1.34	21.8	0.999
Sulfamethoxazole		0.219	0.211	0.226	1.48	1.47	1.49	30.3	0.999
Exponential Model									
L-Dopa	n	4.622	-2.72	11.9	-3.81	-9.85	2.24	1.55E-4	0.997
	n_2	-0.931	-3.08	1.21					
Succinic Acid	n	1.16	1.15	1.17	0.596	0.589	0.604	3.945	1
	n_2	-0.299	-0.304	-0.295					
2-Chlorophenol	n	0.628	0.628	0.628	0.917	0.917	0.917	8.260	1
	n_2	0.102	0.102	0.102					
Ethylbenzene	n	0.173	0.0685	0.277	0.966	0.945	0.988	9.256	0.999
	n_2	0.272	0.204	0.339					
Methyl Orange	n	0.627	0.627	0.627	1.50	1.50	1.50	31.550	1
	n_2	-0.104	-0.104	-0.104					

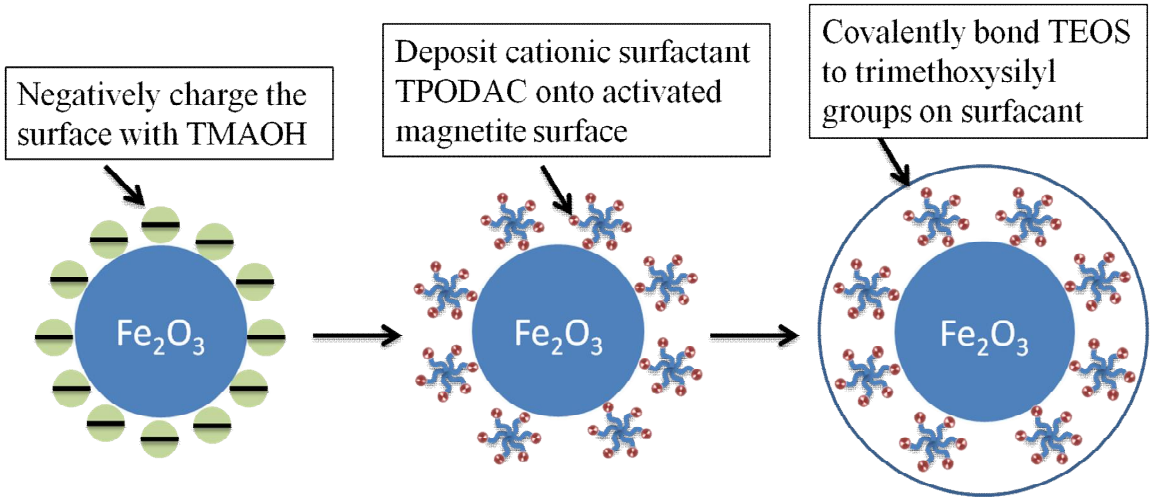

Figure 1. Mag-PCMA synthesis is done with stepwise reagent addition. Silica is interspersed between the surfactant and maghemite covalently securing the micelles to the iron oxide core and leaving void space for contaminant sorption.

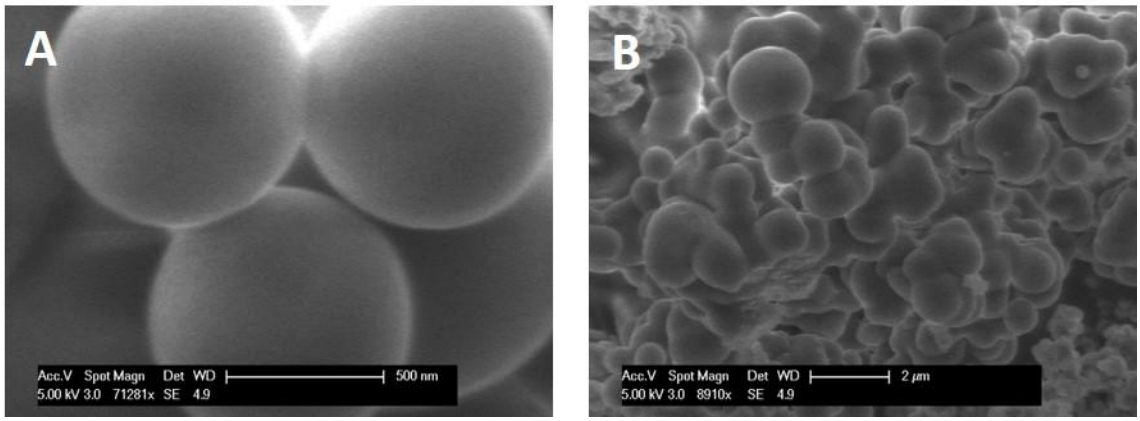

Figure 2. SEM of (A) Mag-PCMA at 71281X (B) Mag-PCMA at 8910X.

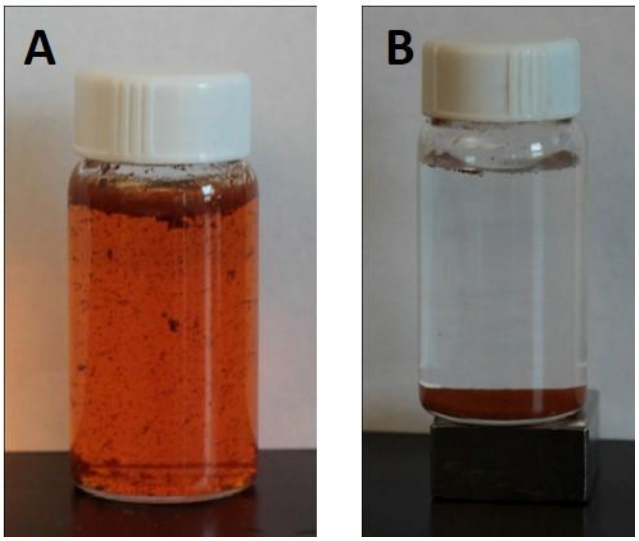

Figure 3. (A) Mag-PCMA particles are introduced into a vial containing contaminated water. (B) A permanent magnet is placed at the bottom of the vial to attract the magnetic particles, demonstrating the rapid removal of Mag-PCMAs from the suspension, within seconds of applying a magnetic field.

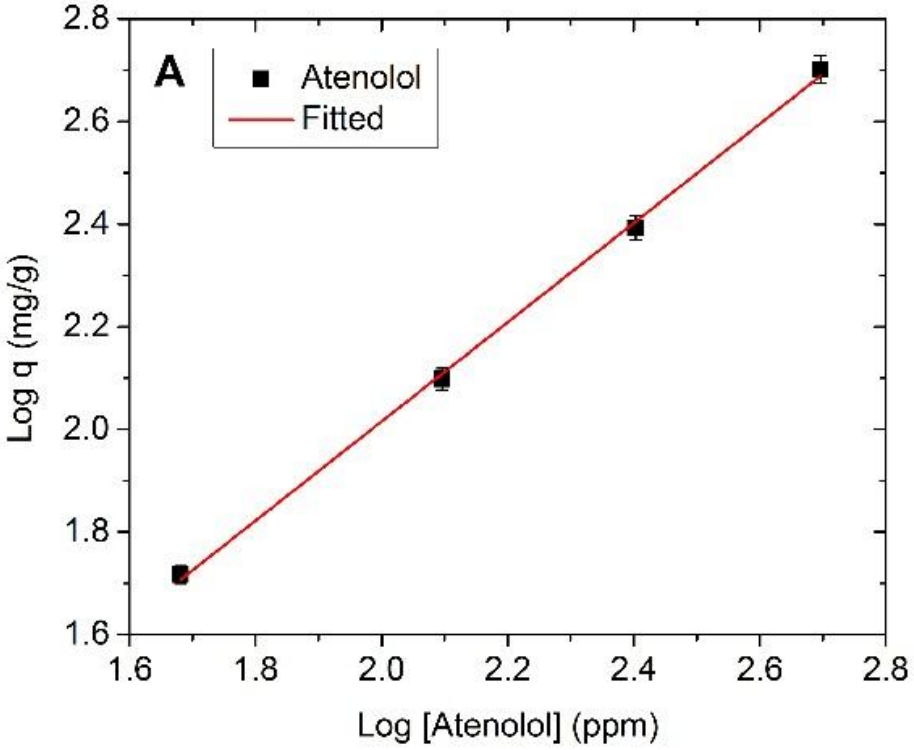
A
Atenolol
Fitted
Log q (mg/g)
Log [Atenolol] (ppm)
2.8
2.6
2.4
2.2
2.0
1.8
1.6
1.6
1.8
2.0
2.2
2.4
2.6
2.8

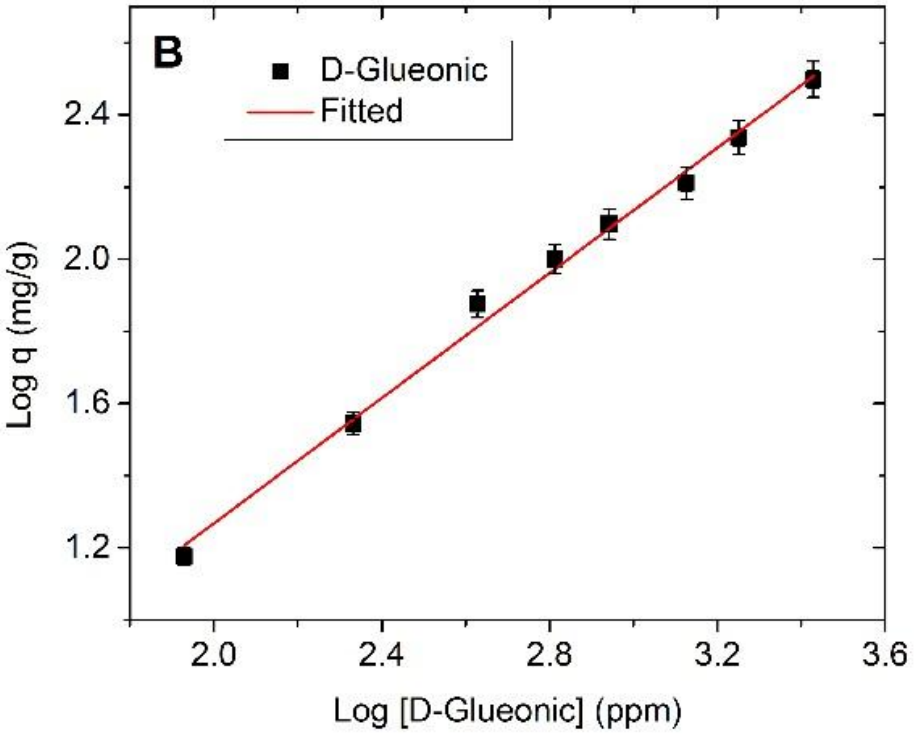
B
D-Glueonic
Fitted
Log q (mg/g)
Log [D-Glueonic] (ppm)
2.4
2.0
1.6
1.2
2.0
2.4
2.8
3.2
3.6

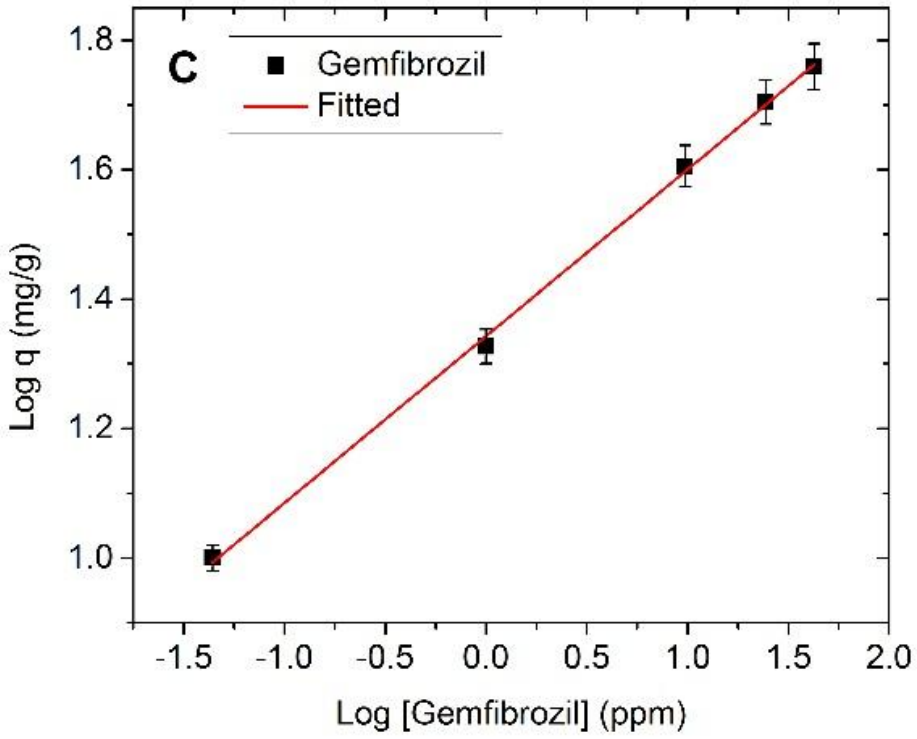
C
Gemfibrozil
Fitted
Log q (mg/g)
Log [Gemfibrozil] (ppm)
1.8
1.6
1.4
1.2
1.0
-1.5
-1.0
-0.5
0.0
0.5
1.0
1.5
2.0

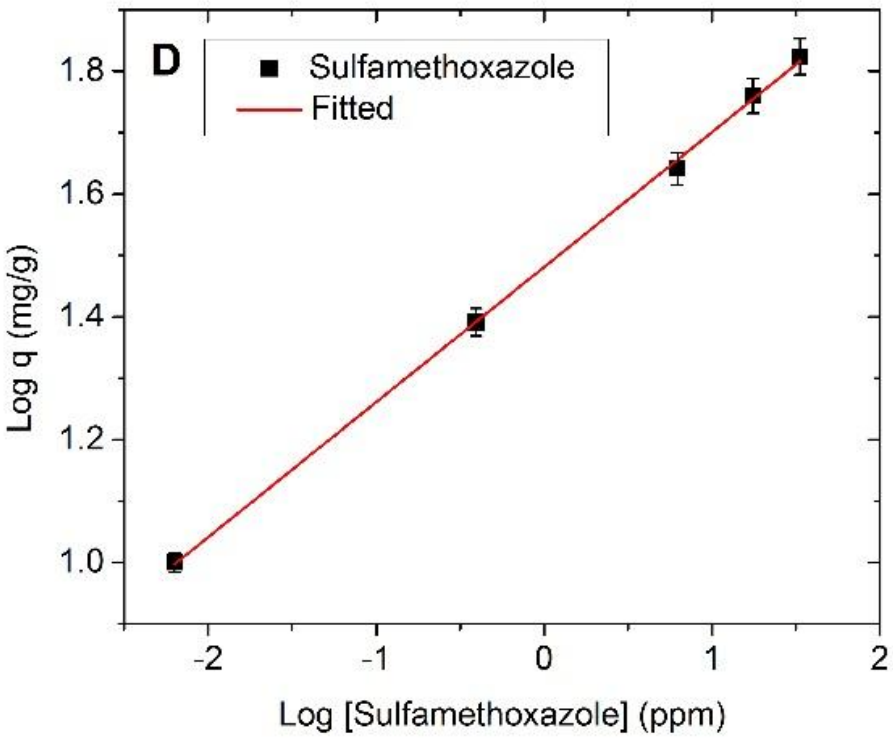
D
Sulfamethoxazole
Fitted
Log q (mg/g)
Log [Sulfamethoxazole] (ppm)
1.8
1.6
1.4
1.2
1.0
-2
-1
0
1
2

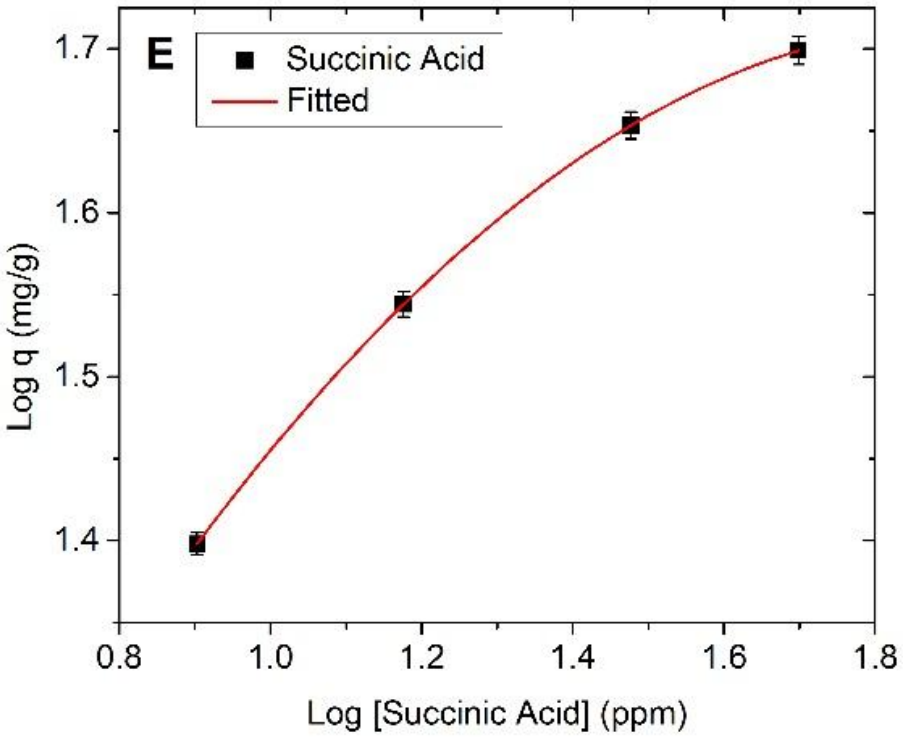
E
Succinic Acid
Fitted
Log q (mg/g)
Log [Succinic Acid] (ppm)
1.7
1.6
1.5
1.4
0.8
1.0
1.2
1.4
1.6
1.8

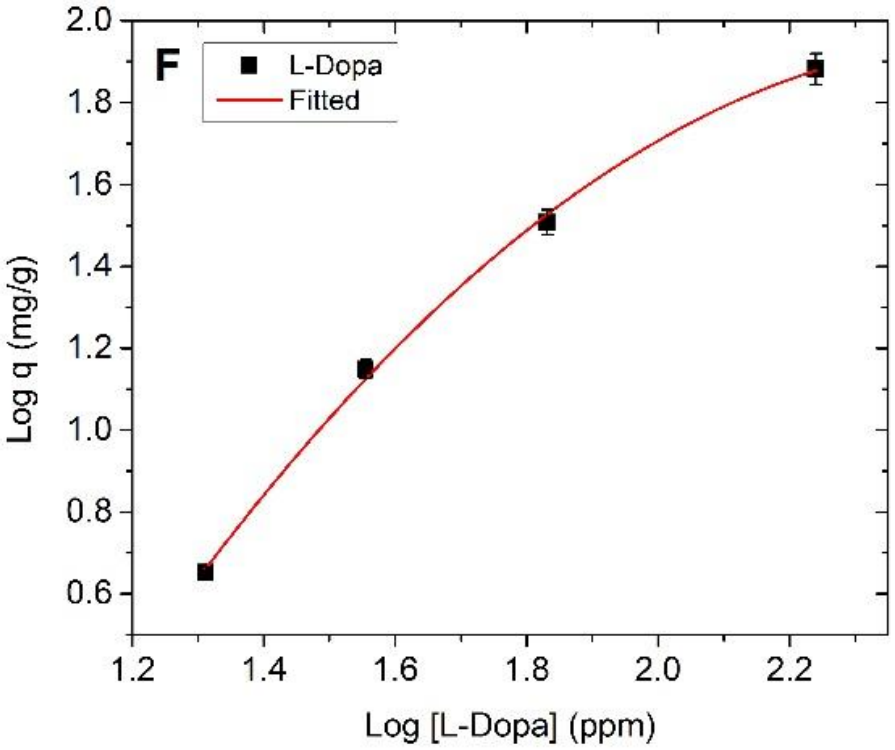
F
L-Dopa
Fitted
Log q (mg/g)
Log [L-Dopa] (ppm)
2.0
1.8
1.6
1.4
1.2
1.0
0.8
0.6
1.2
1.4
1.6
1.8
2.0
2.2

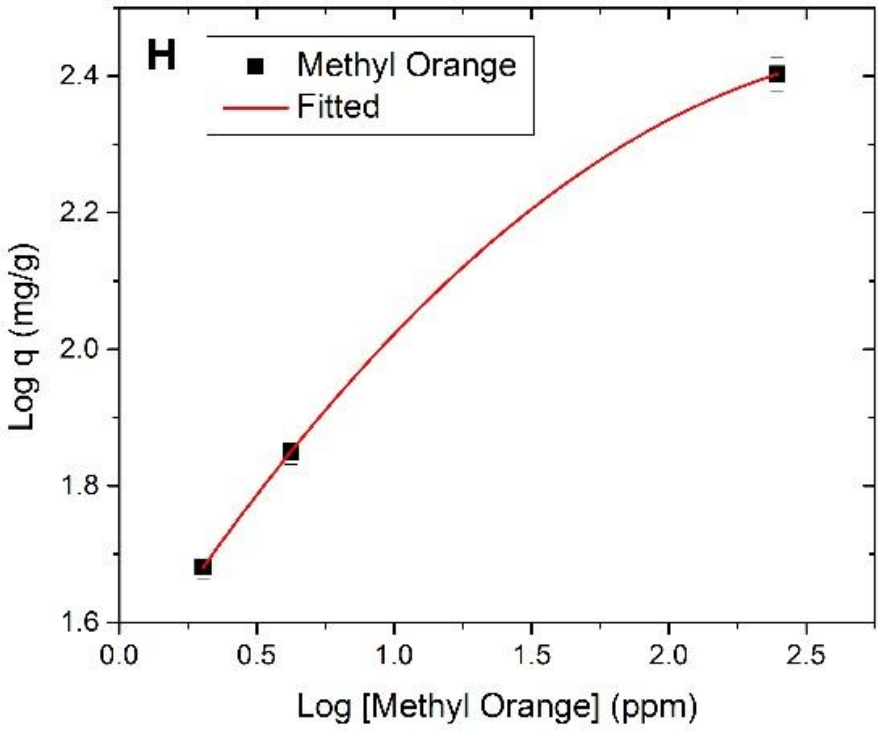
H
Methyl Orange
Fitted
Log q (mg/g)
Log [Methyl Orange] (ppm)
2.4
2.2
2.0
1.8
1.6
0.0
0.5
1.0
1.5
2.0
2.5

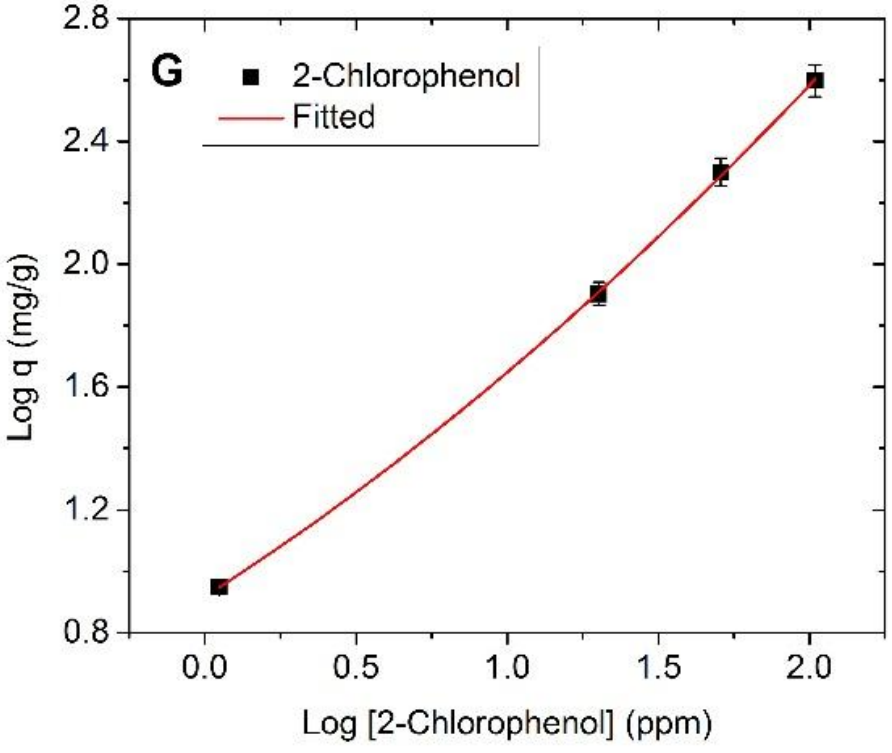
G
2-Chlorophenol
Fitted
Log q (mg/g)
Log [2-Chlorophenol] (ppm)
2.8
2.4
2.0
1.6
1.2
0.8
0.0
0.5
1.0
1.5
2.0

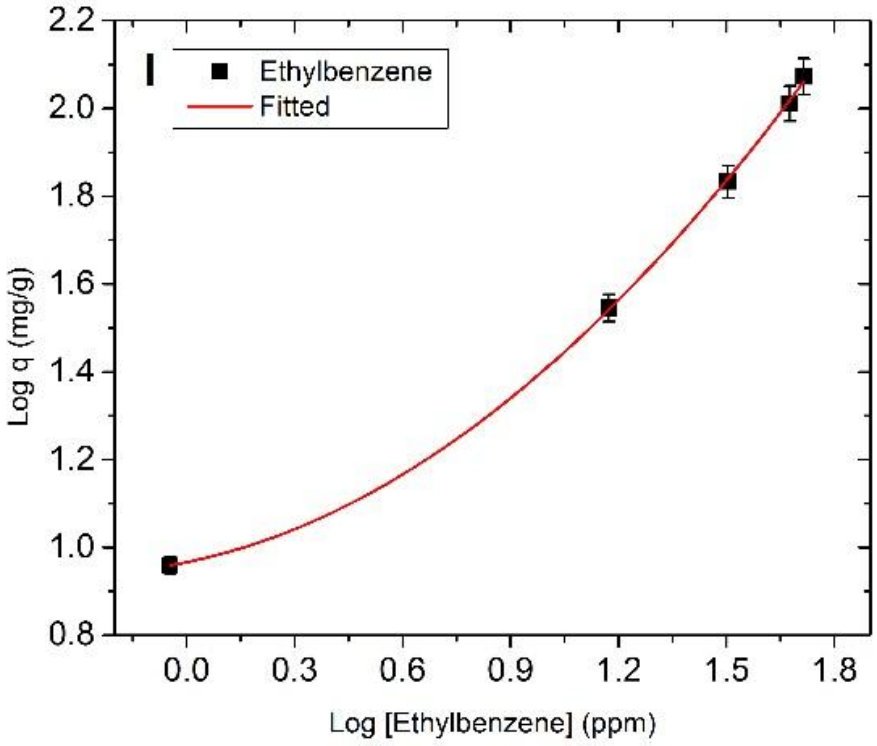

Figure 4. Non-competitive sorption onto Mag-PCMAs across a concentration range for: (A) atenolol; (B) D-gluconic; (C) gemfibrozil; (D) sulfamethoxazole; (E) succinic acid; (F) L-dopa; (G) methyl orange; (H) 2-chlorophenol; (I) ethylbenzene.

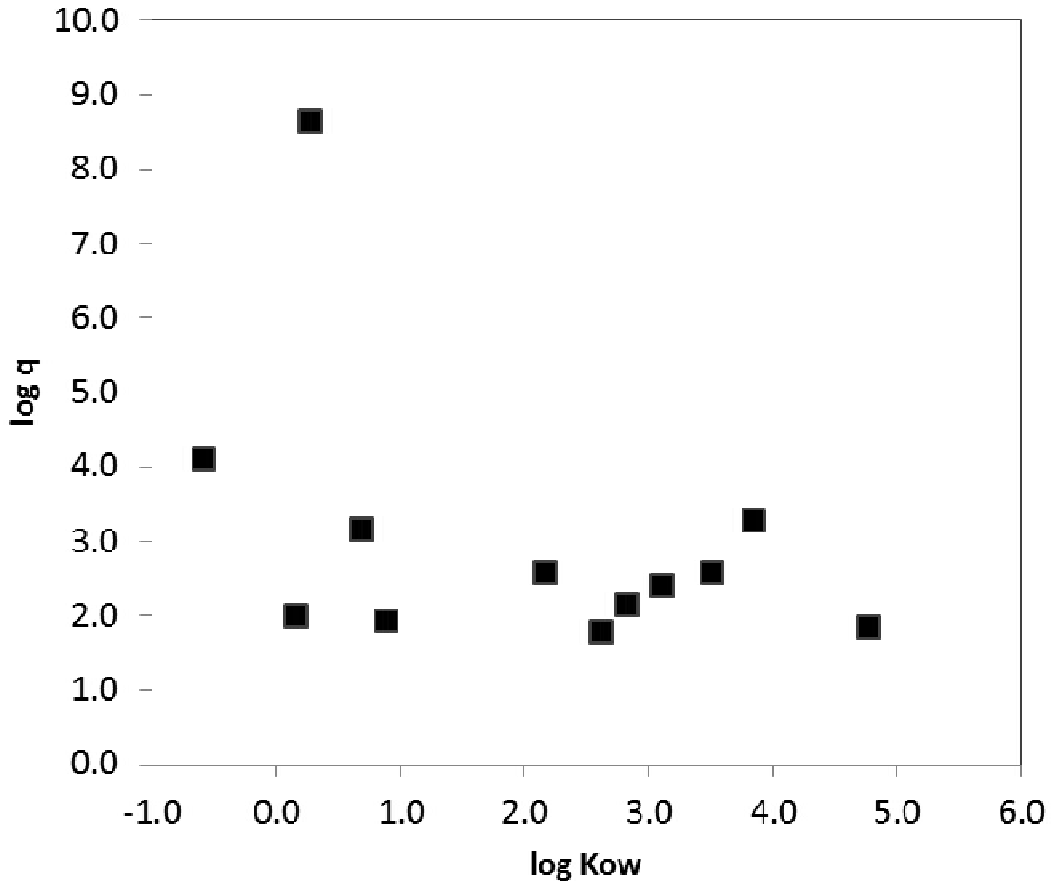

Figure 5. Sorption onto Mag-PCMAs for various compounds as a function of log K_{ow}. D-gluconic acid not included since it represents a major outlier with a log K_{ow} of -6.0.

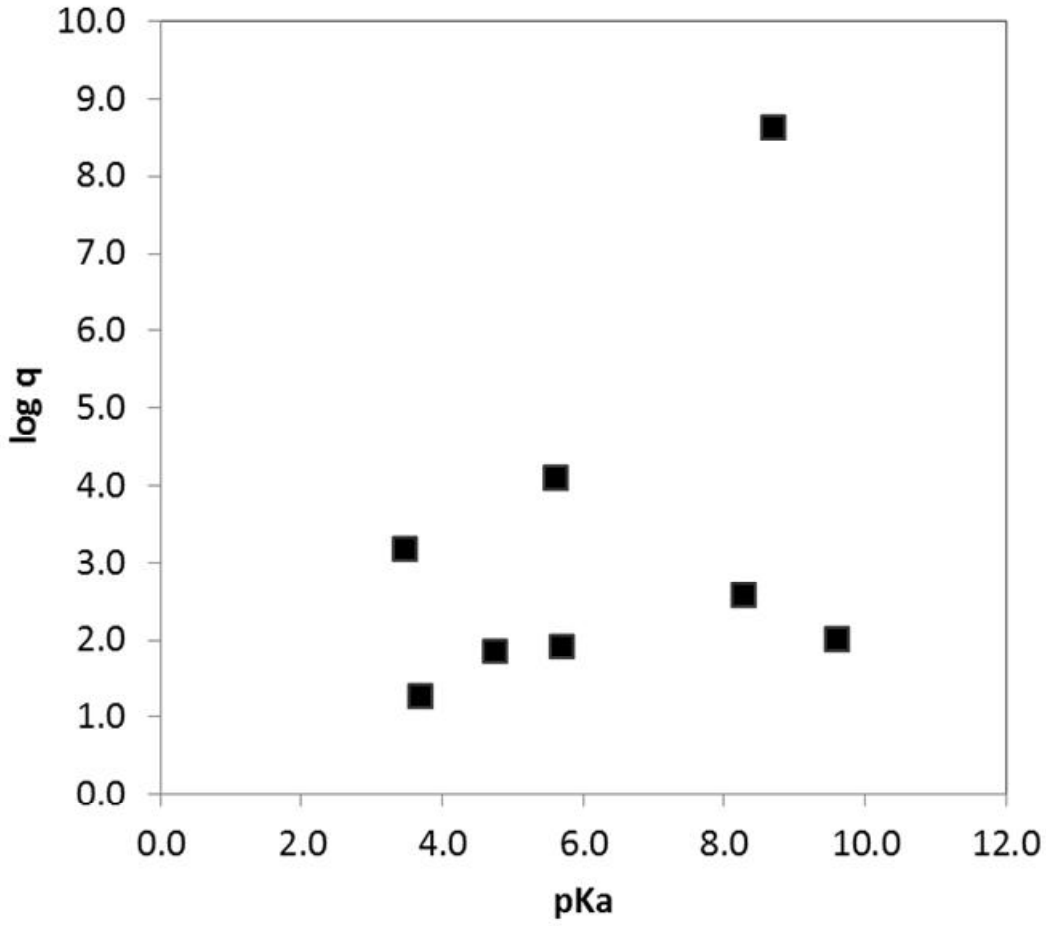

Figure 6. Sorption onto Mag-PCMAs for various compounds as a function of pKa. All ionizable compounds considered.

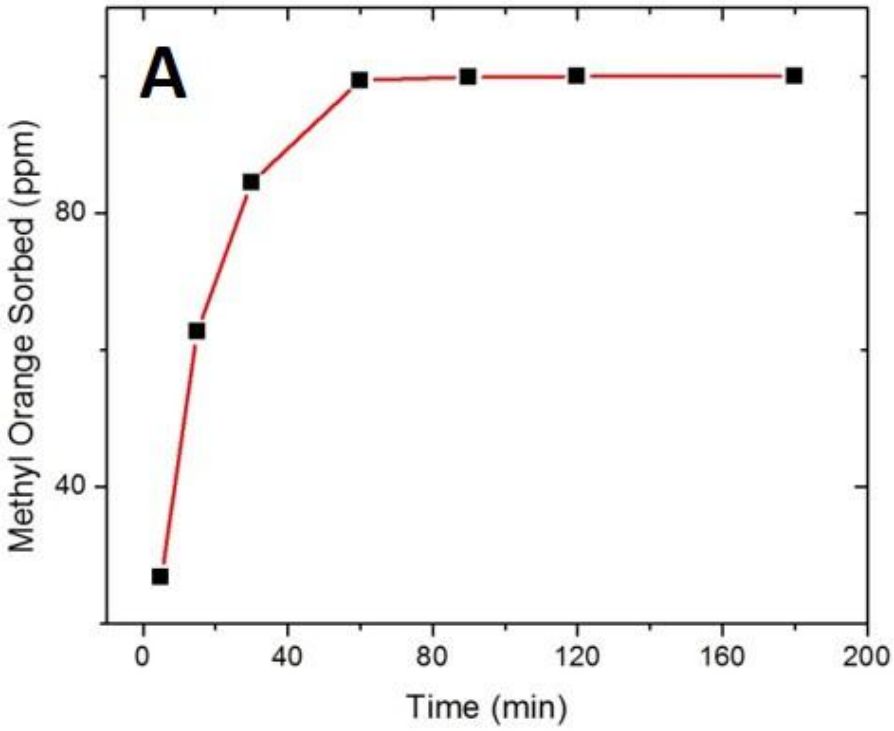
A
Methyl Orange Sorbed (ppm)
80
40
0
40
80
120
160
200
Time (min)

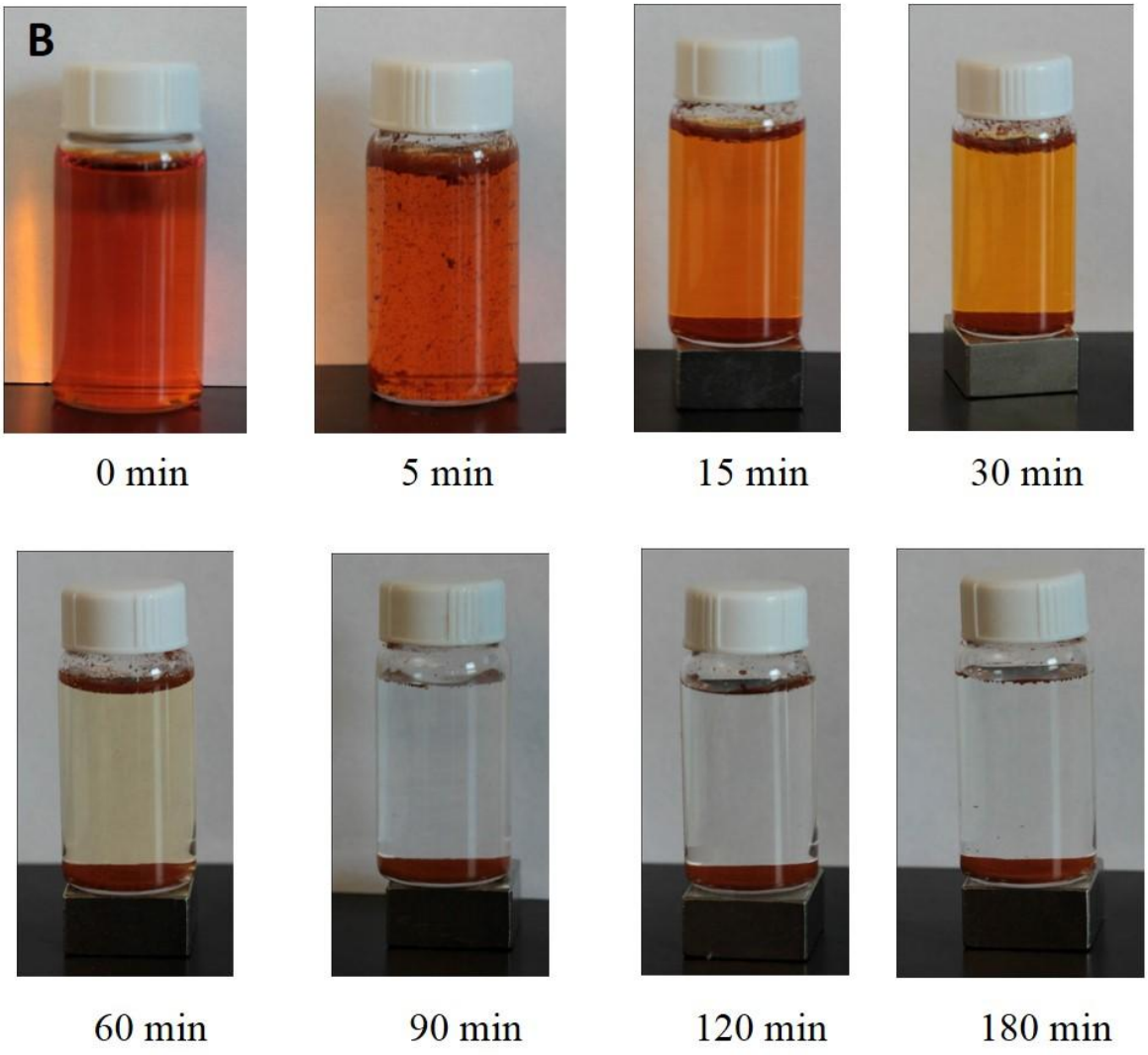

Figure 7. (A) Methyl orange equilibration kinetics (B) Methyl orange color change in sorption time sequence

4.5. References

Ai, Z.H., Cheng, Y., Zhang, L.Z. and Qiu, J.R. (2008) Efficient removal of Cr(VI) from aqueous solution with Fe@Fe2O3 core-shell nanowires. Environmental Science & Technology 42(18), 6955-6960.

Ambashta, R.D. and Sillanpaa, M. (2010) Water purification using magnetic assistance: A review. Journal of Hazardous Materials 180(1-3), 38-49.

Bolong, N., Ismail, A.F., Salim, M.R. and Matsuura, T. (2009) A review of the effects of emerging contaminants in wastewater and options for their removal. Desalination 239(1-3), 229-246.

Carlsson, C., Johansson, A.K., Alvan, G., Bergman, K. and Kuhler, T. (2006) Are pharmaceuticals potent environmental pollutants? Part I: Environmental risk assessments of selected active pharmaceutical ingredients. Science of the Total Environment 364(1-3), 67-87.

Chang, H., Hu, J.Y., Wang, L.Z. and Shao, B. (2008) Occurrence of sulfonamide antibiotics in sewage treatment plants. Chinese Science Bulletin 53(4), 514-520.

Clark, K.K. and Keller, A.A. (2012) Adsorption of perchlorate and other oxyanions onto magnetic permanently confined micelle arrays (Mag-PCMAs). Water Research 46(3), 635-644.

Hao, C.Y., Lissemore, L., Nguyen, B., Kleywegt, S., Yang, P. and Solomon, K. (2006) Determination of pharmaceuticals in environmental waters by liquid chromatography/electrospray ionization/tandem mass spectrometry. Analytical and Bioanalytical Chemistry 384(2), 505-513.

Hoeger, B., Kollner, B., Dietrich, D.R. and Hitzfeld, B. (2005) Water-borne diclofenac affects kidney and gill integrity and selected immune parameters in brown trout (Salmo trutta f. fario). Aquatic Toxicology 75(1), 53-64.

Kim, Y., Choi, K., Jung, J.Y., Park, S., Kim, P.G. and Park, J. (2007) Aquatic toxicity of acetaminophen, carbamazepine, cimetidine, diltiazem and six major sulfonamides, and their potential ecological risks in Korea. Environment International 33(3), 370-375.

Kolok, A.S., Snow, D.D., Kohno, S., Sellin, M.K. and Guillette, L.J. (2007) Occurrence and biological effect of exogenous steroids in the Elkhorn River, Nebraska, USA. Science of the Total Environment 388(1-3), 104-115.

Kuster, M., de Alda, M.J., Hernando, M.D., Petrovic, M., Martin-Alonso, J. and Barcelo, D. (2008) Analysis and occurrence of pharmaceuticals, estrogens, progestogens and polar pesticides in sewage treatment plant effluents, river water and drinking water in the Llobregat river basin (Barcelona, Spain). Journal of Hydrology 358(1-2), 112-123.

Lai, H.T., Hou, J.H., Su, C.I. and Chen, C.L. (2009) Effects of chloramphenicol, florfenicol, and thiamphenicol on growth of algae Chlorella pyrenoidosa, Isochrysis galbana, and Tetraselmis chui. Ecotoxicology and Environmental Safety 72(2), 329-334.

Langmuir, D. (1997) Aqueous environmental geochemistry, Prentice Hall.

Latham, A.H. and Williams, M.E. (2008) Controlling transport and chemical functionality of magnetic nanoparticles. Accounts of Chemical Research 41(3), 411-420.

Lee, C.M. (2003) Environmental Organic Chemistry, 2nd Edition (Schwarzenback, Rene P.; Gschwend, Philip M.; Imboden, Dieter M.). Journal of Chemical Education 80(10), 1143.

Lin, A.Y.C., Plumlee, M.H. and Reinhard, M. (2006) Natural attenuation of pharmaceuticals and alkylphenol polyethoxylate metabolites during river transport: Photochemical and biological transformation. Environmental Toxicology and Chemistry 25(6), 1458-1464.

Lyssimachou, A. and Arukwe, A. (2007) Alteration of brain and interrenal StAR protein, P450scc, and Cyp11 beta mRNA levels in Atlantic salmon after nominal waterborne exposure to the synthetic pharmaceutical estrogen ethynylestradiol. Journal of Toxicology and Environmental Health-Part a-Current Issues 70(7), 606-613.

Murray, K.E., Thomas, S.M. and Bodour, A.A. (2010) Prioritizing research for trace pollutants and emerging contaminants in the freshwater environment. Environmental Pollution 158(12), 3462-3471.

Nakada, N., Kiri, K., Shinohara, H., Harada, A., Kuroda, K., Takizawa, S. and Takada, H. (2008) Evaluation of pharmaceuticals and personal care products as water-soluble molecular markers of sewage. Environmental Science & Technology 42(17), 6347-6353.

Pedrouzo, M., Reverte, S., Borrull, F., Pocurull, E. and Marce, R.M. (2007) Pharmaceutical determination in surface and wastewaters using high-performance liquid chromatography-(electrospray)-mass spectrometry. Journal of Separation Science 30(3), 297-303.

Pomati, F., Castiglioni, S., Zuccato, E., Fanelli, R., Vigetti, D., Rossetti, C. and Calamari, D. (2006) Effects of a complex mixture of therapeutic drugs at environmental levels on human embryonic cells. Environmental Science & Technology 40(7), 2442-2447.

Santos, J.L., Aparicio, I., Callejon, M. and Alonso, E. (2009) Occurrence of pharmaceutically active compounds during 1-year period in wastewaters from four wastewater treatment plants in Seville (Spain). Journal of Hazardous Materials 164(2-3), 1509-1516.

Shannon, M.A., Bohn, P.W., Elimelech, M., Georgiadis, J.G., Marinas, B.J. and Mayes, A.M. (2008) Science and technology for water purification in the coming decades. Nature 452(7185), 301-310.

Stulten, D., Zuhlke, S., Lamshoft, M. and Spiteller, M. (2008) Occurrence of diclofenac and selected metabolites in sewage effluents. Science of the Total Environment 405(1-3), 310-316.

Toprak, M.S., McKenna, B.J., Mikhaylova, M., Waite, J.H. and Stucky, G.D. (2007) Spontaneous assembly of magnetic microspheres. Advanced Materials 19(10), 1362-+.

Tuutijarvi, T., Lu, J., Sillanpaa, M. and Chen, G. (2009) As(V) adsorption on maghemite nanoparticles. Journal of Hazardous Materials 166(2-3), 1415-1420.

Wang, H.T., Keller, A.A. and Clark, K.K. (2011) Natural organic matter removal by adsorption onto magnetic permanently confined micelle arrays. Journal of Hazardous Materials 194, 156-161.

Wang, P., Shi, Q.H., Shi, Y.F., Clark, K.K., Stucky, G.D. and Keller, A.A. (2009) Magnetic Permanently Confined Micelle Arrays for Treating Hydrophobic Organic Compound Contamination. Journal of the American Chemical Society 131(1), 182-188.

Xu, W.H., Zhang, G., Zou, S.C., Li, X.D. and Liu, Y.C. (2007) Determination of selected antibiotics in the Victoria Harbour and the Pearl River, South China using high-performance liquid chromatography-electrospray ionization tandem mass spectrometry. Environmental Pollution 145(3), 672-679.

Yantasee, W., Warner, C.L., Sangvanich, T., Addleman, R.S., Carter, T.G., Wiacek, R.J., Fryxell, G.E., Timchalk, C. and Warner, M.G. (2007) Removal of heavy metals from aqueous systems with thiol functionalized superparamagnetic nanoparticles. Environmental Science & Technology 41(14), 5114-5119.

Yavuz, C.T., Mayo, J.T., Yu, W.W., Prakash, A., Falkner, J.C., Yean, S., Cong, L.L., Shipley, H.J., Kan, A., Tomson, M., Natelson, D. and Colvin, V.L. (2006) Low-field magnetic separation of monodisperse Fe3O4 nanocrystals. Science 314(5801), 964-967.

Zhang, S.Y., Zhang, Q.A., Darisaw, S., Ehie, O. and Wang, G.D. (2007) Simultaneous quantification of polycyclic aromatic hydrocarbons (PAHs), polychlorinated biphenyls (PCBs), and pharmaceuticals and personal care products (PPCPs) in Mississippi river water, in New Orleans, Louisiana, USA. Chemosphere 66(6), 1057-1069.

Chapter 5. Micelle Array Confined Superparamagnetic Nanoparticle Adsorbents Porous Structure Optimization for Higher and Faster Removal of Emerging Organic Contaminants and PAHs

5.1. Introduction

Emerging organic contaminants (EOCs) are relatively new group of unregulated as contaminants due to the limited ecotoxicological information available. EOCs include a wide range of compounds across various chemical classes, such as pharmaceuticals and personal care products (PPCPs), pesticides, surfactants, various industrial additives, and endocrine disruptors (EDCs) (Huang and Keller 2013, Murray et al. 2010). The presence of these EOCs in fresh water or wastewater poses possible toxicological effects to the environment and living organisms (Thomaidi et al. 2015, Yan et al. 2014). Current treatment options that are typically considered for the removal of EOCs from aquatic systems include adsorption and ozonation or advanced oxidation processes, since conventional water treatment processes such as coagulation/flocculation/sedimentation, filtration, and chlorination do not provide an effective removal efficiency many EOCs (Stackelberg et al. 2004). While conventional and advanced oxidation processes can be effective for the removal of EOCs, these processes lead to the formation of oxidation intermediates that are mostly unknown at this point. In addition, unwanted oxidation byproducts, such as halogenated organic compounds or bromate, form in oxidation

processes involving chlorine and ozone (Adams et al. 2002). Several studies have evaluated the adsorption of EOCs on activated carbon (Yoon et al. 2003, Yu et al. 2008), but high adsorbent usage rates can be expected if activated carbon is employed to adsorb polar organic contaminants (Quinlivan et al. 2005).

Magnetic core hybrid nanoparticle adsorbents have shown promise for application in water decontamination owing to their large surface area, and high ratio of surface-to-volume (Huang and Keller 2013, 2015, Su et al. 2015, Su et al. 2014). With the superparamagnetic feature, these nanoparticle sorbents could be extracted and recycled from wastewater system via applying an external magnetic field (Huang and Keller 2015, Wang and Keller 2008). In previous studies, we synthesized magnetic permanently confined micelle arrays (Mag-PCMAs) with a magnetite core and a silica porous layer that permanently confines canonic surfactant micelles within the mesopores, and had been successfully applied to remove hydrophobic compounds (Wang and Keller 2008), pesticides (Clark and Keller 2012b), natural organic matter (Wang et al. 2011), oxyanions (Clark and Keller 2012a) and emerging organic contaminants (Huang and Keller 2013). However, since the cationic surfactant is permanently anchor on the silica framework through –Si–O–Si– covalent bonding (Wang and Keller 2008), the surfactant would occupy most of the pore space. It would reduce the pore space for contaminant adsorption, which may lower the adsorption capacity or kinetics.

Recently, a micelle swelling agent was used to expand the micelles as well as generate cavities within the materials for increasing the removal of HOCs (Shi et al. 2012). Thus, one potential strategy to optimize Mag-PCMAs' porous structure would be to add a micelle swelling agent during the synthesis and later remove it to increase pore volume and surface area. In this study, we introduced 1,3,5-trimethyl benzene (TMB) as a micelle swelling agent to the synthesis of Mag-PCMAs and investigated the effect of different amounts of TMB on the porous structure of Mag-PCMAs, as well as the effect on removal efficiency and sorption kinetics of three EOCs and two PAHs. Relevant physicochemical properties for the contaminants are presented in Table 1. In addition, since the optimized Mag-PCMAs can be regenerated and reused, they provide a sustainable approach for decontamination of EOCs and PAHs.

5.2. Experimental

5.2.1. Chemicals

Maghemite (iron (III) oxide) nanoparticles (30 nm in diameter) were purchased from Alfa Aesar (USA). Tetramethyl ammonium hydroxide (TMAOH) (25 wt % in water), 3-(trimethoxysily)propyl-octadecyldimethyl-ammonium chloride (TPODAC) (72 wt % in methanol), ammonia (28%), methanol, tetraethyl orthosilicate (TEOS), gemfibrozil, and sulfamethoxazolewere purchased from Sigma-Aldrich (USA). Methyl orange, acenaphthene (99% pure), phenanthrene (98% pure), and 1,3,5-trimethyl benzene (TMB)

were purchased from Acros Organics (Geel, Belgium). All chemicals were used as received, without further purification. All solutions were prepared with deionized water (18 MΩ-cm) from a Barnstead NANOpure Diamond Water Purification System (USA).

5.2.2. Synthesis of Mag-PCMAs

0.1 g maghemite nanoparticles were dispersed in 40 mL of TMAOH solution (25% by weight) under constant mixing overnight as pre-treatment to activate the surface. Then 2.5 mL of TPODAC and 0.8 mL of TMB were added to maghemite redispersed in water and ethanol in a volumetric ratio of 1:6 under constant stirring. 5 mL of 28% ammonium hydroxide was added for base-catalyzed sol-gel hydrolysis along with 1 mL of TEOS to bind the surfactant onto the magnetic iron core. The mixture was stirred overnight at room temperature (22–25 °C), then transferred into a hydrothermal bomb, and treated at 110 °C for 24 h. After being rinsed with ethanol, the particles were dried under vacuum at 60 °C overnight to remove TMB. This method was adapted and modified from the synthesis of Mag-PCMAs reported in a previous study (Huang and Keller 2013). The new material was denominated Mag-PMCAs-30, as the weight ratio of TMB to TPODAC is 30%. To investigate the effect of the amount of micelle swelling agent on the sorption capacity and kinetic for EOCs and PAHs onto Mag-PCMAs, Mag-PCMAs-0 and Mag-PMCAs-60 were synthesized following the same procedure as Mag-PMCAs-30 except that the amount of TMB was changed to 0 mL and 1.6 mL, respectively.

5.2.3 Characterization of Mag-PCMAs

Transmission electron microscopy (TEM) images were obtained using a JEOL 1230 Transmission Electron Microscope operated at 80 kV. Electron microscopic images were analyzed by a Philips Electron Optics environmental scanning electron microscope (ESEM) using an accelerating voltage of 3.00 kV. The surface area and pore volume of Mag-PCMAs were determined using a computer-controlled nitrogen gas adsorption analyzer (TriStar 3000). Before measurements, the samples were degassed at 90 °C in a nitrogen flow for 12 h. Thermogravity measurements were used to investigate the amount of surfactant confined on magnetic particle sorbents; thermogravimetric analyses (TGA) were carried out on a TA Instruments Discovery under an air flow of 25 mL/min with a heating rate of 10 °C/min. Magnetization measurements were performed on a Quantum Design MPMS 5XL superconducting quantum interference device (SQUID) Magnetometer.

5.2.4. Batch sorption of EOCs and PAHs

For most experiments 20 mg of the Mag-PCMAs (Mag-PCMAs-0, Mag-PCMAs-30, and Mag-PCMAs-60) particles were mixed in 20 ml of glass vial with 20.0 ml of EOCs or PAHs solution. Adsorption kinetics studies were carried out at the same conditions as previously stated but for a set amount of time, varying from 5 min to 24 h. The sorption isotherms of EOCs and PAHs onto Mag-PCMAs were determined by the same procedure

as the sorption kinetics determination and the equilibration time was 24 h uniformly, to ensure sorption equilibrium to be reached. The concentration of adsorbent was varied from 0.05 to 1 g/L to study the adsorption isotherms of EOCs and PAHs onto Mag-PMCAs. Additionally, solutions with varying initial concentrations of EOCs and PAHs, which ranged from 0.5 mg/L to 100 mg/L were treated with 20 mg of Mag-PCMA particles. These vials were placed in an end-over-end shaker on a Dayton-6Z412A Parallel Shaft (USA) roller mixer with a speed of 70 rpm. After this mixing, the Mag-PCMAs particles were separated from the mixture with an Eclipse magnet N821permanent hand-held magnet (50 mm ×50 mm ×12.5 mm; 243.8 g; pull force: 40.1 N). All experiments were conducted at ambient temperature (22–25 °C).

5.2.5. Regeneration and reuse of Mag-PCMAs

To investigate the regeneration and reuse of the three different Mag-PCMAs, 10 mg/L methyl orange were used with the same adsorption process, followed by separation of the Mag-PCMAs from solution with the handheld magnet. The Mag-PCMAs collected was then extracted with methanol. The regenerated Mag-PCMA particles were then reused for subsequent methyl orange sorption experiments. The sorption, extraction, and reuse processes were repeated for five times. Changes in sorption capacity was determined at every cycle.

5.2.6. Analysis

A Shimadzu high performance liquid chromatograph (HPLC) system (SPD-M10AVP, Shimadzu, MD) equipped with an Ascentis C-18 column (250 × 4.6 mm, 10 μm) and a UV-Vis spectrometer (BioSpec 1601, Shimadzu, MD) were used for EOCs and PAHs analysis.

Removal efficiency and sorption capacity of EOCs or PAHs was calculated as:

$$Removal\ efficiency = \frac{C_0 - C_t}{C_0} \times 100\% \quad (1)$$

$$Sorption\ capacity = q_e = \frac{(C_0 - C_t) \cdot V}{m} \quad (2)$$

where C_0 and C_t are the initial and final concentrations of EOCs (mg/L), m is the mass of Mag-PCMAs (g), and V is the volume of solution (L).

The equilibrium adsorption of EOCs or PAHs was evaluated according to Langmuir and Freundlich isotherms by Eq. 3 and Eq. 4, respectively (Morel and Hering 1993):

$$\frac{C_e}{q_e} = \frac{1}{K_L \cdot q_m} + \frac{C_e}{q_m} \quad (3)$$

$$\log q_e = \log K_F + \frac{1}{n} \log C_e \quad (4)$$

where C_e is solute concentration (mg/L) at equilibrium and q_e is amount adsorbed (mg/g), q_m is the maximum sorption capacity (mg/g). K_L and K_F is the Langmuir and Freundlich sorption equilibrium constant (L/mg), respectively.

Kinetics were analyzed using the pseudo-first-order and pseudo-second-order model by Eq. 5 (Coleman et al. 1956):

$$\frac{t}{q_t} = \frac{1}{k_2 q_e^{\,2}} + \frac{1}{q_e} t \qquad (5)$$

where k_2 ($\frac{g}{mg \cdot h}$) are the equilibrium rate constant of kinetics.

5.3. Results and discussion

5.3.1. Mag-PCMAs synthesis and characterization

The synthesis of Mag-PCMAs is schematically presented in Figure 1, and the core/shell structure of Mag-PCMAs is demonstrated by TEM micrograph in Figure 2. SEM images (Figure 2A, C and E) show that the roughness of Mag-PCMAs' surface changed by adjusting the ratio of micelle swelling agent to surfactant. It suggests that adding TMB during synthesis increases the surface area and pore volume, which is in agreement with the specific BET surface area and the total pore volume calculated based on the nitrogen sorption data (Table 2). In particular, comparing the SEM observation of Mag-PCMAs-0 (Figure 2B) and Mag-PCMAs-60 (Figure 2E), there are large cavities in the silica framework of Mag-PCMAs-60, while the surface of Mag-PCMAs-0 was smoother without any obvious cells. Similar observation could be obtained in TEM micrograph (Figure 2B, D and F), Mag-PCMAs-30 (Figure 2D) and Mag-PCMAs-60 (Figure 2F) show more mesoporous structure and channels inside their particles, which is induced by the micelle swelling agent.

The TGA curves of the different Mag-PCMAs (Figure 3) did not show any significant difference, suggesting that incorporating TMB in the synthesis and post-synthesis removal did not affect the mass percentage of the surfactant confined within the ordered silica framework. Surfactant mass percentage can be determined by the difference of initial and final mass of the sample in TGA curve, and was around 45.46%, 48.58% and 44.63% of the total mass of Mag-PCMAs-0, Mag-PCMAs-30 and Mag-PCMAs-60, respectively. The derivative curve indicates three weight loss steps at about 220, 310, and 600 °C, which can be referred to the decomposition of quaternary ammonium group, the decomposition and carbonization of alkyl chain, and the burn off of carbon, respectively (Wang and Keller 2008).

Magnetic characterization with a SQUID magnetometer at 300 K indicated that Mag-PCMAs-0, Mag-PCMAs-30 and Mag-PCMAs-60 have magnetization saturation values of 5.48, 5.24 and 7.09 emu/g, respectively (Figure 4), indicating a relatively high magnetization. Additionally, no remanence was detected in any of the Mag-PCMAs particles, indicating a superparamagnetism feature due to the nanosized maghemite. Due to the strong magnetization, Mag-PCMAs suspended in water can be quickly separated from the dispersion with a magnet (1000 Oe), indicate that the Mag-PCMAs possesses excellent magnetic responsivity.

5.3.2. Sorption kinetics of EOCs and PAHs

Time dependent removal of methyl orange (initial concentration= 100 mg/L) by the three different types of Mag-PCMAs (1 g/L) showed rapid adsorption of EOCs in the first 30 minutes with above 98% removal efficiency, and thereafter, the rate decreased gradually and reached equilibrium, as shown in Figure 5A. However the removal rate increased significantly with the amount of TMB used during synthesis (Figure 5 A and B). Removal is demonstrated visually in Figure 5B, where the color of methyl orange contaminated solution faded to clear after 60, 30 and 15 min treatment with Mag-PCMA-0, Mag-PCMA-30, and Mag-PCMA-60, respectively. As all of 3 different Mag-PCMAs showed fast sorption rates of EOCs, the sorption kinetics were conducted with mixing times of 1, 5, 10, 15, 30 and 360 minutes for 3 EOCs and 2 PAHs. The kinetic model was then used to investigate the adsorption rate (Figure 5C). The results show that for the sorption kinetics of different EOCs and PAHs onto specific Mag-PCMAs, k_2 decreased with an increasing molecular weight of EOCs or PAHs. It is expected as the EOCs or PAHs would first diffuse through the porous silica framework to interact with the confined surfactant micelles, and the diffusion rates of different compounds are limited by the molecular sizes and weights (Weber and Morris 1963). The negative relationship between k_2 and molecular weight suggests the sorption kinetics of EOCs and PAHs onto Mag-PCMAs are dominated by the diffusion rate (Yeom et al. 1996). For the sorption of the same EOCs or PAHs onto different Mag-PCMAs, higher k_2 was obtained with higher

portion of micelle swelling agent was utilized to synthesize. It was attributed by larger pore size and more porous channels presented (Figure 2), which would provide fast rate of diffusion and mass transfer.

5.3.3. Sorption isothermal of EOCs and PAHs

Figure 6 presents the experimental results of the sorption for EOCs and PAHs along with the fit of the Langmuir and Frenundlich isotherm model (fitted parameter values are summarized in Table 4.). Based on the correlation coefficients (R^2) in Table 4, the Freundlich model was a better fit, suggesting it's likely to be a multilayer sorption process (Weber et al. 1991). For the compounds with relatively high $\log K_{ow}$ (>3.5), the sorption of different EOCs or PAHs onto specific Mag-PCMA, K_F increased with an increasing $\log K_{ow}$, suggesting the sorption mechanism was dominated by hydrophobic interaction (Schwarzenbach et al. 2005, Wang et al. 2009). While for the compound with relatively low $\log K_{ow}$ (<1), the relationship between K_F and $\log K_{ow}$ was less obvious, and another potential mechanism could be electrostatic interactions as the confined surfactant micelles are cationic (Clark and Keller 2012a, Huang and Keller 2013). For the sorption of the same EOCs or PAHs onto different Mag-PCMAs, higher sorption capacities were achieved with increasing percentage of TMB used in the synthesis (Table 4). It suggests that with larger pore size and higher pore volume (Table 1) sorption capacity increases.

The large amount of surfactant micelles confined in the silica framework (Figure 3) also contributed.

5.3.4. Regeneration and reuse of Mag-PCMAs

To demonstrate the regenerability and reusability of the modified Mag-PCMAs, the recovery of methyl orange sorbed onto the Mag-PCMA was investigated using methanol extraction. Methyl orange removal performance by three different Mag-PCMAs during five continuous cycles of regeneration and reuse are shown in Figure 7. No significant losses of sorption capacity of methyl orange was observed for the regenerated Mag-PCMA after 5 cycles, indicating good reusability of Mag-PCMAs.

5.4. Conclusions

The porous structure of the synthesized magnetic nanoparticle sorbents were optimized by introducing a micelle swelling agent and removing it after synthesis. The sorbents are core/shell structure with a magnetite core and a silica porous layer that permanently confines surfactant micelles within the framework. The surfactant, TPODAC, has a reactive -Si $(OCH_3)_3$ group on its hydrophilic end, which allows the surfactant micelles to permanently anchor on the silica framework through covalent bonding. This strong binding of the surfactant enables the Mag-PCMAs to be regenerable at a lower operating cost. The optimized Mag-PCMAs showed higher sorption kinetic rate as well as higher sorption capacity to EOCs and PAHs. The Mag-PCMAs are promising sorbents

for fast, effective and sustainable remediation of EOCs and PAHs. Based on the fast sorption kinetics and high sorption capacity for EOCs and PAHs, with high regeneration performance of Mag-PCMAs, larger scale continuous batch reactors can be designed for water treatment.

Table 1. Properties of selected EOCs and PAHs for Sorption Studies (Huang and Keller 2013, Watts 1998)

	Compound name	Molecular weight (g/mol)	Octanol–water partition coefficient $\log K_{ow}$
EOCs	Methyl Orange	327.3	0.680
	Sulfamethoxazole	253.3	0.890
	Gemfibrozil	250.3	4.770
PAHs	Acenaphthene	154.2	3.920
	Phenanthrene	178.2	4.520

Table 2. Surface area and pore volume of Mag-PCMAs-0, Mag-PCMAs-30, and Mag-PCMAs-60.

	Surface area (m^2/g)	Pore volume (cm^3/g)
Mag-PCMAs-0	1.345	0.029
Mag-PCMAs-30	1.606	0.045
Mag-PCMAs-60	1.631	0.047

Table 3. Kinetic parameters for EOCs and PAHs sorption on Mag-PCMAs

EOCs/PAHs	Mag-PCMAs	q_e (mg/g)	k_2 (g/h·mg)	R^2
Methyl Orange	Mag-PCMAs-0	108.7	0.077	0.995
	Mag-PCMAs-30	102.9	0.200	0.998
	Mag-PCMAs-60	102.9	0.271	0.999
Sulfamethoxazole	Mag-PCMAs-0	50.25	0.066	0.999
	Mag-PCMAs-30	51.02	0.082	1.000
	Mag-PCMAs-60	50.00	0.235	1.000
Gemfibrozil	Mag-PCMAs-0	50.00	13.33	1.000
	Mag-PCMAs-30	50.77	19.41	1.000
	Mag-PCMAs-60	50.00	16.00	1.000
Acenaphthene	Mag-PCMAs-0	0.839	888.8	0.992
	Mag-PCMAs-30	0.828	1042	1.000
	Mag-PCMAs-60	0.825	1130	1.000
Phenanthrene	Mag-PCMAs-0	0.945	361.5	1.000
	Mag-PCMAs-30	0.943	488.9	0.996
	Mag-PCMAs-60	0.945	699.6	1.000

Table 4. Isotherm parameters for EOCs and PAHs sorption on Mag-PCMAs

EOCs and PAHs	Mag-PCMAs	Langmuir			Freundlich		
		q_m (mg/g)	K_L (L/mg)	R^2	K_F ((mg/g)/(L/mg)$^{-n}$)	1/n	R^2
Sulfamethoxazole	Mag-PCMAs-0	87.41	0.718	0.996	43.57	0.206	0.999
	Mag-PCMAs-30	94.07	0.764	0.996	46.08	0.216	0.959
	Mag-PCMAs-60	113.1	0.749	0.996	66.63	0.144	0.981
Gemfibrozil	Mag-PCMAs-0	66.49	-12.23	0.957	9.759	1.732	0.997
	Mag-PCMAs-30	238.1	1.077	0.977	50.93	1.286	0.960
	Mag-PCMAs-60	454.5	0.038	0.968	33.24	1.208	0.990
Methyl Orange	Mag-PCMAs-0	175.4	11.40	1.000	117.6	0.108	0.991
	Mag-PCMAs-30	185.2	-1.038	0.997	113.5	0.133	0.997
	Mag-PCMAs-60	400.0	0.148	0.908	229.0	0.154	0.995
Acenaphthene	Mag-PCMAs-0	0.478	-16.36	0.986	9.216	0.899	0.981
	Mag-PCMAs-30	0.612	-20.30	0.935	9.938	1.156	0.991
	Mag-PCMAs-60	1.366	-13.21	0.948	14.61	1.278	0.995
Phenanthrene	Mag-PCMAs-0	0.359	-20.04	0.984	9.369	0.663	0.971
	Mag-PCMAs-30	0.571	-14.45	0.968	26.63	1.175	0.991
	Mag-PCMAs-60	1.233	-32.44	0.956	65.35	1.574	1.000

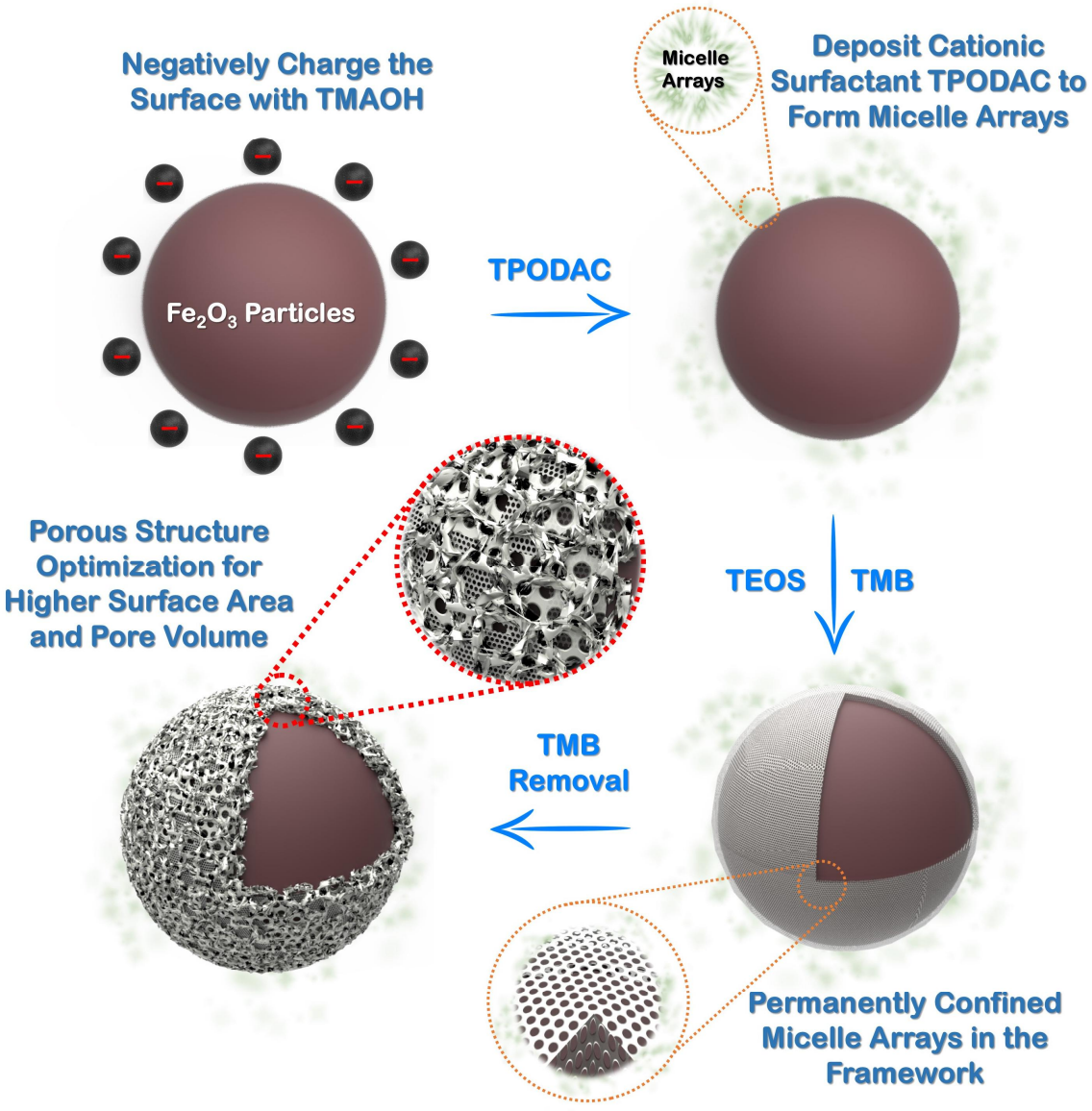

Figure 1. Schematic representation of Mag-PCMAs synthesis with TMB additive

(note: the core and shell are not drawn to scale).

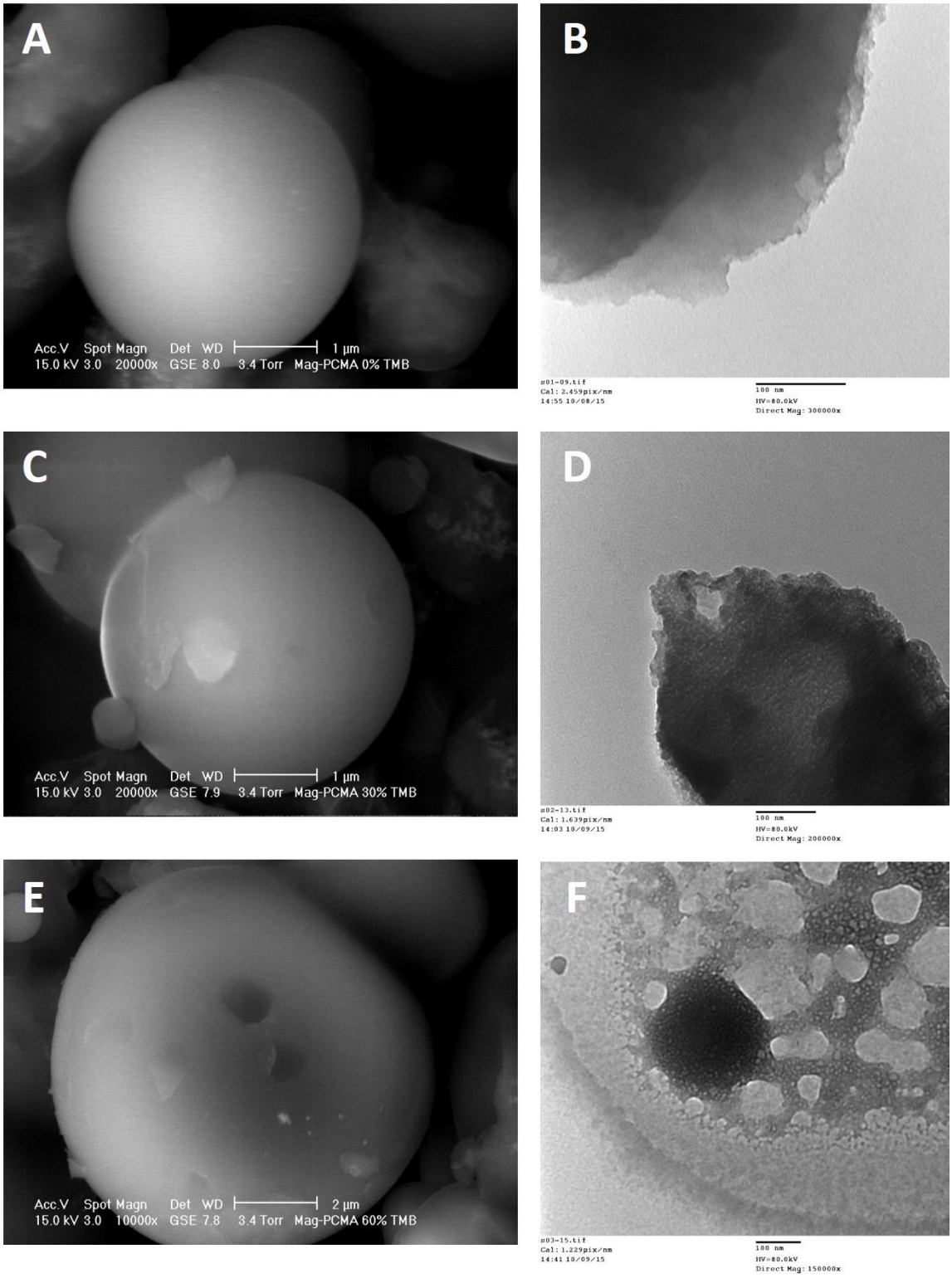

Figure 2. (A) ESEM micrographs of Mag-PCMAs-0 at 20,000×, scale bar=1 μm; (B) TEM micrographs of Mag-PCMAs-0 at 300,000×, scale bar=100 nm; (C) ESEM

micrographs of Mag-PCMAs-30 at 20,000×, scale bar = 1 μm; (D) TEM micrographs of Mag-PCMAs-30 at 200,000×, scale bar=100 nm; (E) ESEM micrographs of Mag-PCMAs-60 at 10,000×, scale bar=2 μm; (F) TEM micrographs of Mag-PCMAs-60 at 150,000×, scale bar=100 nm.

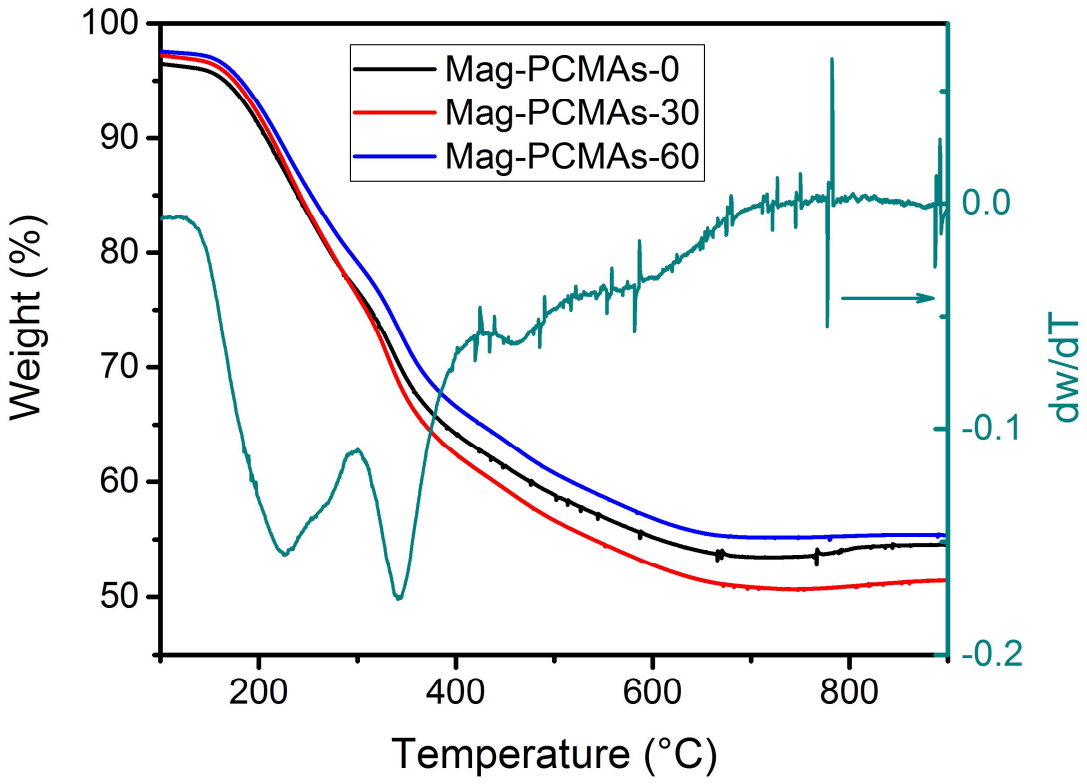

Figure 3. Thermogravimetric analysis (TGA) of Mag-PCMAs-0, Mag-PCMAs-30, and Mag-PCMAs-60.

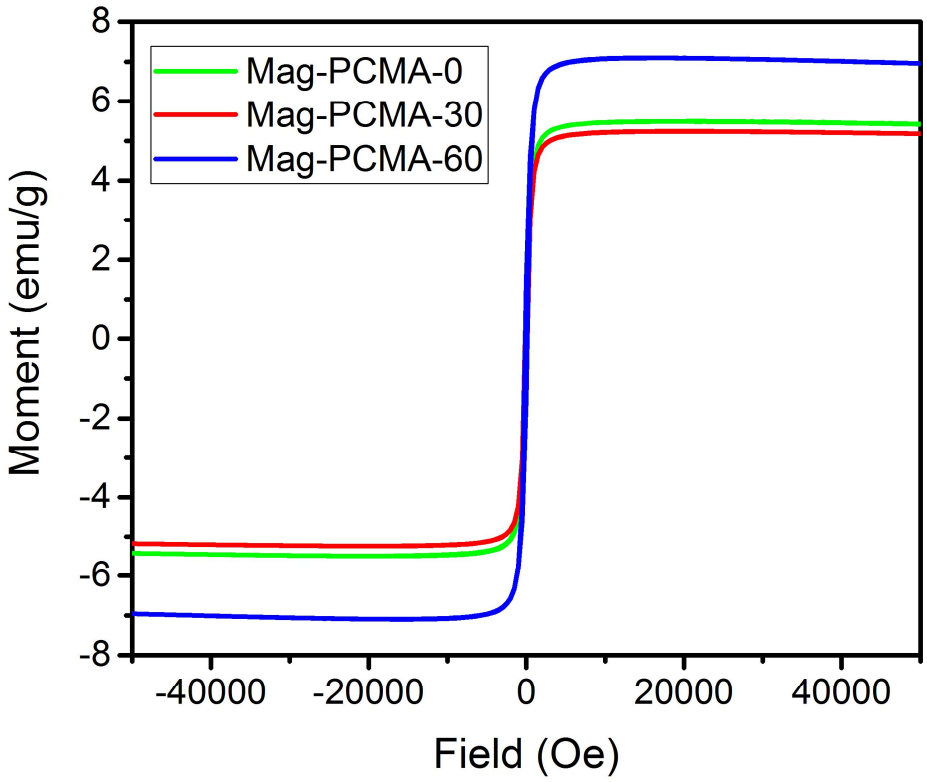

Figure 4. The magnetic hysteresis loops of Mag-PCMAs-0, Mag-PCMAs-30, and Mag-PCMAs-60.

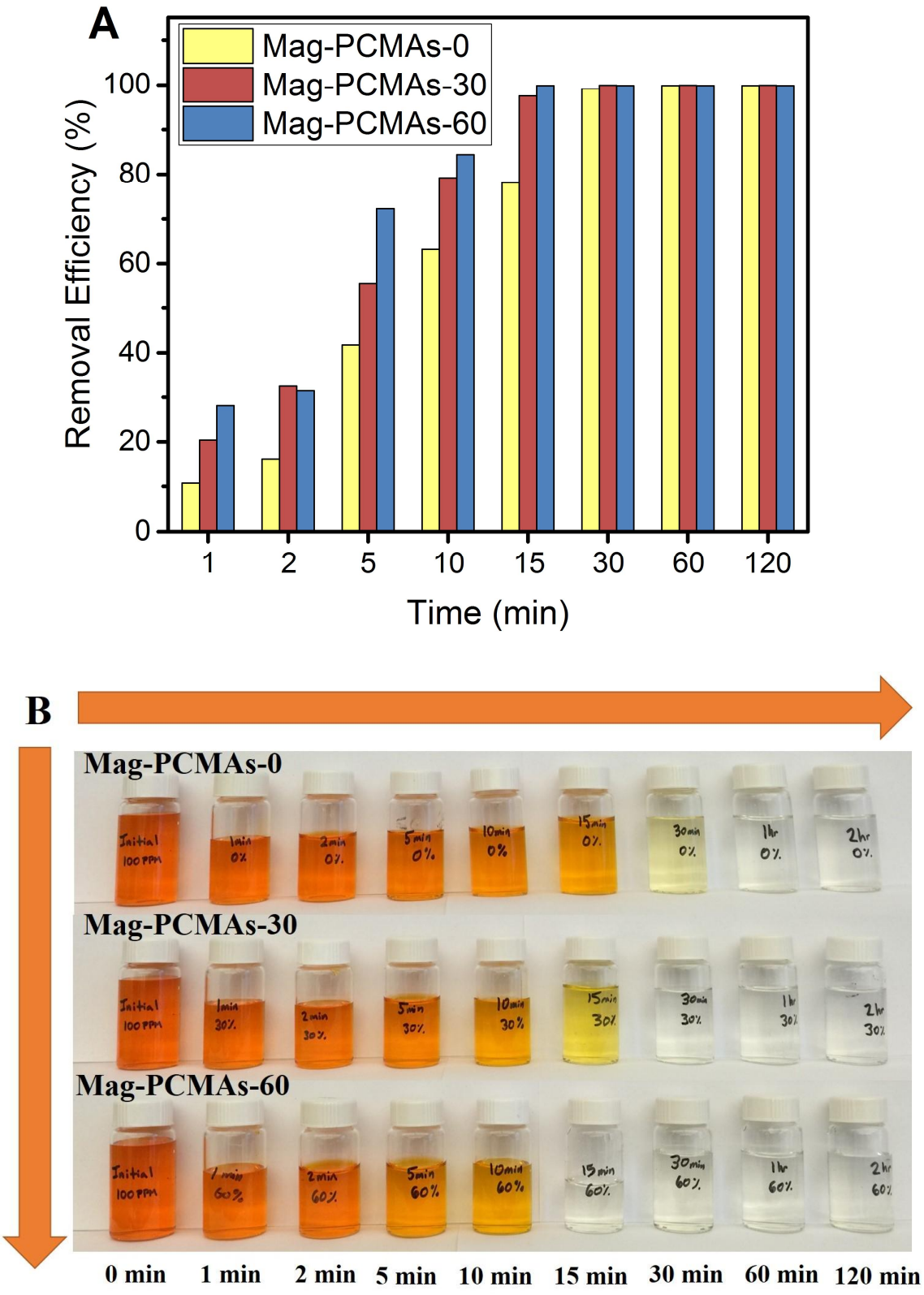
A
Mag-PCMAs-0
Mag-PCMAs-30
Mag-PCMAs-60
Removal Efficiency (%)
0
20
40
60
80
100
1
2
5
10
15
30
60
120
Time (min)
B
Mag-PCMAs-0
Mag-PCMAs-30
Mag-PCMAs-60
0 min
1 min
2 min
5 min
10 min
15 min
30 min
60 min
120 min

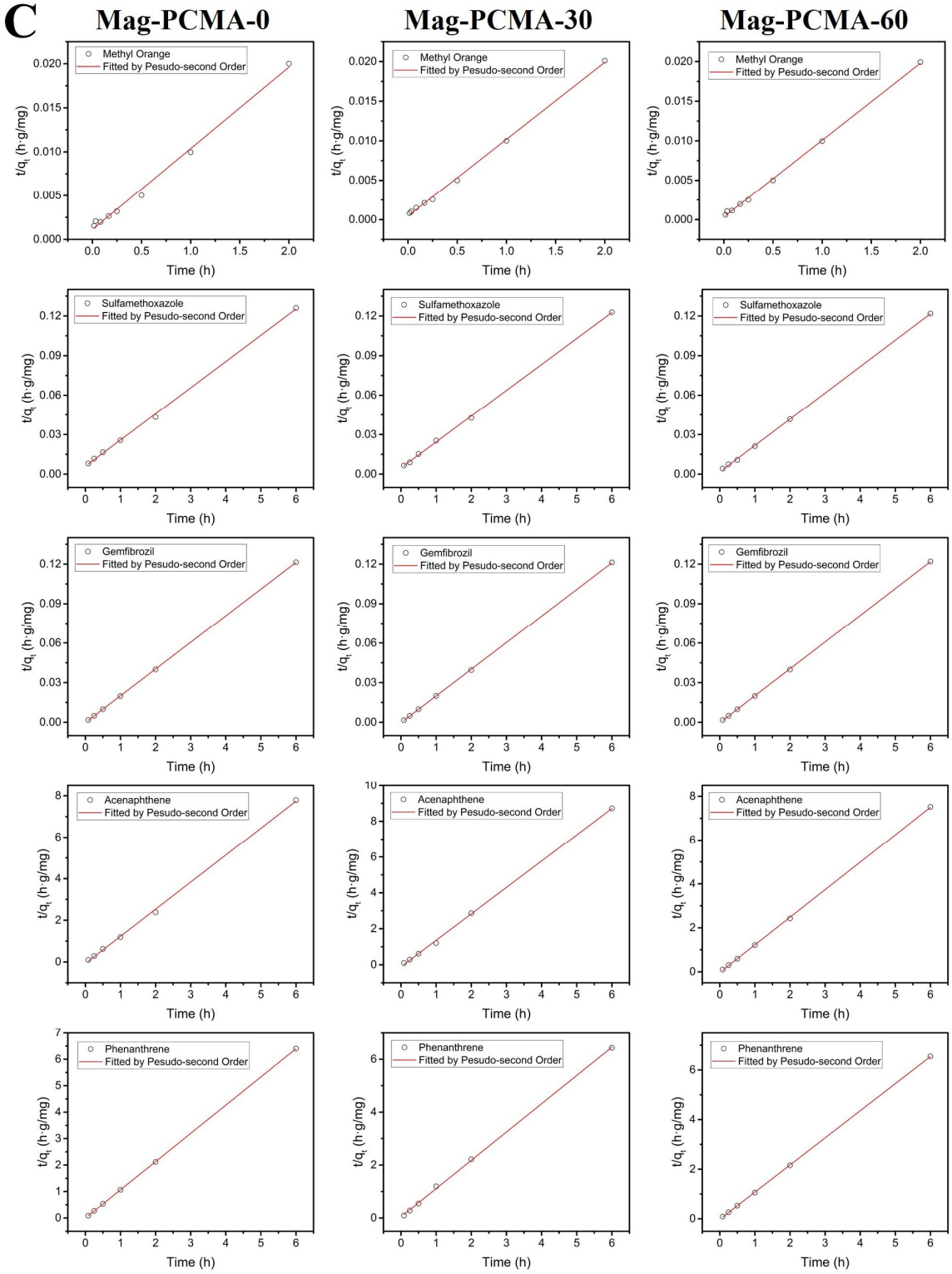
C
Mag-PCMA-0
Mag-PCMA-30
Mag-PCMA-60
Methyl Orange
Fitted by Pesudo-second Order
Sulfamethoxazole
Fitted by Pesudo-second Order
Gemfibrozil
Fitted by Pesudo-second Order
Acenaphthene
Fitted by Pesudo-second Order
Phenanthrene
Fitted by Pesudo-second Order
t/q_t (h·g/mg)
Time (h)

Figure 5. Methyl Orange sorption onto Mag-PCMAs (A) removal efficiency versus time; and (B) visualization of color changes across time sequence; (C) EOCs and PAHs (methyl orange, sulfamethoxazole, gemfibrozil, acenaphthene and phenanthrene) sorption kinetics fitted by Pseudo-second order onto Mag-PCMAs in solution, symbols represent experimental data, and red line represents model prediction.

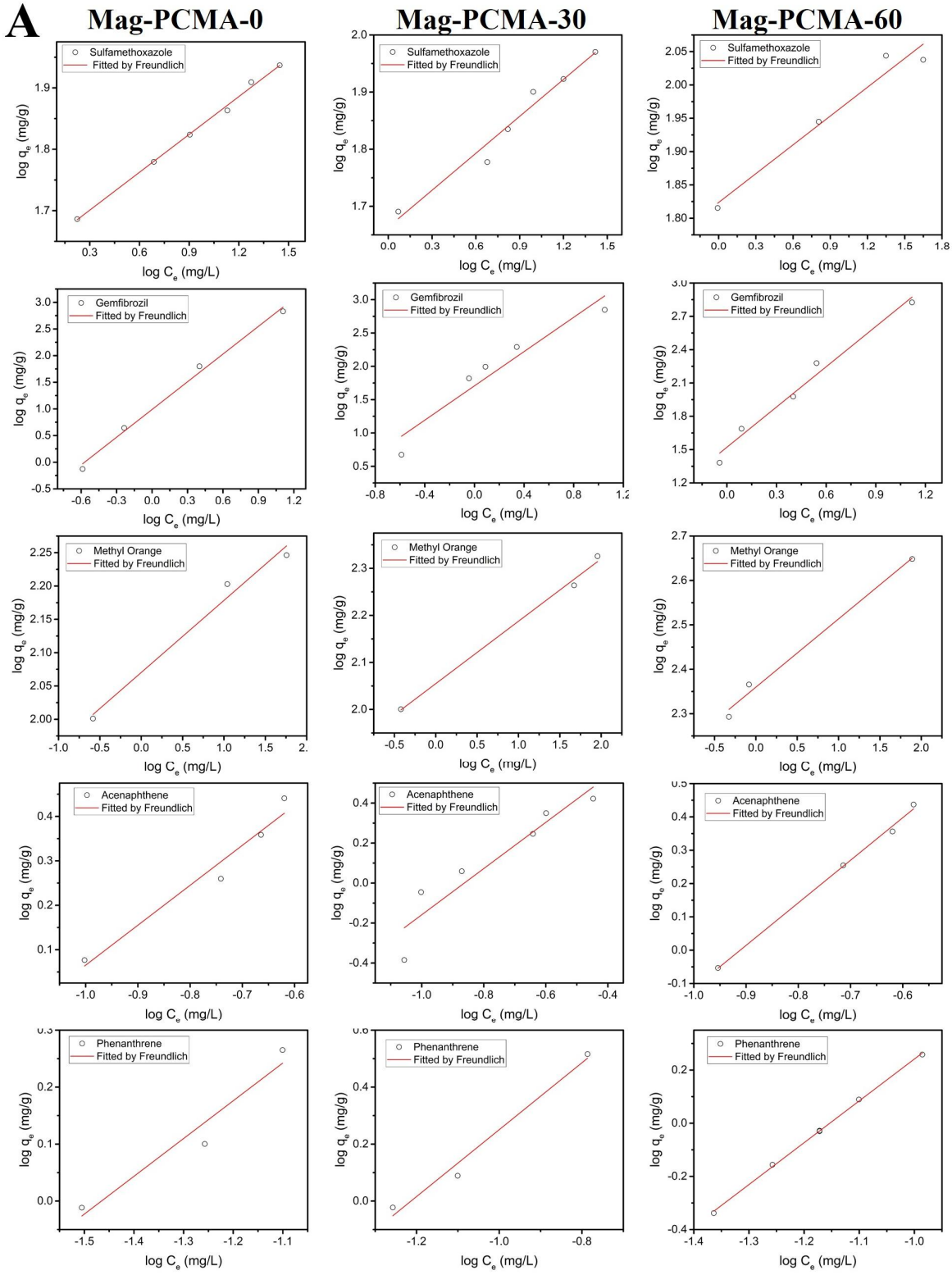
A
Mag-PCMA-0
Mag-PCMA-30
Mag-PCMA-60
Sulfamethoxazole
Fitted by Freundlich
Gemfibrozil
Fitted by Freundlich
Methyl Orange
Fitted by Freundlich
Acenaphthene
Fitted by Freundlich
Phenanthrene
Fitted by Freundlich
log q_e (mg/g)
log C_e (mg/L)

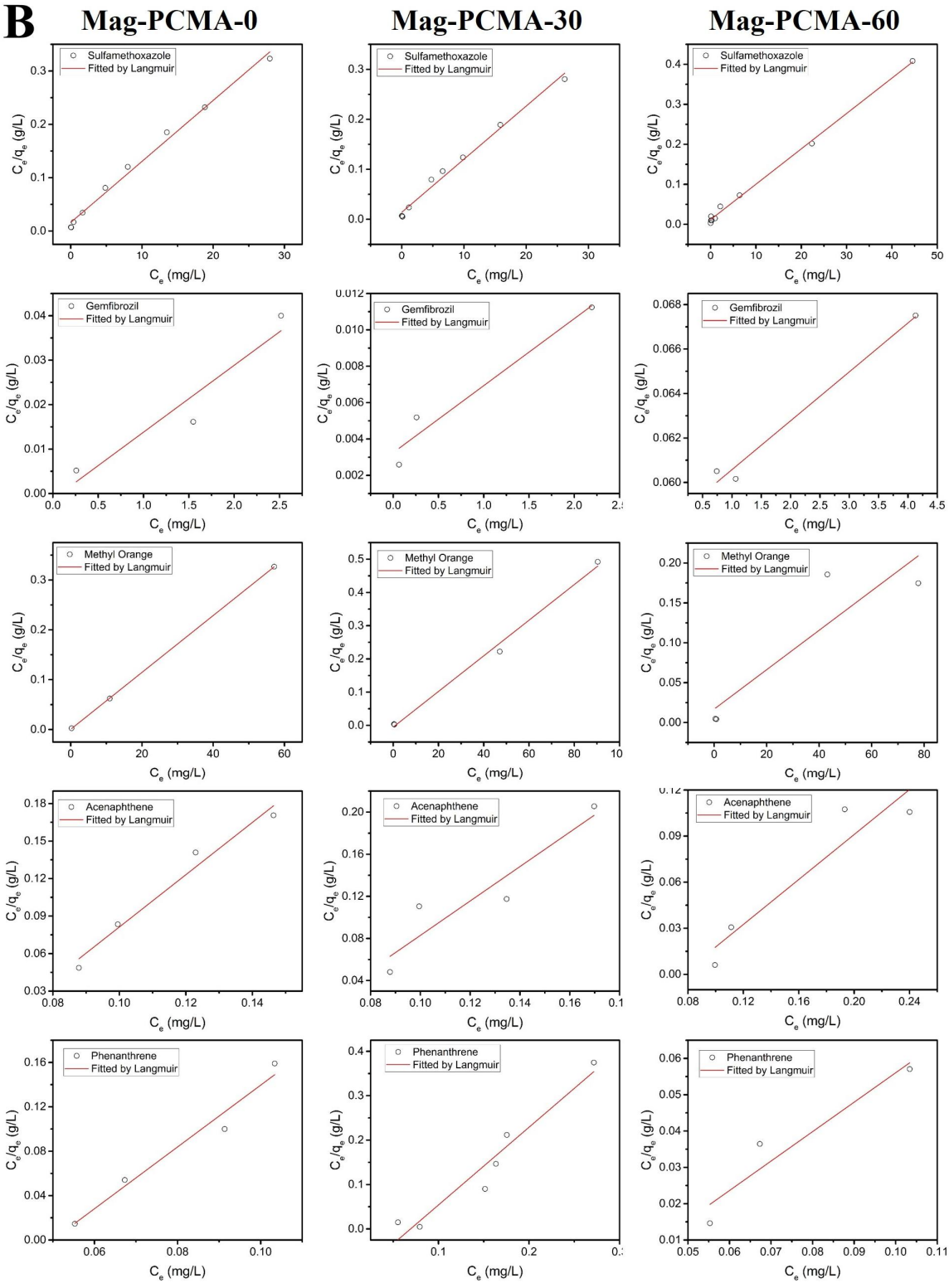
B
Mag-PCMA-0
Mag-PCMA-30
Mag-PCMA-60
Sulfamethoxazole
Fitted by Langmuir
Gemfibrozil
Fitted by Langmuir
Methyl Orange
Fitted by Langmuir
Acenaphthene
Fitted by Langmuir
Phenanthrene
Fitted by Langmuir
Ce/qe (g/L)
Ce (mg/L)

Figure 6. Adsorption of EOCs and PAHs (sulfamethoxazole, gemfibrozil, methyl orange, acenaphthene and phenanthrene) onto Mag-PCMA in solution with (A) Freundlich and (B) Langmuir adsorption isotherms fit, symbols represent experimental data, and red line represents model prediction.

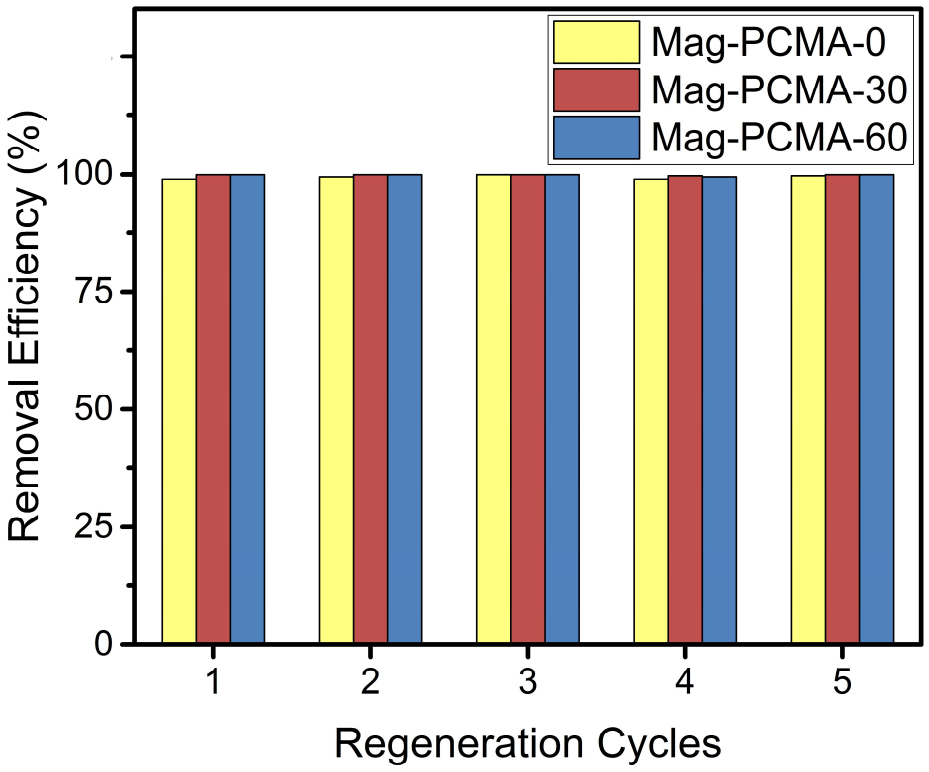

Figure 7. Sorption of acenaphthene onto Mag-PCMA during five regeneration cycles.

5.5. References

Adams, C., Wang, Y., Loftin, K. and Meyer, M. (2002) Removal of antibiotics from surface and distilled water in conventional water treatment processes. Journal of Environmental Engineering-Asce 128(3), 253-260.

Clark, K.K. and Keller, A.A. (2012a) Adsorption of perchlorate and other oxyanions onto magnetic permanently confined micelle arrays (Mag-PCMAs). Water Research 46(3), 635-644.

Clark, K.K. and Keller, A.A. (2012b) Investigation of two magnetic permanently confined micelle array sorbents using nonionic and cationic surfactants for the removal of PAHs and pesticides from aqueous media. Water, Air, & Soil Pollution 223(7), 3647-3655.

Coleman, N.T., Mcclung, A.C. and Moore, D.P. (1956) Formation Constants for Cu(Ii)-Peat Complexes. Science 123(3191), 330-331.

Huang, Y.X. and Keller, A.A. (2013) Magnetic Nanoparticle Adsorbents for Emerging Organic Contaminants. Acs Sustainable Chemistry & Engineering 1(7), 731-736.

Huang, Y.X. and Keller, A.A. (2015) EDTA functionalized magnetic nanoparticle sorbents for cadmium and lead contaminated water treatment. Water Research 80, 159-168.

Morel, F.M.M. and Hering, J.G. (1993) Principles and Applications of Aquatic Chemistry, Wiley.

Murray, K.E., Thomas, S.M. and Bodour, A.A. (2010) Prioritizing research for trace pollutants and emerging contaminants in the freshwater environment. Environmental Pollution 158(12), 3462-3471.

Quinlivan, P.A., Li, L. and Knappe, D.R.U. (2005) Effects of activated carbon characteristics on the simultaneous adsorption of aqueous organic micropollutants and natural organic matter. Water Research 39(8), 1663-1673.

Schwarzenbach, R.P., Gschwend, P.M. and Imboden, D.M. (2005) Environmental organic chemistry, John Wiley & Sons.

Shi, Y.F., Li, B., Wang, P., Dua, R. and Zhao, D.Y. (2012) Micelle swelling agent derived cavities for increasing hydrophobic organic compound removal efficiency by

mesoporous micelle@silica hybrid materials. Microporous and Mesoporous Materials 155, 252-257.

Stackelberg, P.E., Furlong, E.T., Meyer, M.T., Zaugg, S.D., Henderson, A.K. and Reissman, D.B. (2004) Persistence of pharmaceutical compounds and other organic wastewater contaminants in a conventional drinking-water-treatment plant. Science of the Total Environment 329(1), 99-113.

Su, Y., Adeleye, A.S., Keller, A.A., Huang, Y., Dai, C., Zhou, X. and Zhang, Y. (2015) Magnetic sulfide-modified nanoscale zerovalent iron (S-nZVI) for dissolved metal ion removal. Water Research.

Su, Y.M., Adeleye, A.S., Huang, Y.X., Sun, X.Y., Dai, C.M., Zhou, X.F., Zhang, Y.L. and Keller, A.A. (2014) Simultaneous removal of cadmium and nitrate in aqueous media by nanoscale zerovalent iron (nZVI) and Au doped nZVI particles. Water Research 63, 102-111.

Thomaidi, V.S., Stasinakis, A.S., Borova, V.L. and Thomaidis, N.S. (2015) Is there a risk for the aquatic environment due to the existence of emerging organic contaminants in treated domestic wastewater? Greece as a case-study. Journal of Hazardous Materials 283, 740-747.

Wang, H., Keller, A.A. and Clark, K.K. (2011) Natural organic matter removal by adsorption onto magnetic permanently confined micelle arrays. Journal of Hazardous Materials 194, 156-161.

Wang, P. and Keller, A.A. (2008) Partitioning of hydrophobic organic compounds within soil-water-surfactant systems. Water Research 42(8-9), 2093-2101.

Wang, P., Shi, Q.H., Shi, Y.F., Clark, K.K., Stucky, G.D. and Keller, A.A. (2009) Magnetic Permanently Confined Micelle Arrays for Treating Hydrophobic Organic Compound Contamination. Journal of the American Chemical Society 131(1), 182-188.

Watts, R.J. (1998) Hazardous wastes: sources, pathways, receptors.

Weber, W.J., Mcginley, P.M. and Katz, L.E. (1991) Sorption Phenomena in Subsurface Systems - Concepts, Models and Effects on Contaminant Fate and Transport. Water Research 25(5), 499-528.

Weber, W.J. and Morris, J.C. (1963) Kinetics of adsorption on carbon from solution. Journal of the Sanitary Engineering Division 89(2), 31-60.

Yan, Z.H., Yang, X.F., Lu, G.H., Liu, J.C., Xie, Z.X. and Wu, D.H. (2014) Potential environmental implications of emerging organic contaminants in Taihu Lake, China: Comparison of two ecotoxicological assessment approaches. Science of the Total Environment 470, 171-179.

Yeom, I.T., Ghosh, M.M. and Cox, C.D. (1996) Kinetic aspects of surfactant solubilization of soil-bound polycyclic aromatic hydrocarbons. Environmental Science & Technology 30(5), 1589-1595.

Yoon, Y.M., Westerhoff, P., Snyder, S.A. and Esparza, M. (2003) HPLC-fluorescence detection and adsorption of bisphenol A, 17 beta-estradiol, and 17 alpha-ethynyl estradiol on powdered activated carbon. Water Research 37(14), 3530-3537.

Yu, Z.R., Peldszus, S. and Huck, P.M. (2008) Adsorption characteristics of selected pharmaceuticals and an endocrine disrupting compound - Naproxen, carbamazepine and nonylphenol - on activated carbon. Water Research 42(12), 2873-2882.

Chapter 6. Magnetic Nanoparticle Adsorbents with Micelle Array Confined in the Framework for PAHs and Metal Contaminants Simultaneous Removal

6.1. Introduction

Polycyclic aromatic hydrocarbons (PAHs) and heavy metal ions such as cadmium (Cd) have posed severe threat to public health and the environment due to their high toxicity and high retention in the environments (Huang and Keller 2015, Vela et al. 2012). Numerous sites are contaminated by both PAHs and heavy metals, including e-wasting processing sites(Luo et al. 2011), manufactured gas plant sites (Thavamani et al. 2012), and river sediments(Feng et al. 2012), which require simultaneous remediation of PAHs and heavy metals. However, most of recent studies have focused on the decontamination of PAHs (Chen et al. 2015, Lee et al. 2015) or heavy metals (Huang et al. 2014, Sargın et al. 2015) individually. There are few studies on simultaneous removal of both heavy metals and organic contaminants from soils or sediments (Maturi and Reddy 2006, Reddy et al. 2010, Song et al. 2008, Veetil et al. 2013).

Surfactants can enhance the removal efficiency of hydrophobic organic compounds (HOC) (Wang and Keller 2008c) including PAHs and pesticides (Clark and Keller 2012b) via micelles, which offer a good hydrophobic environment into which HOCs can partition or ‘dissolve’ (Wang and Keller 2008a). Surfactants can also be used for metal

contaminant remediation via complexation reactions and electronic interaction (Mulligan et al. 1999). However, one major drawback of applying surfactant for aquatic systems and soil remediation is the non-specific binding of the surfactants to clays and the organic matter naturally present (Wang and Keller 2008b), which would cause the displacement and subsequent loss of the surfactant molecules during treatment (Hanna et al. 2002). In this study, we proposed using a nonionic surfactant, Triton X-100, confined within a mesoporous silica matrix, which would reduce surfactant loss during use.

Recently, magnetic sorbents have emerged as a new generation of materials for environmental decontamination (Huang and Keller 2013, 2015, Su et al. 2015, Su et al. 2014). In previous studies, we synthesized magnetic permanently confined micelle arrays (Mag-PCMAs) with a magnetite core and a silica porous layer that permanently confines cationic surfactant micelles within the mesopores, and had been successfully applied to remove HOCs (Wang and Keller 2008c), pesticides (Clark and Keller 2012b), natural organic matter (Wang et al. 2011), oxyanions (Clark and Keller 2012a) and emerging organic contaminants (Huang and Keller 2013). However, the simultaneous removal of PAHs and metal contaminants by Mag-PCMAs with nonionic surfactant has not been well studied.

In this study, acenaphthene and cadmium were selected to represent PAHs and metal contaminants, respectively, to study their sorption isotherms and kinetics onto Mag-PCMAs in aqueous solution. Simultaneous removal of acenaphthene and cadmium was

investigated. Furthermore, the influence of pH, water hardness (Ca^{2+}, Mg^{2+}), and natural organic matters (NOM) on the performance of acenaphthene and cadmium sorption by the synthesized sorbent were studied.

6.2. Experimental

6.2.1. Chemicals

Maghemite (iron (III) oxide) nanoparticles (30 nm in diameter) was purchased from Alfa Aesar (USA). Tetramethyl ammonium hydroxide (TMAOH) (25 wt % in water), Triton X-100, ammonia (28%), methanol, tetraethyl orthosilicate (TEOS), were purchased from Sigma-Aldrich (USA). Acenaphthene (99% pure) was purchased from Acros Organics (Geel, Belgium). Cadmium chloride anhydrous, calcium chloride dehydrate, and magnesium chloride were purchased from Fisher Scientific (USA). Standard Suwannee River NOM was obtained from the International Humic Substances Society (IHSS, USA). NOM stock solution (100 mg/L) was prepared by mixing a known amount of NOM with DI water for 24 h. The pH of the stock solutions was then adjusted to 8 with 0.1 M and 0.01 M NaOH and HCl. All chemicals were used as received, without further purification. All solutions were prepared with deionized water (18 MΩ-cm) from a Barnstead NANOpure Diamond Water Purification System (USA).

6.2.2. Synthesis of Mag-PCMA

The core–shell structured Mag-PCMA were synthesized through a solvothermal reaction, which is cooperative assembly of silica oligomers and surfactant on the maghemite nanoparticles, as illustrated in Figure 1. 0.1 g maghemite nanoparticles were dispersed in 40 mL of TMAOH solution under constant mixing overnight as pre-treatment to activate the surface, which would help to generate a negative charge on the maghemite particles surface resulting in better binding of silicate and surfactant. Then 1.5 mL of Triton X-100, nonionic surfactant was added to maghemite redispersed in water and ethanol in a volumetric ratio of 1:6 under constant stirring. 5 mL of 28% ammonium hydroxide was added for base-catalyzed sol-gel hydrolysis along with 1 mL of TEOS to bind the surfactant onto the magnetic iron core. The mixture was stirred for 2 h at room temperature (22–25 °C). This method was adapted from the synthesis of Mag-PCMAs reported in a previous study (Huang and Keller 2013).

6.2.3 Characterization of Mag-PCMA

Transmission electron microscopy (TEM) images were obtained using a JEOL 1230 Transmission Electron Microscope operated at 80 kV. Thermogravity measurements were used to investigate the amount of surfactant confined on magnetic particle sorbents; thermogravimetric analyses (TGA) were carried out on a Mettler Toledo TGA/sDTA851e apparatus under an air flow of 100 mL/min with a heating rate of 5 °C/min. Magnetization

measurements were performed on a Quantum Design MPMS 5XL superconducting quantum interference device (SQUID) Magnetometer. The zeta potential was measured using a Malvern Zetasizer (Nano-ZS; Malvern Instruments, Southborough, MA) with pH ranging from 4 to 10.

6.2.4. Batch sorption of PAHs and metal ions

For the individual isothermal experiments 5.0 mg of Mag-PCMA particles were mixed with 20 mL of acenaphthene or cadmium (Cd^{2+}) solution (1 mg/L) in 20 ml glass vial or 50 mL conical tubes, respectively, and the pH was adjusted to the desired condition (range from 4 to 10) by using 0.1 M and 0.01 M NaOH and HCl. Then, these tubes or vials were placed in an end-over-end shaker on a Dayton-6Z412A Parallel Shaft (USA) roller mixer with a speed of 70 rpm at room temperature for 24 h to ensure sufficient equilibration time. Adsorption kinetics studies were carried out at the same conditions as previously stated but for a set amount of time, varying from 1 min to 24 h, with pH=7. After this mixing, the Mag-PCMA particles were separated from the mixture with an Eclipse magnet. All experiments were conducted at ambient temperature (22–25 °C).

The concentration of adsorbent was varied from 0.25 to 1.25 g/L to study the individual adsorption isotherms of acenaphthene, NOM, or Cd^{2+} onto Mag-PCMA at pH 7. Additionally, solutions with varying initial concentrations of acenaphthene, NOM, or

Cd^{2+}, which ranged from 0.5 mg/L to 50 mg/L were treated with the same procedure as above at pH 7 and 5.0 mg Mag-PCMA.

Simultaneous sorption was conducted with various dosages of Mag-PCMA particles (1 mg to 25 mg) mixed with 20 mL of acenaphthene and Cd^{2+} solution (1 mg/L) with or without 20 mg/L NOM present. The influence of solution pH and ionic strength on the simultaneous removal was investigated by mixing 10 mg of Mag-PCMA particles with 20 mL of acenaphthene and Cd^{2+} solution (1 mg/L) under various solution pH (ranging from 4 to 10) and concentration of Ca^{2+} or Mg^{2+} (ranging from 1 mg/L to 50 mg/L), respectively.

6.2.5. Regeneration and reuse of Mag-PCMA

To investigate the regeneration and reuse of Mag-PCMA, 1 mg/L acenaphthene were used with the same adsorption process, followed by separation of the Mag-PCMA from solution with the handheld magnet. The Mag-PCMA collected was then extracted with methanol. The regenerated Mag-PCMA particles were then reused for subsequent acenaphthene sorption experiments. The sorption, extraction, and reuse processes were repeated for five times. Changes in sorption capacity was determined at every cycle.

6.2.6. Analysis

An Agilent 7900 inductively coupled plasma with mass spectroscopy (ICP-MS) was used to analyze the concentration of Cd^{2+}. A Shimadzu high performance liquid

chromatograph (HPLC) system (SPD-M10AVP, Shimadzu, MD) equipped with an Ascentis C-18 column (250 × 4.6 mm, 10 μm) and a UV-Vis spectrometer (BioSpec 1601, Shimadzu, MD) were used for PAH analysis.

Removal efficiency and sorption capacity of PAHs and metal ions was calculated as:

$$Removal\ efficiency = \frac{C_0 - C_t}{C_0} \times 100\% \quad (1)$$

$$Sorption\ capacity = q_e = \frac{(C_0 - C_t) \cdot V}{m} \quad (2)$$

where C_0 and C_t are the initial and final concentrations of PAHs or metal ions (mg/L), m is the mass of Mag-PCMAs (g), and V is the volume of solution (L).

The equilibrium adsorption of PAHs and metal ions was evaluated according to Langmuir and Freundlich isotherms by Eq. 3 and Eq. 4, respectively (Morel and Hering 1993):

$$\frac{C_e}{q_e} = \frac{1}{K_L \cdot q_m} + \frac{C_e}{q_m} \quad (3)$$

$$\log q_e = \log K_F + \frac{1}{n} \log C_e \quad (4)$$

where C_e is solute concentration (mg/L) at equilibrium and q_e is amount adsorbed (mg/g), q_m is the maximum sorption capacity (mg/g). K_L (L/mg) and K_F (mg/g)/ $(L/mg)^{-n}$ is the Langmuir and Freundlich sorption equilibrium constant , respectively.

Kinetics were analyzed using the pseudo-second-order model by Eq. 4 (Coleman et al. 1956):

$$\frac{t}{q_t} = \frac{1}{k_2 q_e^{\,2}} + \frac{1}{q_e} t \qquad (5)$$

where k_2 ($\frac{g}{mg \cdot h}$) are the equilibrium rate constant of kinetics.

6.3. Results and discussion

6.3.1. Mag-PCMA characterization

The core/shell structure of a Mag-PCMAs is shown in TEM images (Figure 2), and the shell layer (silica porous framework) is approximately 20 nm as determined by TEM. The size of particles varied from hundred nanometers to several micrometers due to the aggregation via magnetic forces or crosslinking of the silica framework. The weight percentage of surfactant within the silica framework of Mag-PCMA ws determined by the difference of initial and final mass of the sample in the TGA measurement and was approximately 7.45% of the total mass of Mag-PCMA. Magnetic characterization by SQUID magnetometer at 300 K showed that maghemite and Mag-PCMA have magnetization saturation values of 52.8 and 14.65 emu/g, respectively (Figure 2C), indicating a relatively high magnetization of Mag-PCMA particles even with a thick silica coating. The zeta potential in the initial pH range of 4 to 10 is presented in Figure 2D for Mag-PCMAs solution in DI water. In this pH range, the zeta potential of Mag-PCMAs was negative (-30.11 to -41.65 mv), and decreased slightly as pH increased. Even though the surfactant, Triton X-100, is nonionic, due to the pretreatment by TMAOH in the

synthesis the surface of maghemite particle was strongly negatively charged (Wang et al. 2009). It suggests the formation of anionic negatively charged surface complexes on the Mag-PCMAs.

6.3.2. Sorption isothermal of PAHs, metal ions and NOM

Figure 3 presents the experimental results of the non-competitive sorption for Cd^{2+}, acenaphthene and NOM for the range of concentrations studied, as well as the fit of the Langmuir and Freundlich isotherm model (fitted parameter values are summarized in Table 1). The Langmuir model provided a slightly better fit for Cd^{2+}, while the Freundlich model fitted acenaphthene and NOM adsorption better, based on the correlation coefficients (R^2) in Table 1. This suggests a multilayer sorption process(Weber et al. 1991). Since Triton X-100 is a nonionic surfactant confined in micelles within the silica framework of Mag-PCMA, there are several potential remediation mechanisms for these three different categories of contaminants. Triton X-100 is a poly(ethylene oxide), and interactions are predominantly between the ethylene oxide groups and the chlorinated and nonchlorinated hydrophobic organic contaminants (Wang and Keller 2008b, c). Due to the hydrophobic cores, the surfactant micelles can enhance the apparent acenaphthene solubility (Rosen and Kunjappu 2012), which would promote the hydrophobic interaction between acenaphthene and the confined micelles. The ethylene oxide chain on the Triton X-100 can form complexes with metal ions(Kikuchi et al. 1992), explaining the sorption

of Cd^{2+} onto Mag-PCMAs. In addition, since the surface of Mag-PCMAs is negatively charged, there are also favorable electrostatic interactions with cationic ions such as Cd^{2+}. NOM consists of both hydrophobic and hydrophilic regions as well as polar groups, such as carboxylic groups(Tan 2014). The sorption mechanism of NOM onto Mag-PCMA could be the hydrophobic interaction between the hydrophobic fraction of NOM and micelles; or/and the hydrogen bond between carboxylic groups on NOM and poly (ethylene oxide) groups on surfactants(Wang et al. 2011).

6.3.3. Sorption kinetics of PAHs and metal contaminants

Time dependent removal of acenaphthene and Cd^{2+} (initial concentration = 1 mg/L) by Mag-PCMAs (0.25 g/L) showed rapid adsorption of acenaphthene and Cd^{2+}; around 95% of the sorption capacities were obtained in the first 30 min, as shown in Figure 4A. The pseudo-second-order (Figure 4B and C) kinetic model was used to investigate the adsorption rate of acenaphthene and Cd^{2+} onto Mag-PCMAs, and the kinetic parameters were listed in Table 2. Mag-PCMA's fast sorption kinetics for both acenaphthene and Cd^{2+} is due to the relatively high portion of the confined surfactant micelles. It also indicates the silica framework did not show significant effect on the diffusion of PAHs and metal contaminants into the micelles.

6.3.4. Simultaneous sorption of PAHs, metal contaminants and NOM

Based on the above studies, Mag-PCMA could remove acenaphthene, Cd^{2+} and NOM from contaminated water, respectively. Thus, it proposed the potential for the simultaneous remediation of acenaphthene, Cd^{2+} and NOM. The simultaneous removal of acenaphthene and Cd^{2+} were presented in Figure 5. Comparing to the individual sorption of acenaphthene or Cd^{2+}, the sorption capacities decreased, indicating some competitive sorption between acenaphthene and Cd^{2+}. It results from the fact that both acenaphthene and Cd^{2+} interact with the poly (ethylene oxide) groups on the surfactant micelles (Kikuchi et al. 1992, Wang and Keller 2008b, c), given that the number of the reactive sites is limited. Competitive sorption is also proved by the fact that as Mag-PCMA dosage increased, the differences of sorption capacity between individual and simultaneous sorption decreased. Noticeably, competitive sorption results in less impact on the adsorption capacity of acenaphthene than on Cd^{2+}. This can be explained by the faster sorption kinetics on acenaphthene, based on the kinetic constant k_2 (Table 2), which allows acenaphthene to occupy the available active sites first. This result also agrees with the fact the difference was less significant with higher Mag-PCMA dosage, since there are more available sites.

Furthermore, as NOM constitutes a major fraction of the organic matter in water, the simultaneous sorption of Cd^{2+} and acenaphthene in the presence of NOM was also investigated, as shown in Figure 6. The sorption capacity of Mag-PCMA for

acenaphthene decreased slightly in the presence of NOM. This is not surprising because NOM also competes for the limited ethylene oxide groups on the surfactant micelles. Furthermore, the concentration of NOM (20 mg/L) was much higher, which would promote the interaction via provide higher driving force and result in higher sorption capacity. On the other hand, the sorption capacity of Cd^{2+} increased in the presence of NOM, since the significant amount of polar groups (e.g. carboxylic groups) on the NOM (Tan 2014) can also complex Cd^{2+} (Otto et al. 2001). The differences were smaller when a higher amount of sorbent was added.

6.3.5. Effect of pH on simultaneous removal

pH is an important factor in water chemistry, which may affect the speciation of solutes. Acenaphthene has a very high pK_a value (>15) (Montgomery 2007), which is over the range of pH (4.0–10.0) considered in the current study, suggesting the group mainly existed in pronated forms (cationic) within the pH range (Atkins and De Paula). Simulation of the aqueous speciation of cadmium using Visual MINTEQ (Gustafsson 2006) software indicates that for pH from 3 to 10, cadmium in DI water at these concentrations is mostly present as Cd^{2+}. Therefore, the protonated form of both Cd^{2+} and acenaphthene are favorable for the electrostatic interactions with Mag-PCMA's negatively charged surface across pH 4 to10 (Figure 2D). In Figure 7, as pH increased, the simultaneous sorption of both Cd^{2+} and acenaphthene increased, particularly, significant

increase occurred on the sorption capacity of Cd^{2+}. It agreed with the trend of Mag-PCMAs' zeta potential (Figure 2D), more negative surface charge of Mag-PCMA as pH increase. It suggests that the dominant mechanism of Cd^{2+} remediation by Mag-PCMA in the simultaneous removal is electrostatic interaction.

6.3.6. Effect of water hardness on simultaneous removal

Water hardness is usually expressed as the total amount of $Ca^{2+}$and/or Mg^{2+} present in the water, which varies in different water matrices. As complexions between poly(ethylene oxide) groups on the surfactant micelles and metal ions are not specific, thus, Ca^{2+} and Mg^{2+} may also compete with simultaneous sorption of Cd^{2+} and acenaphthene (Kikuchi et al. 1992). Figure 8 shows the simultaneous removal performance of Cd^{2+} and acenaphthene using Mag-PCMA in the presence of different concentrations of Ca^{2+} or Mg^{2+}. No significant difference was found on the sorption capacity of acenaphthene as either Ca^{2+} or Mg^{2+} concentration up to 50 mg/L. However, the sorption capacity of Cd^{2+} sharply decreased when more Mg^{2+} were presented, while no obvious change was observed with Ca^{2+} presence. It is not surprising as previous study suggests that alkaline earth metal ion complexes with Triton X-100, and Ca^{2+} showed low formation constant (Kikuchi et al. 1992).

6.3.7. Regeneration and reuse of Mag-PCMA

To demonstrate the regenerability and reusability of the Mag-PCMA, the recovery of acenaphthene sorbed onto the Mag-PCMA was investigated using methanol extraction. The removal of acenaphthene during five continuous cycles of regeneration and reuse are shown in Fig. 9. No significant losses of sorption capacity of acenaphthene was observed for the regenerated Mag-PCMA after 5 cycles, indicating good reusability of Mag-PCMA.

6.4. Conclusions

Micelle array confined magnetic (Mag-PCMA) nanoparticle adsorbents with nonionic surfactant were successfully synthesized, and the novel sorbents performed well to remove Cd^{2+}, acenaphthene and NOM, respectively. The isotherm study indicated that hydrophobic interaction played an important role in the sorption process of acenaphthene while complexation reaction is the most likely dominant mechanism for Cd^{2+} sorption. The kinetic study showed that the Mag-PCMA had a rapid sorption towards PAHs and metal contaminants. Mag-PCMA can simultaneously remove Cd^{2+} and acenaphthene with or without NOM presented. The simultaneous sorption of Cd^{2+} and acenaphthene by Mag-PCMAs was no significantly affected by the change of water hardness and increased with an increase of pH. Moreover, the sorbent had showed excellent performance of regeneration and can be used at least five times without significant loss of sorption

capacity for acenaphthene. It demonstrated that Mag-PCMA could provide a fast, effective and sustainable approach for simultaneous decontamination of PAHs, metal ions and NOM.

Table 1. Isotherm parameters for Cd^{2+}, acenaphthene and NOM sorption on Mag-PCMA

	Langmuir			Freundlich		
	q_m (mg/g)	K_L (L/mg)	R^2	K_F ((mg/g)/(L/mg)$^{-n}$)	1/n	R^2
Cd^{2+}	1.479	62.44	0.999	1.806	0.273	0.998
Acenaphthene	0.391	-10.31	0.997	48.00	1.641	0.999
NOM	4.193	0.131	0.908	0.242	1.104	0.991

Table 2. Kinetic parameters for Cd^{2+} and acenaphthene sorption on Mag-PCMA

	q_e (mg/g)	k_2 (g/h·mg)	R^2
Cd^{2+}	0.778	0.974	0.978
Acenaphthene	4.193	1.429	0.975

Figure 1. Schematic representation of Mag-PCMA synthesis (note: the core and shell are not drawn to scale).

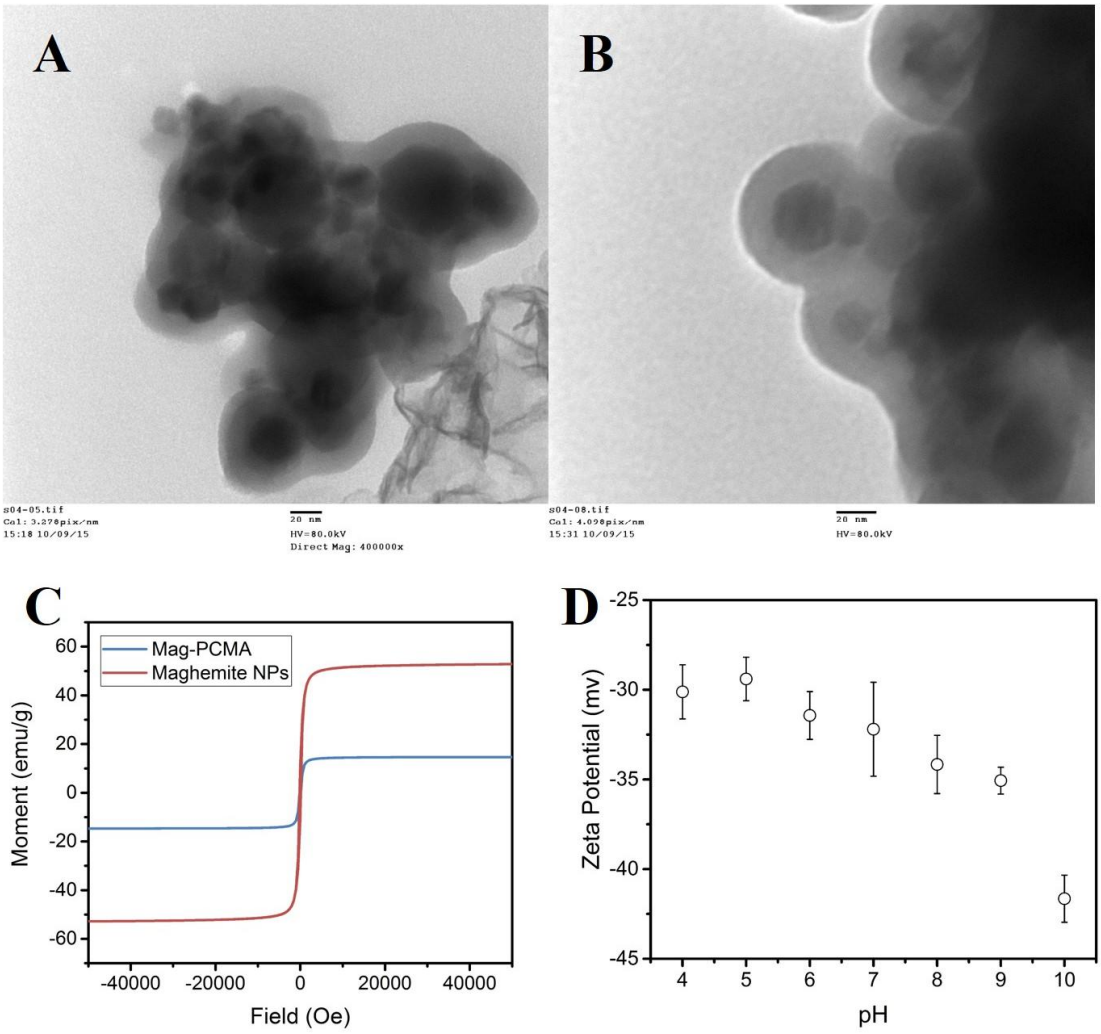

Figure 2. TEM micrographs of Mag-PCMA (A) at 400,000×, scale bar=20 nm and (B) at 500,000×, scale bar=20 nm; (C) the magnetic hysteresis loops of Mag-PCMA and maghemite nanoparticles; (D) zeta potential of Mag-PCMA particles as a function of pH.

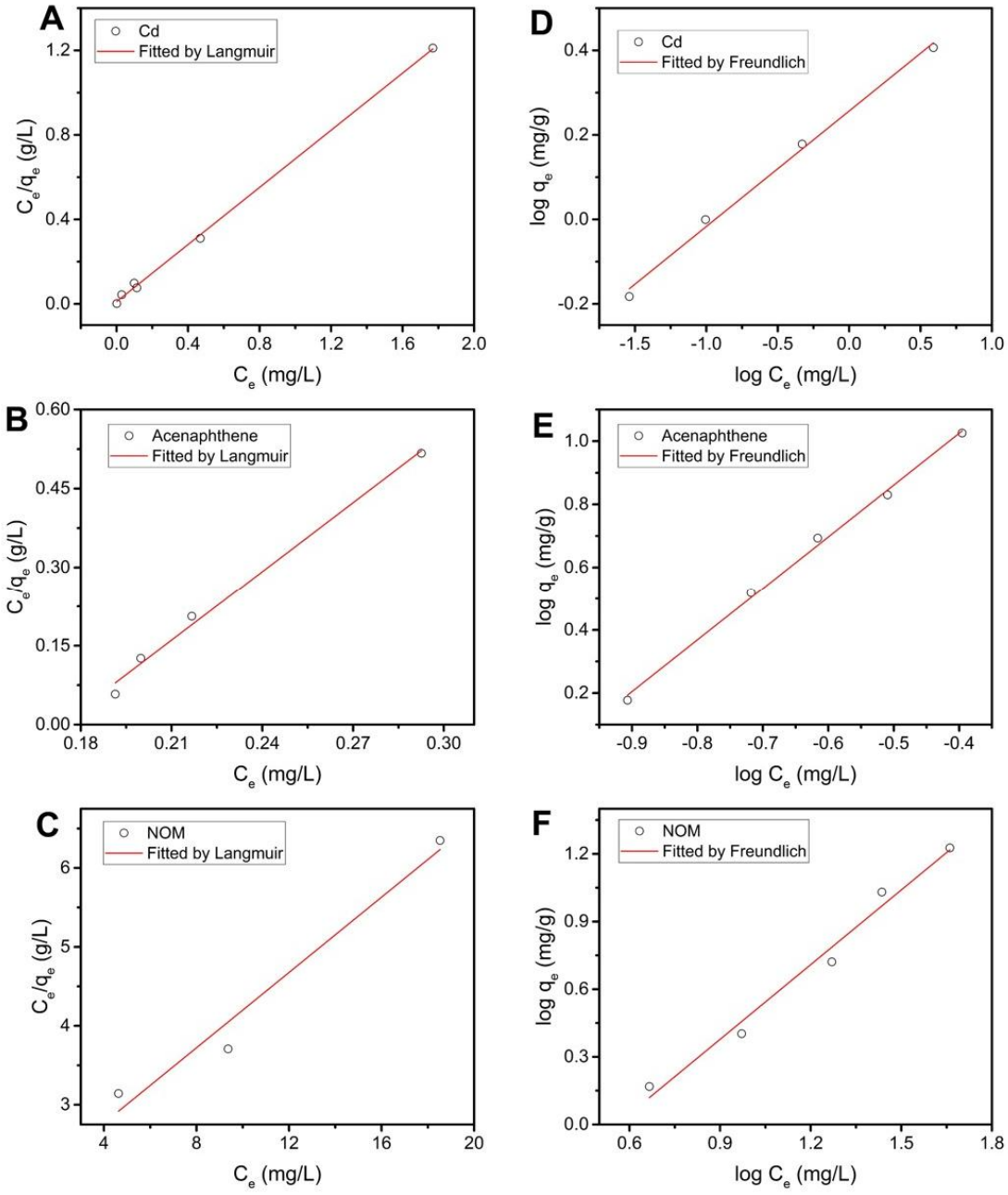

Figure 3. Langmuir adsorption isotherms fit for (A) Cd^{2+}; (B) acenaphthene; and (C) NOM onto Mag-PCMA at pH 7; and Freundlich adsorption isotherms fit for (D) Cd^{2+}; (E) acenaphthene; and (F) NOM onto Mag-PCMA at pH 7, symbols represent experimental data, and red line represents model prediction.

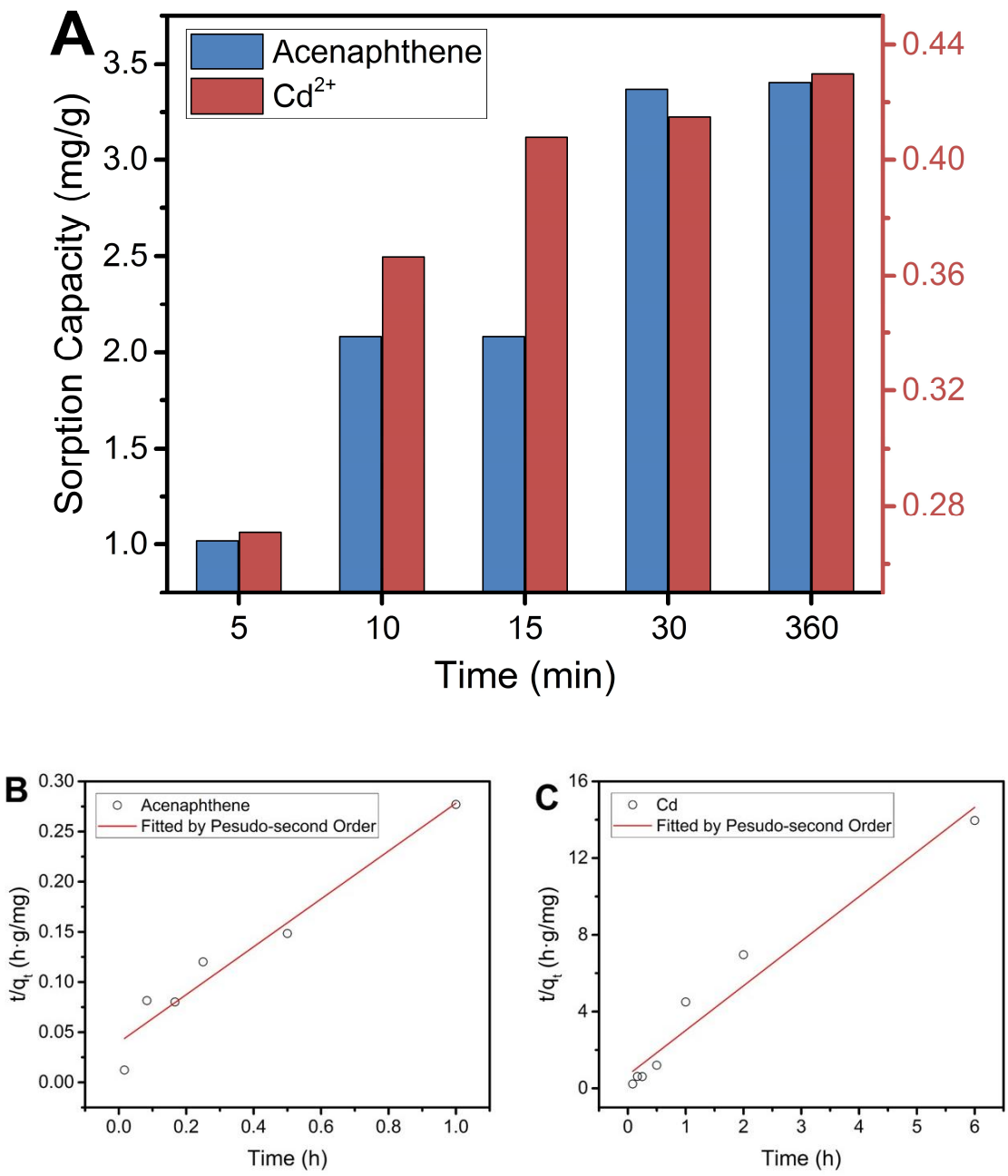

Figure 4. (A) Sorption capacity of acenaphthene and Cd^{2+} versus time; and sorption kinetics fitted by Pseudo-second order of (B) acenaphthene; (C) Cd^{2+} onto Mag-PCMA in solution at pH 7, symbols represent experimental data, and red line represents model prediction.

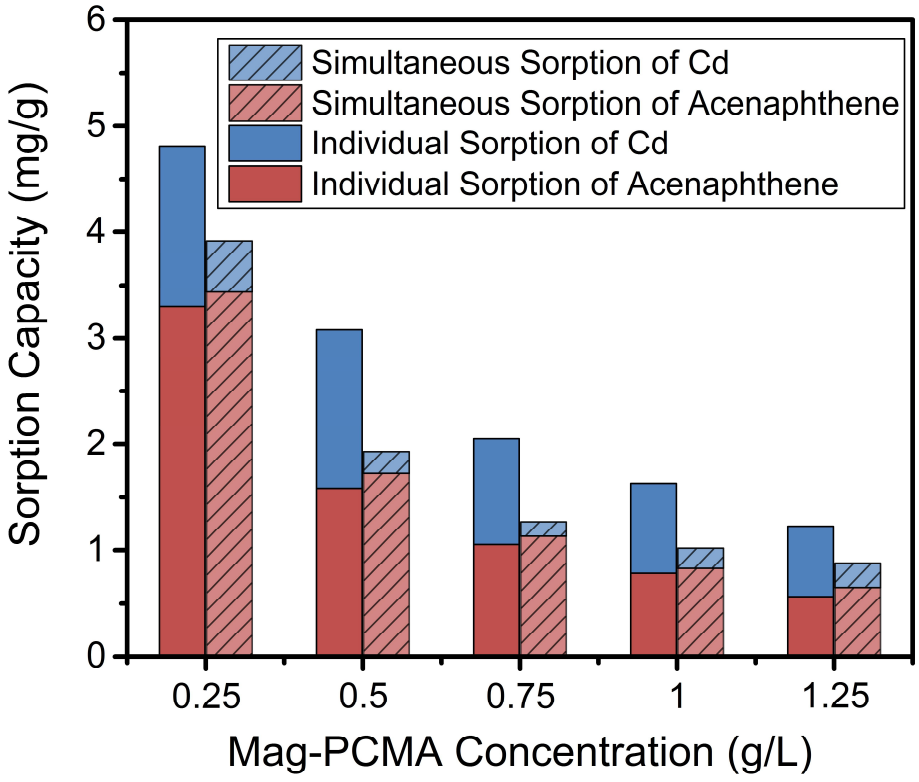

Figure 5. Simultaneous sorption of Cd^{2+} and acenaphthene as a function of adsorbent dose with a fixed initial concentration of 1 mg/L Cd^{2+} and acenaphthene equally. Individual sorption capacity of Cd^{2+} and acenaphthene under same conditions are presented for comparison.

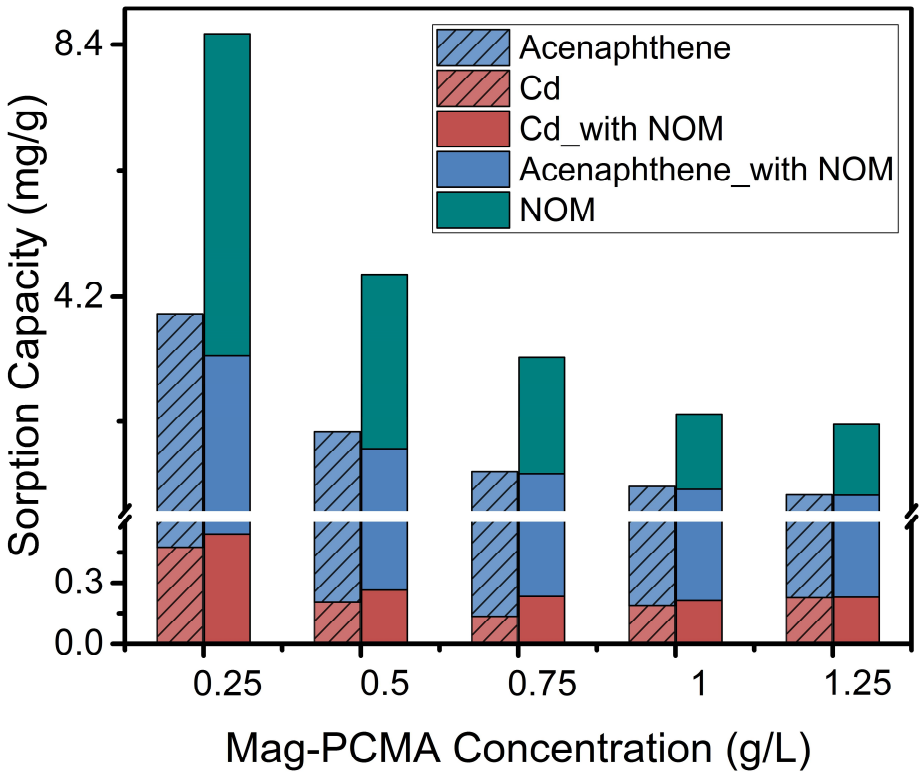

Figure 6. Simultaneous sorption of Cd^{2+}, acenaphthene and NOM as a function of adsorbent dose with a fixed initial concentration of 1 mg/L of Cd^{2+} and acenaphthene equally in the presence of 20 mg/L NOM.

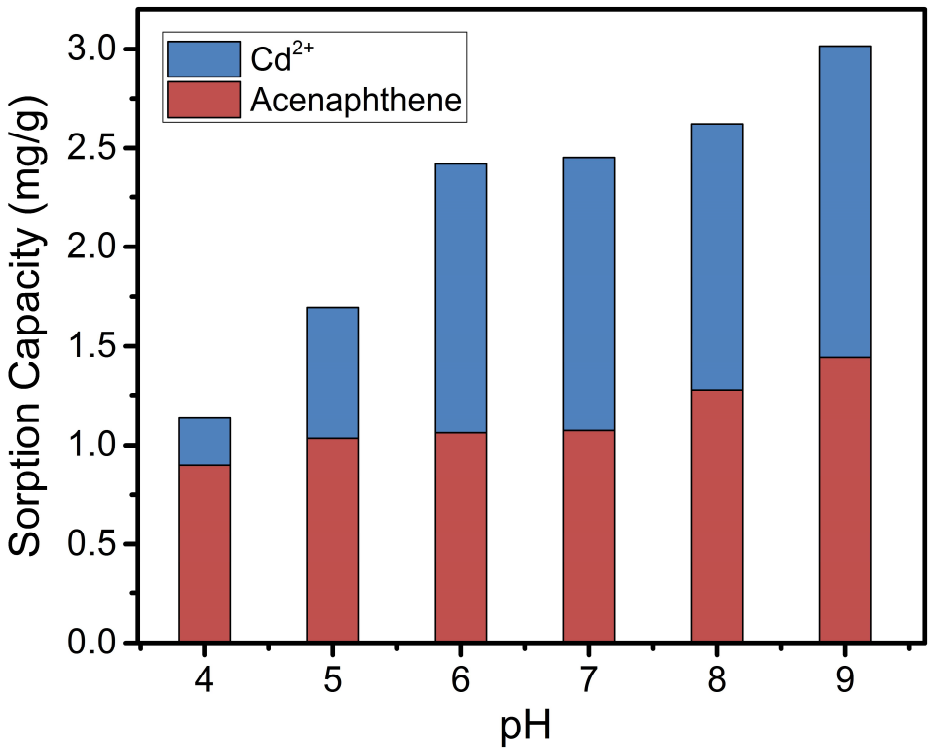

Figure 7. Simultaneous sorption of Cd^{2+} and acenaphthene as a function of pH.

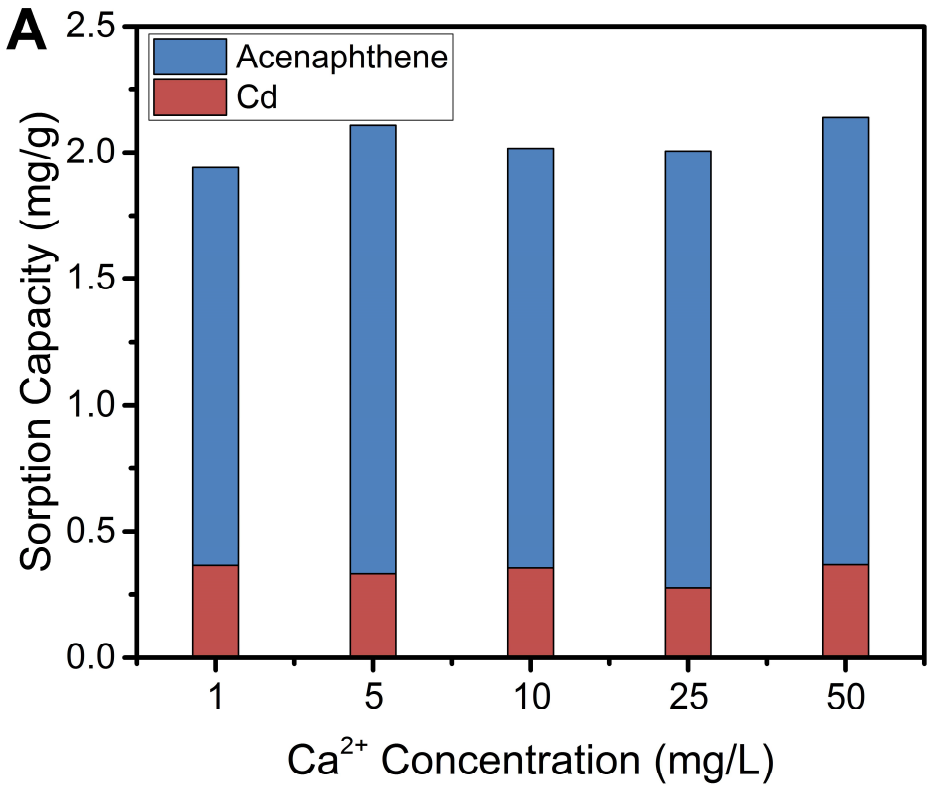
A
Acenaphthene
Cd
Sorption Capacity (mg/g)
2.5
2.0
1.5
1.0
0.5
0.0
1
5
10
25
50
Ca2+ Concentration (mg/L)

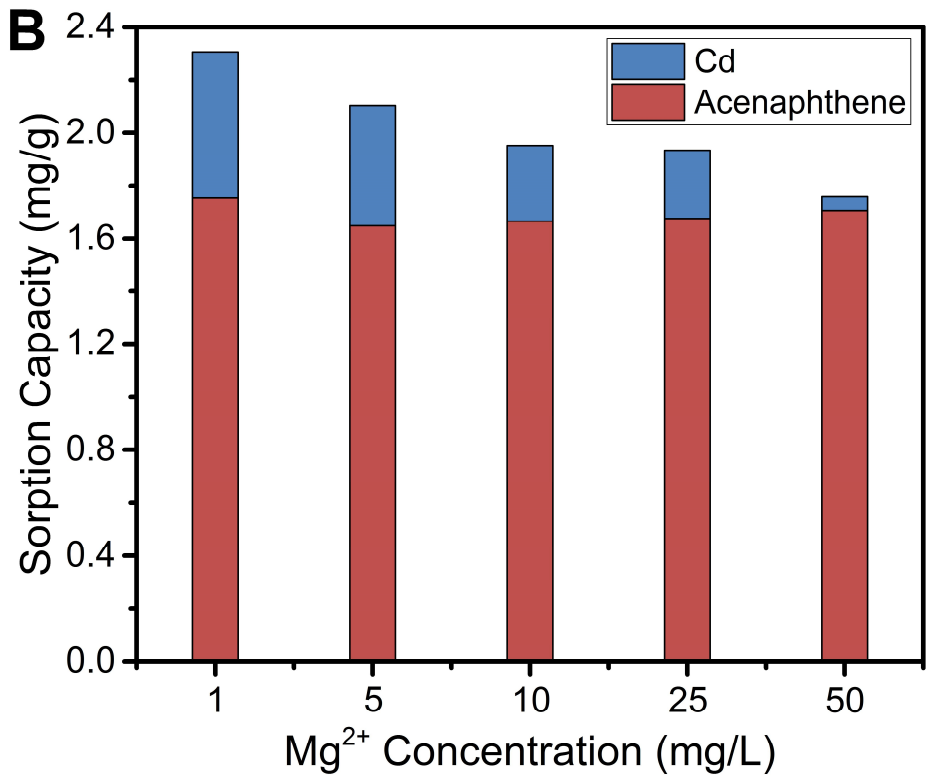
B
Cd
Acenaphthene
Sorption Capacity (mg/g)
2.4
2.0
1.6
1.2
0.8
0.4
0.0
1
5
10
25
50
Mg2+ Concentration (mg/L)

Figure 8. Simultaneous sorption of Cd^{2+} and acenaphthene in the presence of (A) Ca^{2+} (from 1 mg/L to 50 mg/L) and (B) Mg^{2+} (from 1 mg/L to 50 mg/L) at pH 7.

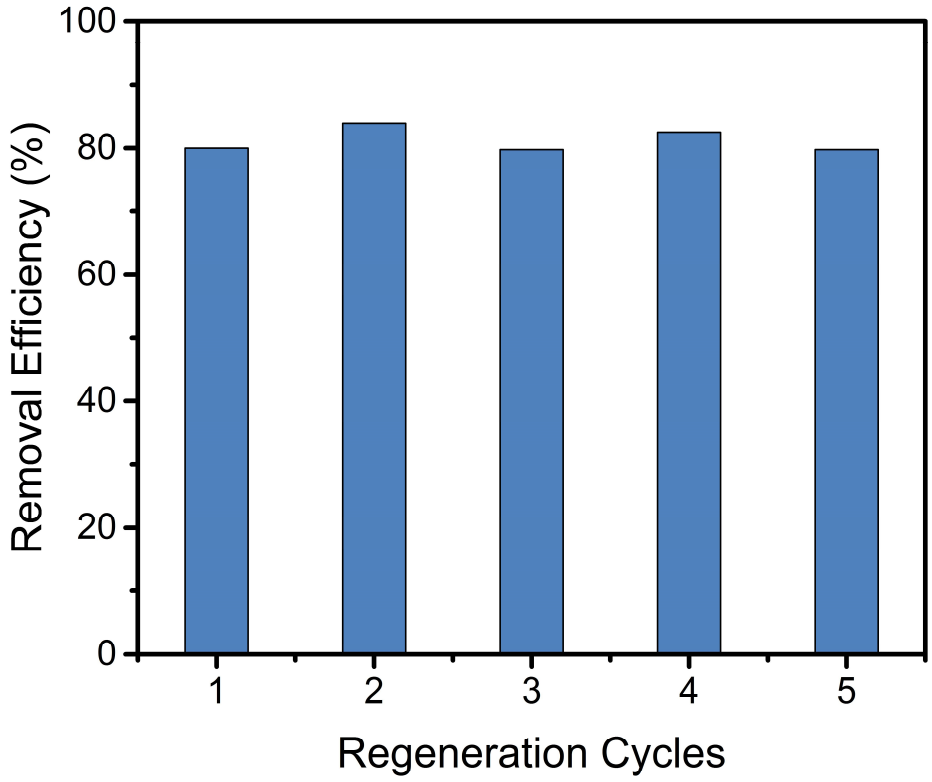

Figure 9. Sorption of acenaphthene onto Mag-PCMA during five regeneration cycles.

6.5. References

Atkins, P. and De Paula, J. Physical chemistry, 2002. Oxford University Press, ca 57, 80.

Chen, C.-F., Binh, N.T., Chen, C.-W. and Dong, C.-D. (2015) Removal of polycyclic aromatic hydrocarbons from sediments using sodium persulfate activated by temperature and nanoscale zero-valent iron. Journal of the Air & Waste Management Association 65(4), 375-383.

Clark, K.K. and Keller, A.A. (2012a) Adsorption of perchlorate and other oxyanions onto magnetic permanently confined micelle arrays (Mag-PCMAs). Water Research 46(3), 635-644.

Clark, K.K. and Keller, A.A. (2012b) Investigation of two magnetic permanently confined micelle array sorbents using nonionic and cationic surfactants for the removal of PAHs and pesticides from aqueous media. Water, Air, & Soil Pollution 223(7), 3647-3655.

Coleman, N.T., Mcclung, A.C. and Moore, D.P. (1956) Formation Constants for Cu(Ii)-Peat Complexes. Science 123(3191), 330-331.

Feng, S.L., Mai, B.X., Wei, G.J. and Wang, X.M. (2012) Genotoxicity of the sediments collected from Pearl River in China and their polycyclic aromatic hydrocarbons (PAHs) and heavy metals. Environmental Monitoring and Assessment 184(9), 5651-5661.

Gustafsson, J.P. (2006) Visual minteq. Capturado em de 26.

Hanna, K., Beurroies, I., Denoyel, R., Desplantier-Giscard, D., Galarneau, A. and Di Renzo, F. (2002) Sorption of hydrophobic molecules by organic/inorganic mesostructures. Journal of Colloid and Interface Science 252(2), 276-283.

Huang, Y.X. and Keller, A.A. (2013) Magnetic Nanoparticle Adsorbents for Emerging Organic Contaminants. Acs Sustainable Chemistry & Engineering 1(7), 731-736.

Huang, Y.X. and Keller, A.A. (2015) EDTA functionalized magnetic nanoparticle sorbents for cadmium and lead contaminated water treatment. Water Research 80, 159-168.

Huang, Y.X., Yang, J.K. and Keller, A.A. (2014) Removal of Arsenic and Phosphate from Aqueous Solution by Metal (Hydr-)oxide Coated Sand. Acs Sustainable Chemistry & Engineering 2(5), 1128-1138.

Kikuchi, Y., Suzuki, T. and Sawada, K. (1992) Liquid—liquid extraction of alkaline earth metal ions with a non-ionic surfactant having a poly (oxyethylene) chain (Triton X-100). Analytica chimica acta 264(1), 65-70.

Lee, H., Jang, Y., Lee, Y.M., Lee, H., Kim, G.-H. and Kim, J.-J. (2015) Enhanced removal of PAHs by Peniophora incarnata and ascertainment of its novel ligninolytic enzyme genes. Journal of environmental management 164, 10-18.

Luo, C., Liu, C., Wang, Y., Liu, X., Li, F., Zhang, G. and Li, X. (2011) Heavy metal contamination in soils and vegetables near an e-waste processing site, south China. Journal of Hazardous Materials 186(1), 481-490.

Maturi, K. and Reddy, K.R. (2006) Simultaneous removal of organic compounds and heavy metals from soils by electrokinetic remediation with a modified cyclodextrin. Chemosphere 63(6), 1022-1031.

Montgomery, J.H. (2007) Groundwater chemicals desk reference, CRC Press.

Morel, F.M.M. and Hering, J.G. (1993) Principles and Applications of Aquatic Chemistry, Wiley.

Mulligan, C.N., Yong, R.N., Gibbs, B.F., James, S. and Bennett, H.P.J. (1999) Metal removal from contaminated soil and sediments by the biosurfactant surfactin. Environmental Science & Technology 33(21), 3812-3820.

Otto, W.H., Burton, S.D., Carper, W.R. and Larive, C.K. (2001) Examination of cadmium (II) complexation by the Suwannee River fulvic acid using 113Cd NMR relaxation measurements. Environmental Science & Technology 35(24), 4900-4904.

Reddy, K.R., Al-Hamdan, A.Z. and Ala, P. (2010) Enhanced soil flushing for simultaneous removal of PAHs and heavy metals from industrial contaminated soil. Journal of Hazardous, Toxic, and Radioactive Waste 15(3), 166-174.

Rosen, M.J. and Kunjappu, J.T. (2012) Surfactants and interfacial phenomena, John Wiley & Sons.

Sargın, İ., Kaya, M., Arslan, G., Baran, T. and Ceter, T. (2015) Preparation and characterisation of biodegradable pollen–chitosan microcapsules and its application in heavy metal removal. Bioresource technology 177, 1-7.

Song, S.S., Zhu, L.Z. and Zhou, W.J. (2008) Simultaneous removal of phenanthrene and cadmium from contaminated soils by saponin, a plant-derived biosurfactant. Environmental Pollution 156(3), 1368-1370.

Su, Y., Adeleye, A.S., Keller, A.A., Huang, Y., Dai, C., Zhou, X. and Zhang, Y. (2015) Magnetic sulfide-modified nanoscale zerovalent iron (S-nZVI) for dissolved metal ion removal. Water Research.

Su, Y.M., Adeleye, A.S., Huang, Y.X., Sun, X.Y., Dai, C.M., Zhou, X.F., Zhang, Y.L. and Keller, A.A. (2014) Simultaneous removal of cadmium and nitrate in aqueous media by nanoscale zerovalent iron (nZVI) and Au doped nZVI particles. Water Research 63, 102-111.

Tan, K.H. (2014) Humic matter in soil and the environment: principles and controversies, CRC Press.

Thavamani, P., Megharaj, M. and Naidu, R. (2012) Multivariate analysis of mixed contaminants (PAHs and heavy metals) at manufactured gas plant site soils. Environmental Monitoring and Assessment 184(6), 3875-3885.

Veetil, D.P., Mercier, G., Blais, J.F., Chartier, M. and Tran, L.H. (2013) Simultaneous removal of Cu and PAHs from dredged sediments using flotation. Journal of Soils and Sediments 13(8), 1502-1514.

Vela, N., Martinez-Menchon, M., Navarro, G., Perez-Lucas, G. and Navarro, S. (2012) Removal of polycyclic aromatic hydrocarbons (PAHs) from groundwater by heterogeneous photocatalysis under natural sunlight. Journal of Photochemistry and Photobiology a-Chemistry 232, 32-40.

Wang, H., Keller, A.A. and Clark, K.K. (2011) Natural organic matter removal by adsorption onto magnetic permanently confined micelle arrays. Journal of Hazardous Materials 194, 156-161.

Wang, P. and Keller, A.A. (2008a) Adsorption of hydrophobic organic compounds onto a hydrophobic carbonaceous geosorbent in the presence of surfactants. Environmental Toxicology and Chemistry 27(6), 1237-1243.

Wang, P. and Keller, A.A. (2008b) Particle-size dependent sorption and desorption of pesticides within a water-soil-nonionic surfactant system. Environmental Science & Technology 42(9), 3381-3387.

Wang, P. and Keller, A.A. (2008c) Partitioning of hydrophobic organic compounds within soil-water-surfactant systems. Water Research 42(8-9), 2093-2101.

Wang, P., Shi, Q.H., Shi, Y.F., Clark, K.K., Stucky, G.D. and Keller, A.A. (2009) Magnetic Permanently Confined Micelle Arrays for Treating Hydrophobic Organic Compound Contamination. Journal of the American Chemical Society 131(1), 182-188.

Weber, W.J., Mcginley, P.M. and Katz, L.E. (1991) Sorption Phenomena in Subsurface Systems - Concepts, Models and Effects on Contaminant Fate and Transport. Water Research 25(5), 499-528.

Chapter 7. Conclusions and Future Works

7.1. Conclusions

This doctoral research developed a series of novel magnetic nanoparticle sorbents with different functional groups for organic and inorganic contaminants remediation in aquatic systems. The decontamination performance were evaluated under various environmental conditions, such as solution pH, in presence of NOM, ionic strength, competitive sorption of other species and et al.. Study was also investigated on the mechanism of the removal for different categories of pollutants, and optimization were carried out to improve the sorption capacities and kinetics. The regeneration and reuse of these novel magnetic nanoparticle sorbents were also studied, which proved the promising utilization in larger scale of water treatment in the future. This dissertation demonstrate a fast, convenient, efficient, and sustainable approach for water treatment.

In the first study, a multiple-time reusable magnetic ligand particle (Mag-Ligand) which includes a metal-binding organic ligand (EDTA) attached to an iron oxide nanoparticle was synthesized successfully in a simple procedure. The superparamagnetic maghemite core allowed rapid separation of Mag-Ligand after sorption, while the attached organic ligand can strongly bind the dissolved metal ion contaminant via complexation reactions. Mag-Ligand showed fast removal ability for both Cd^{2+} (<2 h) and Pb^{2+} (<15 min) with relatively high sorption capacity (79.4 and 100.2 mg/g for Cd^{2+} and

Pb^{2+}, respectively). The remediation performance was relatively stable across a wide pH range (4-10), and slightly affected by increased water hardness (up to 100 mg/L Ca^{2+} or 60 mg/L Mg^{2+} present in the solution). The Mag-Ligand exhibited the potentially wide application in the removal of metal ions in various aqueous matrices.

The second project followed up on the first one by exploring the promising wide range of removing metal ions as well as extending the application to adsorb or collect ions of valuable elements. In this study, the adsorption capacities, isotherms and kinetics of nine different metal ions, including three rare earth elements, onto Mag-Ligand, at different initial metal ion concentrations in individual sorption were determined. Creatively, the isothermal titration calorimeter technology was utilized to obtain the thermodynamic quantification of the interactions between nanoparticle sorbents and metal ions. The difference in magnitude of binding of Mag-Ligand with different metal ions led to the similar sequence of sorption capacities. In addition, the performance of Mag-Ligand for multiple metal ions in competitive sorption was investigated to address the fact that natural aquatic systems contain a wide variety of dissolved heavy metal ions at trace level. The sequence of selective in competitive sorption was demonstrated to be associated with the individual sorption kinetics. The study revealed the sorption mechanisms in individual and competitive sorption were dominated by complexation reaction between metal ions and ligand and adsorption onto the porous structure of Mag-Ligand. This project provided more thermodynamic data and foundational understanding

of using Mag-Ligand in more complex aquatic systems, with pushing the limit to engineering side further.

In the third study, attention was directed at the remediation of EOCs. Magnetic permanently confined micelle arrays (Mag-PCMAs) with a core–shell structure were synthesized by coating the surface of maghemite particles with a silica/surfactant mesostructured hybrid layer. The sorption kinetics and isotherms of 2 legacy contaminants and 7 newly occurred synthetic chemicals, including pharmaceuticals and industrial additives onto Mag-PCMAs were determined. The mechanisms of removing these rather soluble EOCs were most likely to be the combination of hydrophobic interactions, hydrogen bonding, and electrostatic interactions. This project has widely extended the categories of contaminants that Mag-PCMAs could be utilized for remediation. Furthermore, Mag-PCMAs showed the potential application in separation and purification for valuable compounds (e.g. pharmaceuticals) due to its high sorption capacity and easy recovery as well as low energy and cost requirement.

As the previous studies showing the wide application of Mag-PCMAs in the environmental decontamination, the fourth project focus on further improving the sorption capacities and kinetics for PAHs and EOCs. The porous structure of the synthesized magnetic nanoparticle sorbents were optimized via introducing a micelle swelling agent and removing it afterward. 3 different Mag-PCMAs were synthesized through changed the amount of micelle swelling agent used during the synthesis. The

results demonstrate that with higher portion of micelle swelling agent, the sorbents obtained higher surface area and pore volume. It results in higher sorption rate and higher equilibrium sorption capacities of both EOCs and PAHs, which have various hydrophobicity. The enlarged surface area and pore volume enable faster diffusion rate for EOCs and PAHs to transfer through the silica framework to have the hydrophobic interactions with the confined surfactant micelles.

As the first four projects were directed on using the magnetic nanoparticle sorbents for the treatment of metal ions and organic contaminants individually, the last project was designed for simultaneous removal of PAHs and metal contaminants regarding to the fact that numerous wastewater is contaminated with various categories of contaminants. Mag-PCMAs with nonionic surfactant were developed, and it showed good removal of metal ions, PAHs and NOM, respectively. Cd^{2+} and acenaphthene were chose as the reprehensive of metal ions and PAHs to study the sorption isothermals and kinetics onto Mag-PCMAs. The adsorption mechanisms of PAHs, metal ions and NOM were investigated. The sorption process of PAHs and metal ions were dominated by hydrophobic interaction and complexation reactions, respectively. The simultaneous removal of PAHs and metal contaminants were studied under various environmental conditions, such as with the presence of NOM, different solution pH and water hardness. The performance of simultaneous removal was relatively stable across a wide range of

ionic strength, and increased with an increase of pH. The presence of NOM slightly stimulated the removal efficiency of metal ions.

7.2. Future works

The primary goal of this study was to develop novel magnetic nanoparticle sorbents for the decontamination of organic and metal pollutants and evaluate these sorbents under different environmental conditions. Beyond this doctoral research, there are some further noteworthy scientific and engineering questions which may need to be answered by future studies for the final application in the realistic scenarios.

7.2.1. Simultaneous removal of numerous low concentration of contaminants

The magnetic nanoparticle sorbents developed in this dissertation showed the promising capability to wide range of different pollutant categories. For most of the studies in this dissertation, the isothermal and kinetics were determined via individual sorption experiments. With more advanced instrument, such as ICP-MS and LC/MS/MS, we are able to push detect limit to much lower concentration of metal ions and organic compounds as well as analyze numerous items at one single run. It would be possible to evaluate the performance of these novel magnetic nanoparticle sorbents for low concentration pollutants. In addition, we can develop high though put method to investigate the removal efficiencies of these sorbents on particular classic of contaminants, such as PAHs, pesticides and et al.. With these data, we would be able to better

understand the mechanisms of the interaction between nanoparticle sorbents and contaminants.

7.2.2. Automated apparatus for continuous utilizing magnetic nanoparticle adsorbents in water treatment

Nowadays, most of the newly developed nanotechnologies for water treatment are applied in the laboratory scale only. One major limitation is the cost of the production and operation. One outstanding feature of the magnetic nanoparticle sorbents developed in this dissertation is its superparamagenic core, which enable for magnetic mixing and separation to lower the energy input and operation cost. Furthermore, these sorbents can be easily regenerated and showed stable performance on reusing, which could further reduce the cost. To further stet into engineering side, a large scale automated apparatus for continuous utilizing magnetic nanoparticle adsorbents needed to be designed and fabricated.

7.2.3. Life-cycle analysis and environmental impact of utilizing magnetic nanoparticle adsorbents in water treatment

The projects in this research were focused on the development and optimization of novel magnetic nanoparticle sorbents as well as their performance on decontamination. These emerging materials did demonstrate higher removal efficiencies on certain pollutants, but limited information on cost and environmental impacts are available.

Furthermore, as rapid development of these engineered nanomaterials, more and more concern were directed at their environmental impact and toxicity. It is necessary to provide such information via conducting life-cycle analysis for further industrial utilization.